NASA TECHNICAL MEMORANDUM

NASA TM X-1553

NASA TM X-1553

PHASE AND GROUP REFRACTIVE INDICES FROM THE COLLISIONLESS MAGNETOIONIC THEORY

by

Lawrence Colin and Kwok-Long Chan

Ames Research Center
Moffett Field, Calif.

and

Jack G. K. Lee

Informatics, Inc.
Palo Alto, Calif.

NATIONAL AERONAUTICS AND SPACE ADMINISTRATION • WASHINGTON, D. C. • APRIL 1968

NASA TM X-1553

PHASE AND GROUP REFRACTIVE INDICES FROM THE COLLISIONLESS MAGNETOIONIC THEORY

By Lawrence Colin and Kwok-Long Chan

Ames Research Center
Moffett Field, Calif.

and

Jack G. K. Lee

Informatics, Inc.
Palo Alto, Calif.

(Tabulation supplement available on request.)

NATIONAL AERONAUTICS AND SPACE ADMINISTRATION

For sale by the Clearinghouse for Federal Scientific and Technical Information
Springfield, Virginia 22151 – CFSTI price $3.00

The supplemental tabulations to this report list the computed phase and group refractive indices for the ordinary mode (MUOSQ, MUOPRIM) and the extraordinary and Z modes (MUXSQ, MUXPRIM). Also listed are the values of auxiliary variables in the computation S_O, S_X, R. The tables include 13 angles of θ: 0°, 10°, 15°, 20°, 30°, 40°, 45°, 50°, 60°, 70°, 75°, 80°, 90°.

The tabulations are available on request from:

Chief, Technical Information Division
National Aeronautics and Space Administration
Ames Research Center
Moffett Field, California, 94035

CUT

Date__________

Please send copy of tabulation supplement to NASA TM X-1553 by Colin, Chan, and Lee.

____
Name of organization

____
Street Number

____
City and State
Attention: Mr.__________
Title__________

Place
stamp
here

Chief, Technical Information Division
National Aeronautics and Space Administration
Ames Research Center
Moffett Field, California, 94035

PHASE AND GROUP REFRACTIVE INDICES FROM THE COLLISIONLESS MAGNETOIONIC THEORY

By Lawrence Colin and Kwok-Long Chan
Ames Research Center

and

Jack G. K. Lee
Informatics, Inc.
Palo Alto, California

SUMMARY

Graphs of phase and group refractive indices computed from the collisionless magnetoionic theory are presented. The indices are computed for both the entire range of electron concentration and the intensity of the earth's magnetic field to be encountered by operational topside ionospheric sounders in the International Satellites for Ionospheric Studies (ISIS) series (Alouette I, Explorer XX, Alouette II, ISIS-A, ISIS-B).

INTRODUCTION

Swept high-frequency radar soundings of the earth's ionospheric plasma have been performed routinely and bottomside ionograms collected for over 40 years by more than 100 ground-based stations. Topside ionograms obtained from sounders on board the earth-orbiting satellites Alouette I and Alouette II have been collected since 1962. The theory of propagation of electromagnetic waves in an ionized medium (i.e., the magnetoionic theory) is well documented and generally accepted (refs. 1 and 2). The key parameters affecting the propagating waves are the phase and group refractive indices which, in turn, define the wave phase and group velocities relative to the velocity of light in free space. These indices are functions of the radar wave frequency, the local ionospheric electron concentration, the earth's magnetic field intensity, the angle between the directions of the wave normal and magnetic field, and the particle collision frequencies. Computations of phase and group refractive indices appropriate to the ionosphere below the F_2 layer peak, for restricted ionospheric models and for particular geographical locations, have been published (refs. 3-5). The earth-orbiting radar sounder has made it necessary to consider these indices at substantially all geographic longitudes and latitudes at heights from 300 to 3000 km. Within this range the collisionless magnetoionic theory is applicable. It is the purpose of this report to present graphs of the indices appropriate to the entire range of electron concentration observable during a sunspot cycle throughout the above geographical region. Applications of these results to the reduction of topside sounder data are reviewed by Jackson (ref. 6). The results are also applicable to other types of experiments involving propagation of electromagnetic energy through cold magnetoionic plasmas.

REFRACTIVE INDICES

The phase and group refractive indices are defined by

$$\mu = c/v_p \tag{1}$$

$$\mu' = c/v_g = \mu + f(\partial\mu/\partial f) \tag{2}$$

where

μ phase refractive index

μ' group refractive index

v_p phase velocity

v_g group velocity

c velocity of light in free space

f electromagnetic wave frequency

The collisionless phase refractive index is given by the Appleton-Hartree equation of the magnetoionic theory (ref. 1):

$$\mu = \left[1 - \frac{X}{1 - \frac{Y^2 \sin^2 \theta}{2(1 - X)} \pm \sqrt{\frac{Y^4 \sin^4 \theta}{4(1 - X)^2} + Y^2 \cos^2 \theta}}\right]^{1/2} \tag{3}$$

where

$$X = f_n{}^2/f^2 = N/12{,}400f^2$$

N electron concentration, electrons/cm^3

f electromagnetic wave frequency, Mc/s

f_n plasma frequency, Mc/s

and

$$Y = f_h/f = 2.8B/f$$

B magnetic induction, gauss

f_h electron gyrofrequency, Mc/s

θ angle between the directions of the wave normal and earth's magnetic field

It can be seen that two modes of propagation are possible in a magnetoionic medium, the ordinary mode (with the plus sign) and the extraordinary mode (with the minus sign). These are usually denoted with appropriate subscripts x and o. For clarity the ordinary and extraordinary phase refractive indices may be written:

$$\mu_o = \left(1 - \frac{X}{S_o}\right)^{1/2} \tag{4}$$

$$\mu_x = \left(1 - \frac{X}{S_x}\right)^{1/2} \tag{5}$$

where

$$S_o = 1 - \frac{Y^2 \sin^2 \theta}{2(1 - X)} + \frac{YR}{2(1 - X)} \tag{6}$$

$$S_x = 1 - \frac{Y^2 \sin^2 \theta}{2(1 - X)} - \frac{YR}{2(1 - X)} \tag{7}$$

$$R = [Y^2 \sin^4 \theta + 4 \cos^2 \theta (1 - X)^2]^{1/2} \tag{8}$$

Applying equation (2) to equations (4) through (8) yields the ordinary and extraordinary group refractive indices:

$$\mu_o' = \frac{1}{\mu_o} \left\{1 - \frac{XY(1 - X)\cos^2 \theta}{S_o^2(Y \sin^2 \theta + R)} \left[1 - \frac{Y \sin^2 \theta}{R} \left(\frac{1 + X}{1 - X}\right)\right]\right\} \tag{9}$$

$$\mu_x' = \frac{1}{\mu_x} \left\{1 + \frac{X(1 - S_x)}{2S_x^2} \left[1 + \frac{Y \sin^2 \theta}{R} \left(\frac{1 + X}{1 - X}\right)\right]\right\} \tag{10}$$

These equations simplify considerably for the special cases of longitudinal propagation ($\theta = 0^\circ$) and transverse propagation ($\theta = 90^\circ$):

(a) longitudinal propagation

$$\mu_O = \left(1 - \frac{X}{1 + Y}\right)^{1/2} \tag{11}$$

$$\mu_X = \left(1 - \frac{X}{1 - Y}\right)^{1/2} \tag{12}$$

$$\mu_O' = \frac{1}{\mu_O}\left[1 - \frac{XY}{2(1 + Y)^2}\right] \tag{13}$$

$$\mu_X' = \frac{1}{\mu_X}\left[1 + \frac{XY}{2(1 - Y)^2}\right] \tag{14}$$

(b) transverse propagation

$$\mu_O = (1 - X)^{1/2} \tag{15}$$

$$\mu_X = \left[1 - \frac{X(1 - X)}{1 - X - Y^2}\right]^{1/2} \tag{16}$$

$$\mu_O' = \frac{1}{\mu_O} \tag{17}$$

$$\mu_X' = \frac{1}{\mu_X}\left[1 + \frac{XY^2}{(1 - X - Y^2)^2}\right] \tag{18}$$

GRAPHS OF μ AND μ'

The variation of μ^2 with X for a given value of Y is compactly illustrated in figure 1(a) for $Y < 1$ and in figure 1(b) for $Y > 1$. The vertical cross-hatching bounded by the solid curves represents the computation of μ_O^2 from equation (4) while the horizontal cross-hatching bounded by the dotted curves represents the computation of μ_X^2 from equation (5). The longitudinal and transverse limits are labelled L and T, respectively, and are computed from equations (11), (12), (15), and (16). The specific case of $Y = 1/2$, $\theta = 45^\circ$ is plotted in figure 1(a) and the case of $Y = 3$, $\theta = 15^\circ$ is plotted in figure 1(b).

For $Y < 1$ (fig. 1(a)) there are one branch for the ordinary mode $(0 \leq X \leq 1)$ and two branches for the extraordinary mode $(0 \leq X \leq 1 - Y$ and $(1 - Y^2)/(1 - Y^2 \cos^2 \theta) \leq X \leq 1 + Y)$. The latter branch of the extraordinary mode is referred to as the Z mode. For $Y > 1$ (fig. 1(b)) the ordinary mode has two branches $(0 \leq X \leq 1$ and $(1 - Y^2)/(1 - Y^2 \cos^2 \theta) \leq X$; the latter branch is called the whistler mode and exists only when $Y^2 \cos^2 \theta > 1)$ while the extraordinary mode has only one branch, the Z mode branch ($0 \leq X \leq 1 + Y$). The ordinary, extraordinary, and Z modes are observed as distinct reflection traces in topside ionograms.

Zeros occur in μ at $X = 1$ (ordinary mode), $X = 1 - Y$ (extraordinary mode), and $X = 1 + Y$ (Z mode). An infinity occurs in μ at $X = (1 - Y^2)/[1 - Y^2 \cos^2 \theta]$ (Z mode for $Y < 1$ and ordinary mode for $Y > 1$). Both the zeros and infinities in μ result in infinities in μ'. It should be noted that the infinity in μ' associated with $X = (1 - Y^2)/[1 - Y^2 \cos^2 \theta]$ is not a wave reflection condition as are the other infinities.

For the extraordinary mode when $Y > 1$ (i.e., the Z mode), μ and μ' exhibit discontinuities at $X = 1$ for $\theta = 0$ (longitudinal propagation), and μ' exhibits a maximum at $X = 1$ for other angles. It can be shown (ref. 3) that the following relationships obtain:

$$\mu_Z = \left(1 - \frac{X}{1 - Y}\right)^{1/2} \qquad \text{for} \qquad X < 1, \theta = 0^\circ \tag{19}$$

$$= \left(1 - \frac{X}{1 + Y}\right)^{1/2} \qquad \text{for} \qquad X > 1, \theta = 0^\circ \tag{20}$$

$$\mu_Z' = \frac{1}{\mu_Z}\left[1 + \frac{XY}{2(1 - Y)^2}\right] \qquad \text{for} \qquad X < 1, \theta = 0^\circ \tag{21}$$

$$= \frac{1}{\mu_Z}\left[1 - \frac{XY}{2(1 + Y)^2}\right] \qquad \text{for} \qquad X > 1, \theta = 0^\circ \tag{22}$$

$$\mu_Z' \cong 1 + \frac{1}{Y^2 \sin^2 \theta} \qquad \text{for} \qquad X = 1, \theta \neq 0^\circ \tag{23}$$

The variations of μ' vs. X for different values of Y and θ, plotted on a reciprocal scale to exhibit the infinities, are shown in figures 2 through 113. Table I contains a key to the order of these figures. Figures 2 through 66 are plots of μ' vs. X for fixed θ, variable Y. Figures 67 through 113 are plots of μ' vs. X for fixed Y, variable θ.

TABLES OF μ AND μ'

For the reader who requires greater accuracy than is obtainable from figures 1 through 113, tabulations of μ and μ' may be obtained by mailing the request card in the back of this report. The tabulated quantities include μ_o^2, μ_x^2, μ_o', μ_x', S_o, S_x and R. The range and increments of the independent variables are:

X	0(0.1)1.9 + Y	for	$Y \leq 1$
	0(0.1)10	for	$Y > 1$
Y	0(0.1)5		
θ	$0^\circ(10^\circ)90^\circ$	and	$15^\circ, 45^\circ, 75^\circ$

When values of X or Y other than these are encountered, it is sufficient, for most purposes, to interpolate between the tabulated results. Interpolation for values of θ other than those given may not be sufficiently accurate, however. A Fortran IV listing of a program to compute the phase and group refractive indices for any θ and for the X and Y intervals and increments mentioned above is given in table II.

Ames Research Center
National Aeronautics and Space Administration
Moffett Field, Calif., 94035, Jan. 5, 1968
188-39-01-01-00-21

REFERENCES

1. Ratcliffe, J. A.: The Magneto-Ionic Theory and Its Applications to the Ionosphere. Cambridge University Press, 1959.

2. Budden, K. G.: Radio Waves in the Ionosphere. Cambridge University Press, 1961.

3. Whale, H. A.; and Stanley, J. P.: Group and Phase Velocities From the Magneto-Ionic Theory. J. Atmospheric Terrest. Phys., vol. 1, no. 2, 1950, pp. 82-94.

4. Shinn, D. H.; and Whale, H. A.: Group Velocities and Group Heights From the Magneto-Ionic Theory. J. Atmospheric Terrest. Phys., vol. 2, no. 2, 1952, pp. 85-105.

5. Becker, W.: Tables of Ordinary and Extraordinary Refractive Indices, Group Refractive Indices and $h'_{o,x}(f)$ Curves for Standard Ionospheric Layer Models. Max-Planck-Institute für Aeronome, no. 4, 1960, Berlin, Springer.

6. Jackson, J. E.: The Analysis of Topside Ionograms. Goddard Space Flight Center Document X-615-67-452, Sept. 1967.

TABLE I.- INDEX TO FIGURES

Figure	Mode	Range of Y	Range of θ, deg
2-14	X	0(0.1)0.9	0(10)90 and 15, 45, 75
15-27	Z	0.1(0.1)1.0	0(10)90 and 15, 45, 75
28-40	Z	1.1(0.1)5.0	0(10)90 and 15, 45, 75
41-53	O	0(0.1)1.0	0(10)90 and 15, 45, 75
54-66	O	1.1(0.1)5.0	0(10)90 and 15, 45, 75
67-76	X	0(0.1)0.9	0(10)90 and 15, 45, 75
77-86	Z	0.1(0.1)1.0	0(10)90 and 15, 45, 75
87-94	Z	1.5(0.5)5.0	0(10)90 and 15, 45, 75
95-105	O	0(0.1)1.0	0(10)90 and 15, 45, 75
106-113	O	1.5(0.5)5	0(10)90 and 15, 45, 75

TABLE II.- COMPUTATION OF GROUP AND PHASE REFRACTIVE INDEX

```
C
C  MAIN PROGRAM ***
C
C*** INPUT DATA ***
C** (1) NTHETA = NO. OF THETA USE FOR COMPUTATION (I3)
C** (2) THETA = ANGLE THETA IN DEGREES (F7.2)
C       (NTHETA OF THEM, ONE THETA PER CARD)
C
      DIMENSION X(200),SO(200),SX(200),RMUOSQ(200),RMUXSQ(200),R(200),
     *          RMUOP(200),RMUXP(200)
      DIMENSION TR(100),XX(100),TSO(100),TSX(100),TMUOSQ(100),
     *          TMUXSQ(100),TMUOP(100),TMUXP(100)
      COMMON/COMINP/C,S,Y,THETA
      COMMON/COMOUT/N,A,XX,TSO,TSX,TMUOSQ,TMUXSQ,TMUOP,TMUXP,TR
      READ(5,8) NTHETA
    8 FORMAT(I3)
      DO 300 I=1,NTHETA
      READ(5,9) THETA
    9 FORMAT(F7.2)
      THETAR = THETA*1.745329E-2
      C = COS(THETAR)
      S = SIN(THETAR)
C**** COMPUTE Y AND A = (1-Y**2)/(1-YL**2), Y = 0(0.1)5
C**** N = TOTAL NO. OF POINTS AROUND X = 1-Y,1,A,AND 1+Y FOR EACH Y
      DO 250 J=1,51
      N =0
      TJ = J
      Y = (TJ-1.0)*0.1
      A = (1.0-Y**2)/(1.0-(Y*C)**2)
C**** CONVERT A TO 2 DECIMAL PLACES
      NA = A*100.0
      TA = NA
      A = TA*0.01
      IF(Y.GT.0.9) GO TO 14
      X1=1.0-Y
      X2=1.0
      X3 = 1.0+Y
      GO TO 15
   14 X1 = 1.0
      X2 = 1.0+Y
   15 IF(Y.GT.1.0) GO TO 16
C**** NX = NO. OF X VALUES USE  FOR COMPUTATION , (X=0(0.1)2+Y IF Y LESS
C       THAN OR EQUAL TO 1, X=0(0.1)10 IF Y GREATER THAN 1)
```

```
      NX = (2.0 + Y)*10.0 + 1.0
      GO TO 17
   16 NX = 101
   17 WRITE(6,18)
   18 FORMAT(1H1,40X,47HCOMPUTATION OF GROUP AND PHASE REFRACTIVE INDEX)
      WRITE(6,19) THETA,Y
   19 FORMAT(1H0,9X,6HTHETA=,F4.1,2X,2HY=,F3.1)
      WRITE(6,21)
   21 FORMAT(1H0,11X,1HX,12X,1HR,11X,5HMUOSQ,11X,2HSO,12X,7HMUOPRIM,7X,
     *5HMUXSQ,11X,2HSX,12X,7HMUXPRIM//)
C**** COMPUTE REFRACTIVE INDEXES FOR VARIOUS X
      DO 100 K=1,NX
      TK = K
      GX   = (TK-1.0)*0.1
      GR   = SQRT((Y*S*S)**2 + (2.0*C*(1.0- GX ))**2)
      CALL ORD(GX,Y,GR,GSO,GMUOSQ,GMUOP)
      CALL EXORD(GX,Y,GR,GSX,GMUXSQ,GMUXP)
      X(K) = GX
      R(K) = GR
      SO(K) = GSO
      SX(K) = GSX
      RMUOSQ(K) = GMUOSQ
      RMUXSQ(K) = GMUXSQ
      RMUOP(K) = GMUOP
      RMUXP(K) = GMUXP
  100 CONTINUE
C**** COMPUTE REFRACTIVE INDEXES AROUND X= 1,1-Y,1+Y,(1-Y**2)/(1-YL**2)
      CALL INTERM(X1)
      CALL INTERM(X2)
      CALL INTERA(A)
      IF(Y.GT.0.9) GO TO 20
      CALL INTERM(X3)
C**** REARRANGE SET XX(K) AND THEIR ASSOCIATE VARIABLES INTO ASCENDING
C**** ORDER
   20 NM1 = N-1
      DO 30 K=1,NM1
      KP1 =K+1
      DO 30 L=KP1,N
      IF(XX(K)-XX(L)) 30,30,25
   25 TEMP1= XX(K)
      TEMP2= TSO(K)
      TEMP3= TSX(K)
      TEMP4= TMUOSQ(K)
      TEMP5= TMUXSQ(K)
      TEMP6= TMUOP(K)
```

```
      TEMP7= TMUXP(K)
      TEMP8= TR(K)
      TR(K)=TR(L)
      XX(K)= XX(L)
      TSO(K)= TSO(L)
      TSX(K)= TSX(L)
      TMUOSQ(K)= TMUOSQ(L)
      TMUXSQ(K)= TMUXSQ(L)
      TMUOP(K) = TMUOP(L)
      TMUXP(K) = TMUXP(L)
      XX(L) = TEMP1
      TSO(L)= TEMP2
      TSX(L)= TEMP3
      TMUOSQ(L)= TEMP4
      TMUXSQ(L)= TEMP5
      TMUOP(L) = TEMP6
      TMUXP(L) = TEMP7
      TR(L)= TEMP8
   30 CONTINUE
      M =1
      DO 200 K=1,NX
   32 IF(M.GT.N) GO TO 44
      IF(XX(M).GT.X(K)) GO TO 44
      IF(X(K)-XX(M).GT.0.009) GO TO 35
      M= M+1
      GO TO 44
   35 IF(ABS(XX(M)-XX(M+1)).GT.0.009) GO TO 40
      M =M+1
      GO TO 35
   40 WRITE(6,45)       XX(M),TR(M),TMUOSQ(M),TSO(M),TMUOP(M),TMUXSQ(M),
     *           TSX(M),TMUXP(M)
      M=M+1
      GO TO 32
   44 WRITE(6,45)       X(K),R(K),RMUOSQ(K),SO(K),RMUOP(K),RMUXSQ(K),
     *                SX(K),RMUXP(K)
   45 FORMAT(1H ,F14.2,4X,E12.5,F12.5,4X,E12.5,F16.5,F12.5,4X,E12.5,
     *F16.5)
  200 CONTINUE
  250 CONTINUE
  300 CONTINUE
      STOP
      END
```

```
C  SUBROUTINE TO COMPUTE REFRACTIVE INDEX FOR X AROUND 1-Y,1,1+Y
C
      SUBROUTINE INTERM(X1)
      DIMENSION TR(100),XX(100),TSO(100),TSX(100),TMUOSQ(100),
     *          TMUXSQ(100),TMUOP(100),TMUXP(100)
      COMMON/COMINP/C,S,Y,THETA
      COMMON/COMOUT/N,A,XX,TSO,TSX,TMUOSQ,TMUXSQ,TMUOP,TMUXP,TR
      IF(X1.LE.0.0) RETURN
C*** X VARIES IN STEP OF 0.01
      DO 10 L=2,10
      TL=L
      X=(TL-1.0)*0.01 + (X1-0.1)
      IF(X.LT.0.0) RETURN
      R= SQRT((Y*S*S)**2 + (2.0*C*(1.0-X))**2)
      CALL ORD(X,Y,R,SO,RMUOSQ,RMUOP)
      CALL EXORD(X,Y,R,SX,RMUXSQ,RMUXP)
      N =N+1
      TR(N) = R
      XX(N) = X
      TSO(N)= SO
      TSX(N)= SX
      TMUOSQ(N) = RMUOSQ
      TMUXSQ(N) = RMUXSQ
      TMUOP(N)  = RMUOP
      TMUXP(N)  = RMUXP
   10 CONTINUE
      RETURN
      END



C  SUBROUTINE TO COMPUTE REFRACTIVE INDEX FOR X AROUND (1-Y**2)/(1-YL**2
C
      SUBROUTINE INTERA(X1)
      DIMENSION TR(100),XX(100),TSO(100),TSX(100),TMUOSQ(100),
     *          TMUXSQ(100),TMUOP(100),TMUXP(100)
      COMMON/COMINP/C,S,Y,THETA
      COMMON/COMOUT/N,A,XX,TSO,TSX,TMUOSQ,TMUXSQ,TMUOP,TMUXP,TR
      IF(X1.LT.0.0) RETURN
C*** X VARIES IN STEP OF 0.01
      DO 10 L=2,10
      TL=L
      X=(TL-1.0)*0.01 + X1
      R= SQRT((Y*S*S)**2 + (2.0*C*(1.0-X))**2)
      CALL ORD(X,Y,R,SO,RMUOSQ,RMUOP)
```

```
      CALL EXORD(X,Y,R,SX,RMUXSQ,RMUXP)
      N =N+1
      TR(N) = R
      XX(N) = X
      TSO(N)= SO
      TSX(N)= SX
      TMUOSQ(N) = RMUOSQ
      TMUXSQ(N) = RMUXSQ
      TMUOP(N)  = RMUOP
      TMUXP(N)  = RMUXP
   10 CONTINUE
      RETURN
      END



C  SUBROUTINE TO COMPUTE THE ORDINARY WAVE GROUP AND PHASE REFRACTIVE
C  INDEX (MUOPRI AND MUO)
C
C  X = (FN/F)SQ
C  Y = FH/F
C  THETA = ANGLE THETA IN DEGREES
C  MUO = PHASE REFRACTIVE INDEX
C  MUOPRI = GROUP REFRACTIVE INDEX
C
      SUBROUTINE ORD(X,Y,R,SO,MUOSQ,MUOPRI)
      REAL MUO1,MUO2,MUOSQ,MUO,MUOPP1,MUOPP2,MUOPRI
      COMMON/COMINP/C,S,Y,THETA
      IF(THETA.EQ.0.0.AND.X.GE.0.99999.AND.X.LE.1.00001) GO TO 39
      SO1=Y*(1.0+C*C*(1.0-2.0*X))+R
      SO2=Y*S**2 + R
      SO = SO1/SO2
      MUO1= Y*(1.0+C**2) + R
      MUO2= SO1
      MUOSQ = (1.0-X)*(MUO1/MUO2)
      IF(MUOSQ.LE.0.0.OR.ABS(MUOSQ).LT.1.0E-5) GO TO 40
      MUO = SQRT(MUOSQ)
      MUOPP1= (1.0-X)-((Y*S*S)*(1.0+X))/R
      MUOPP2= (Y*C*C*X)/(SO**2*(Y*S**2+R))
      MUOPRI= (1.0-MUOPP2*MUOPP1)/MUO
      RETURN
   39 SO = 1.0
   40 MUOSQ = 0.0
      MUOPRI=10000.0
      RETURN
```

```
C   SUBROUTINE TO COMPUTE THE EXTRAORDINARY WAVE GROUP AND PHASE
C   REFRACTIVE INDEX(MUXPRI AND MUX)
C
C   X = (FN/F)SQ
C   Y = FH/F
C   THETA =  ANGLE THETA IN DEGREES
C   MUX    =   PHASE REFRACTIVE INDEX
C   MUXPRI=  GROUP REFRACTIVE INDEX
C
      SUBROUTINE EXORD(X,Y,R,SX,MUXSQ,MUXPRI)
      REAL MUX1,MUX2,MUX3,MUX4,MUX24,MUXSQ,MUX,MUXPP1,MUXPP2,MUXPRI
      COMMON/COMINP/C,S,Y,THETA
      IF(THETA.EQ.0.0) GO TO 60
      IF(ABS(1.0-Y).GE.0.01) GO TO 10
      IF(X.LT.0.01) GO TO 15
   10 IF(ABS(1.0-X).GT.0.001) GO TO 20
      IF(Y.EQ.0.0) GO TO 75
      SX = 10000.0
      MUXSQ = 1.0
      MUXPRI = 1.0 + 1.0/((Y*S)**2)
      RETURN
   20 SX1 = (1.0-X)+Y**2*(X*C**2-1.0)
      SX2 = 2.0*(1.0-X)-(Y*S)**2+Y*R
      SX = 2.0*(SX1/SX2)
   25 MUX1= 1.0+Y-X
      MUX2= SX1
      MUX3= (1.0-X)*SX2
      MUX4= 2.0*(1.0-X)**2-(Y*S)**2+Y*R
      MUX24 = MUX2*MUX4
      MUXSQ =(1.0-X-Y)*((MUX1*MUX3)/MUX24)
      IF(MUXSQ.LE.0.0.OR.ABS(MUXSQ).LT.1.0E-5) GO TO 50
      MUX = SQRT(MUXSQ)
      MUXPP1 = (X*(1.0-SX))/(2.0*SX**2)
      MUXPP2 = 1.0+((Y*S**2)/R)*((1.0+X)/(1.0-X))
      MUXPRI = (1.0+MUXPP1*MUXPP2)/MUX
      RETURN
   60 IF(ABS(1.0-Y).GE.0.01) GO TO 65
      IF(X.LT.1.0) GO TO 49
      IF(ABS(1.0-X).LT.0.001) GO TO 15
      SX = 2.0
      MUXSQ = 1.0 - X/(1.0+Y)
```

```
      IF(MUXSQ.LE.0.0.OR.ABS(MUXSQ).LT.1.0E-5) GO TO 50
      MUXPRI = (1.0 - (X*Y)/(2.0*(1.0+Y)**2))/SQRT(MUXSQ)
      RETURN
   65 IF(Y.LT.1.0) GO TO 70
      IF(ABS(1.0-X).GT.0.001) GO TO 20
      SX = 10000.
      MUXSQ = 1.0
      MUXPRI = 10000.0
      RETURN
   70 IF(ABS(1.0-X).GT.0.001) GO TO 20
      IF(Y.EQ.0.0) GO TO 75
      GO TO 15
   75 SX = 1.0
      GO TO 50
   15 SX =0.0
      MUXSQ = 10000.0
      MUXPRI= 10000.0
      RETURN
   49 SX =0.0
   50 MUXSQ = 0.0
      MUXPRI= 10000.0
      RETURN
      END
```

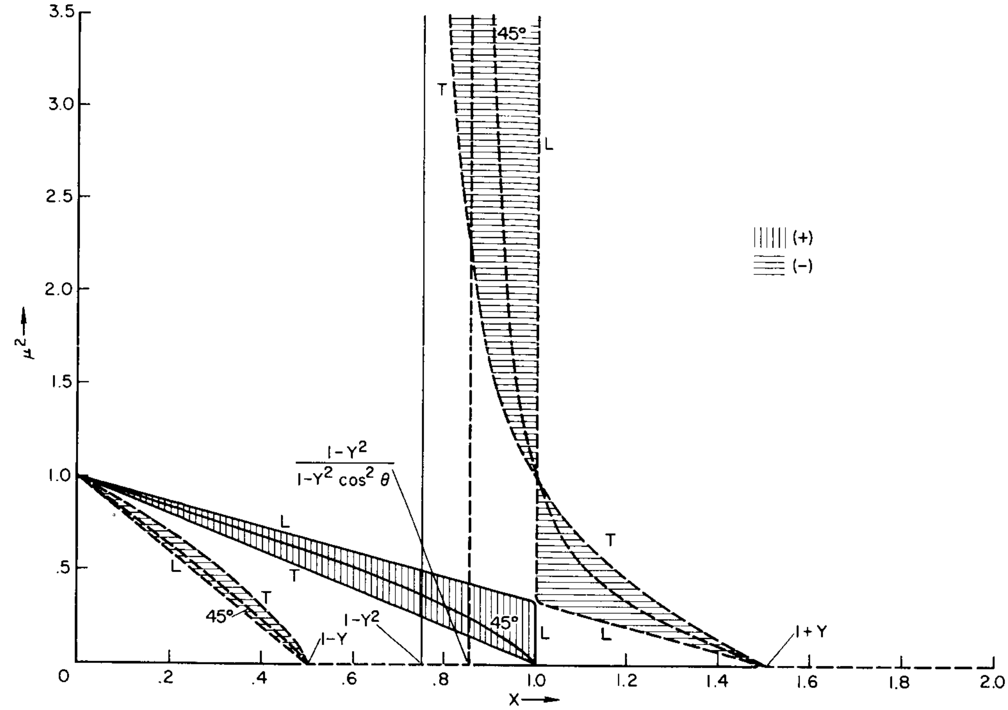

(a) Y = 1/2

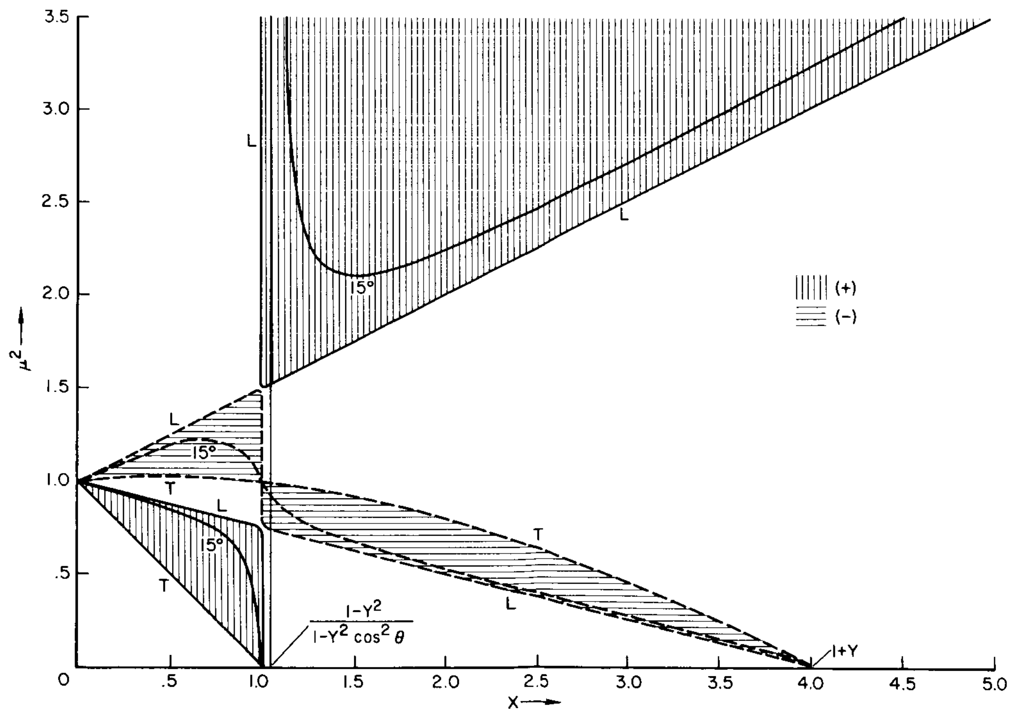

(b) Y = 3

Figure 1.- Variation of μ^2 with X.

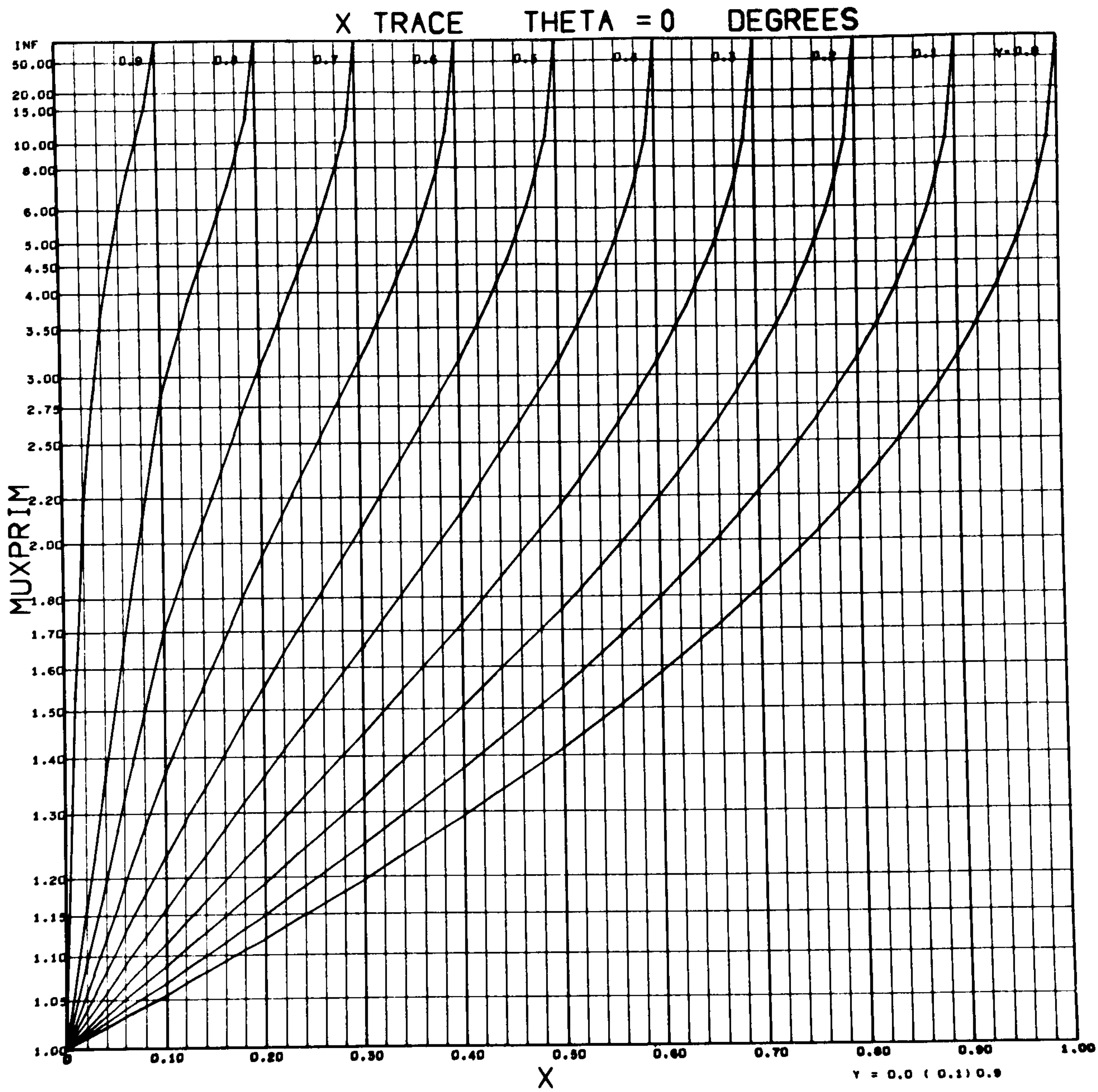

Figure 2.- Variation of μ' vs. X; Y = 0 - 0.9; $\theta = 0^{\circ}$.

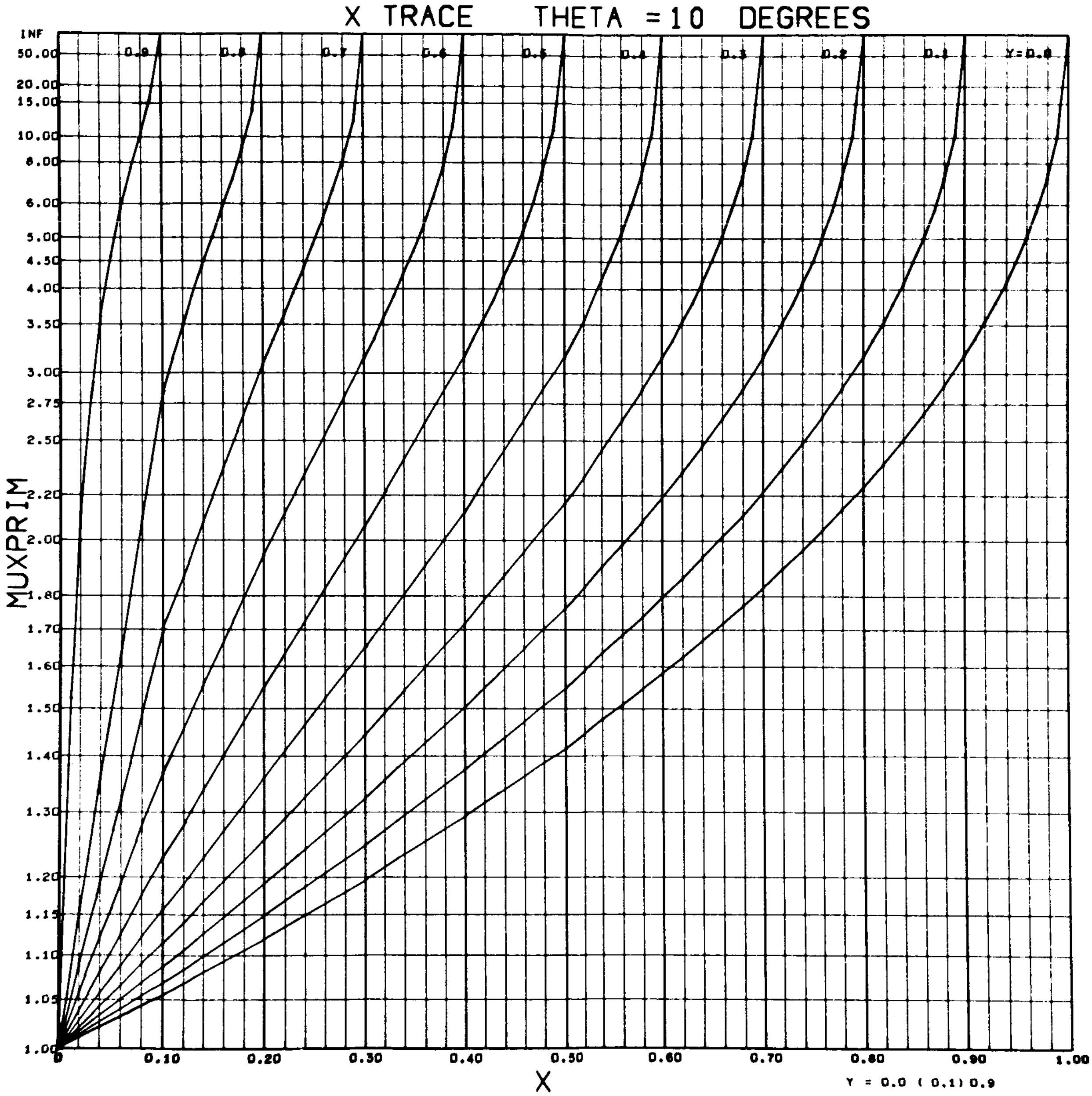

Figure 3.- Variation of μ' vs. X; Y = 0 - 0.9; $\theta = 10^{\circ}$.

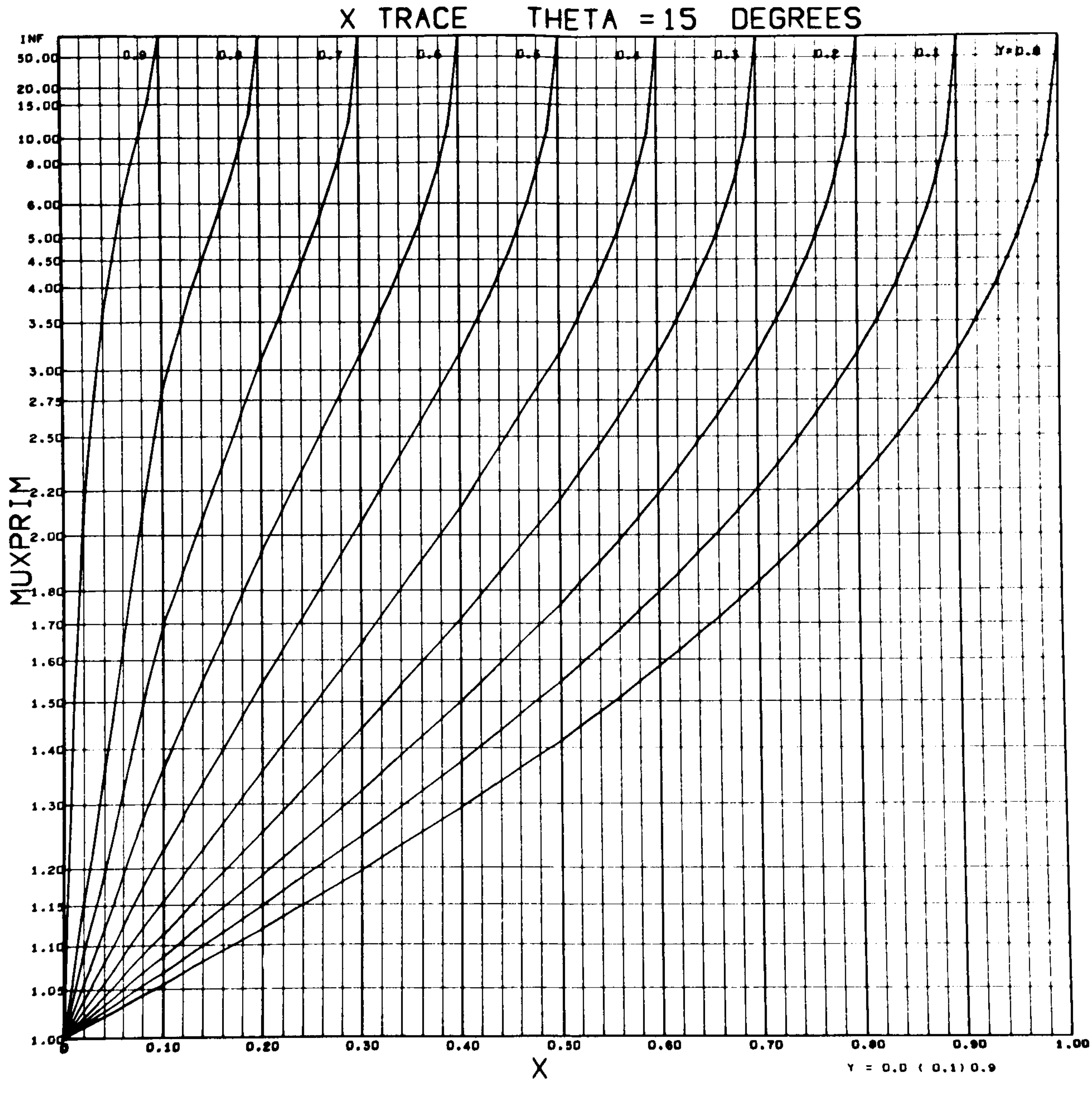

Figure 4.- Variation of μ' vs. X; Y = 0 - 0.9; $\theta = 15^{\circ}$.

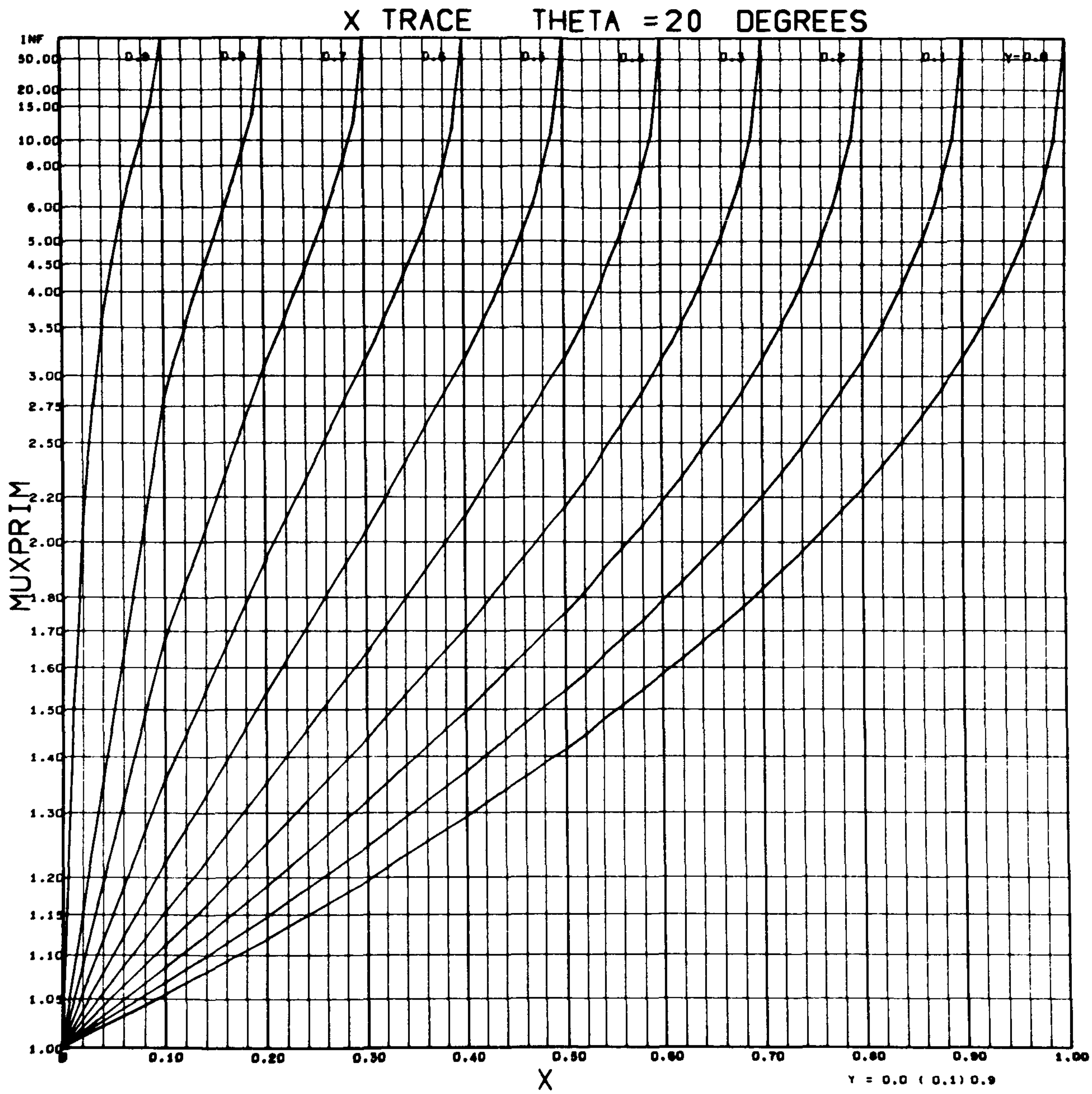

Figure 5.- Variation of μ' vs. X; Y = 0 - 0.9; $\theta = 20^{\circ}$.

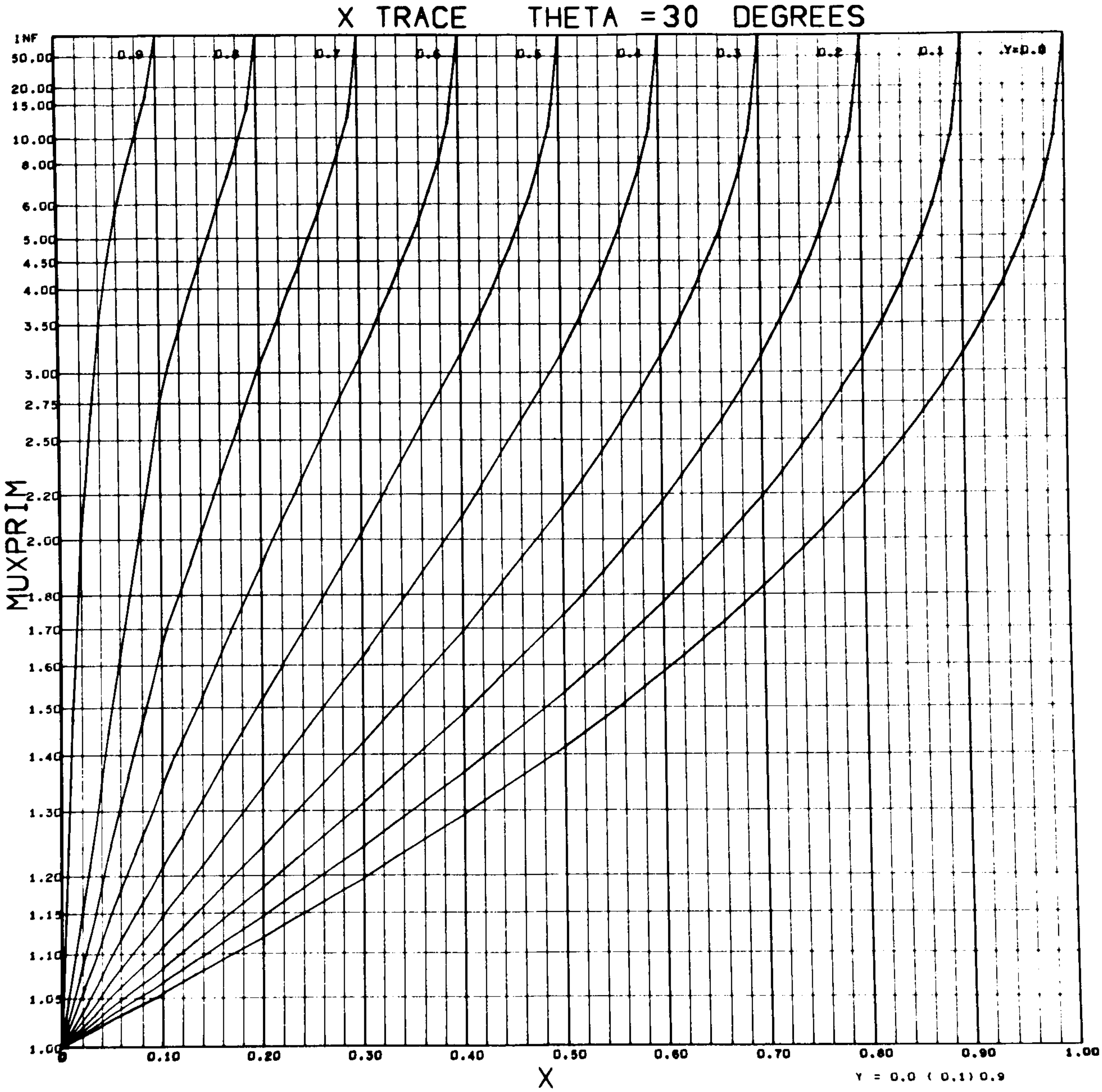

Figure 6.- Variation of μ' vs. X; Y = 0 - 0.9; θ = 30°.

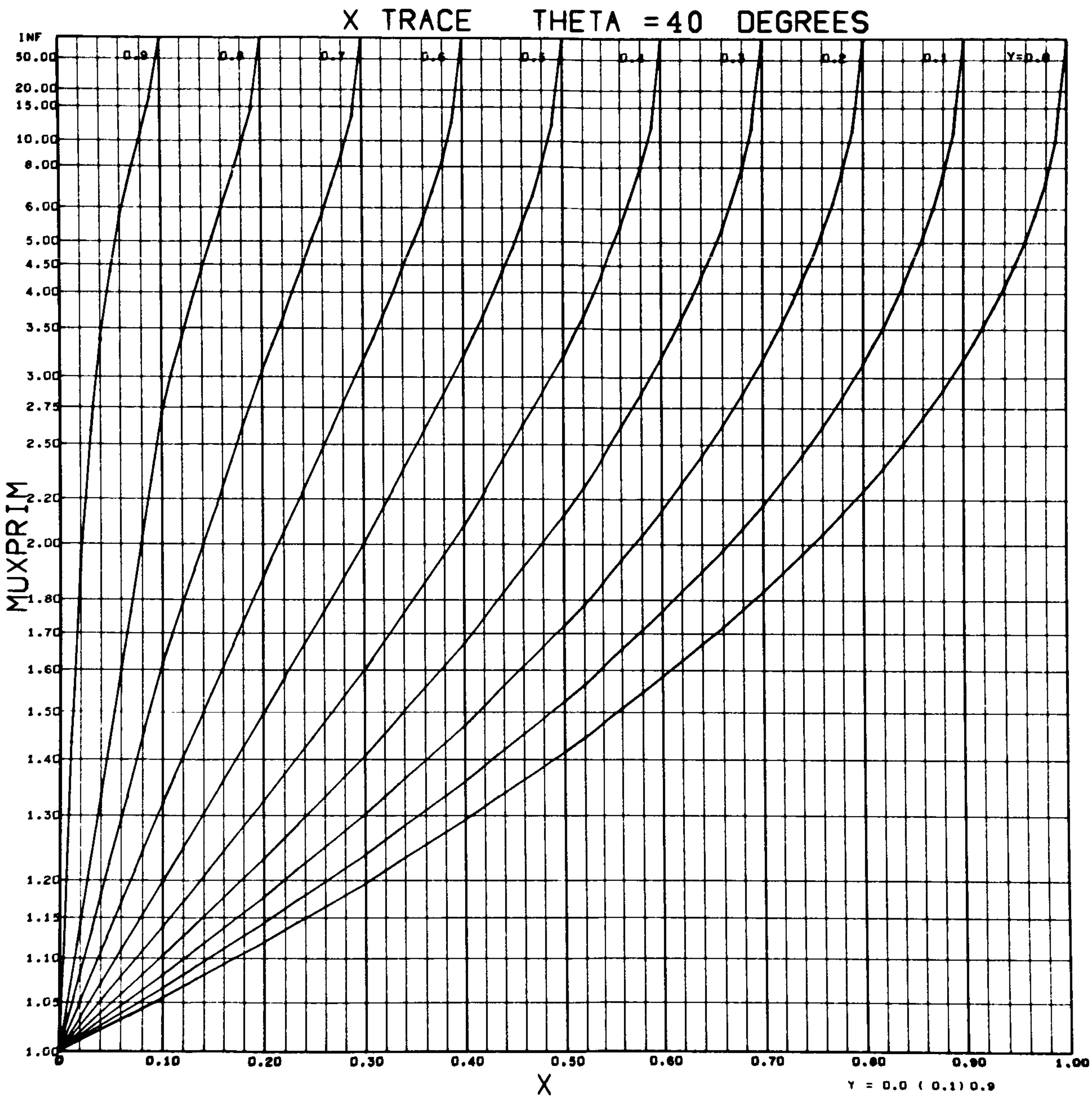

Figure 7.- Variation of μ' vs. X; Y = 0 - 0.9; $\theta = 40^{\circ}$.

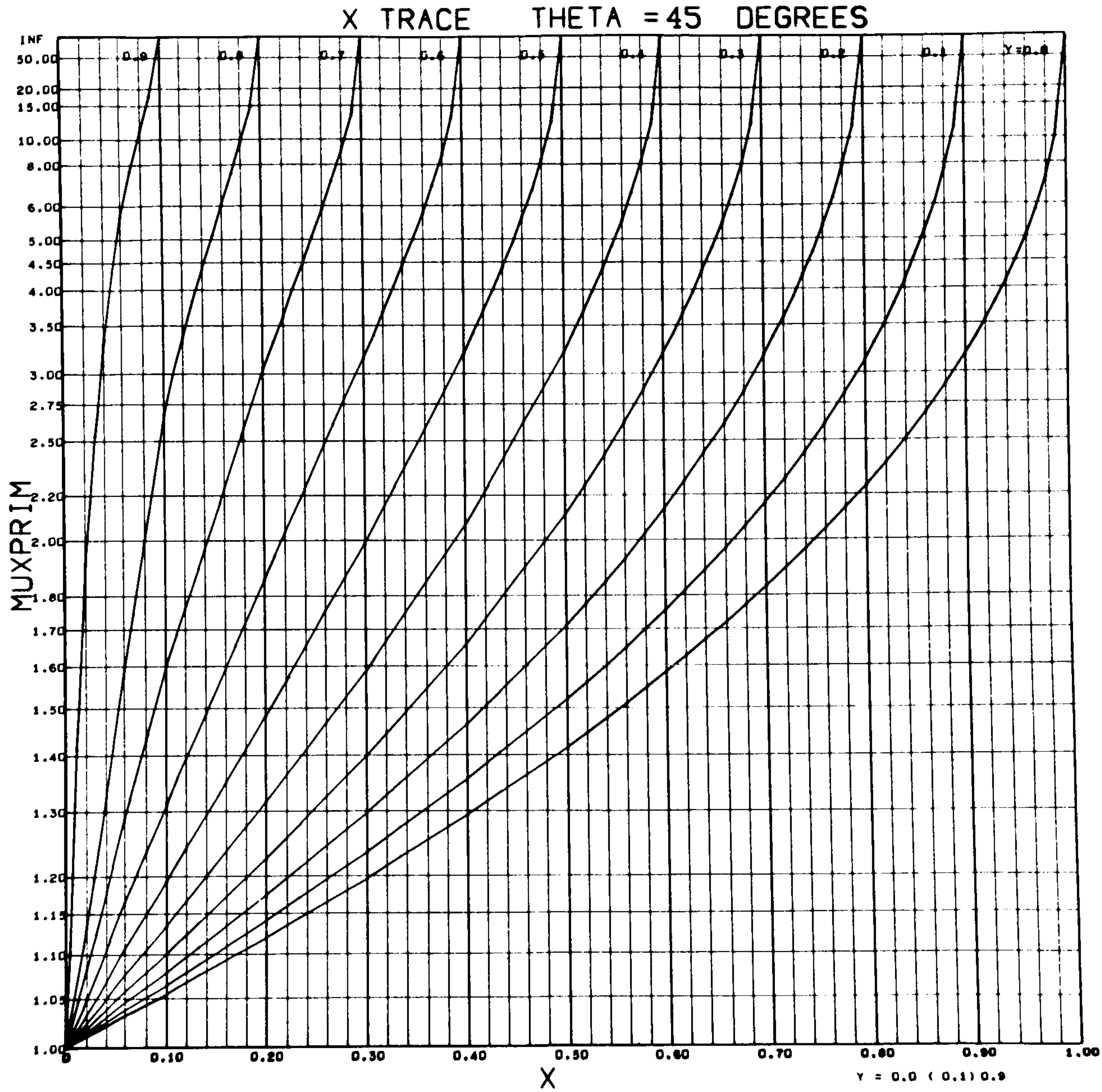

Figure 8.- Variation of μ' vs. X; Y = 0 - 0.9; $\theta = 45^{\circ}$.

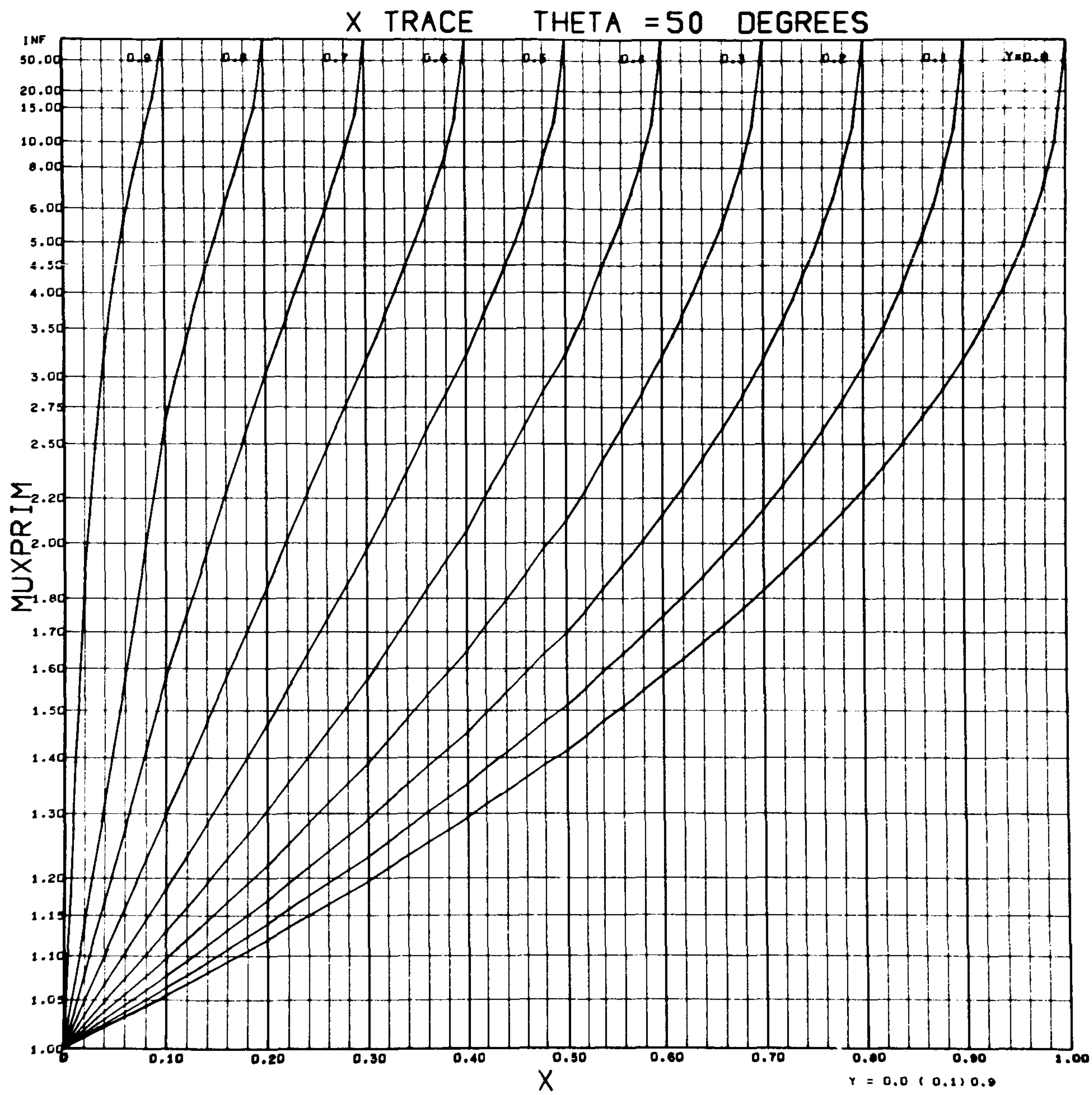

Figure 9.- Variation of μ' vs. X; Y = 0 - 0.9; $\theta = 50^{\circ}$.

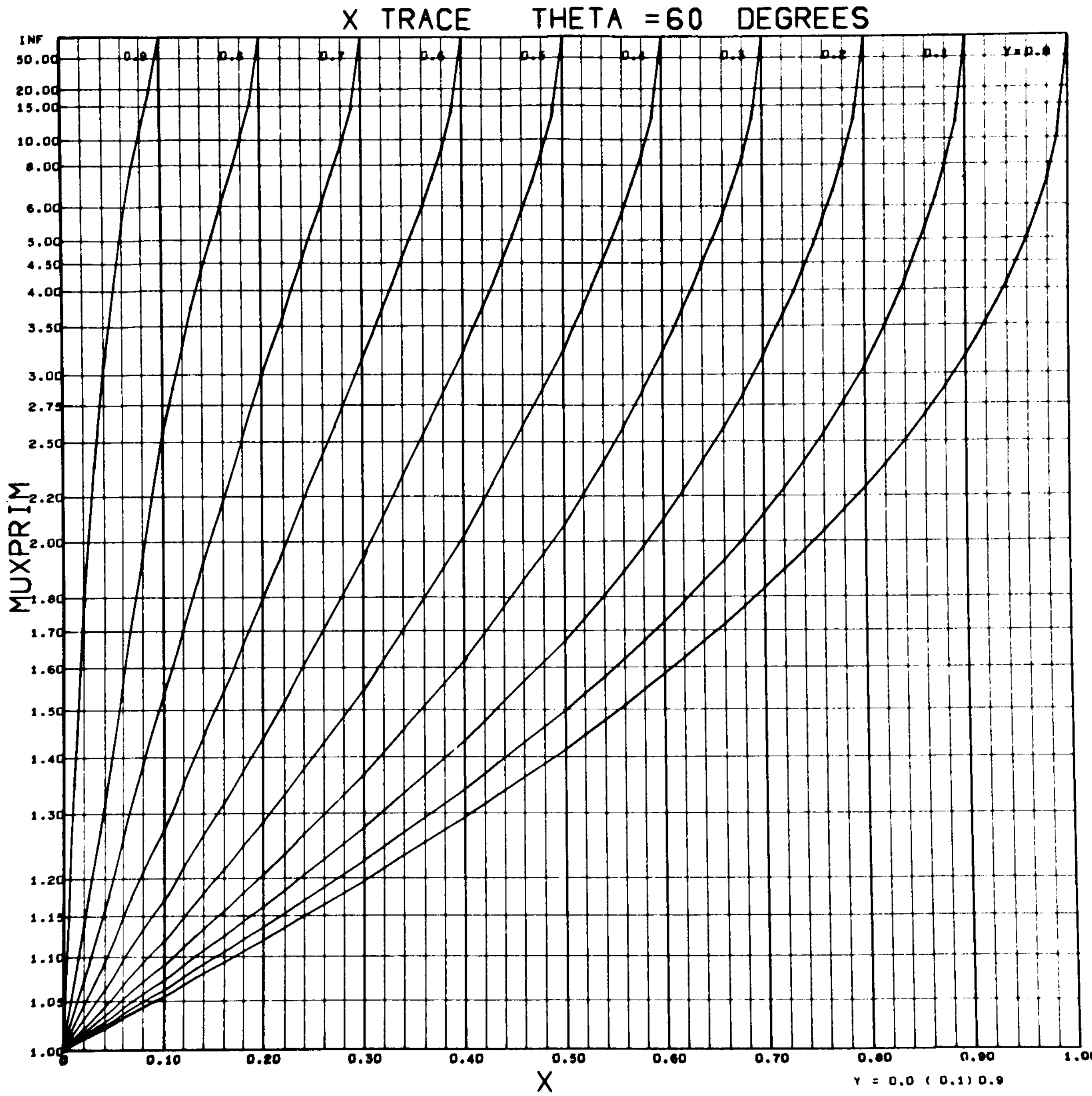

Figure 10.- Variation of μ' vs. X; Y = 0 - 0.9; θ = 60°.

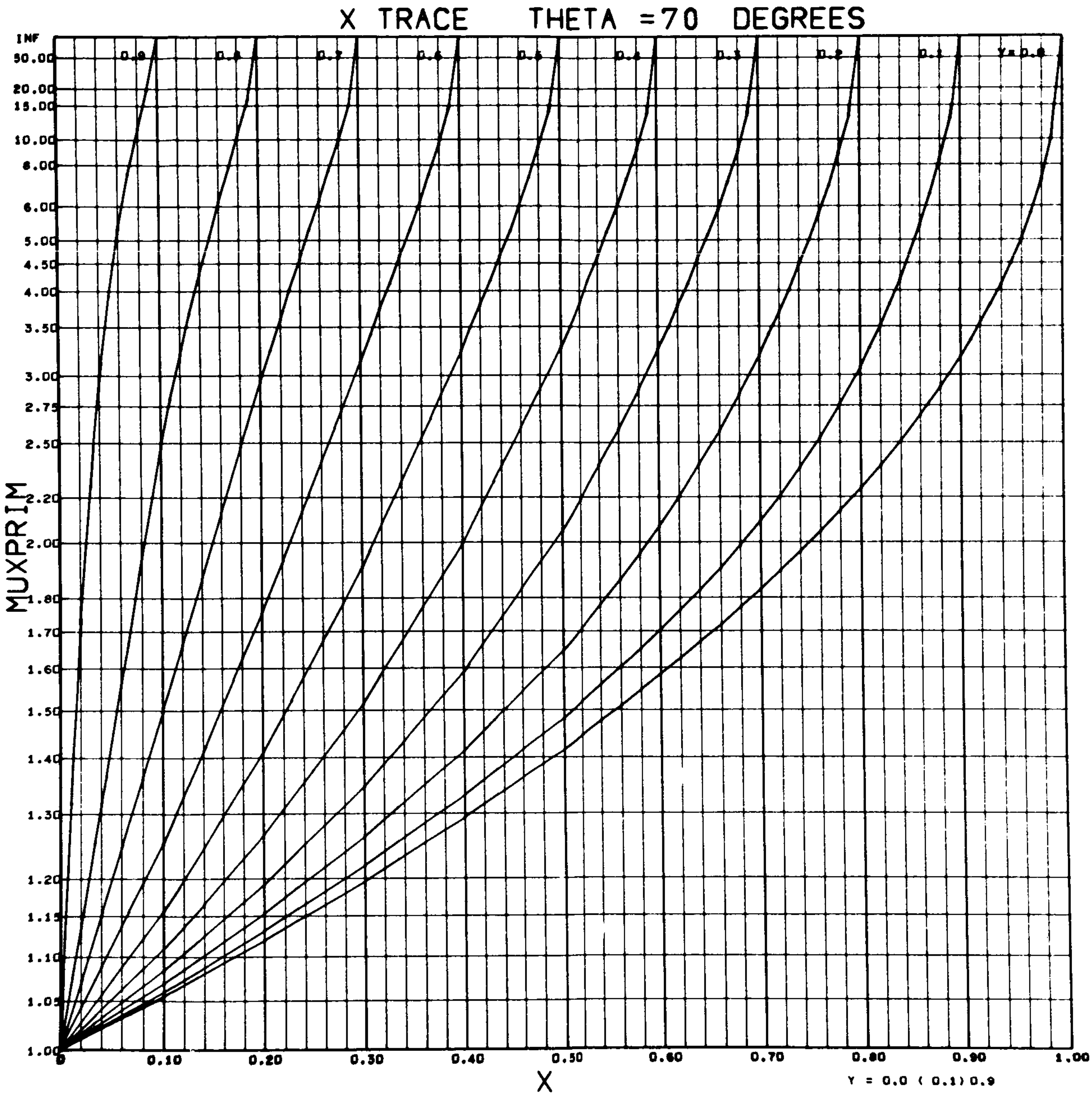

Figure 11.- Variation of μ' vs. X; Y = 0 - 0.9; θ = 70°.

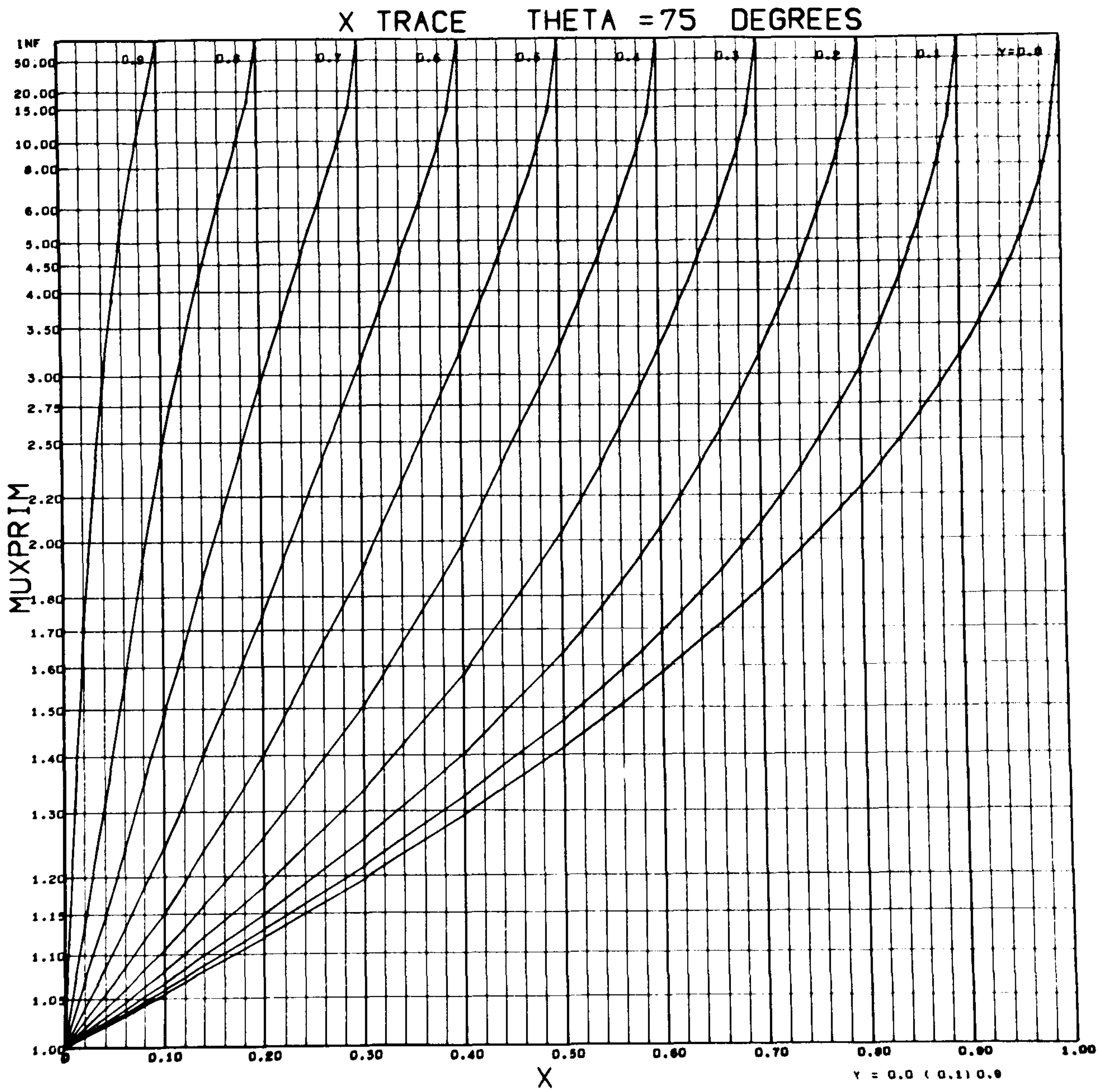

Figure 12.- Variation of μ' vs. X; Y = 0 - 0.9; θ = 75°.

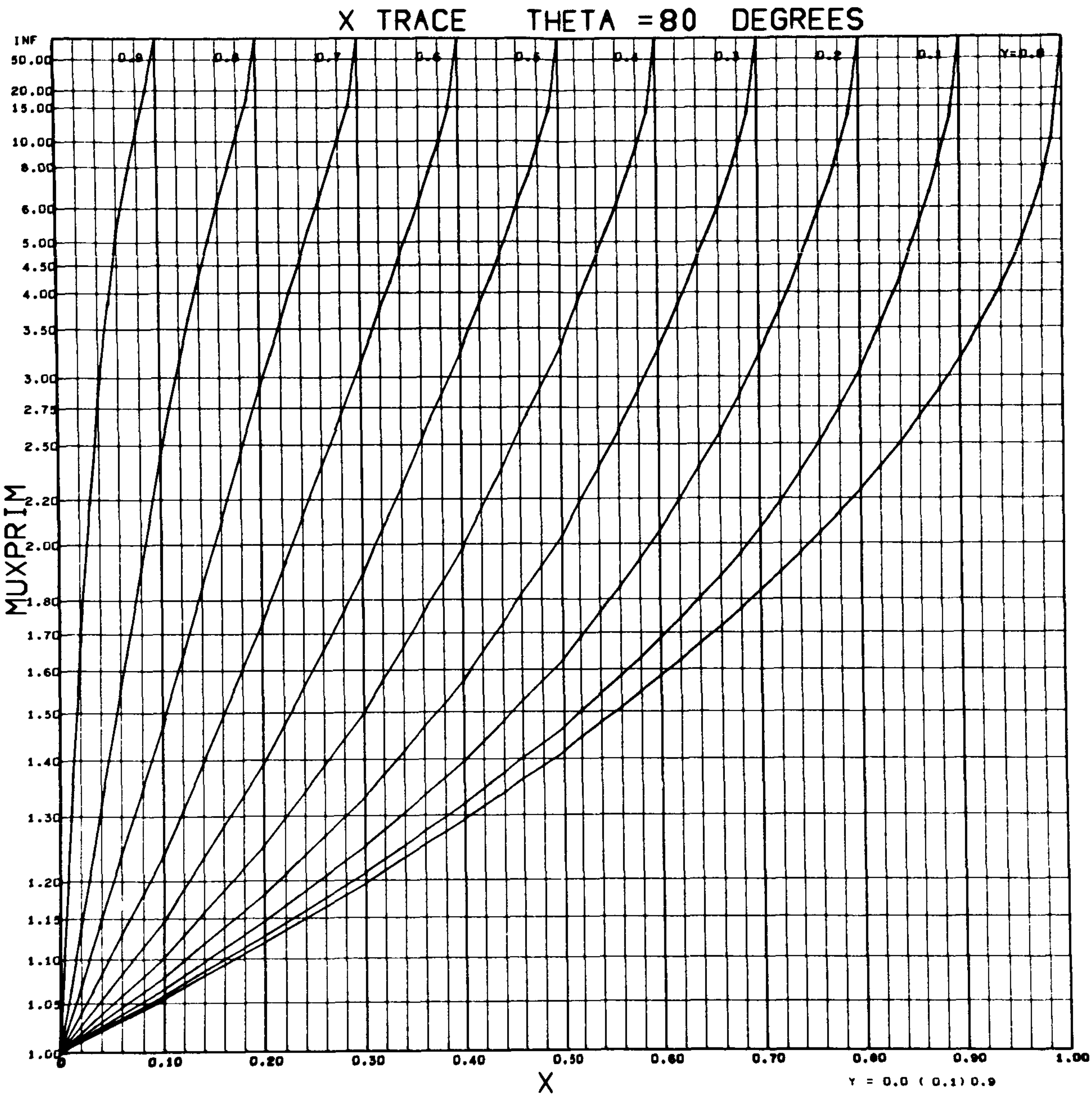

Figure 13.- Variation of μ' vs. X; Y = 0 - 0.9; $\theta = 80^{\circ}$.

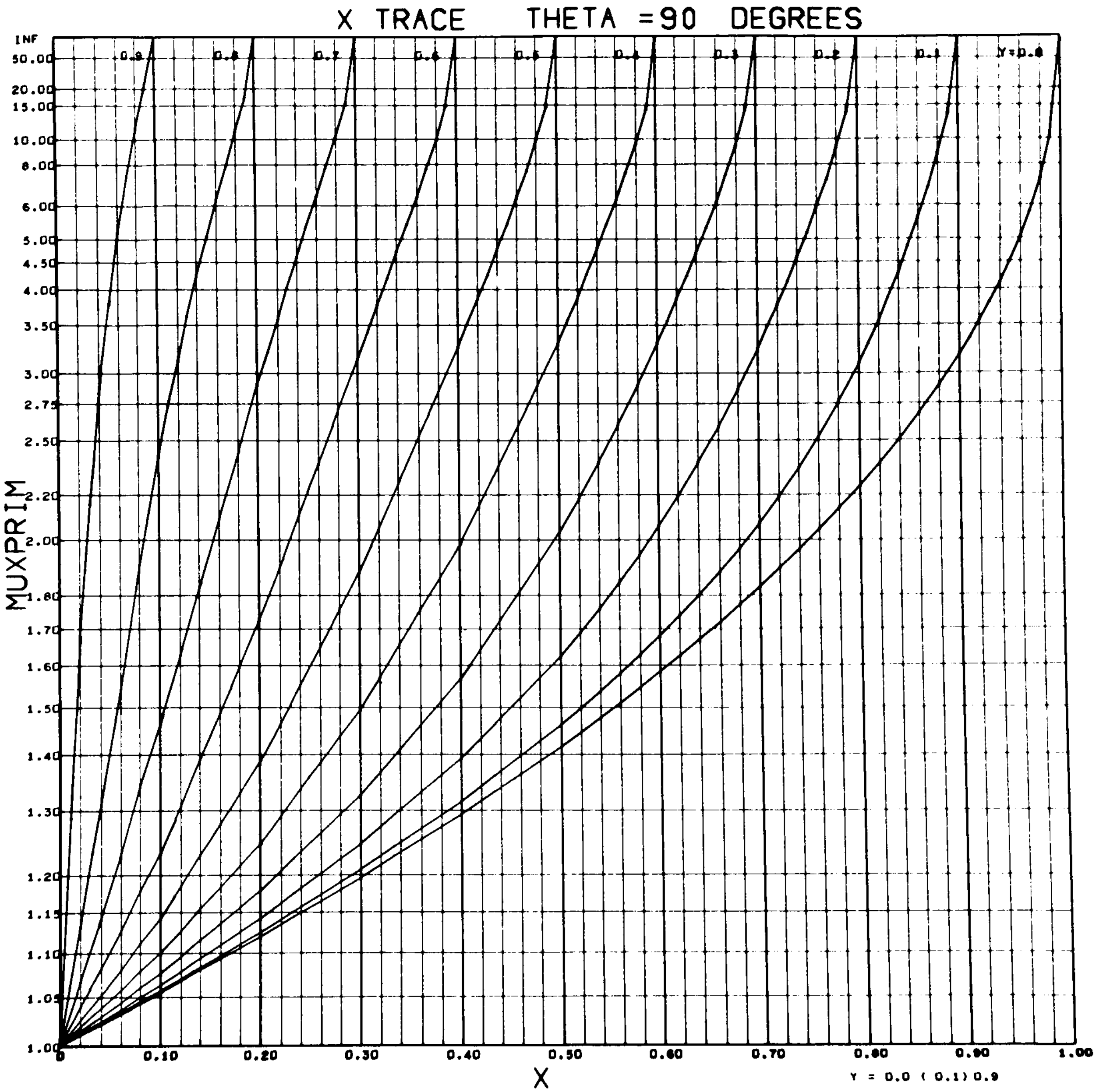

Figure 14.- Variation of μ' vs. X; Y = 0 - 0.9; $\theta = 90^\circ$.

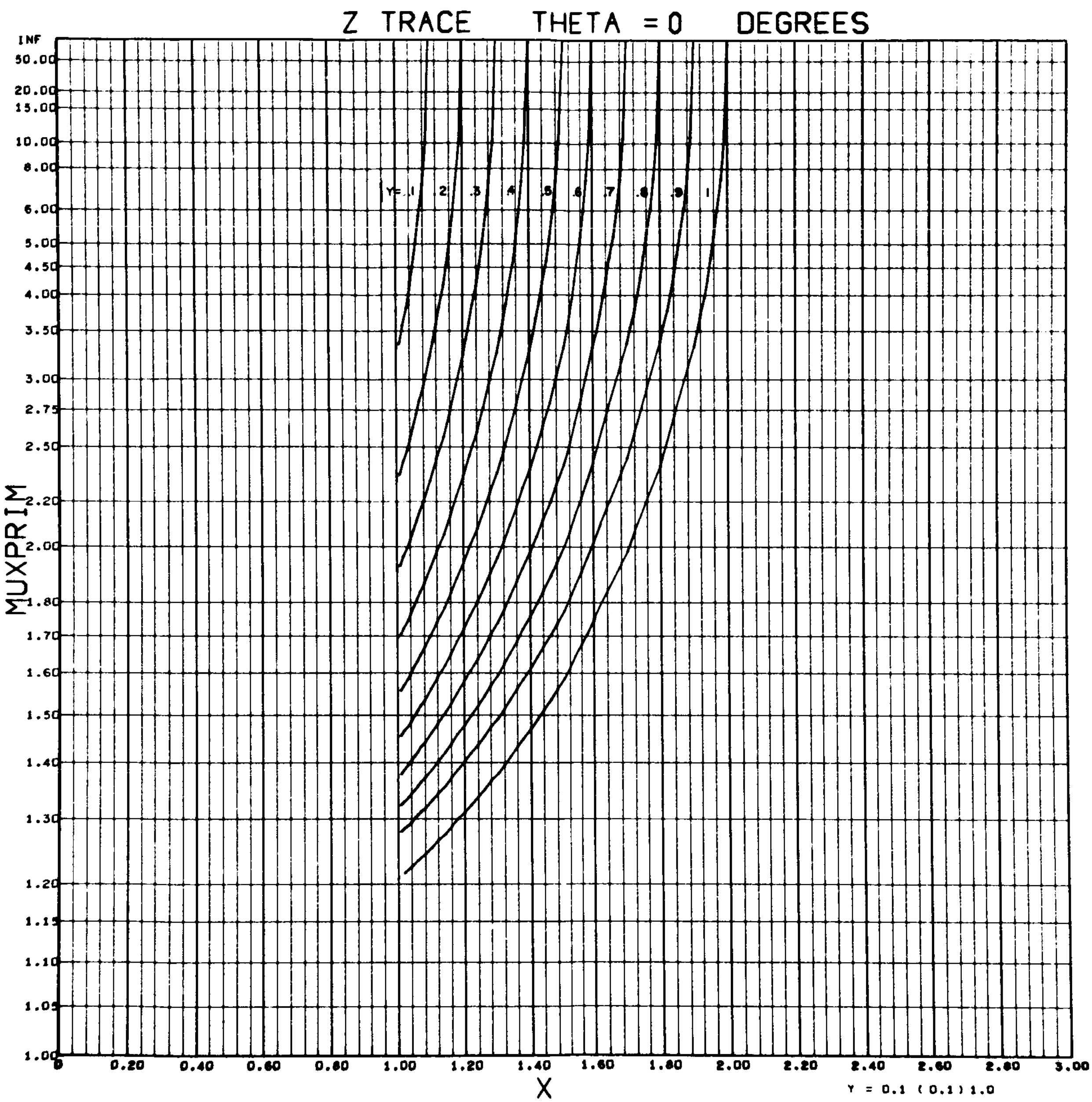

Figure 15.- Variation of μ' vs. X; Y = 0.1 - 1.0; $\theta = 0^{\circ}$.

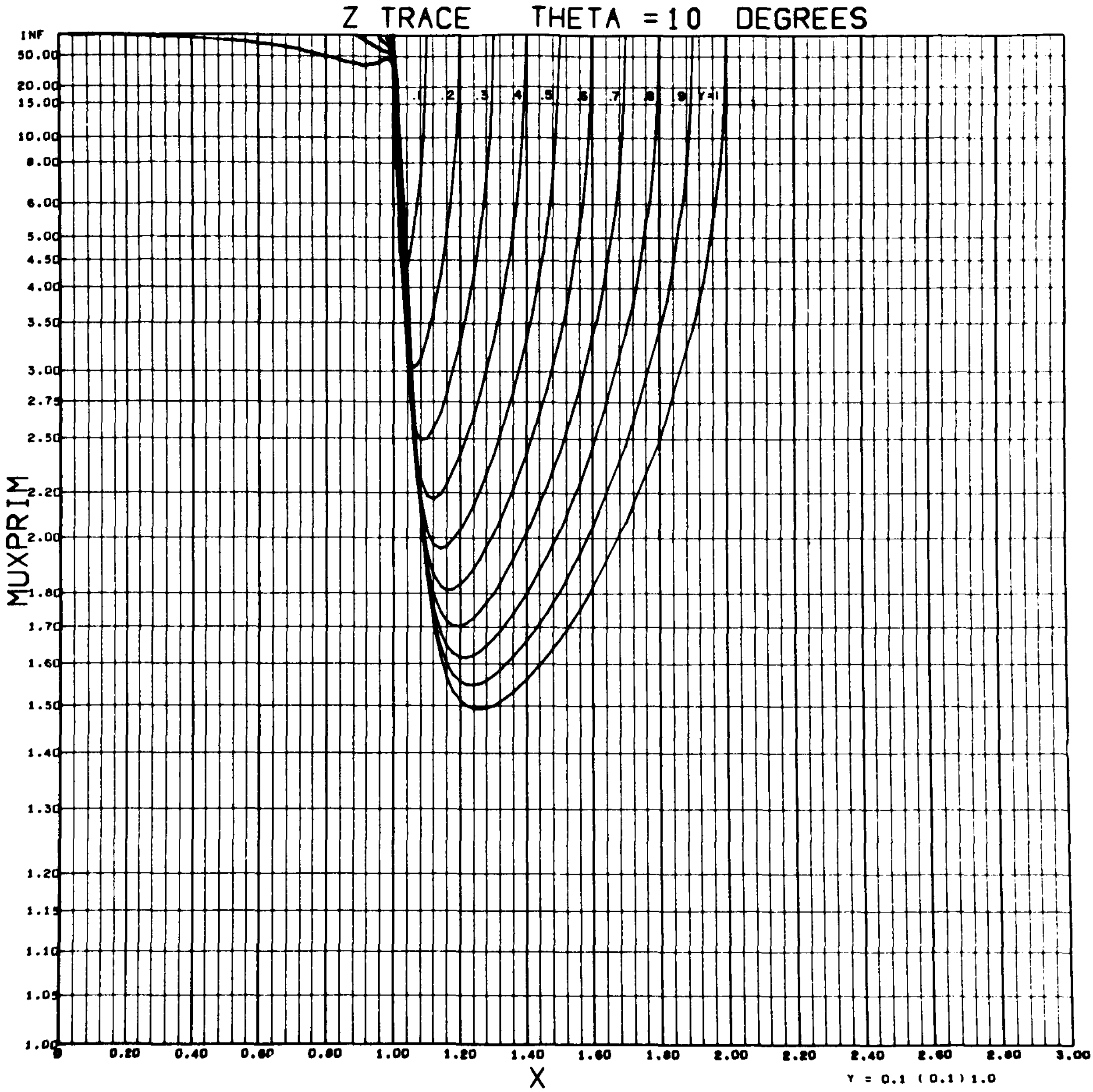

Figure 16.- Variation of μ' vs. X; Y = 0.1 - 1.0; $\theta = 10^{\circ}$.

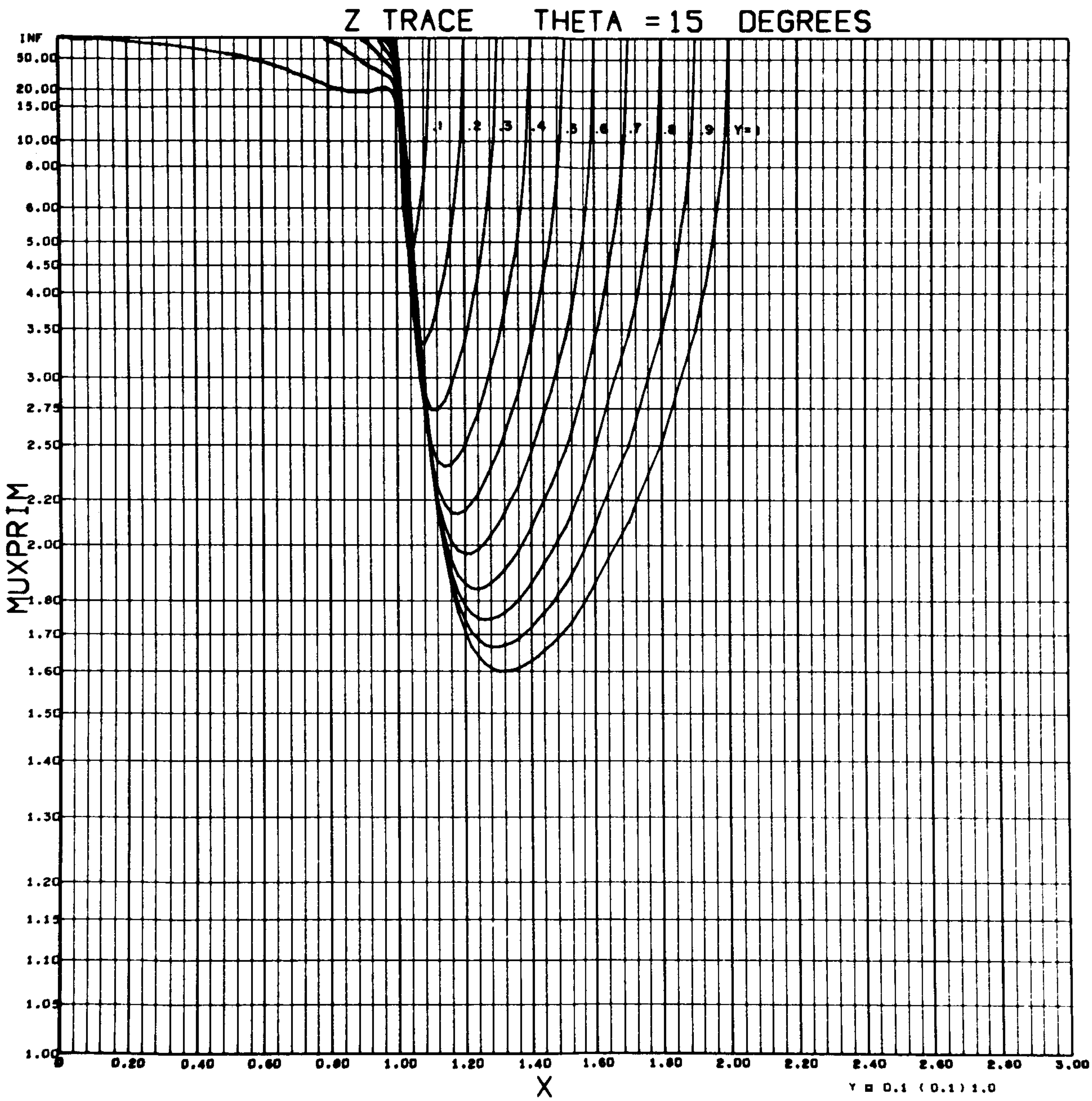

Figure 17.- Variation of μ' vs. X; Y = 0.1 - 1.0; $\theta = 15^{\circ}$.

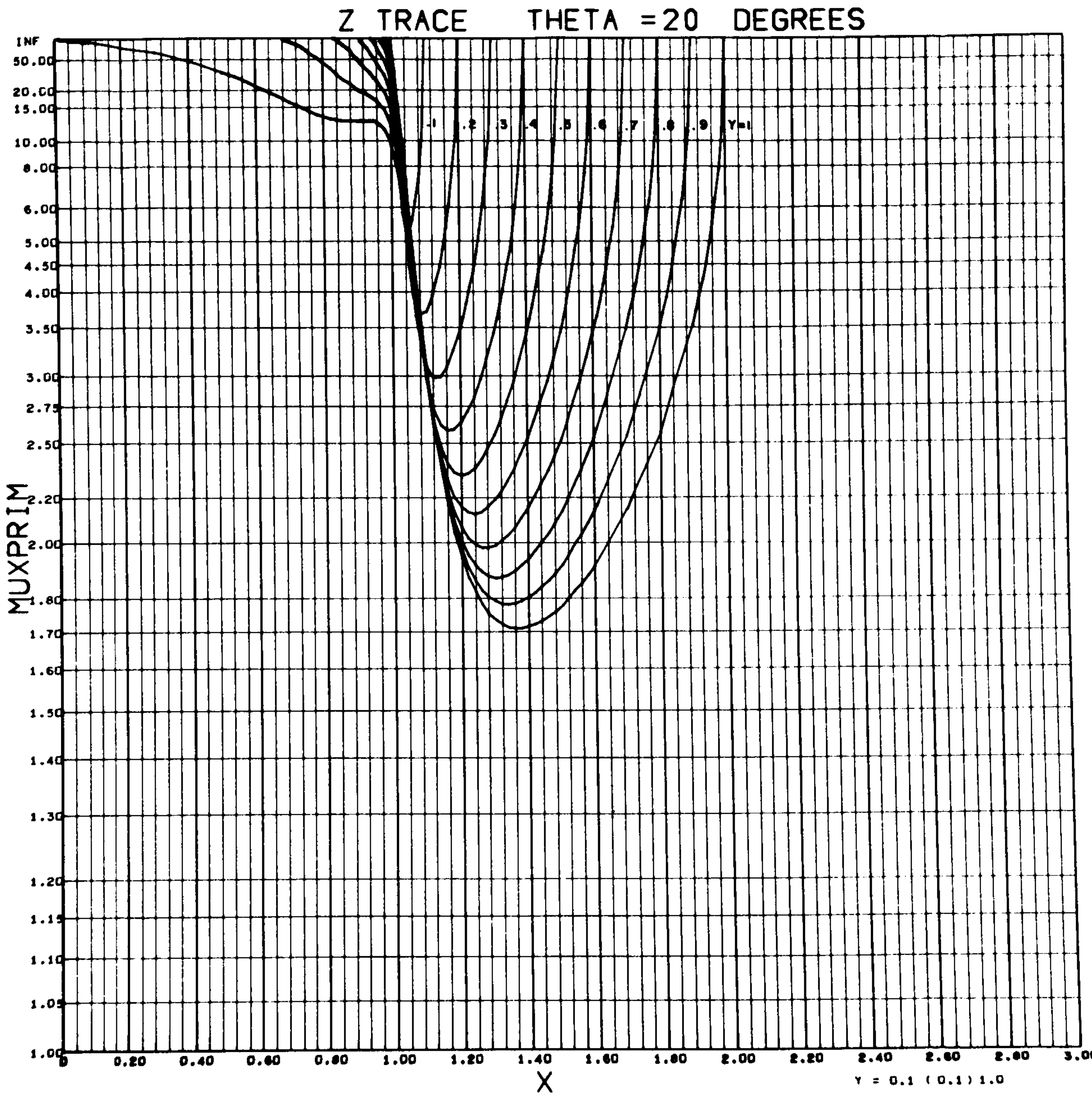

Figure 18.- Variation of μ' vs. X; Y = 0.1 - 1.0; $\theta = 20^{\circ}$.

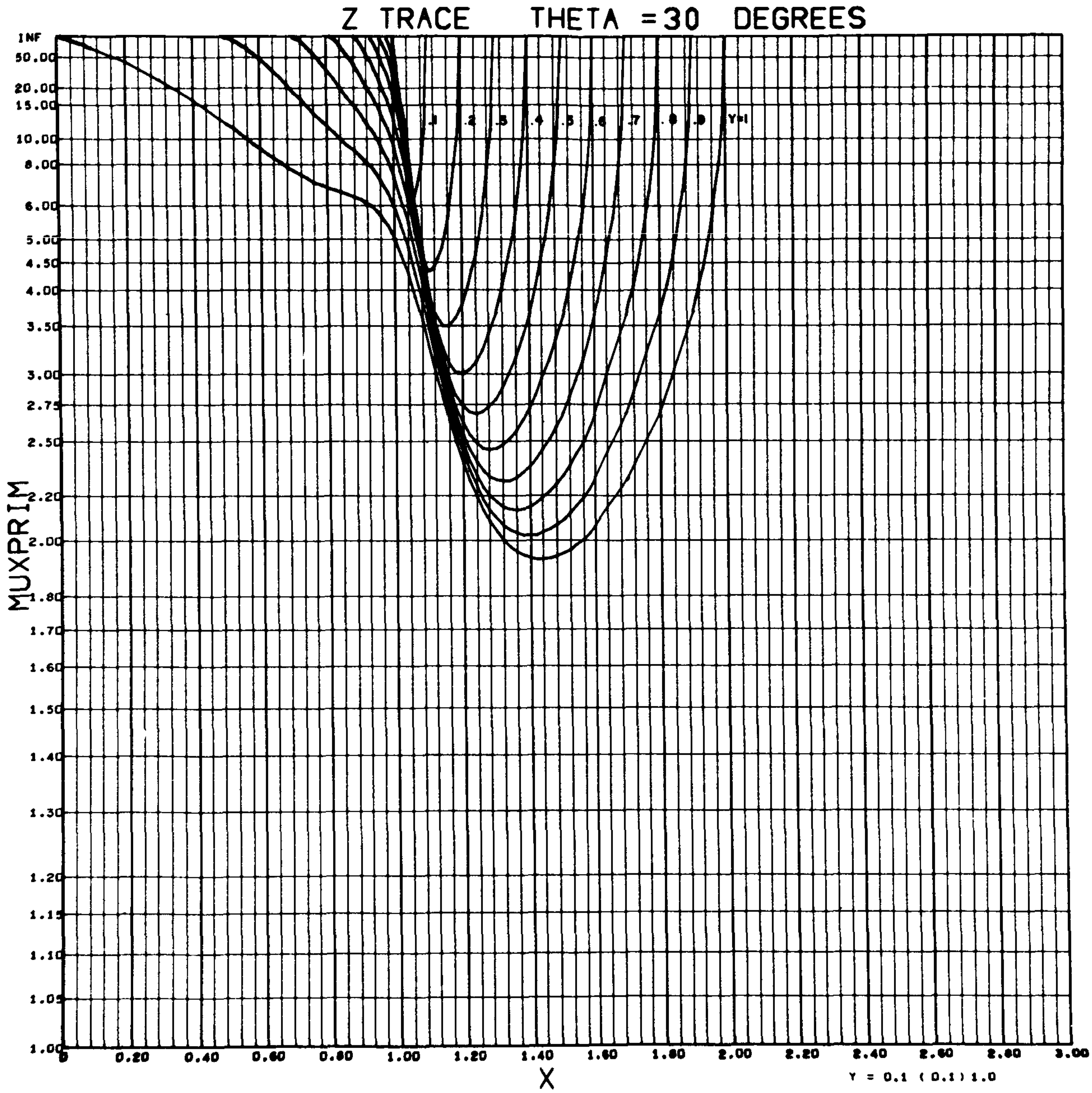

Figure 19.- Variation of μ' vs. X; Y = 0.1 - 1.0; $\theta = 30^\circ$.

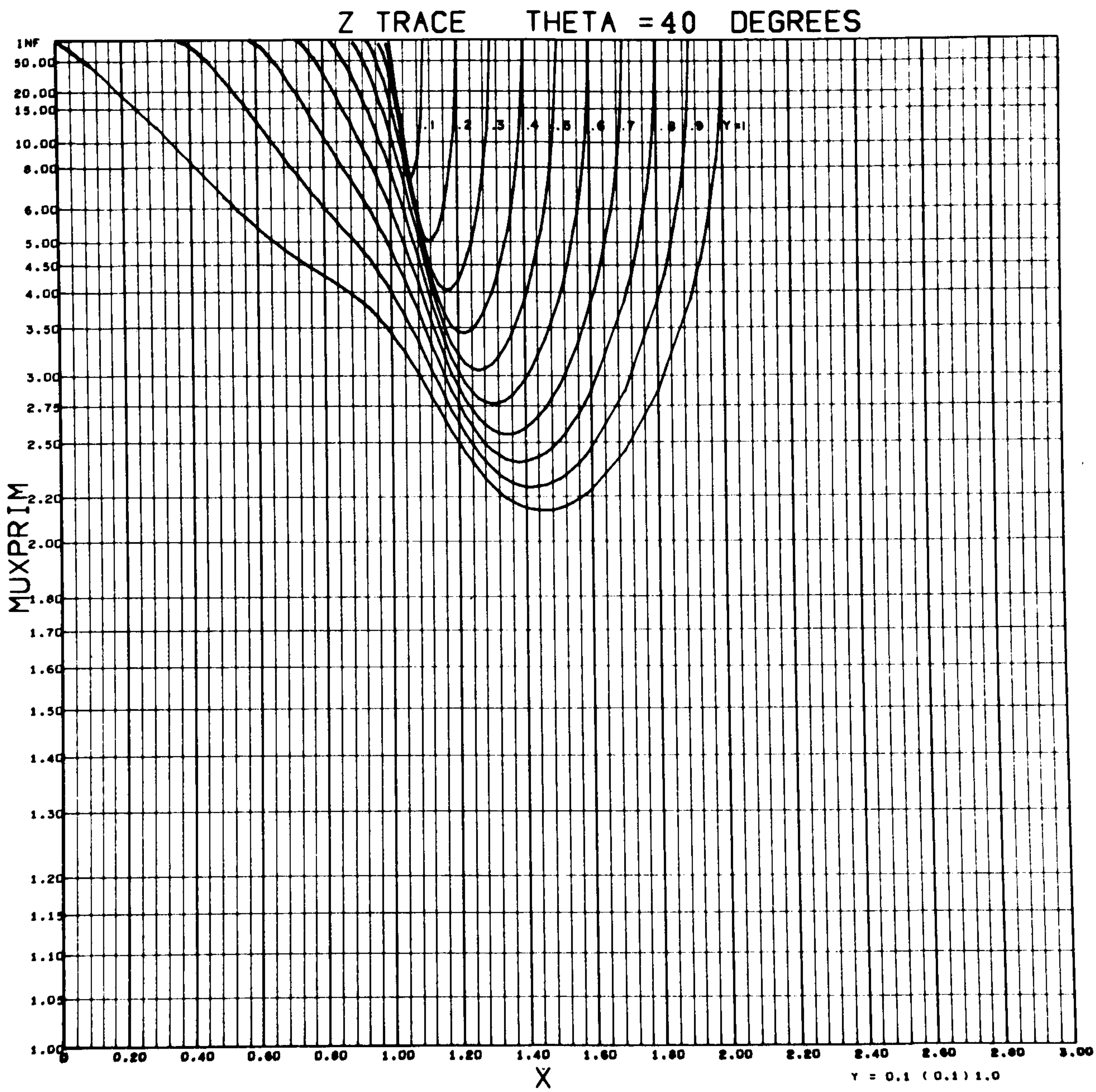

Figure 20.- Variation of μ' vs. X; Y = 0.1 - 1.0; θ = 40°.

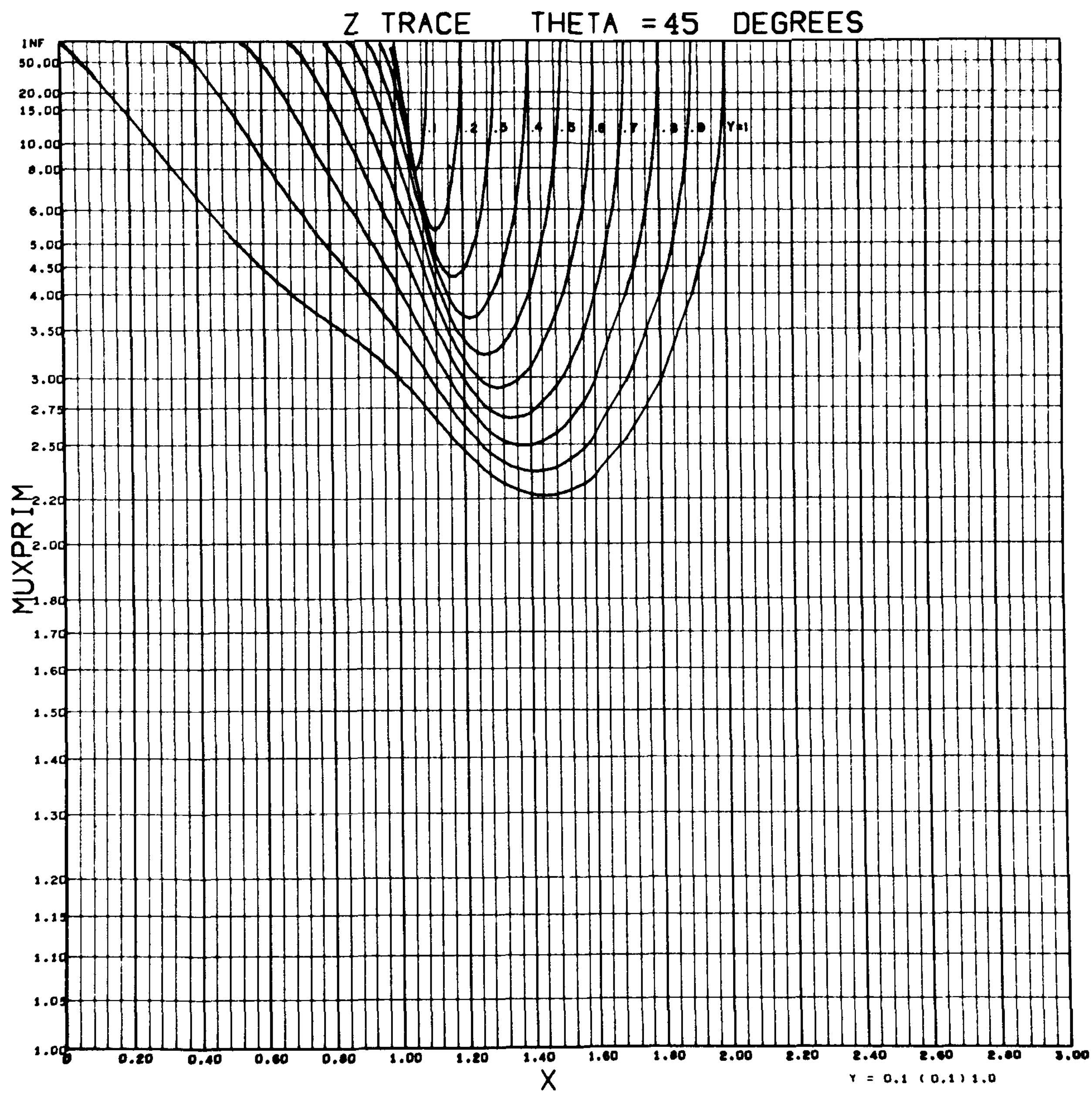

Figure 21.- Variation of μ' vs. X; Y = 0.1 - 1.0; θ = 45°.

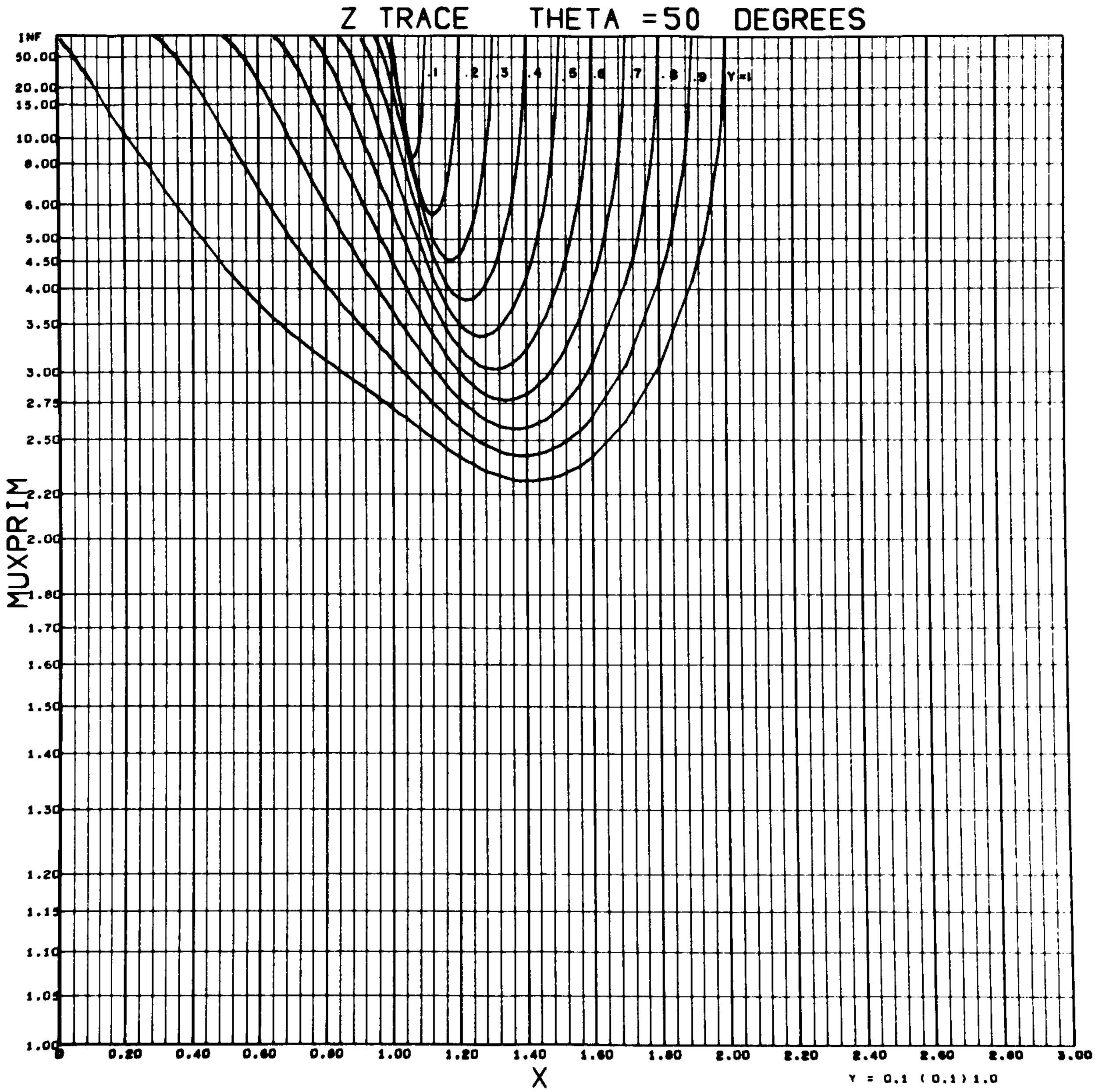

Figure 22.- Variation of μ' vs. X; Y = 0.1 - 1.0; θ = 50°.

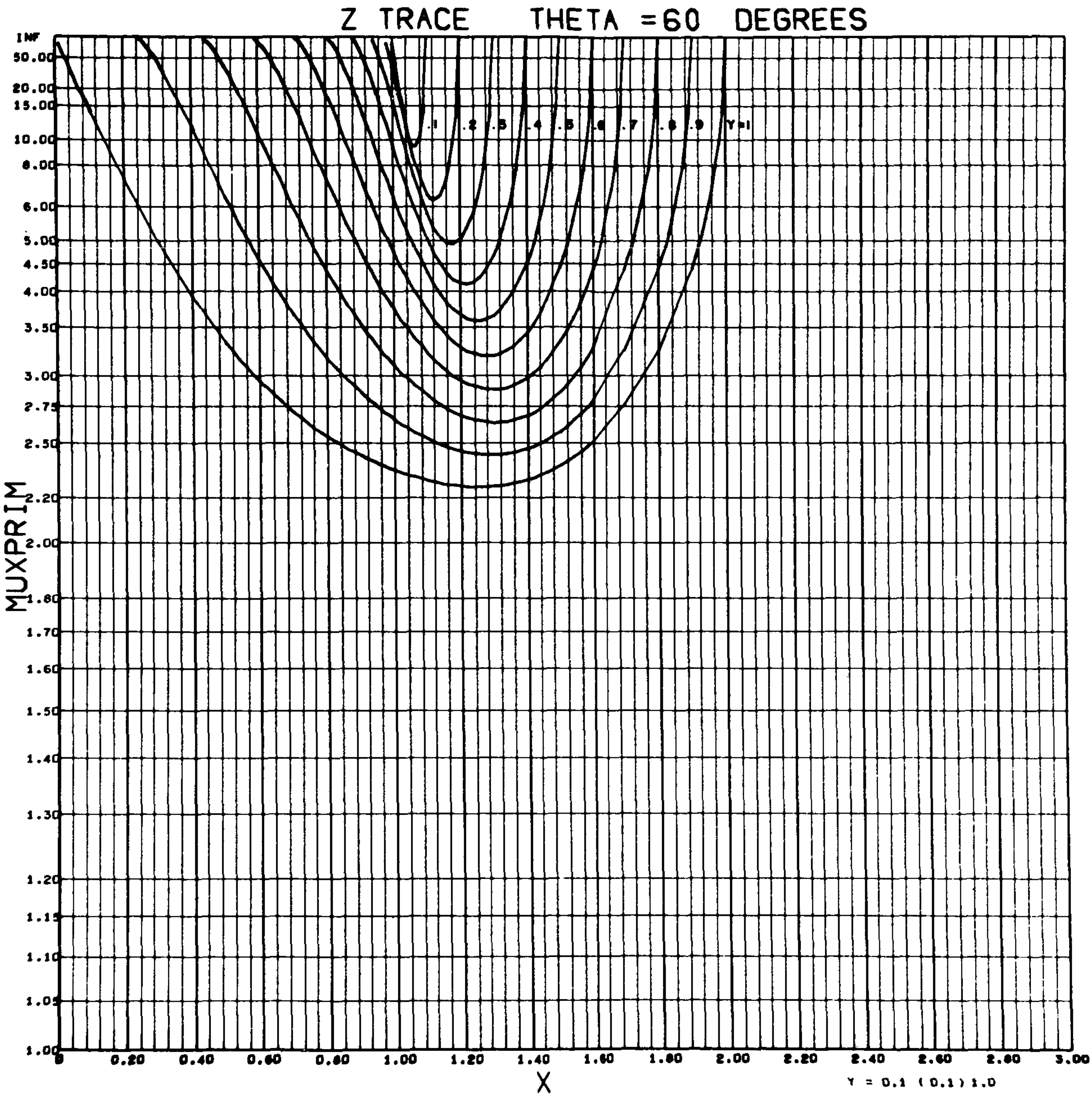

Figure 23.- Variation of μ' vs. X; Y = 0.1 - 1.0; θ = 60°.

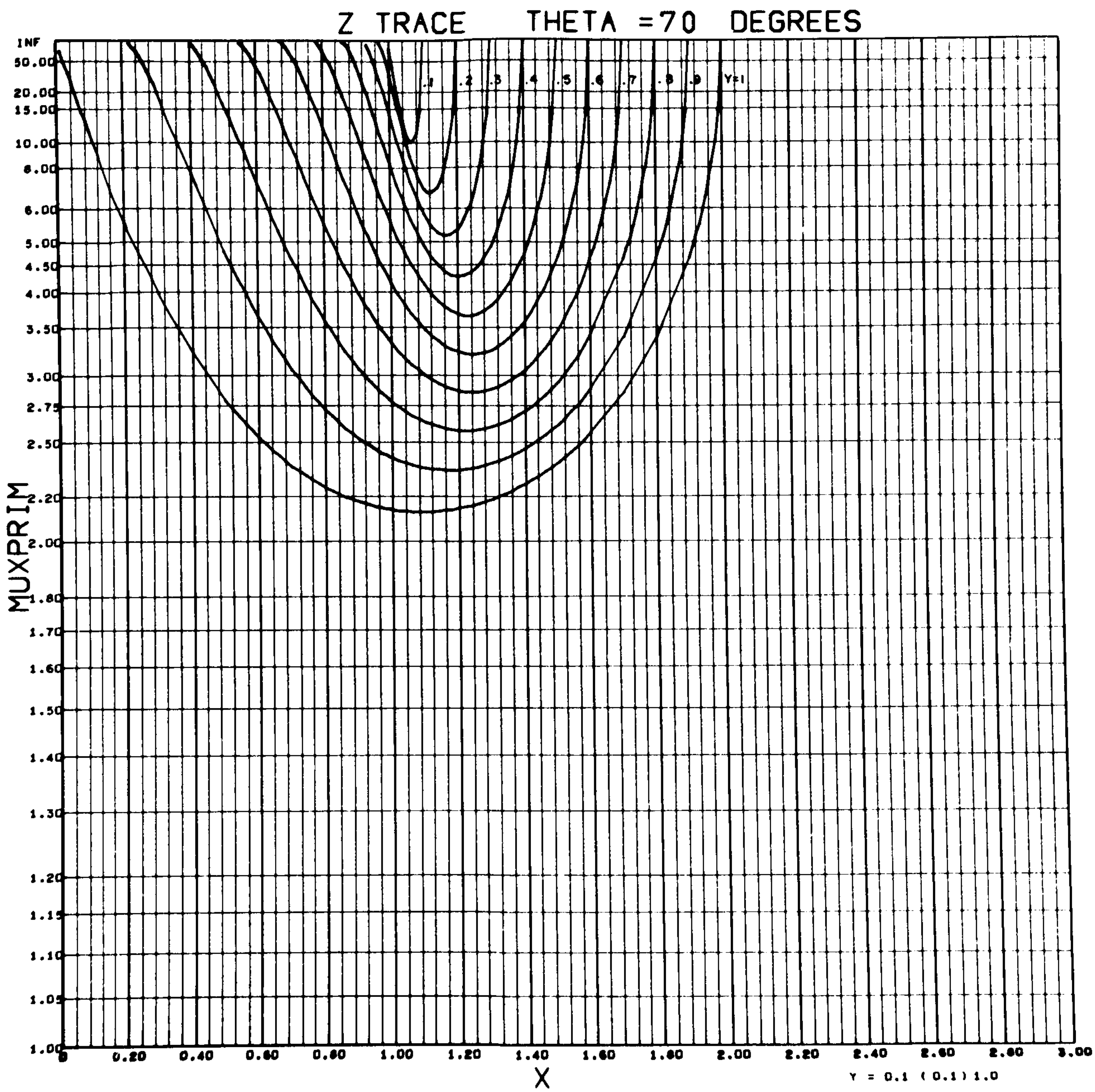

Figure 24.- Variation of μ' vs. X; Y = 0.1 - 1.0; θ = 70°.

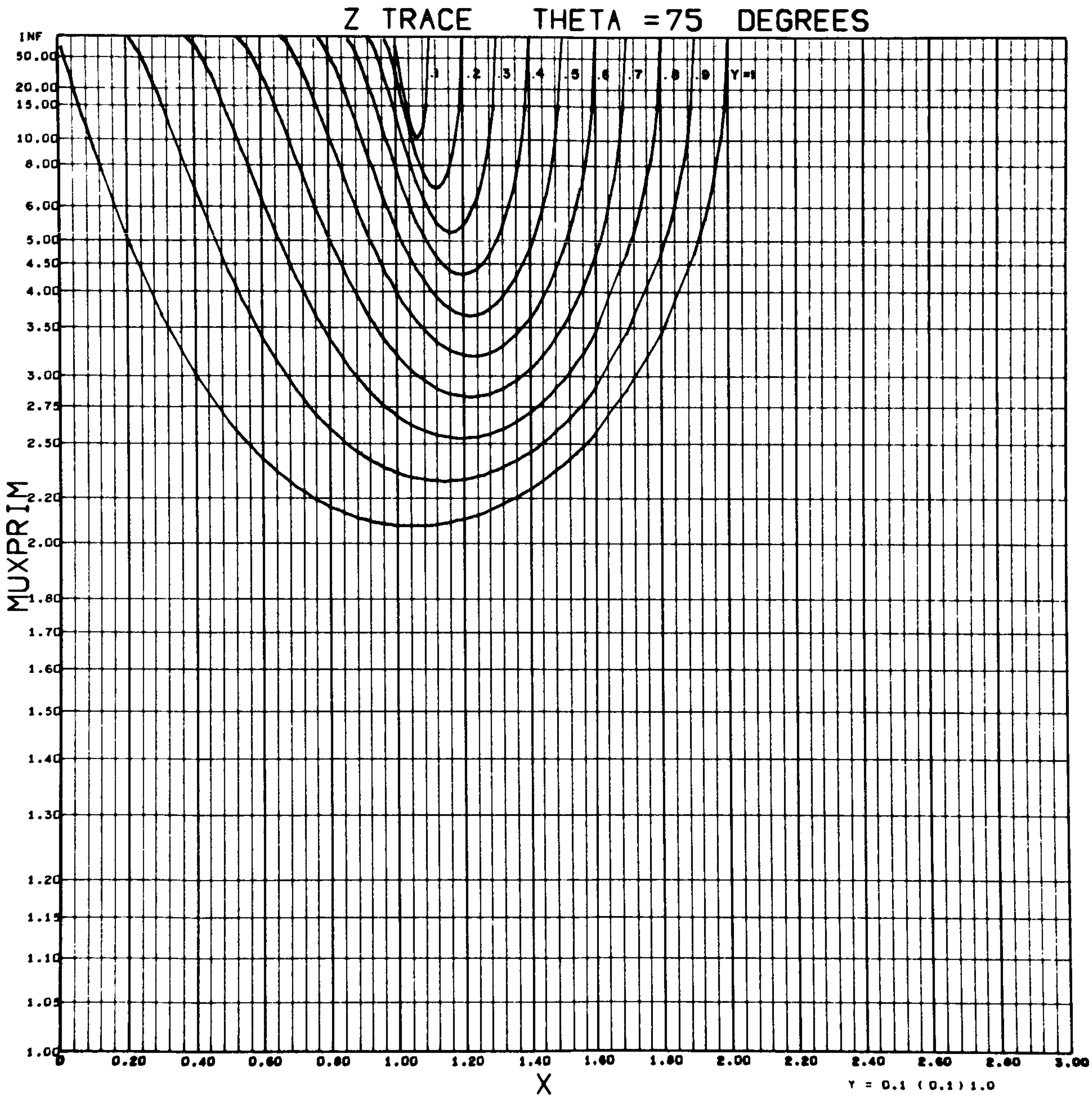

Figure 25.- Variation of μ' vs. X; Y = 0.1 - 1.0; θ = 75°.

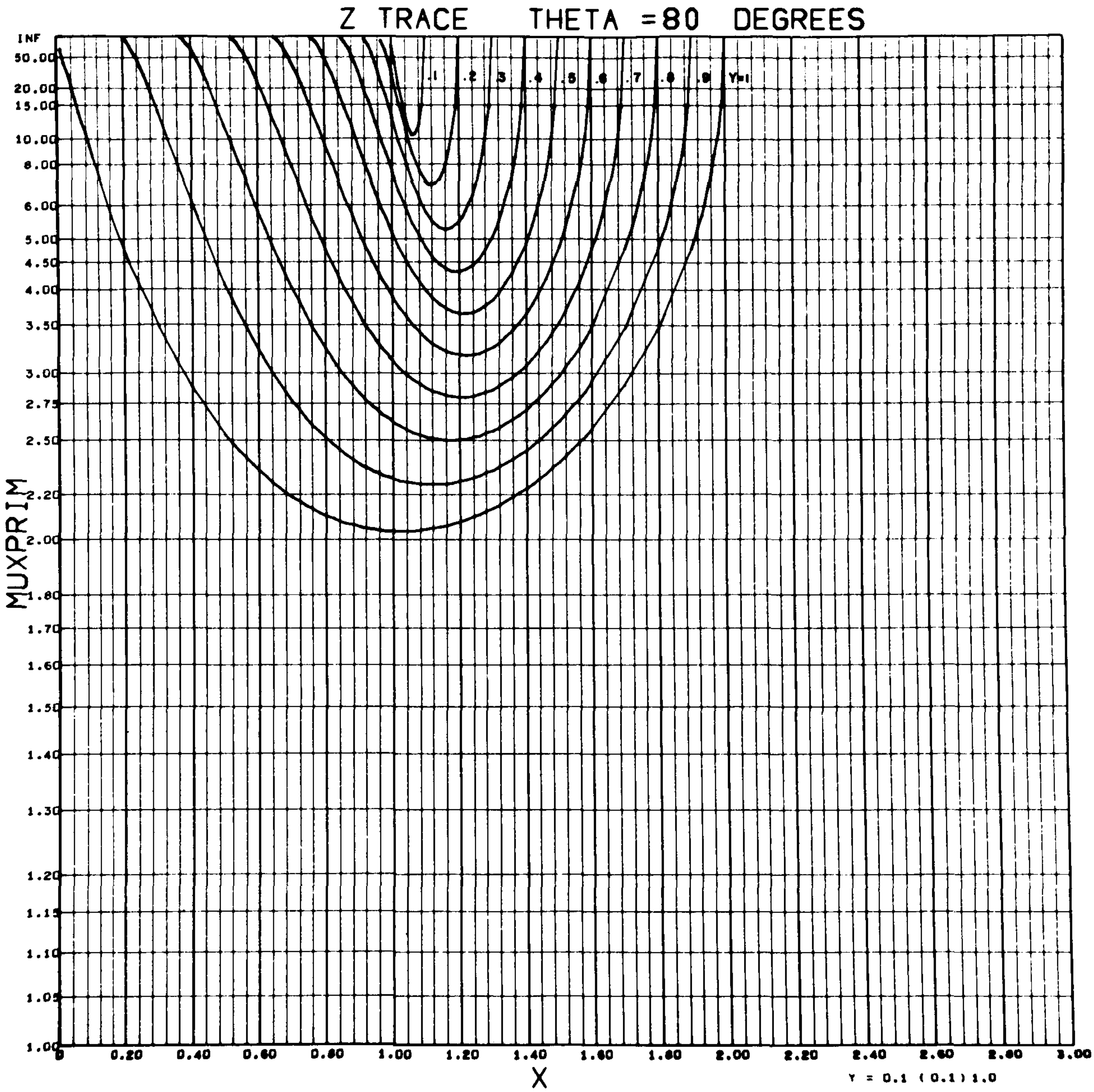

Figure 26.- Variation of μ' vs. X; Y = 0.1 - 1.0; $\theta = 80^{\circ}$.

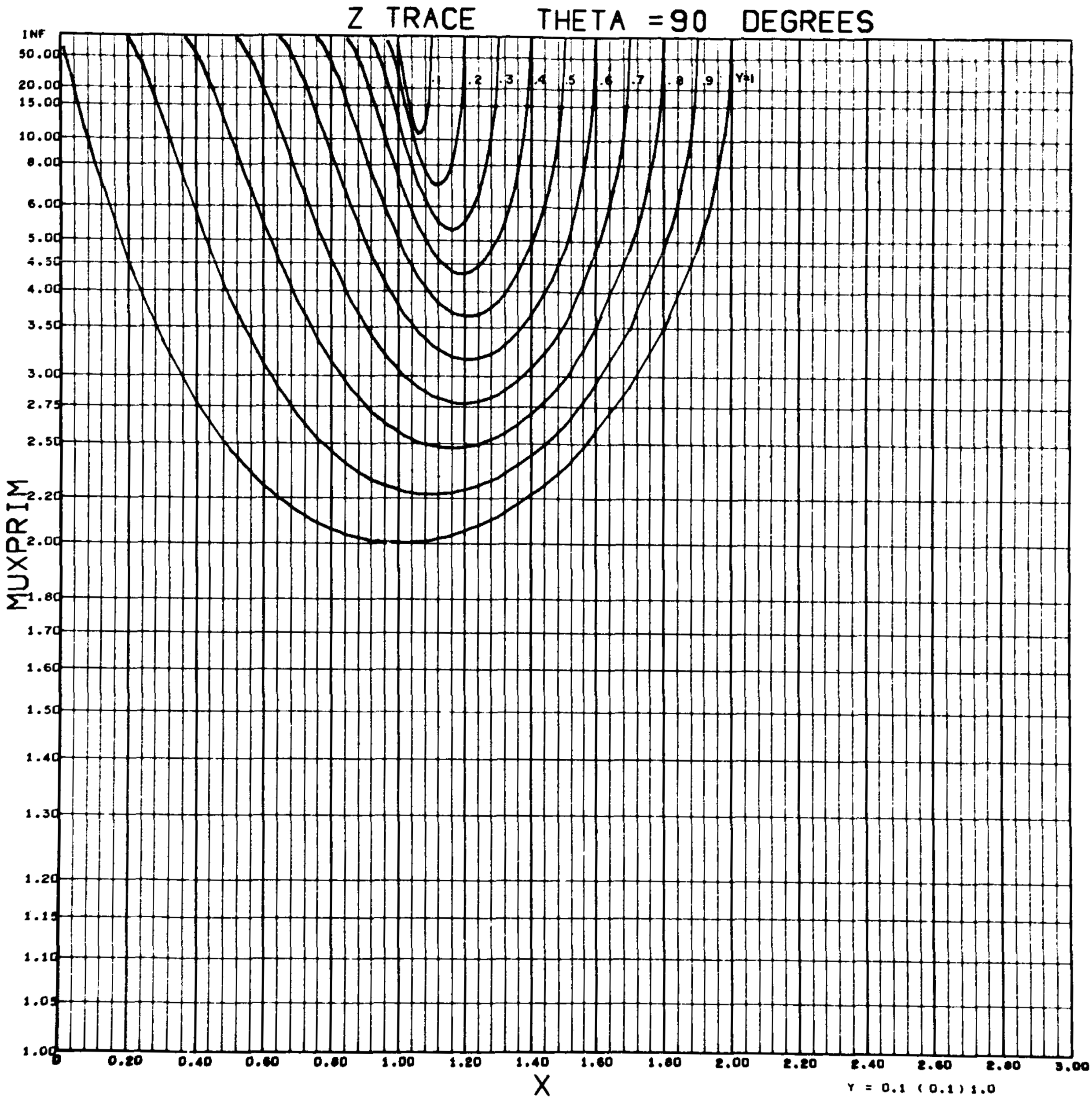

Figure 27.- Variation of μ' vs. X; Y = 0.1 - 1.0; θ = 90°.

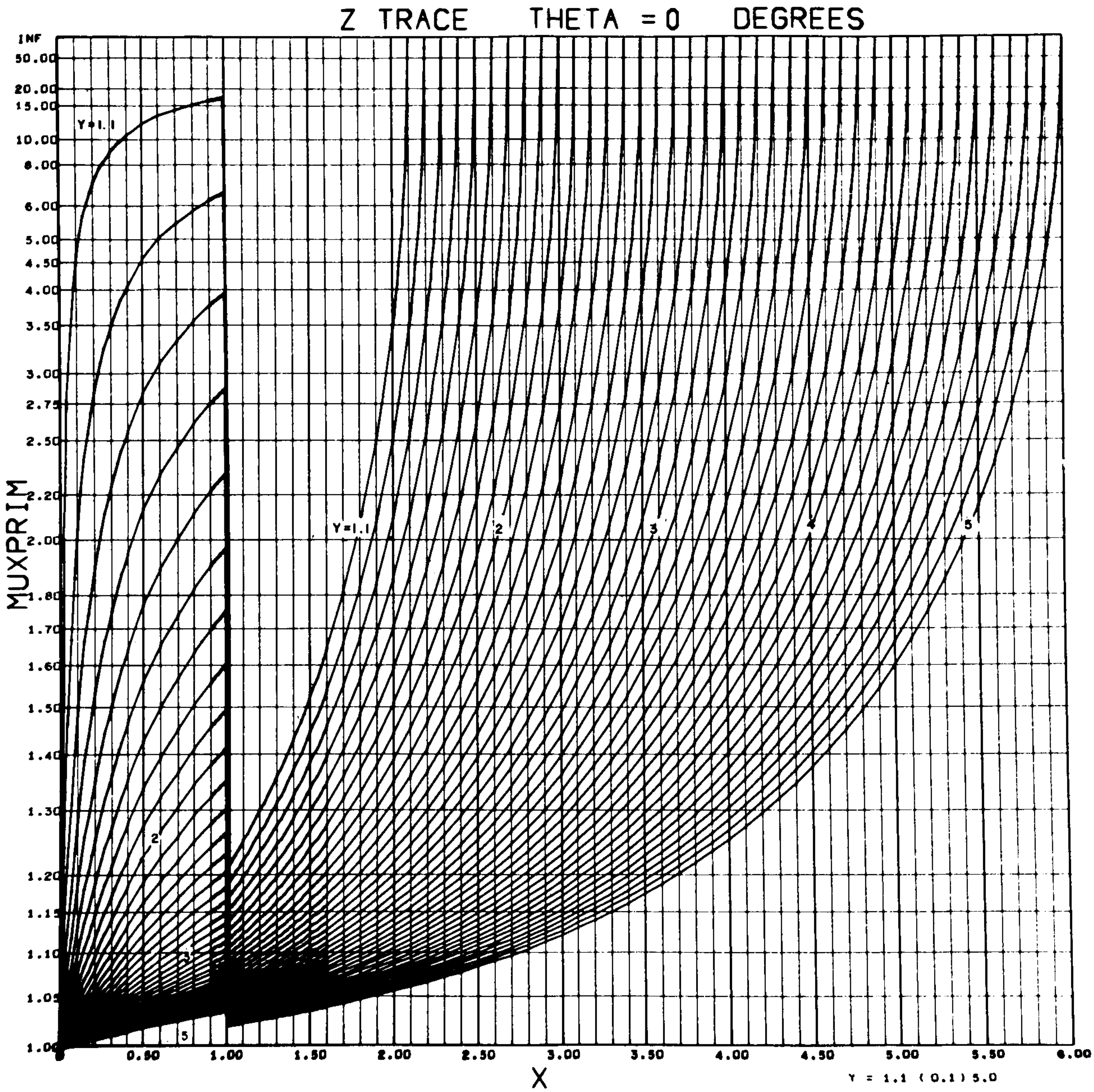

Figure 28.- Variation of μ' vs. X; Y = 1.1 - 5.0; $\theta = 0^{\circ}$.

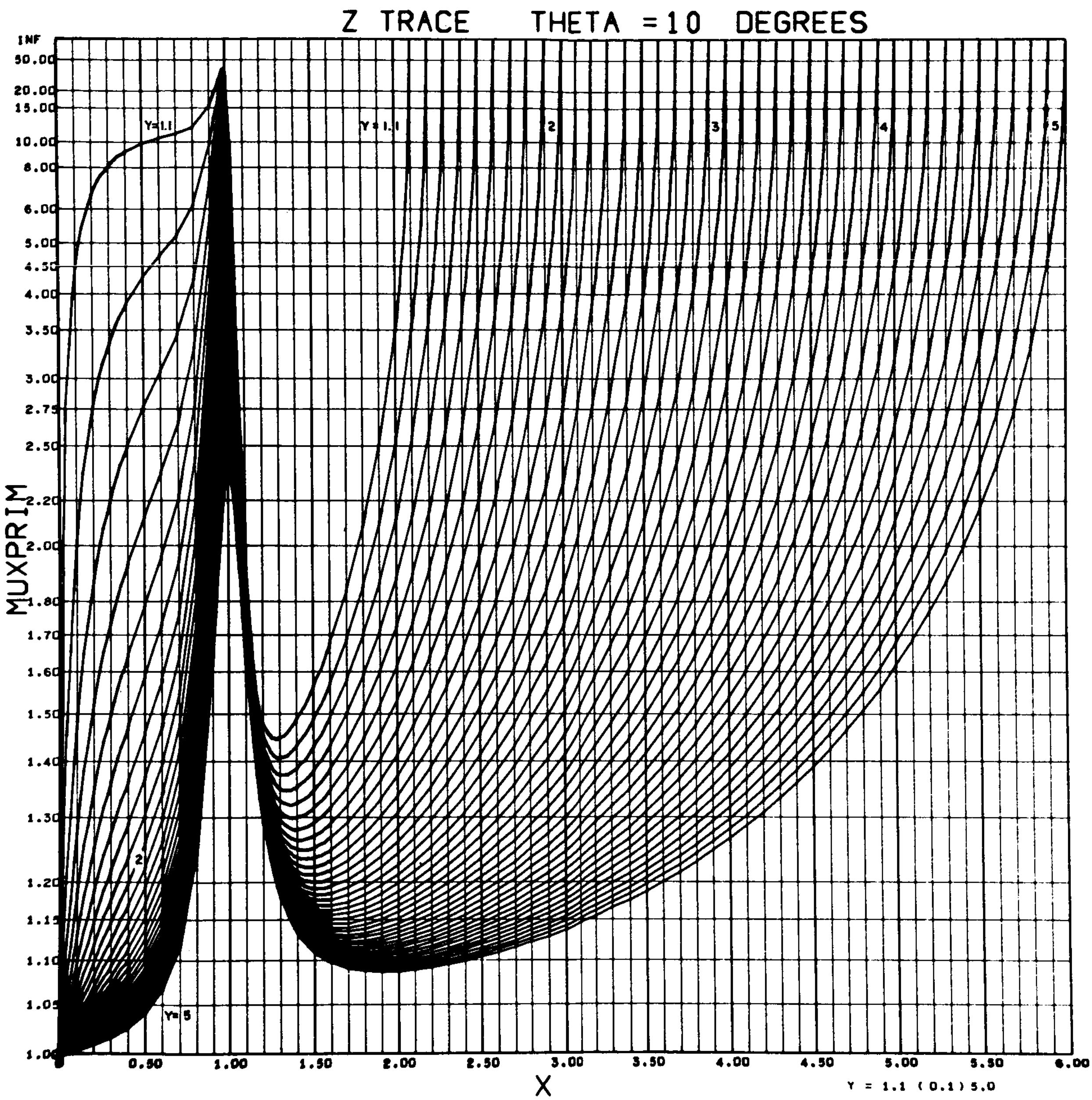

Figure 29.- Variation of μ' vs. X; Y = 1.1 - 5.0; $\theta = 10^{\circ}$.

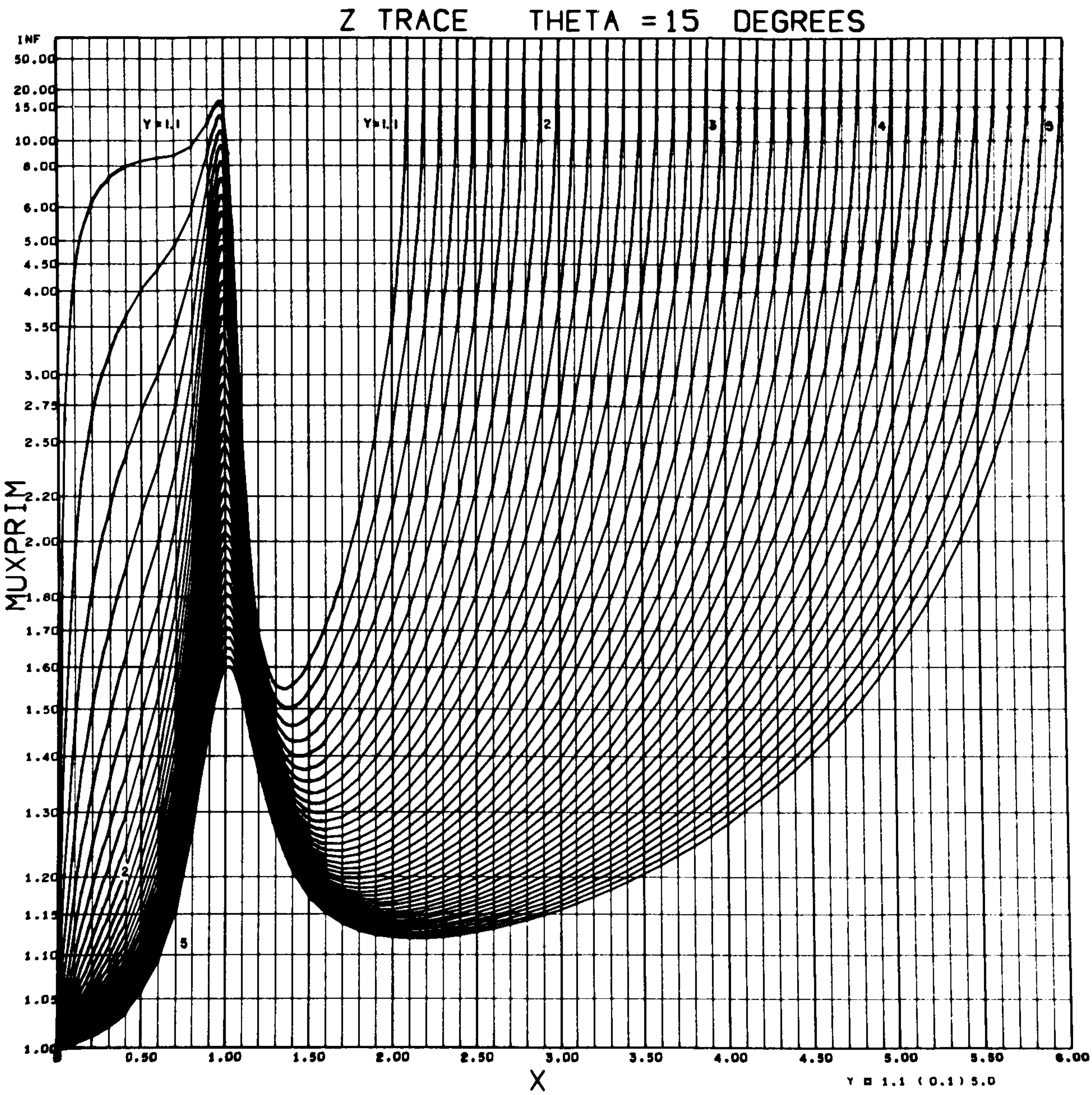

Figure 30.- Variation of μ' vs. X; Y = 1.1 - 5.0; $\theta = 15^{\circ}$.

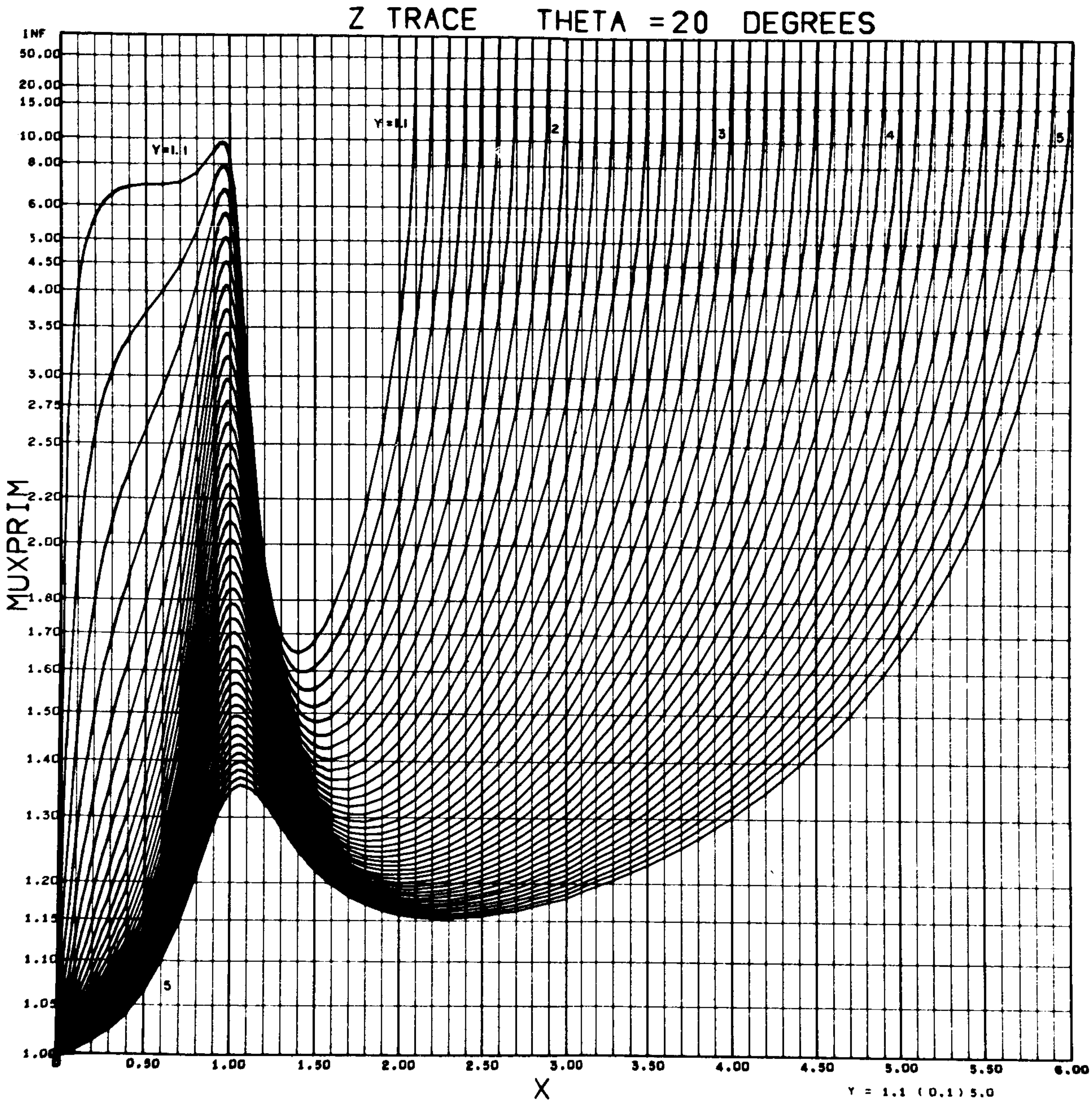

Figure 31.- Variation of μ' vs. X; Y = 1.1 - 5.0; $\theta = 20^{\circ}$.

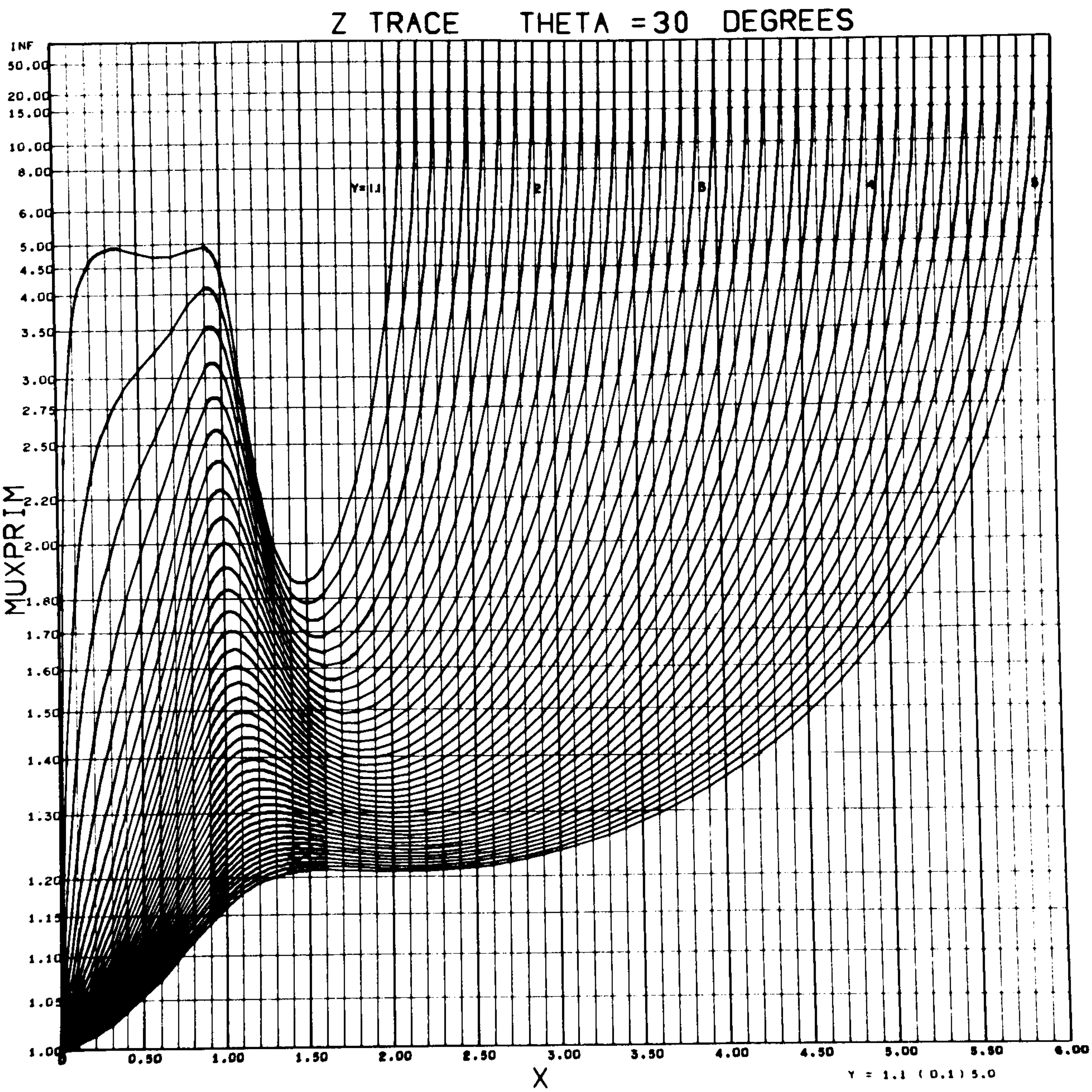

Figure 32.- Variation of μ' vs. X; Y = 1.1 - 5.0; $\theta = 30^{\circ}$.

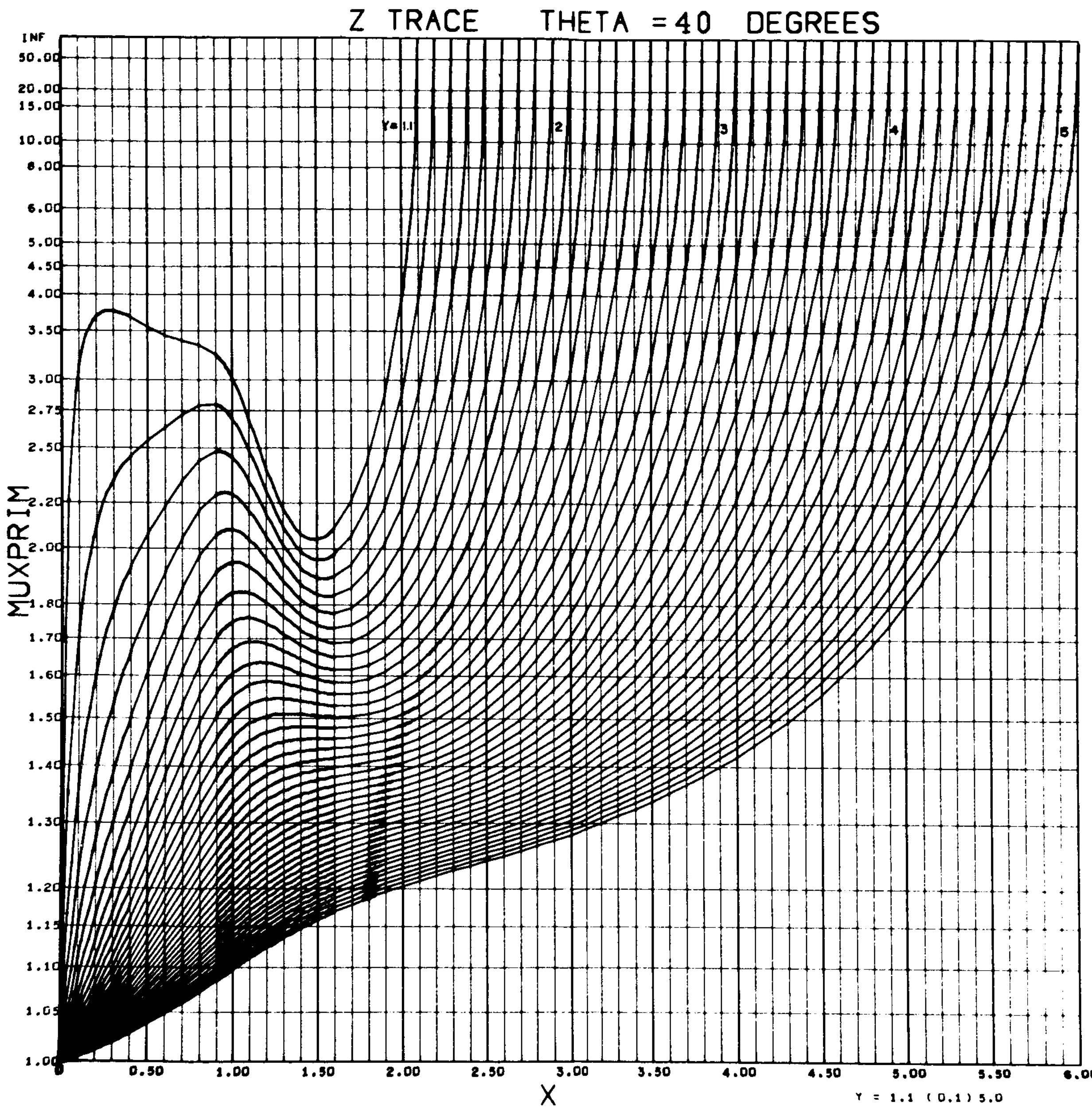

Figure 33.- Variation of μ' vs. X; Y = 1.1 - 5.0; $\theta = 40^{\circ}$.

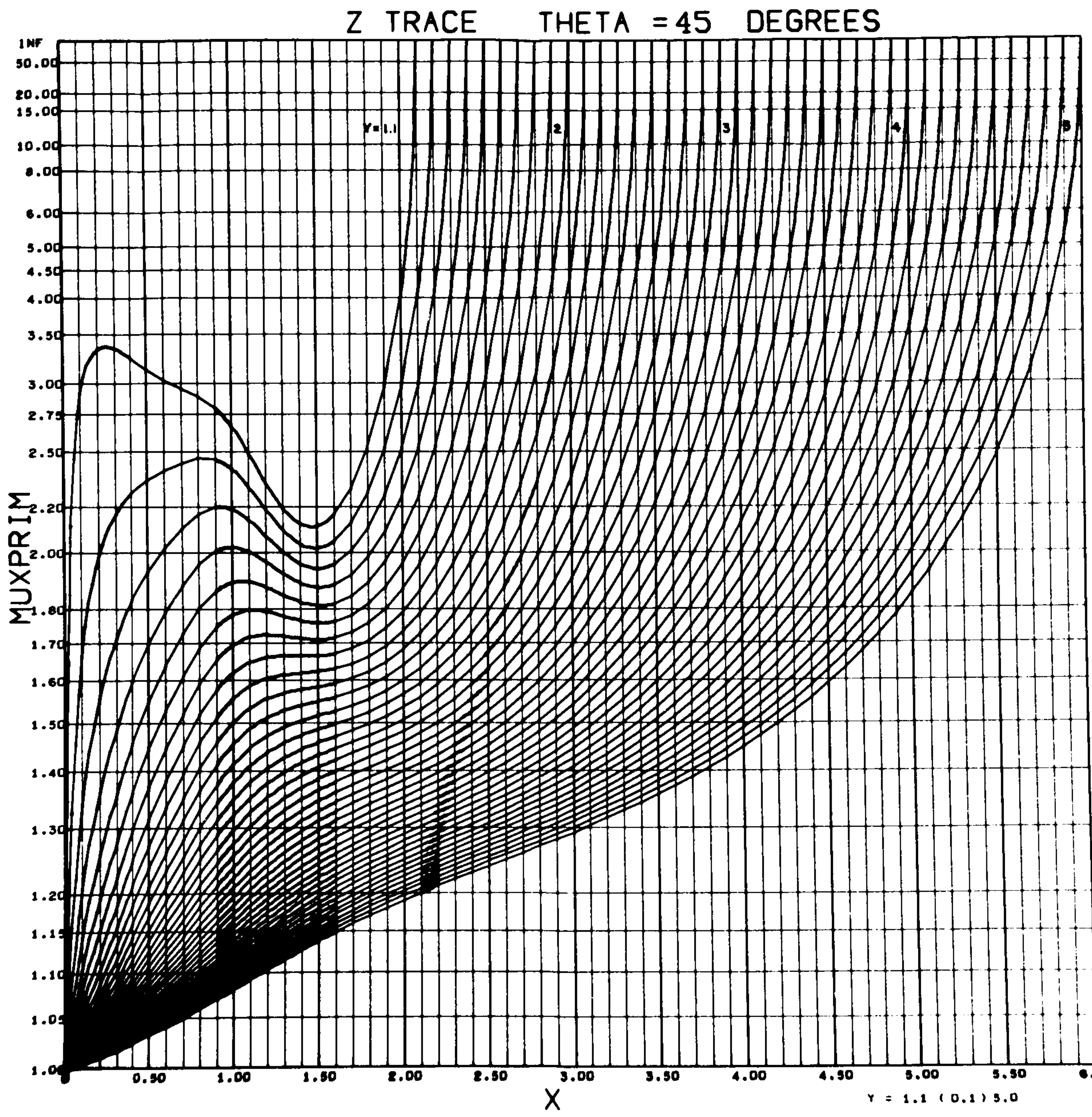

Figure 34.- Variation of μ' vs. X; Y = 1.1 - 5.0; $\theta = 45^{\circ}$.

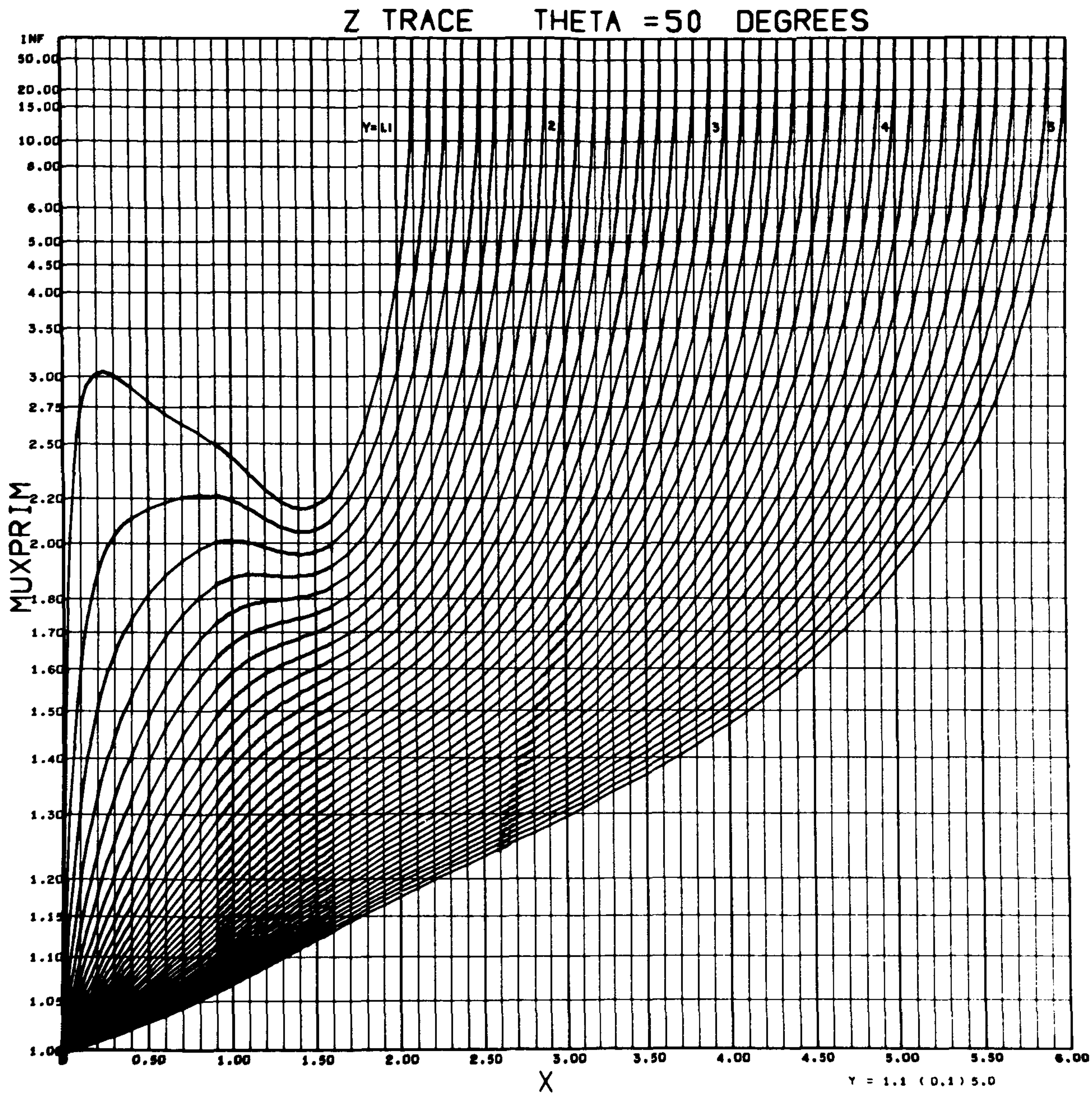

Figure 35.- Variation of μ' vs. X; Y = 1.1 - 5.0; θ = 50°.

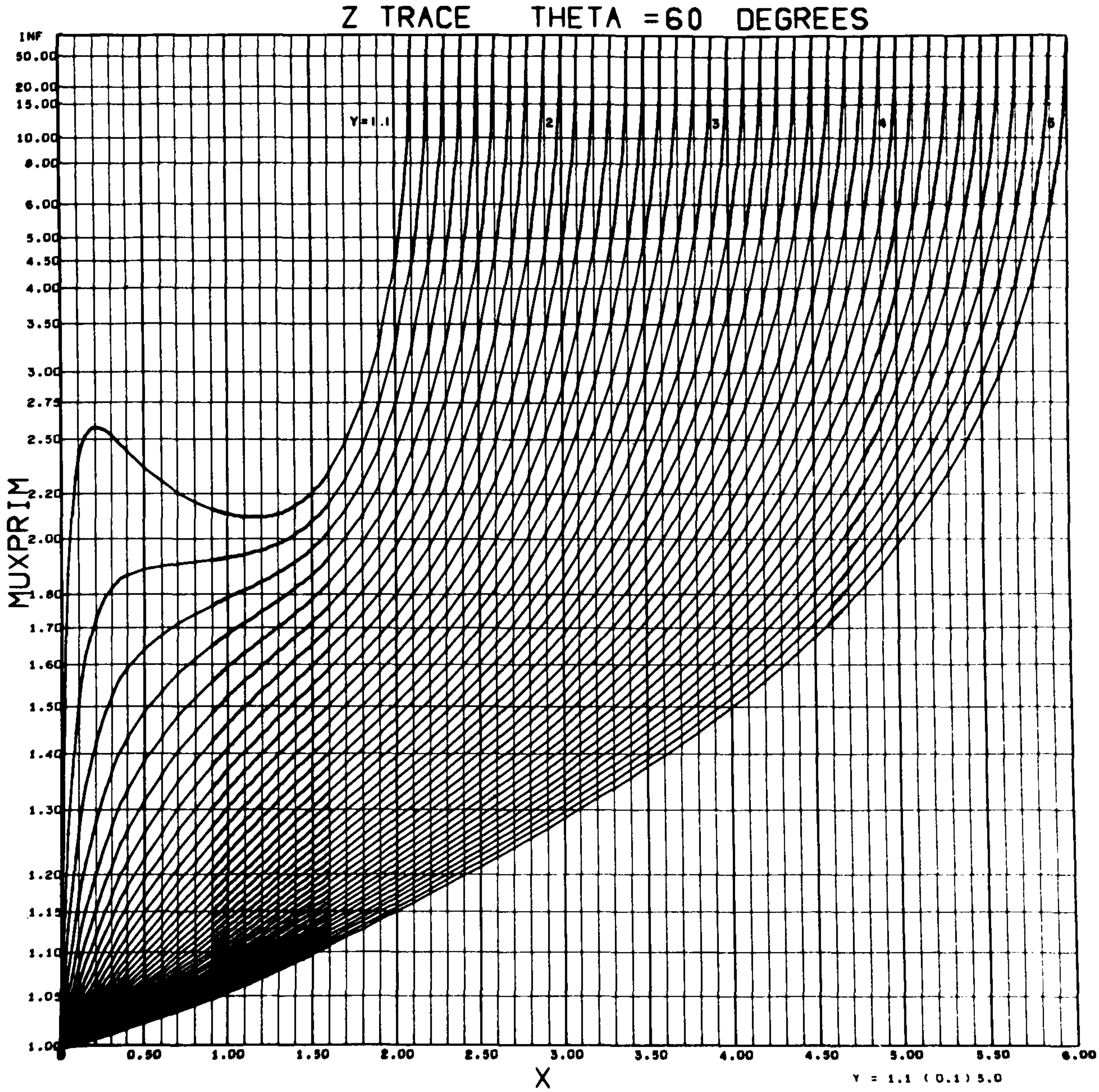

Figure 36.- Variation of μ' vs. X; Y = 1.1 - 5.0; $\theta = 60^{\circ}$.

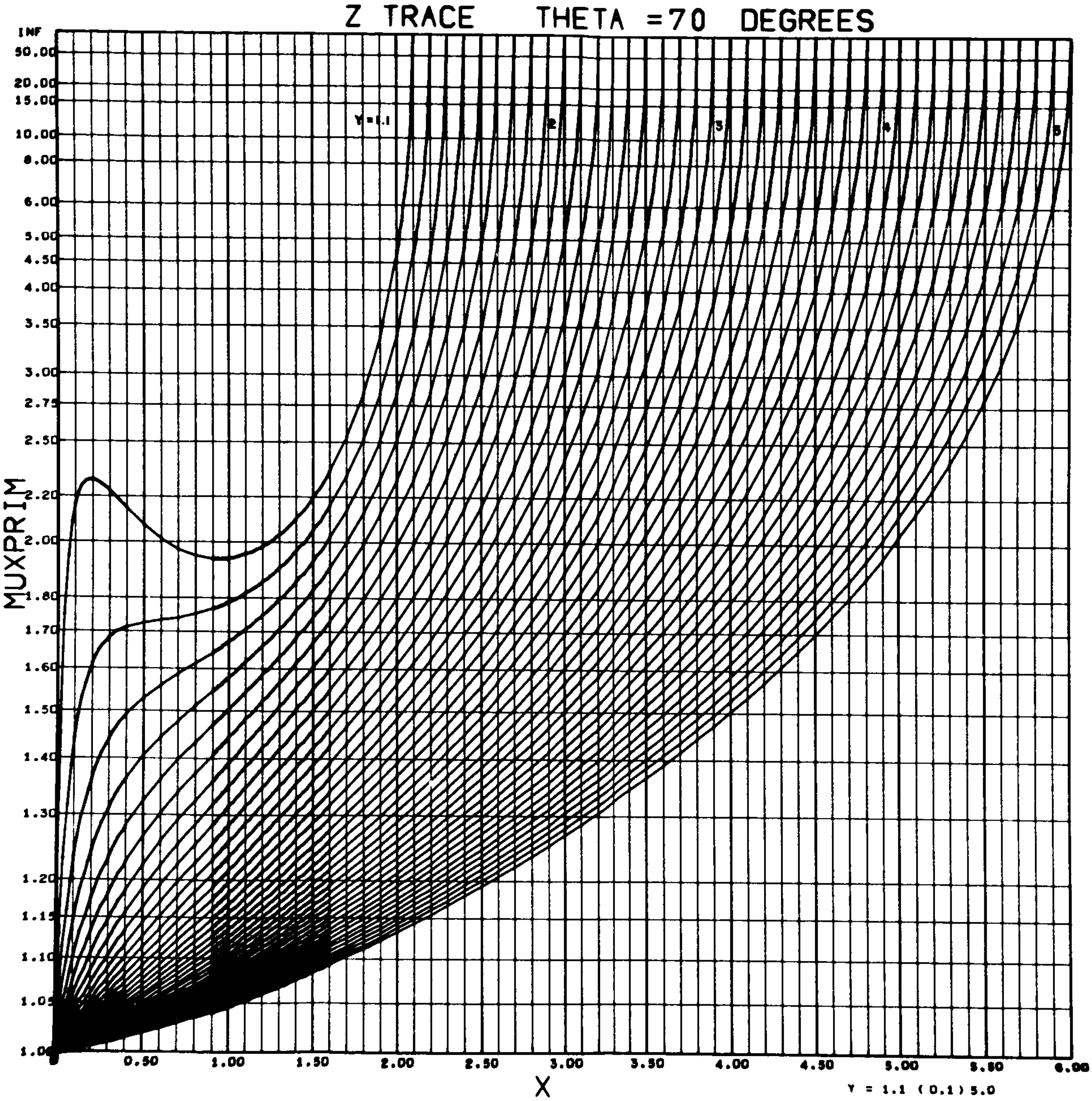

Figure 37.- Variation of μ' vs. X; Y = 1.1 - 5.0; $\theta = 70^{\circ}$.

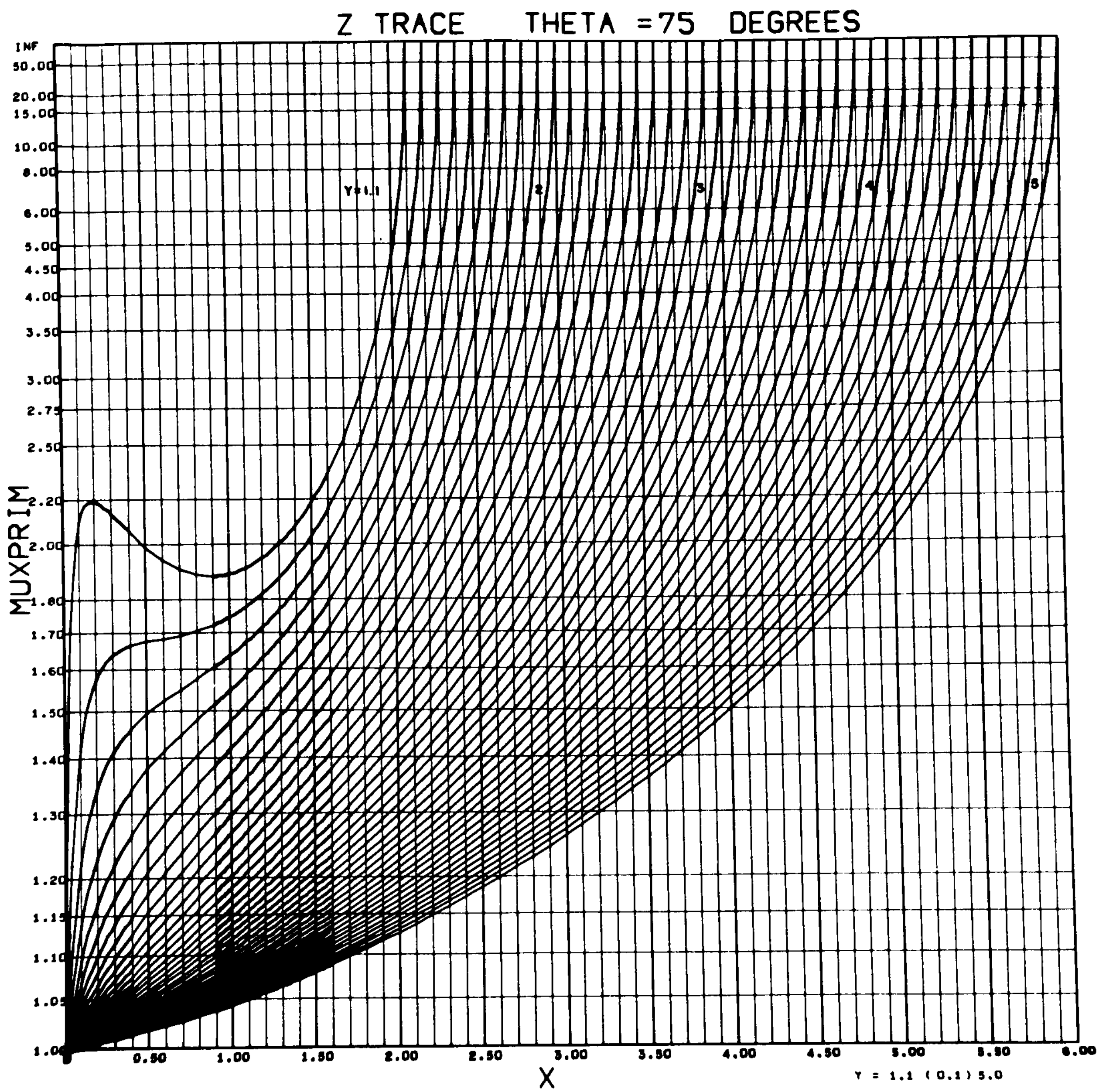

Figure 38.- Variation of μ' vs. X; Y = 1.1 - 5.0; $\theta = 75^{o}$.

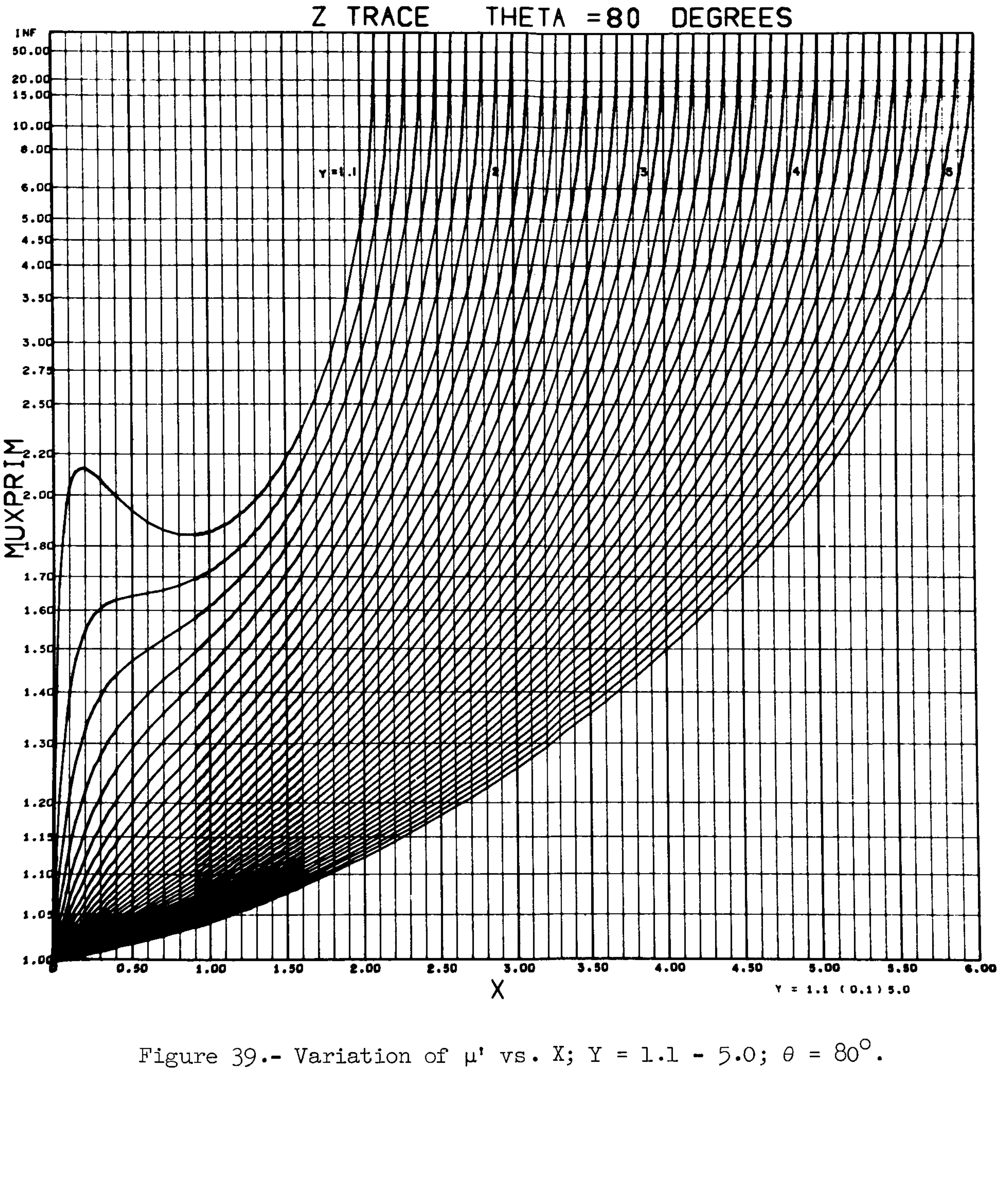

Figure 39.- Variation of μ' vs. X; Y = 1.1 - 5.0; $\theta = 80^{\circ}$.

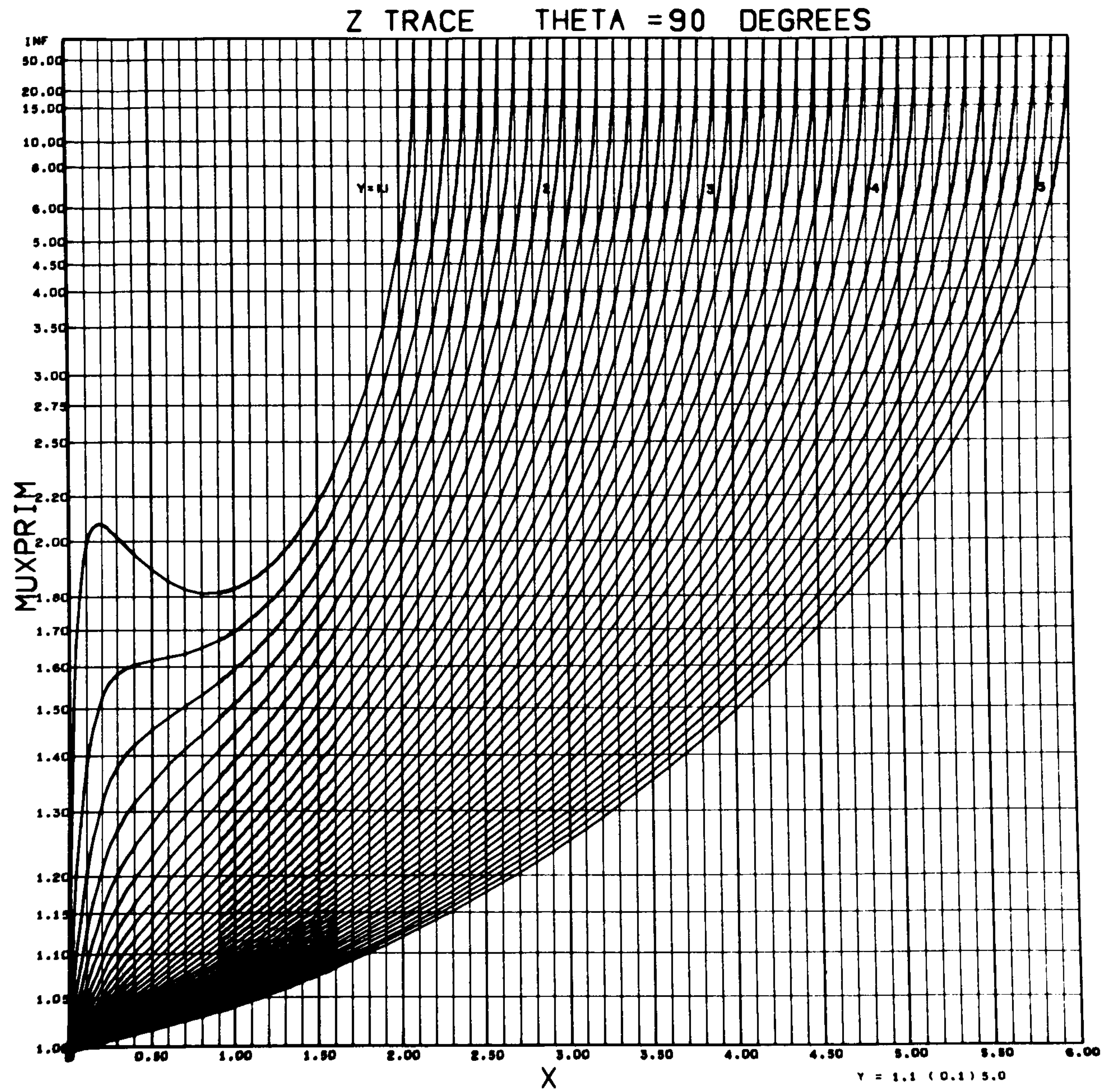

Figure 40.- Variation of μ' vs. X; Y = 1.1 - 5.0; $\theta = 90^{\circ}$.

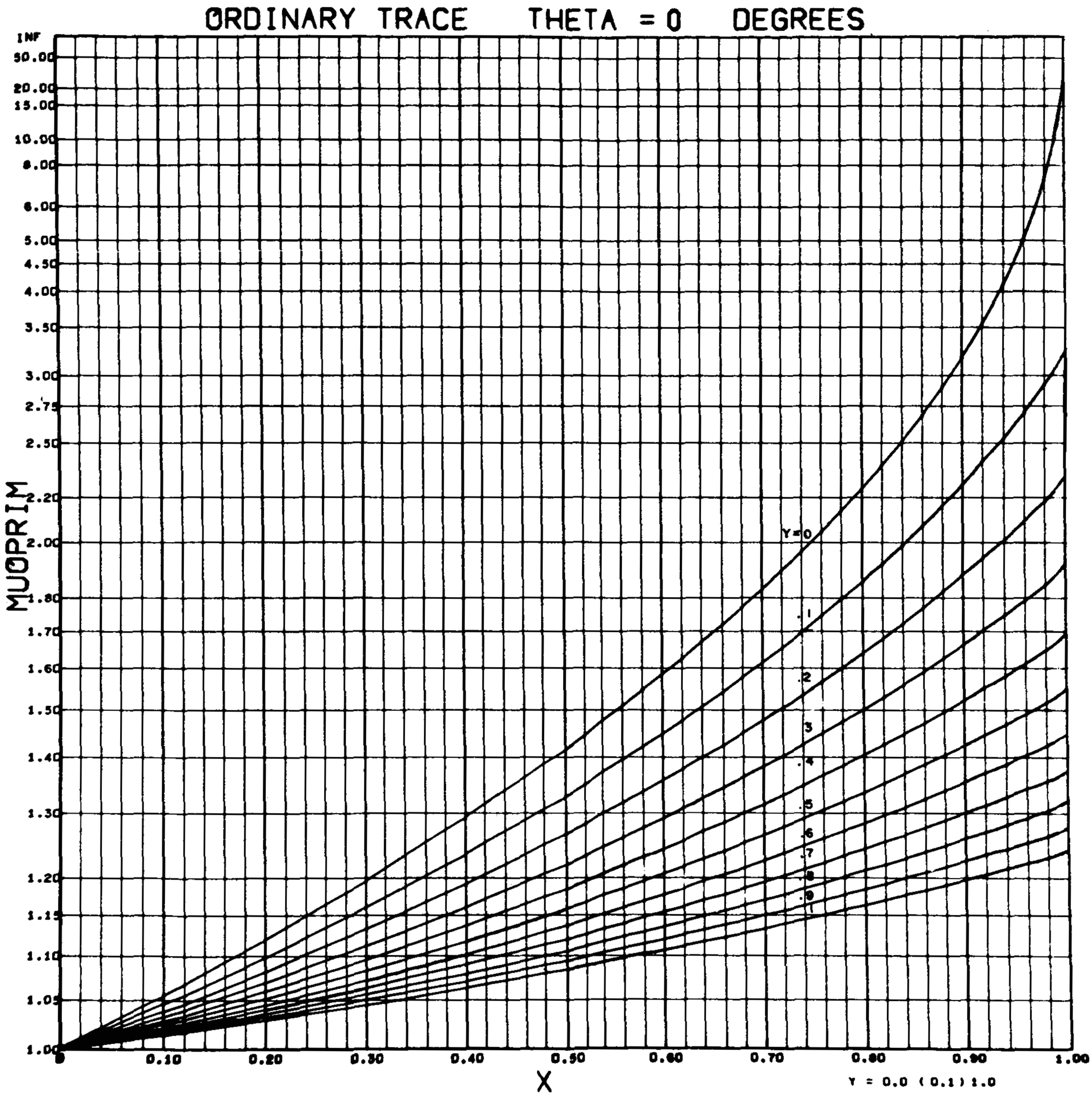

Figure 41.- Variation of μ' vs. X; Y = 0 - 1.0; $\theta = 0^{\circ}$.

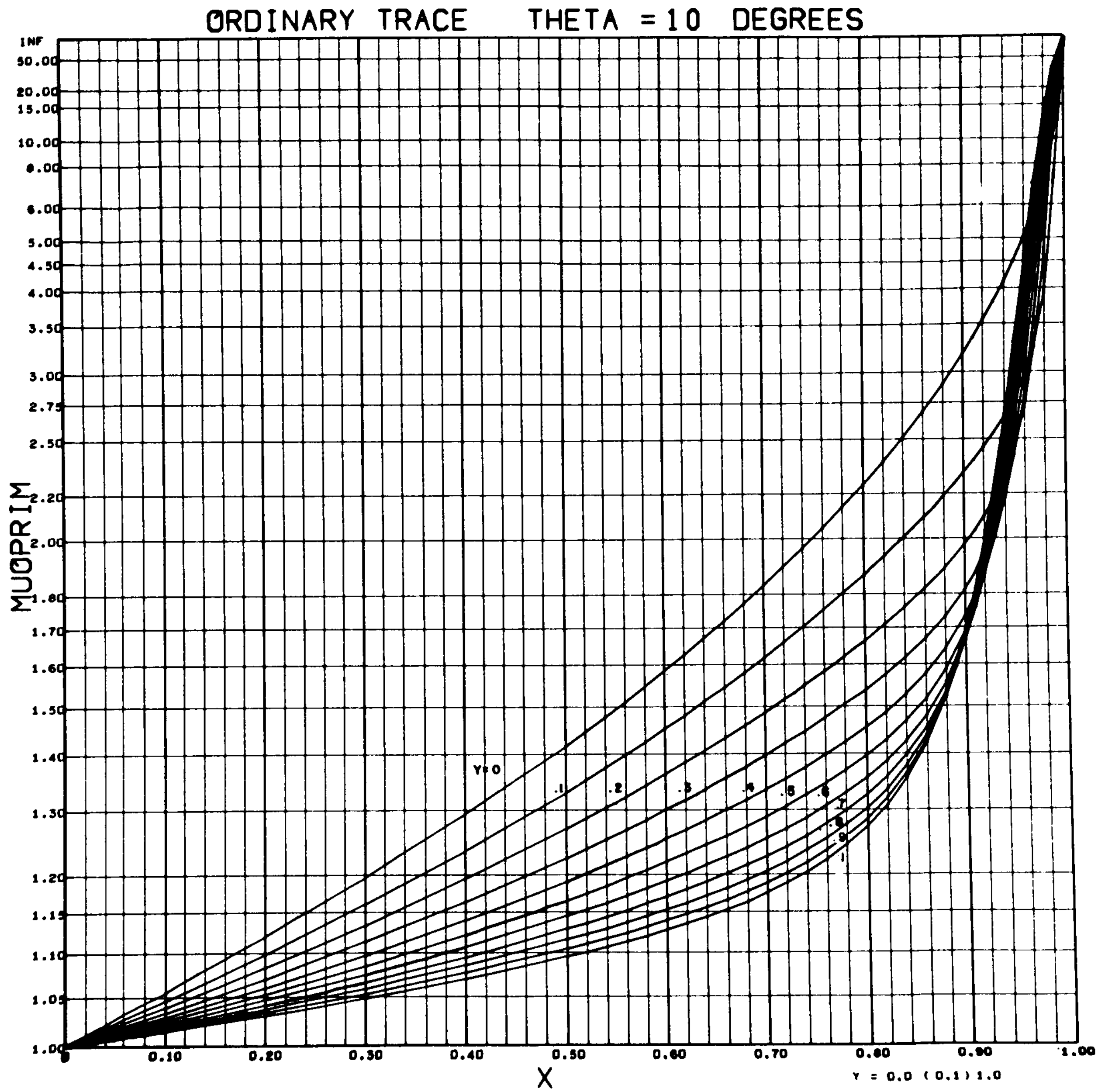

Figure 42.- Variation of μ' vs. X; Y = 0 - 1.0; $\theta = 10^{\circ}$.

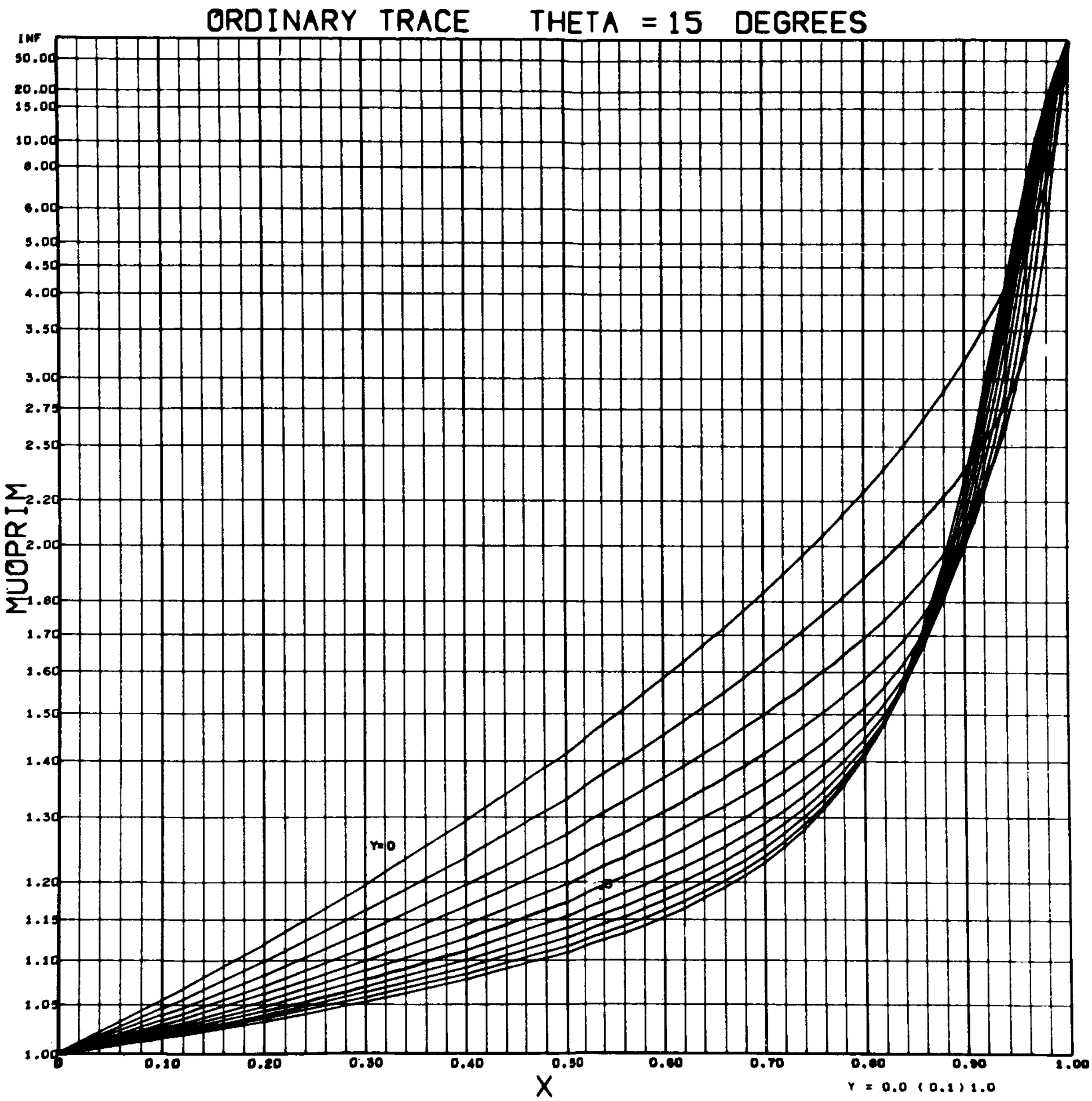

Figure 43.- Variation of μ' vs. X; Y = 0 - 1.0; $\theta = 15^{\circ}$.

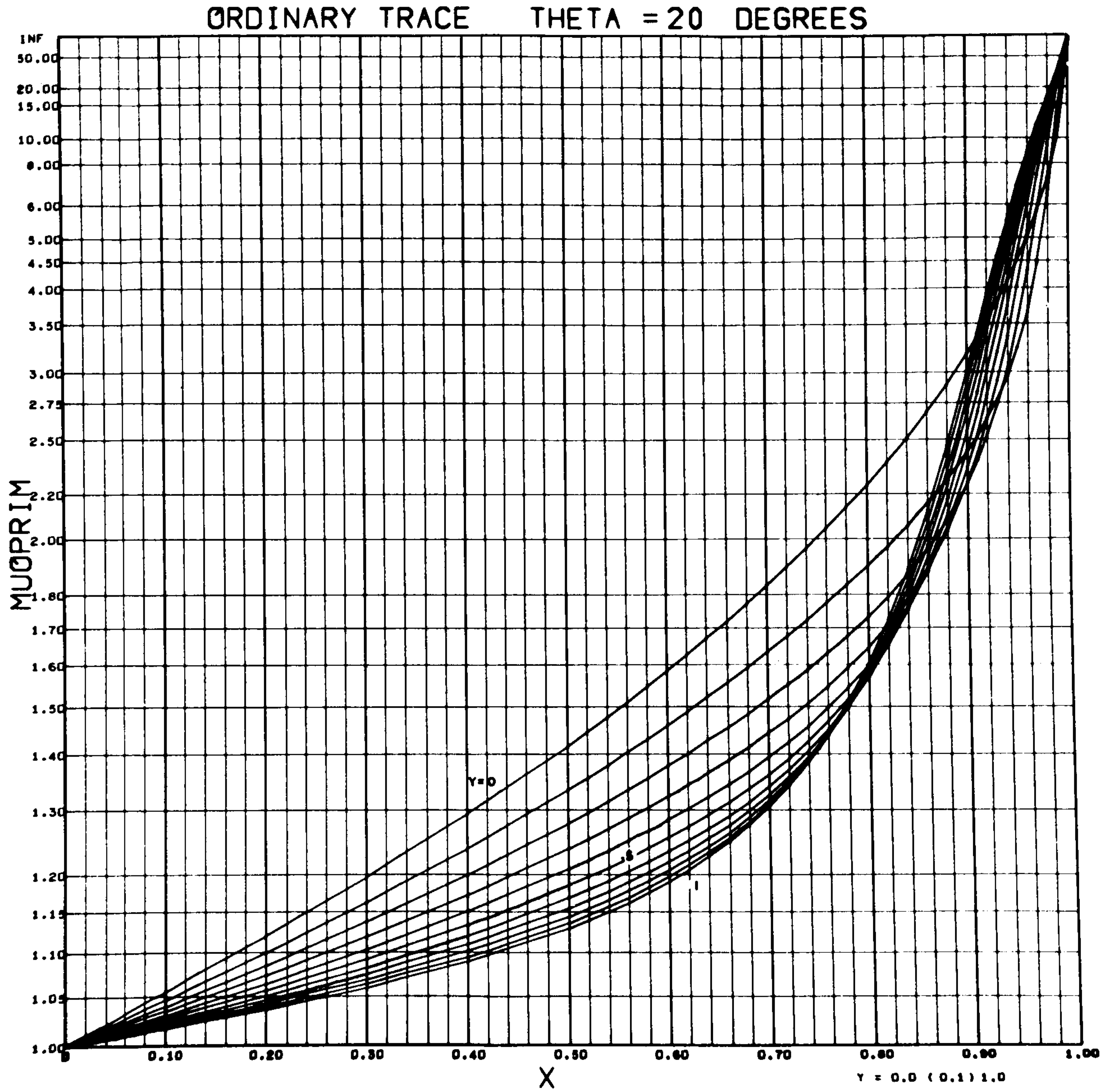

Figure 44.- Variation of μ' vs. X; Y = 0 - 1.0; $\theta = 20^{\circ}$.

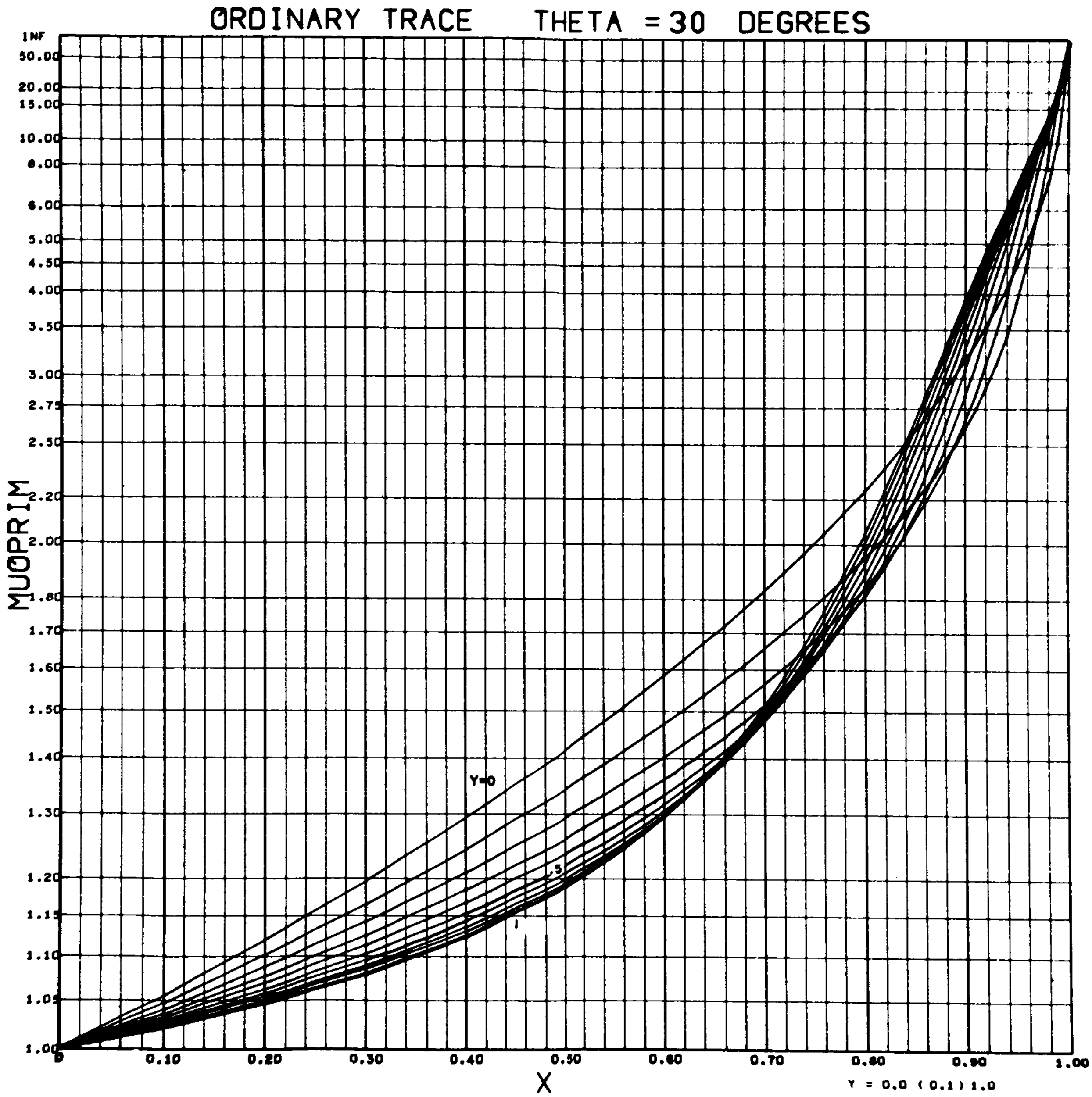

Figure 45.- Variation of μ' vs. X; Y = 0 - 1.0; $\theta = 30^{\circ}$.

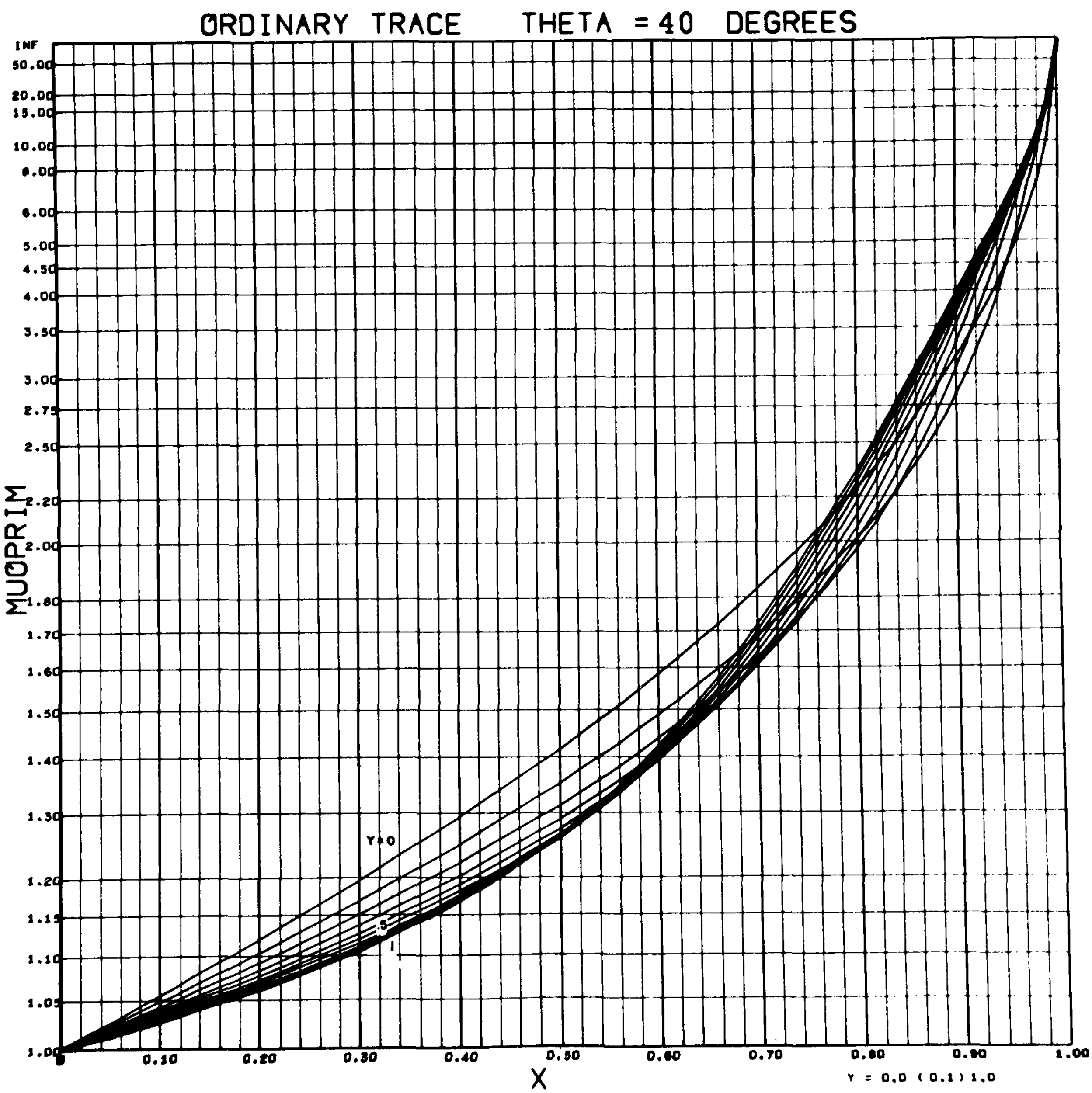

Figure 46.- Variation of μ' vs. X; Y = 0 - 1.0; $\theta = 40^{\circ}$.

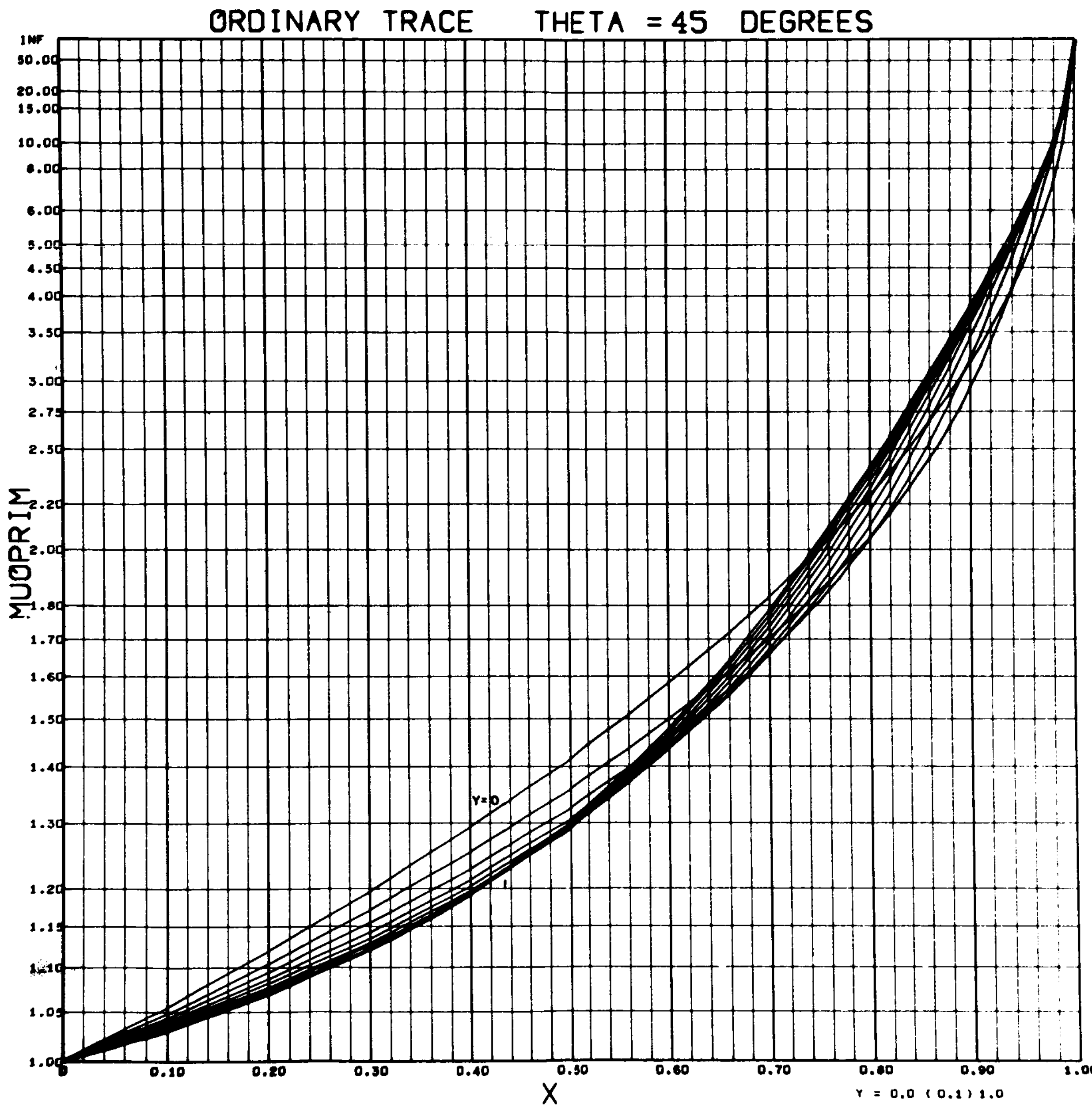

Figure 47.- Variation of μ' vs. X; Y = 0 - 1.0; θ = 45°.

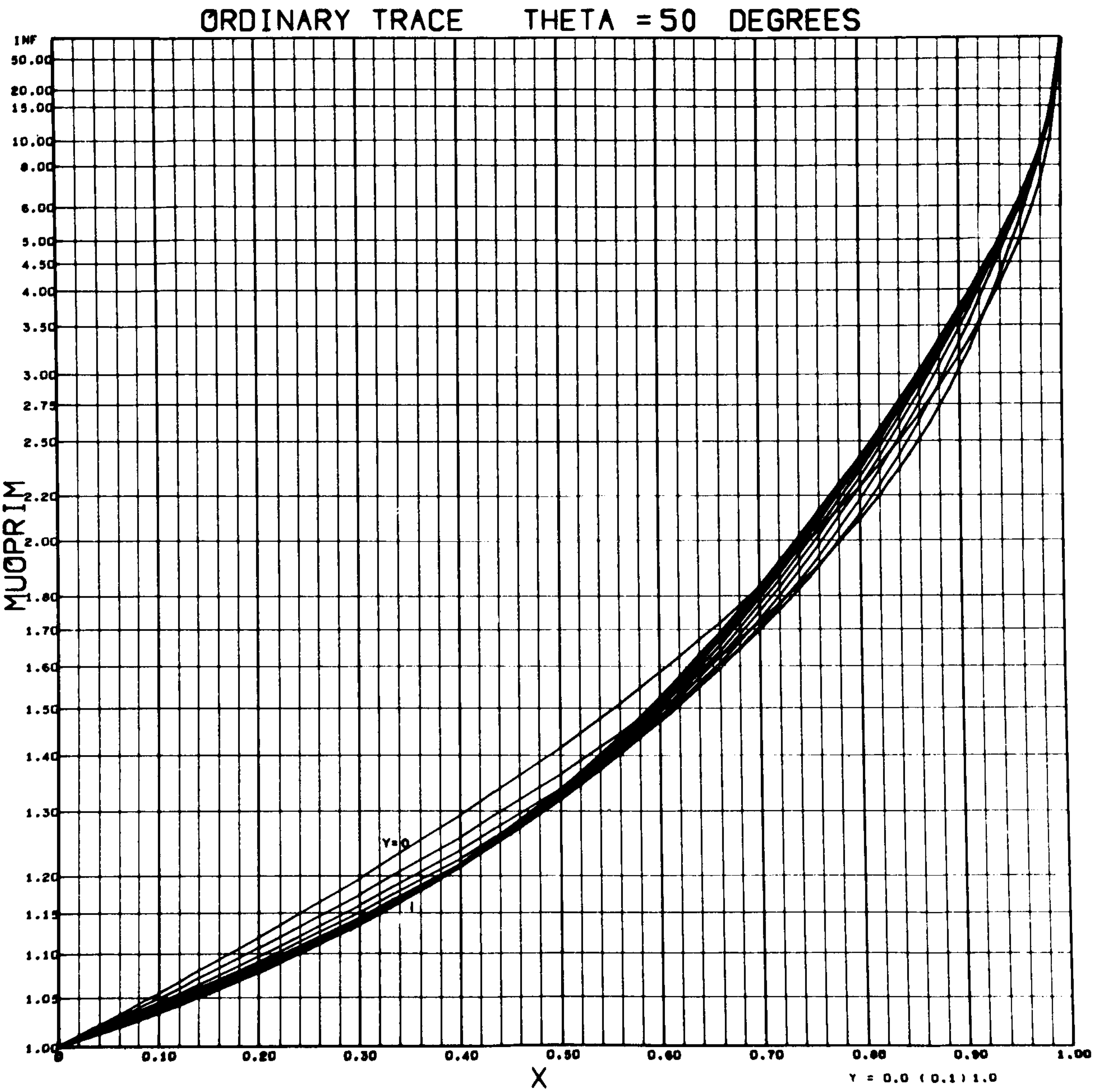

Figure 48.- Variation of μ' vs. X; Y = 0 - 1.0; $\theta = 50^{\circ}$.

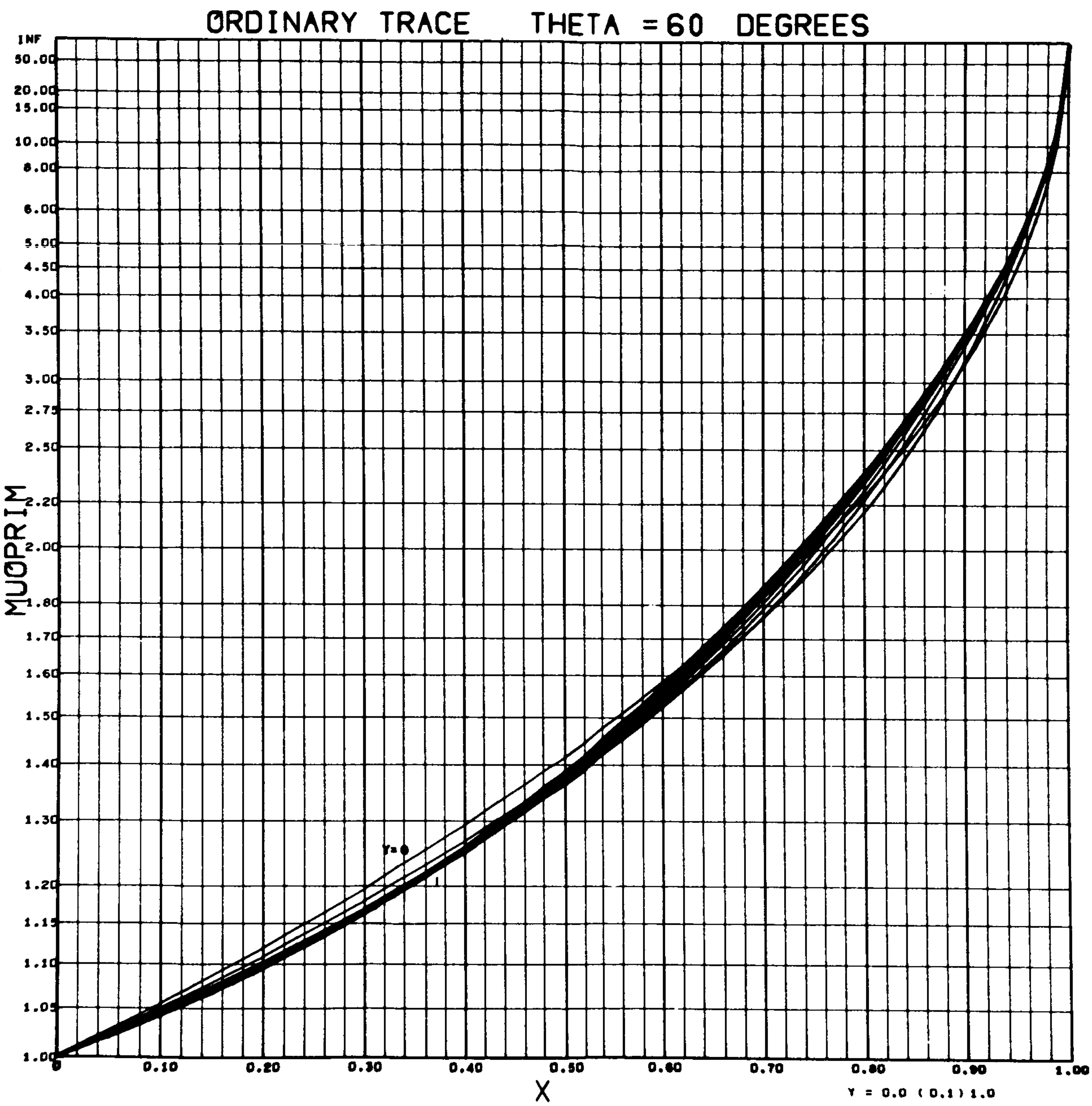

Figure 49.- Variation of μ' vs. X; Y = 0 - 1.0; $\theta = 60^{\circ}$.

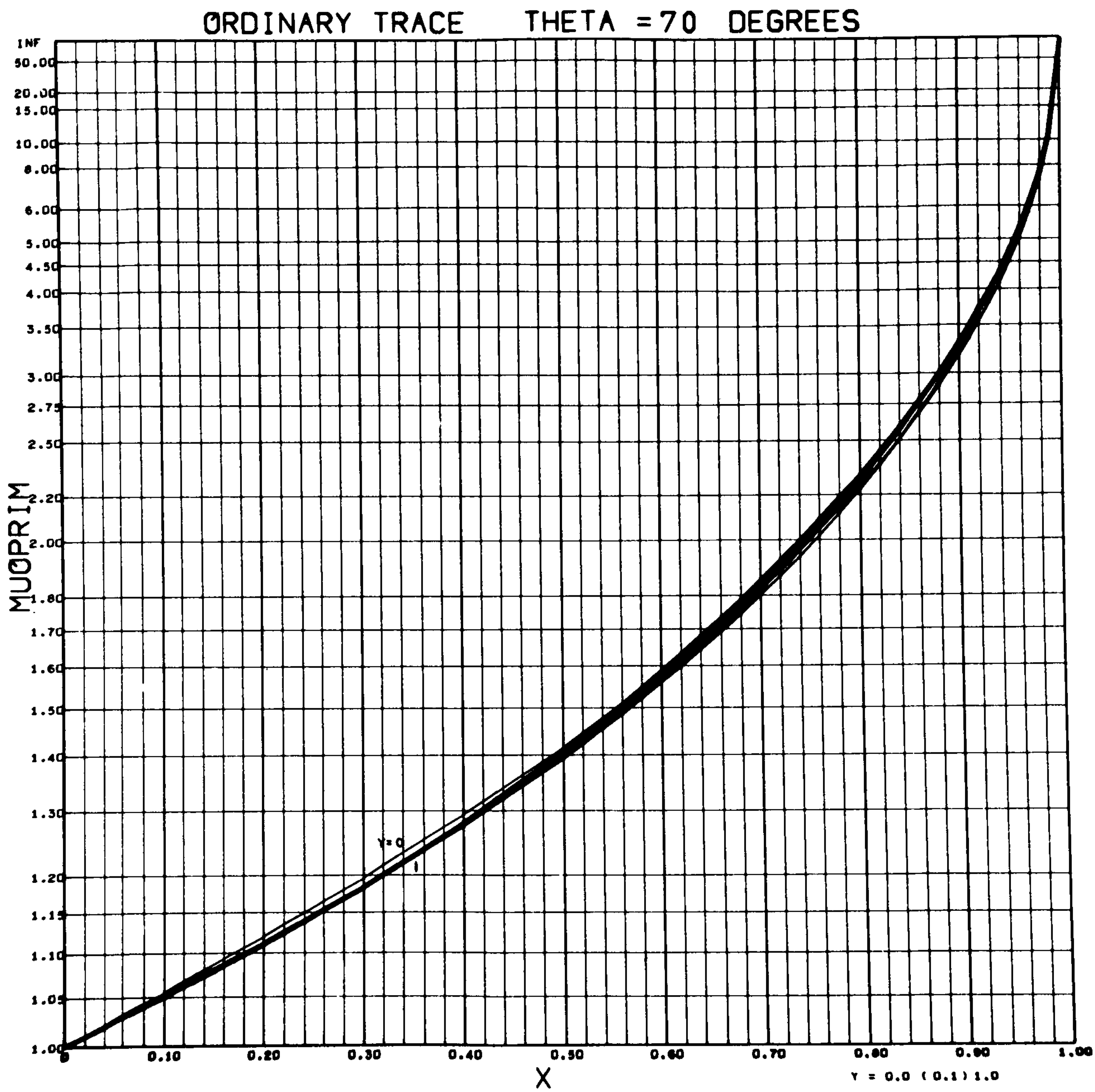

Figure 50.- Variation of μ' vs. X; Y = 0 - 1.0; $\theta = 70^{\circ}$.

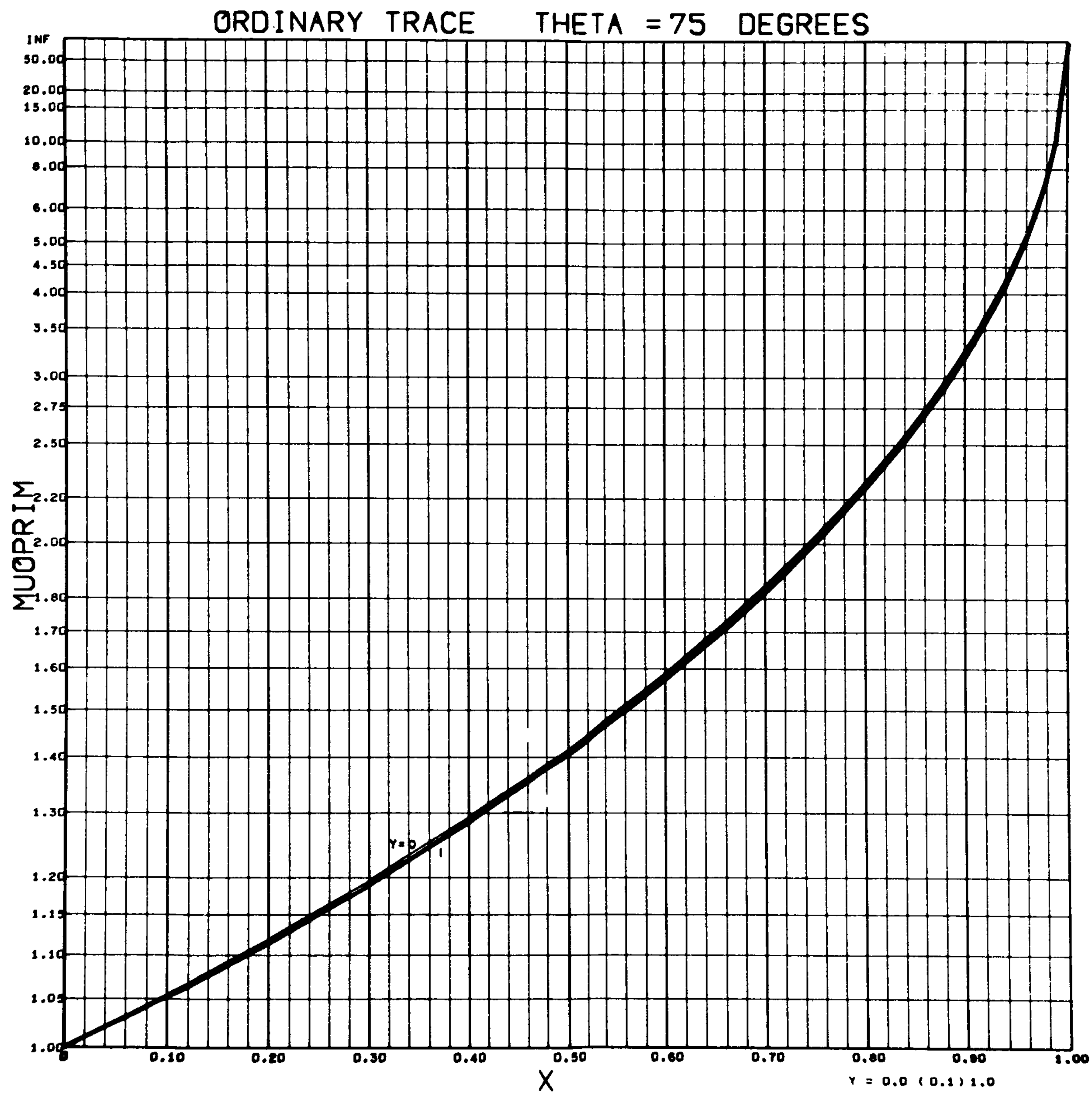

Figure 51.- Variation of μ' vs. X; Y = 0 - 1.0; $\theta = 75^{\circ}$.

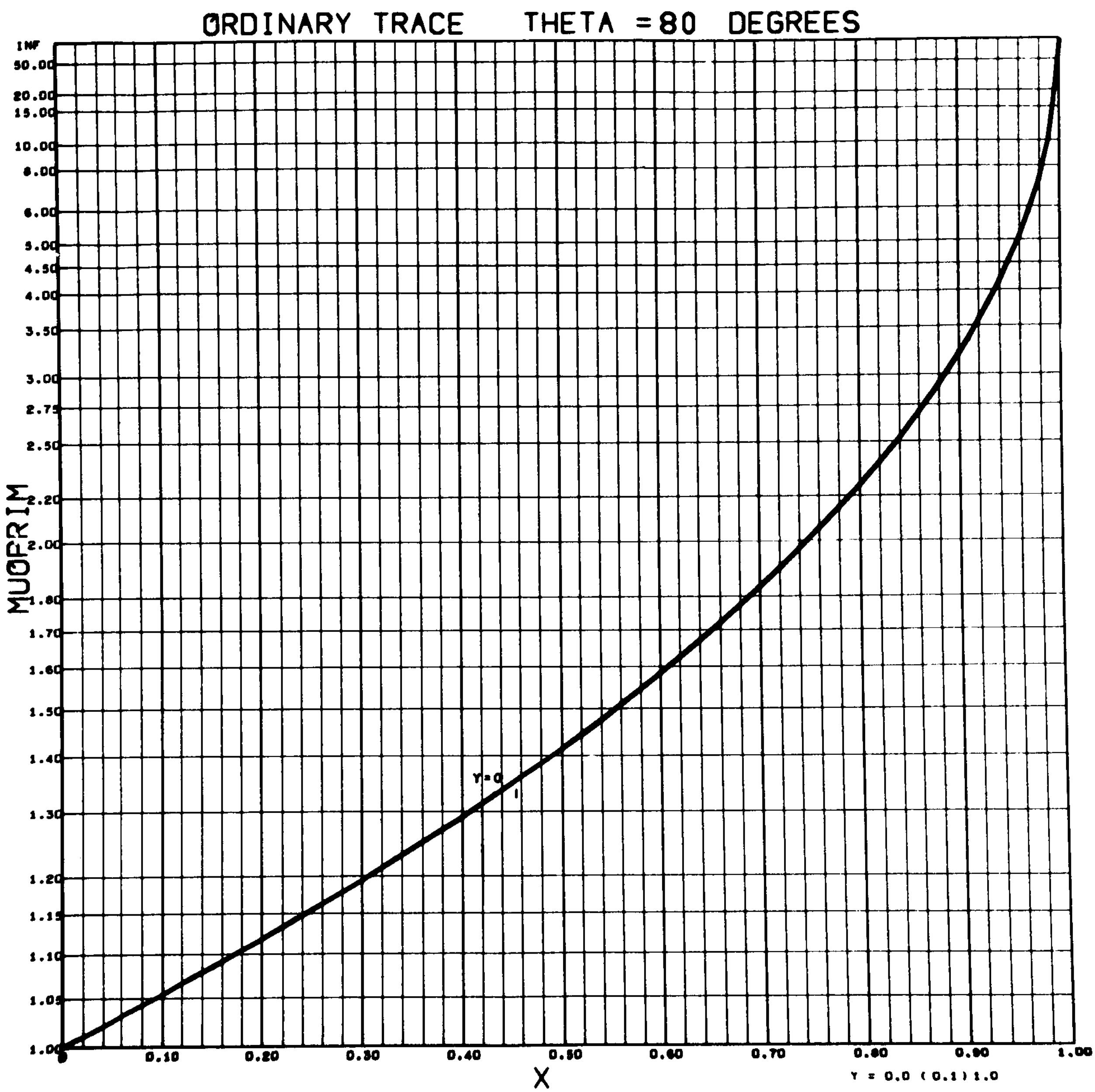

Figure 52.- Variation of μ' vs. X; Y = 0 - 1.0; $\theta = 80^{\circ}$.

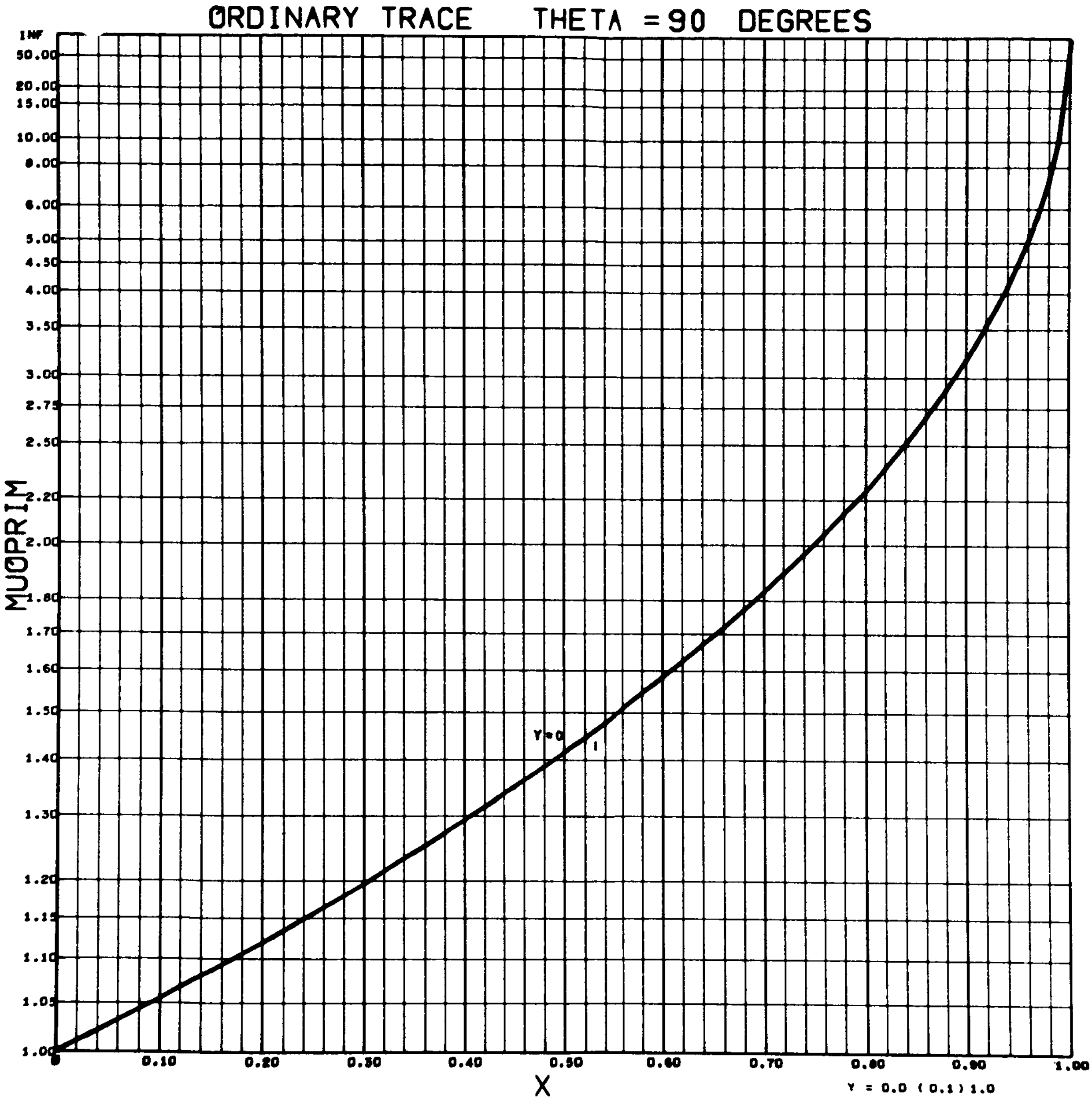

Figure 53.- Variation of μ' vs. X; Y = 0 - 1.0; $\theta = 90^{\circ}$.

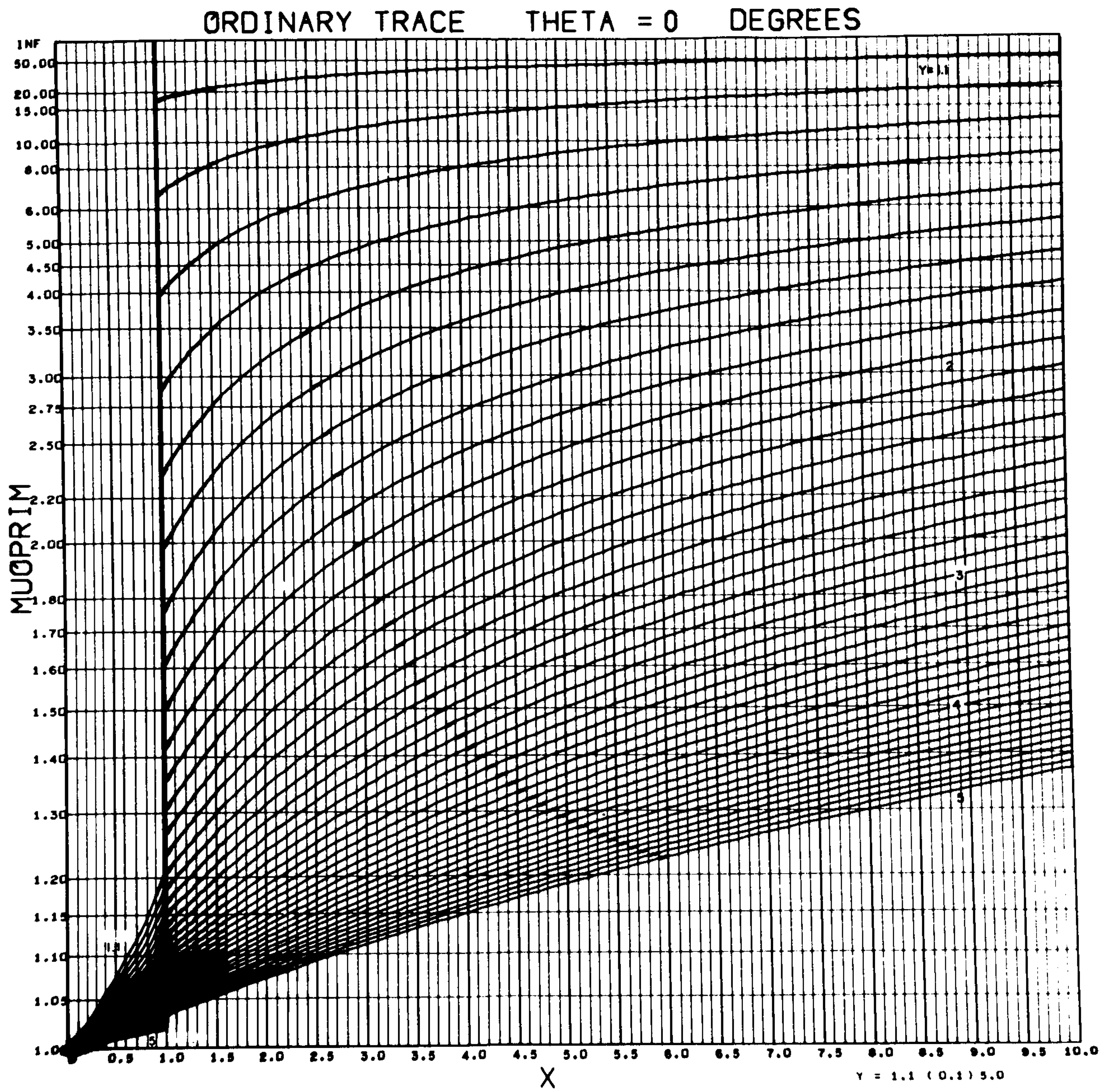

Figure 54.- Variation of μ' vs. X; Y = 1.1 - 5.0; θ = 0.

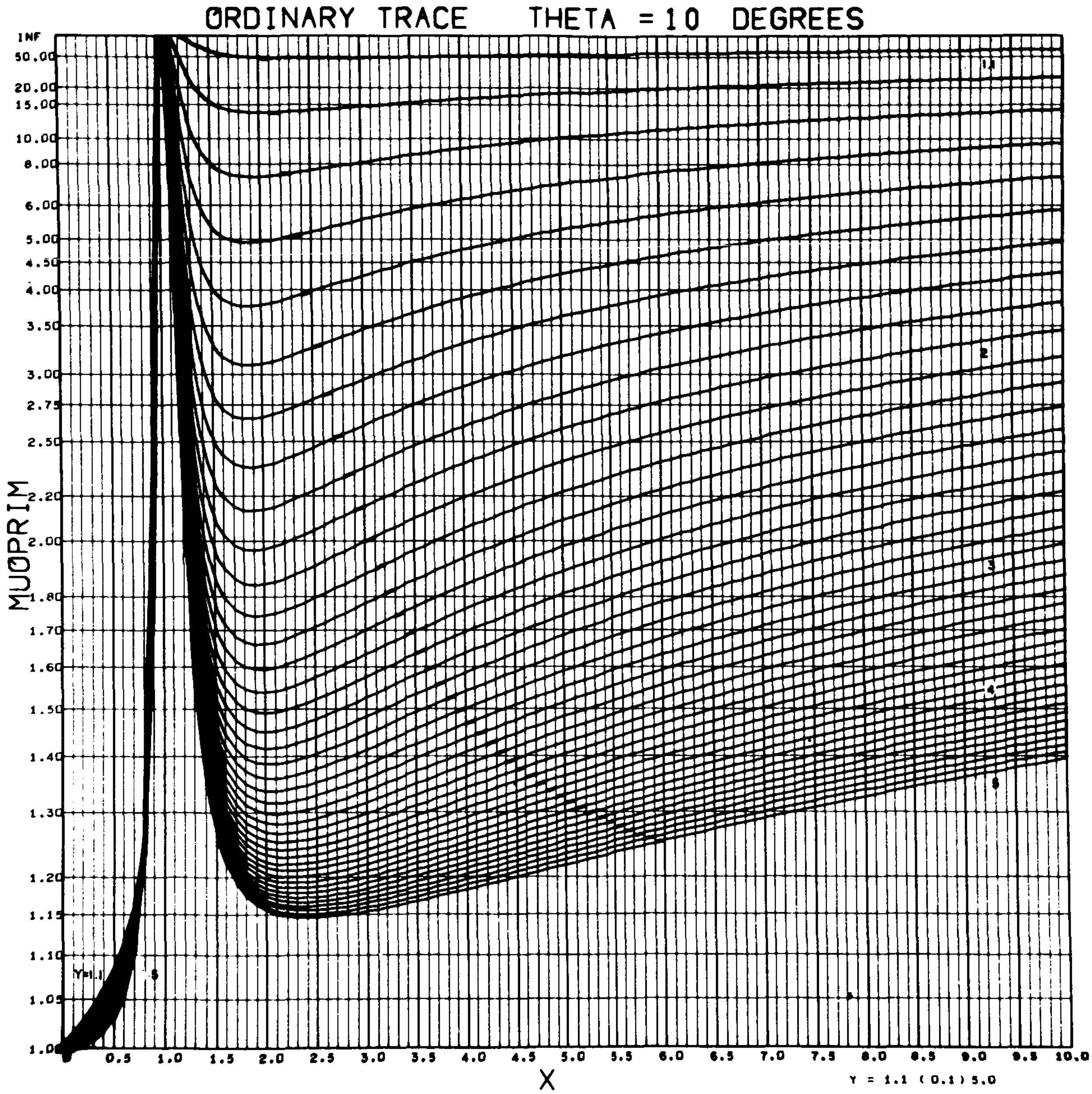

Figure 55.- Variation of μ' vs. X; Y = 1.1 - 5.0; $\theta = 10^{\circ}$.

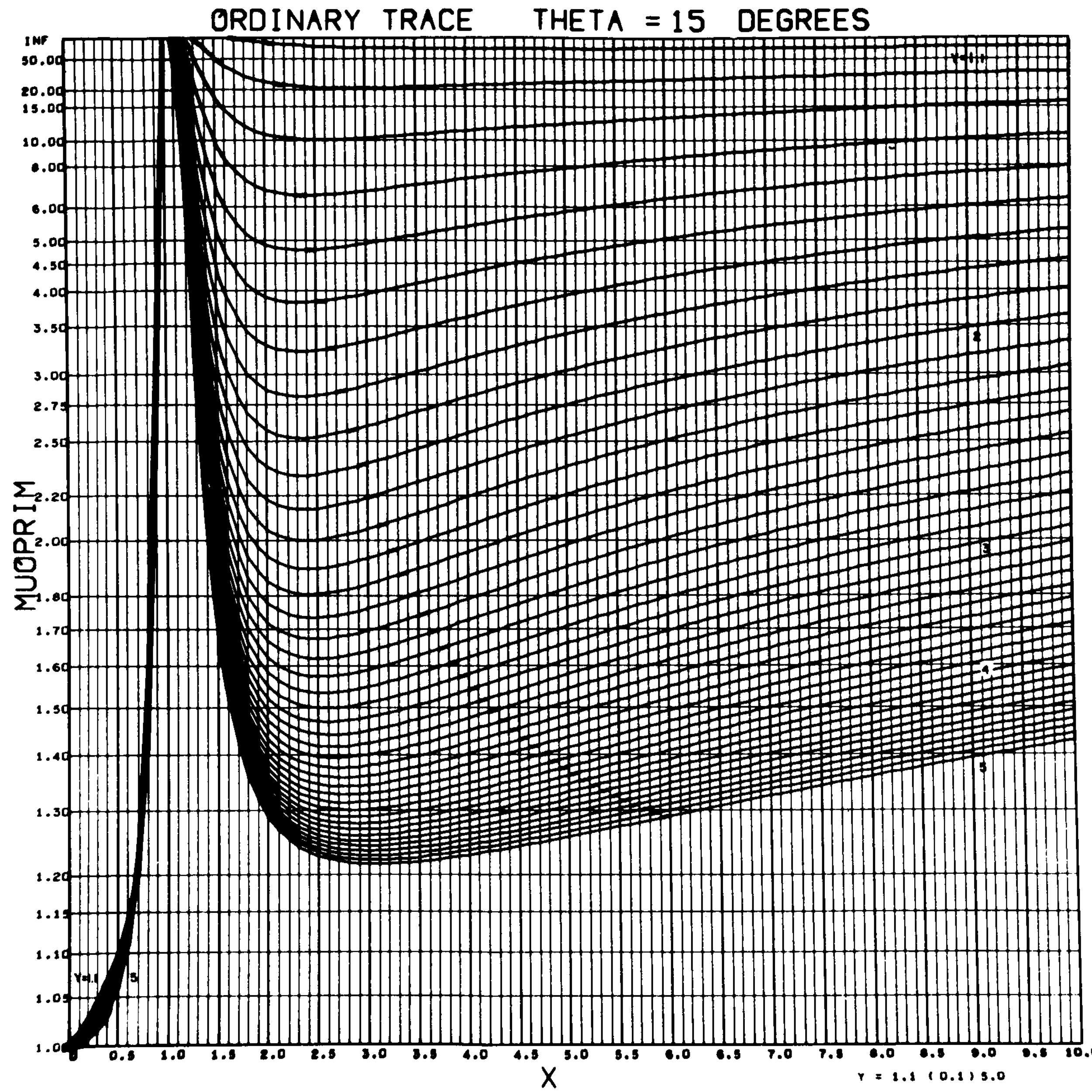

Figure 56.- Variation of μ' vs. X; Y = 1.1 - 5.0; $\theta = 15^{\circ}$.

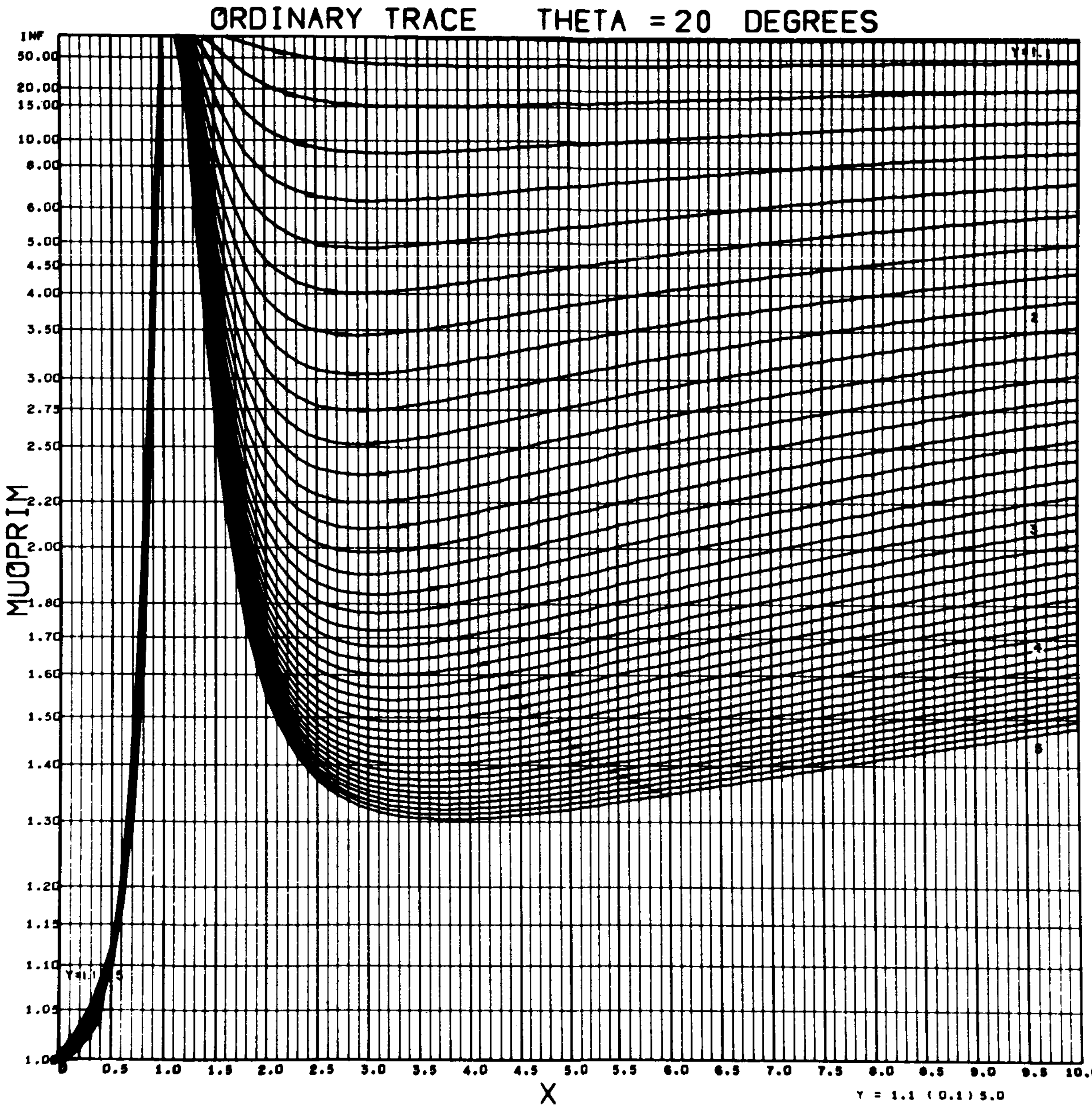

Figure 57.- Variation of μ' vs. X; Y = 1.1 - 5.0; $\theta = 20^{\circ}$.

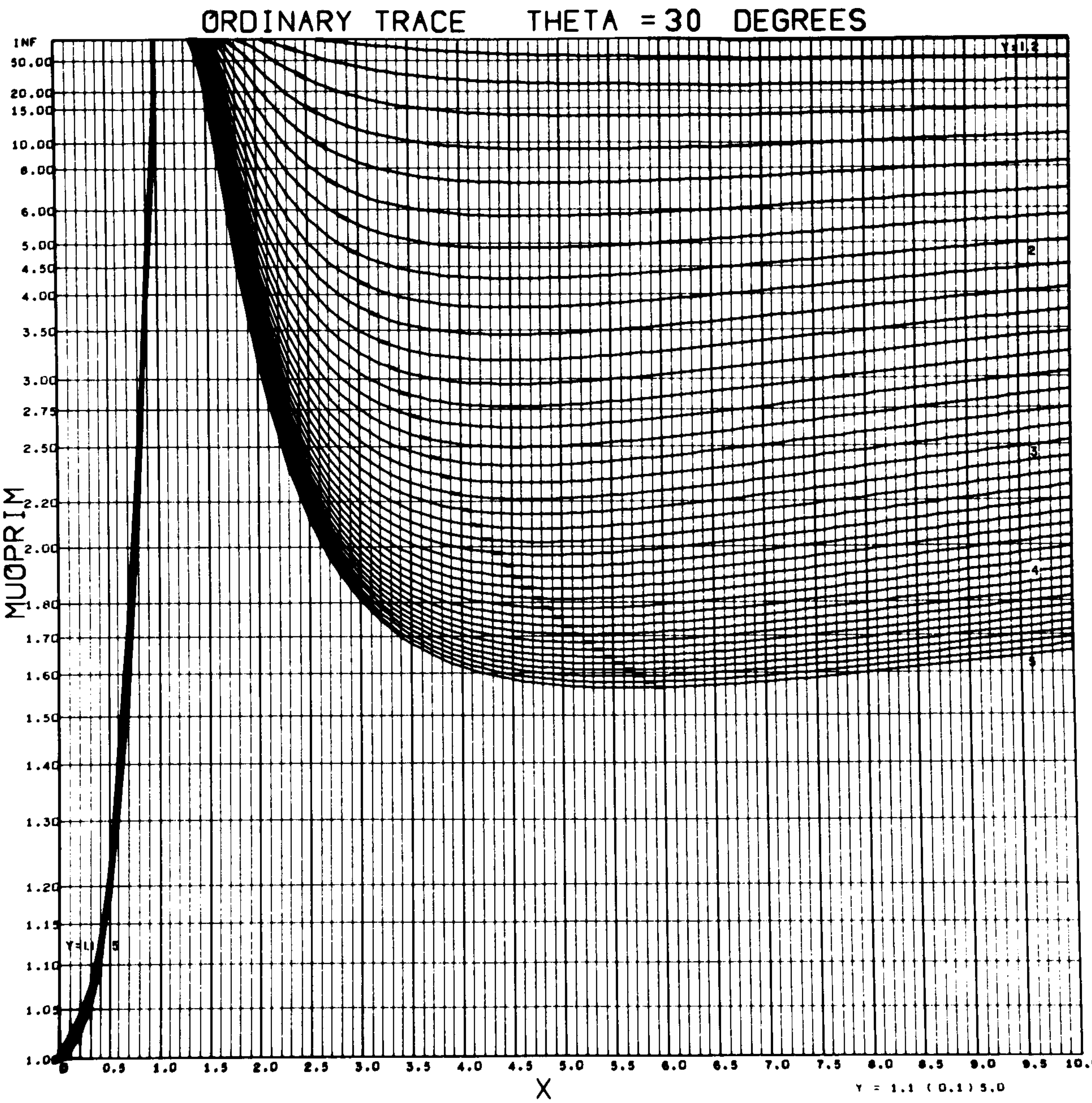

Figure 58.- Variation of μ' vs. X; Y = 1.1 - 5.0; θ = 30°.

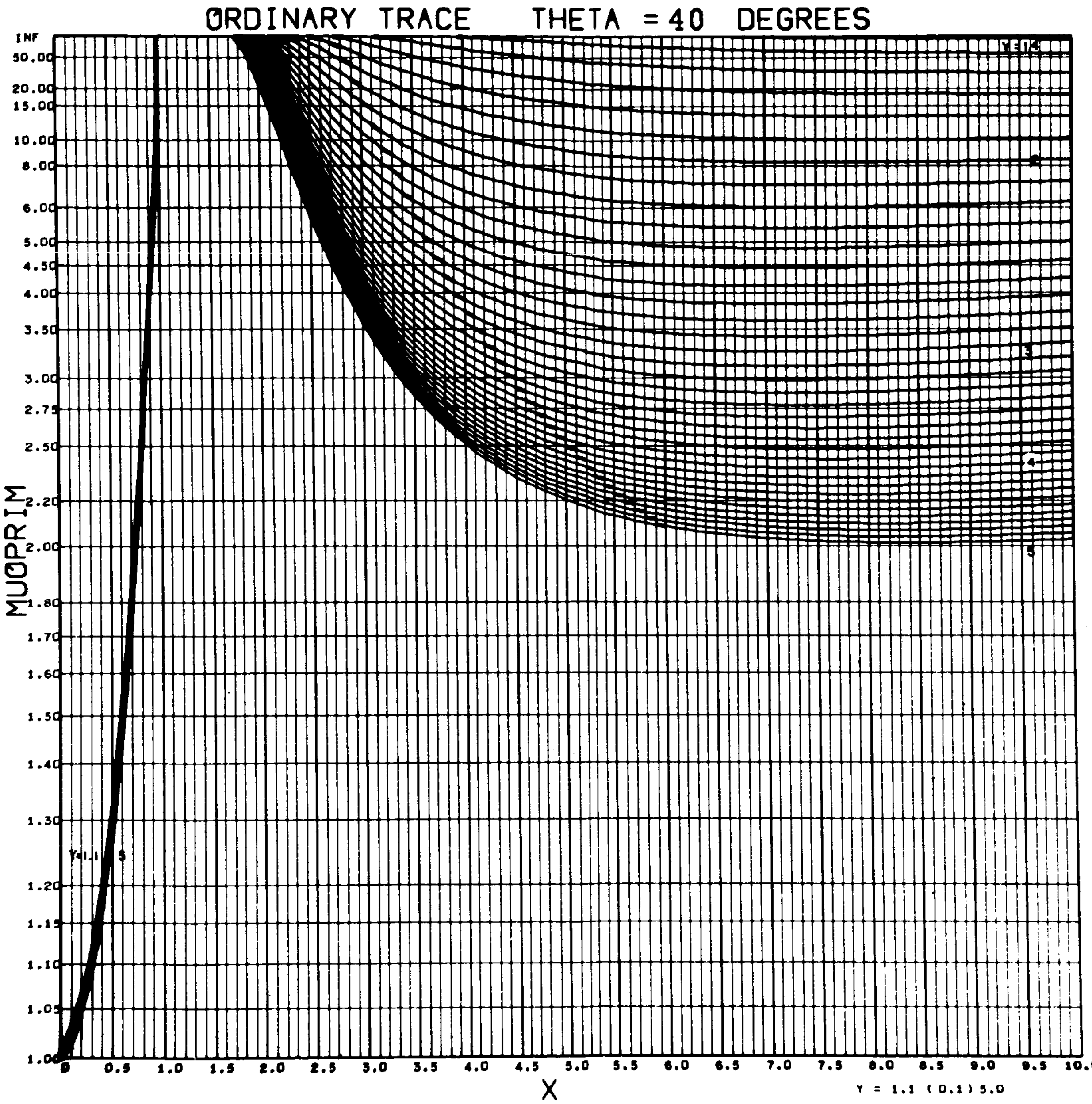

Figure 59.- Variation of μ' vs. X; Y = 1.1 - 5.0; $\theta = 40^{\circ}$.

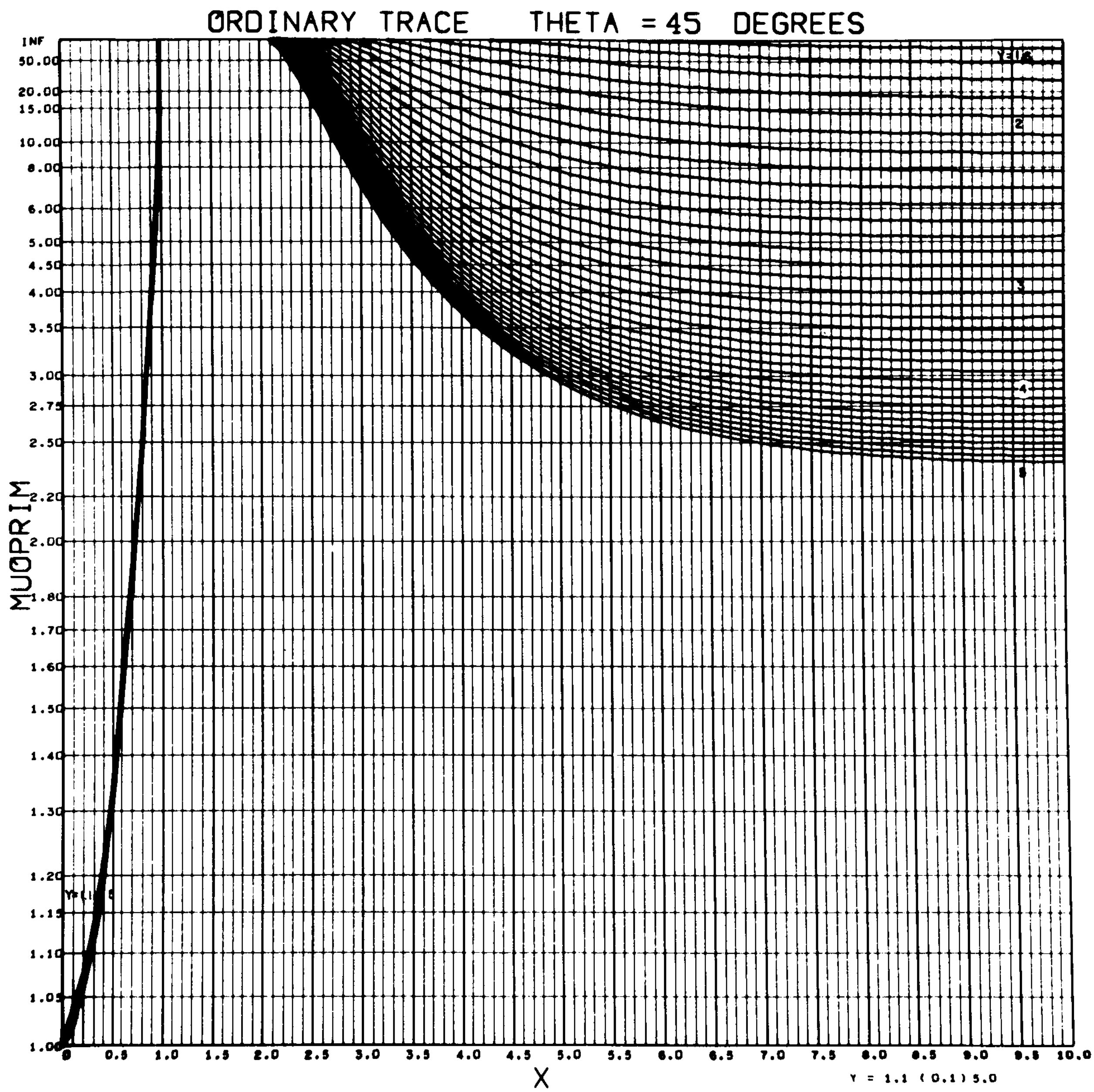

Figure 60.- Variation of μ' vs. X; Y = 1.1 - 5.0; $\theta = 45^{\circ}$.

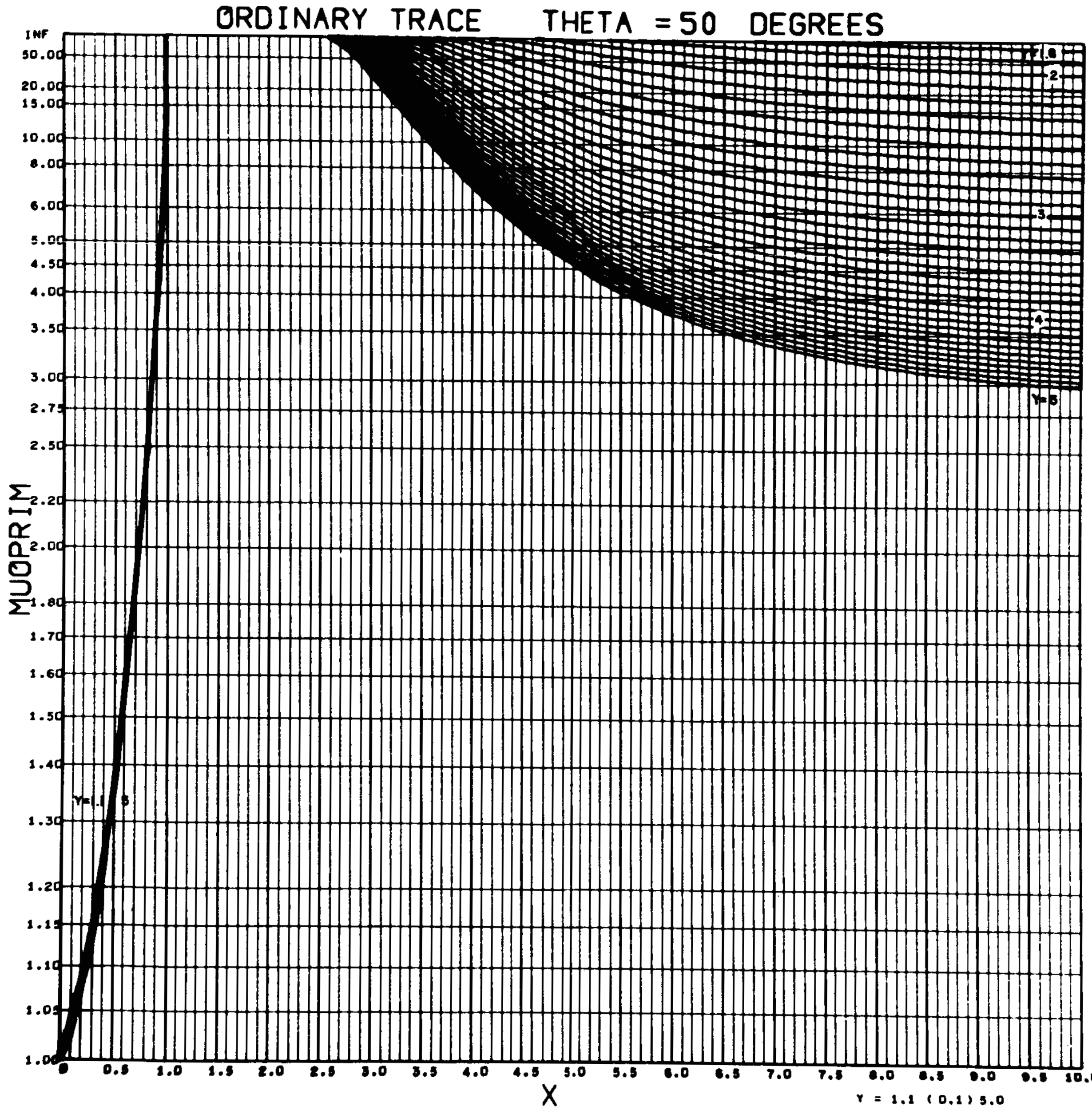

Figure 61.- Variation of μ' vs. X; Y = 1.1 - 5.0; $\theta = 50^{\circ}$.

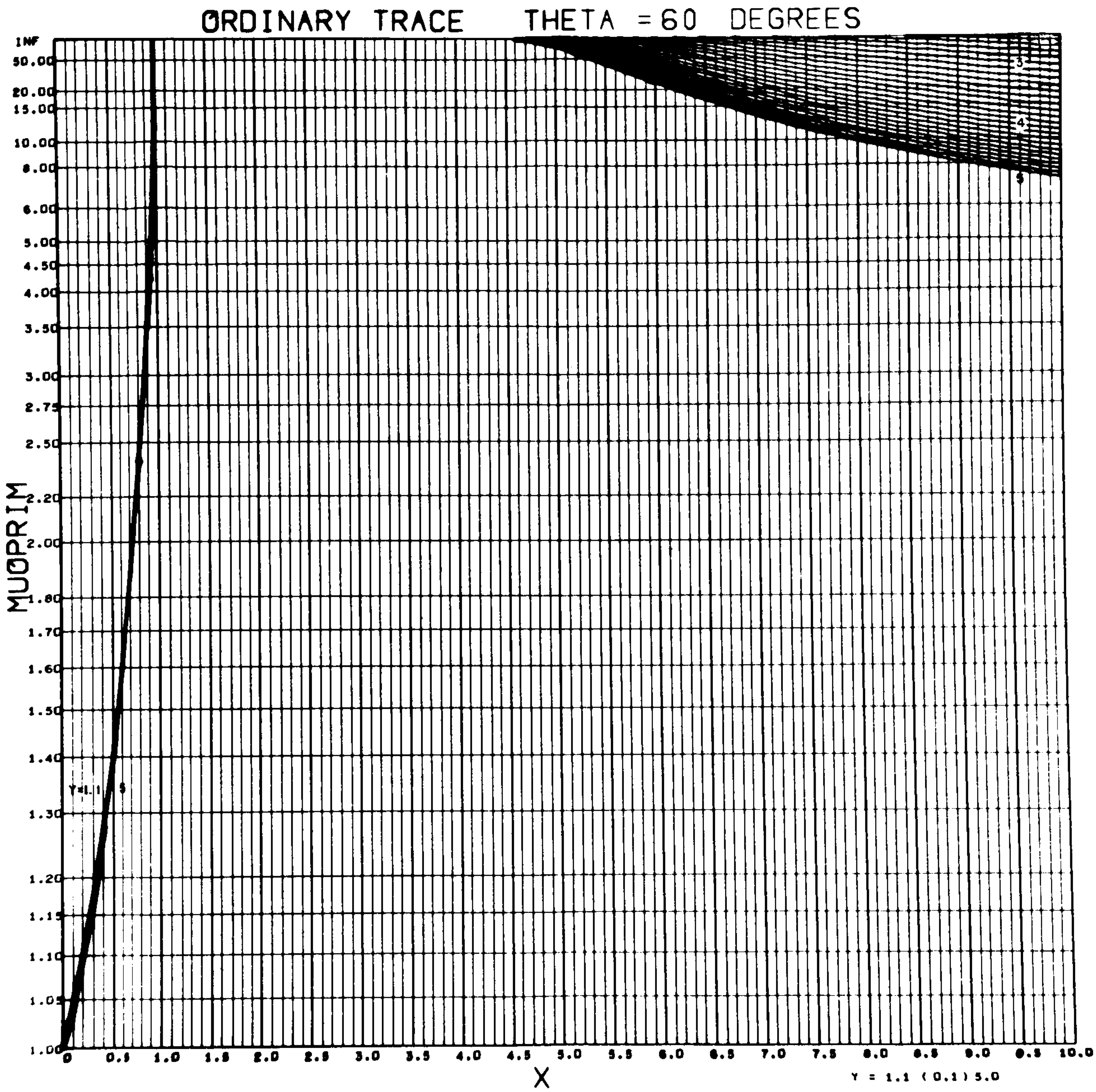

Figure 62.- Variation of μ' vs. X; Y = 1.1 - 5.0; $\theta = 60^\circ$.

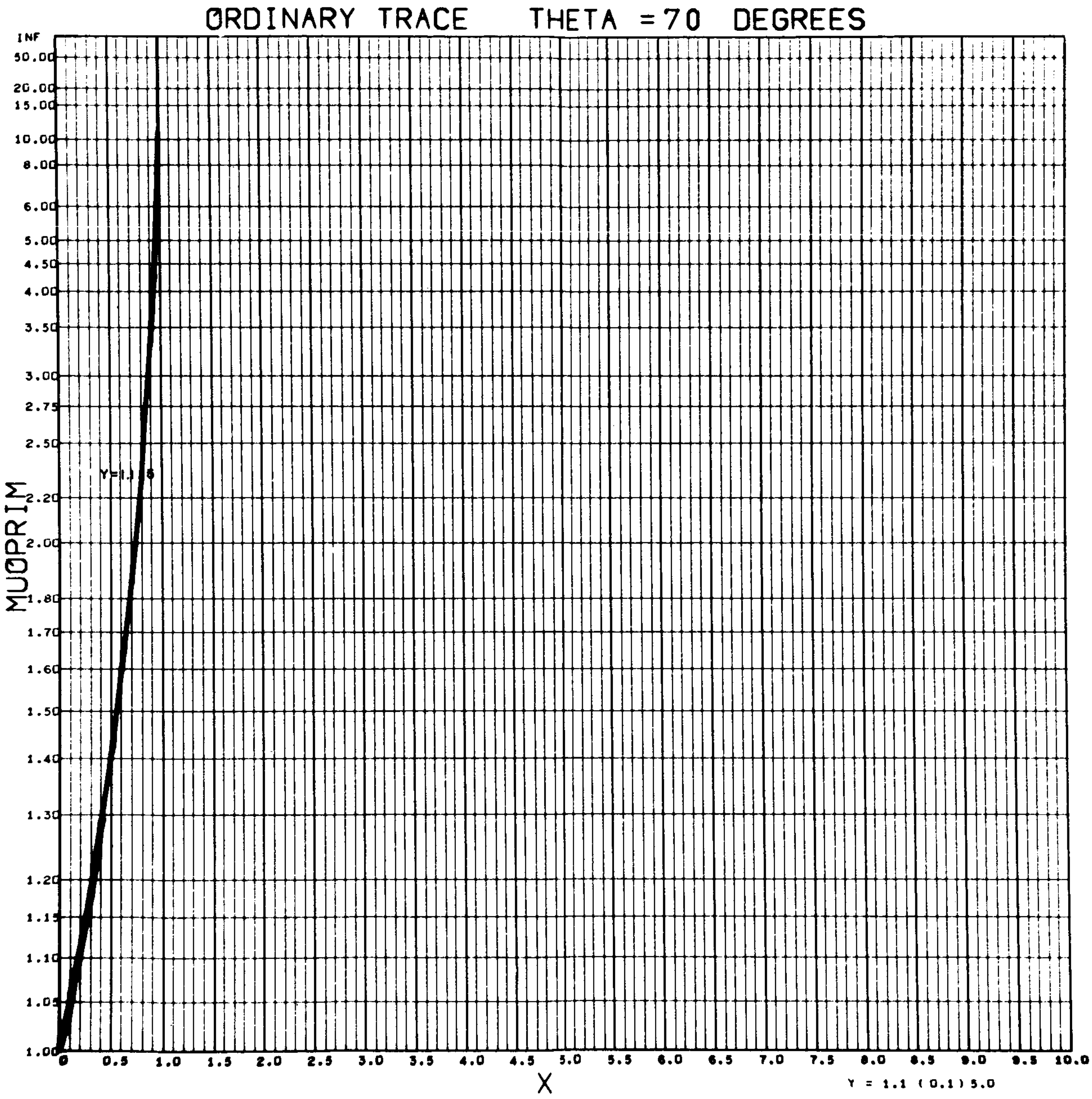

Figure 63.- Variation of μ' vs. X; Y = 1.1 - 5.0; θ = 70°.

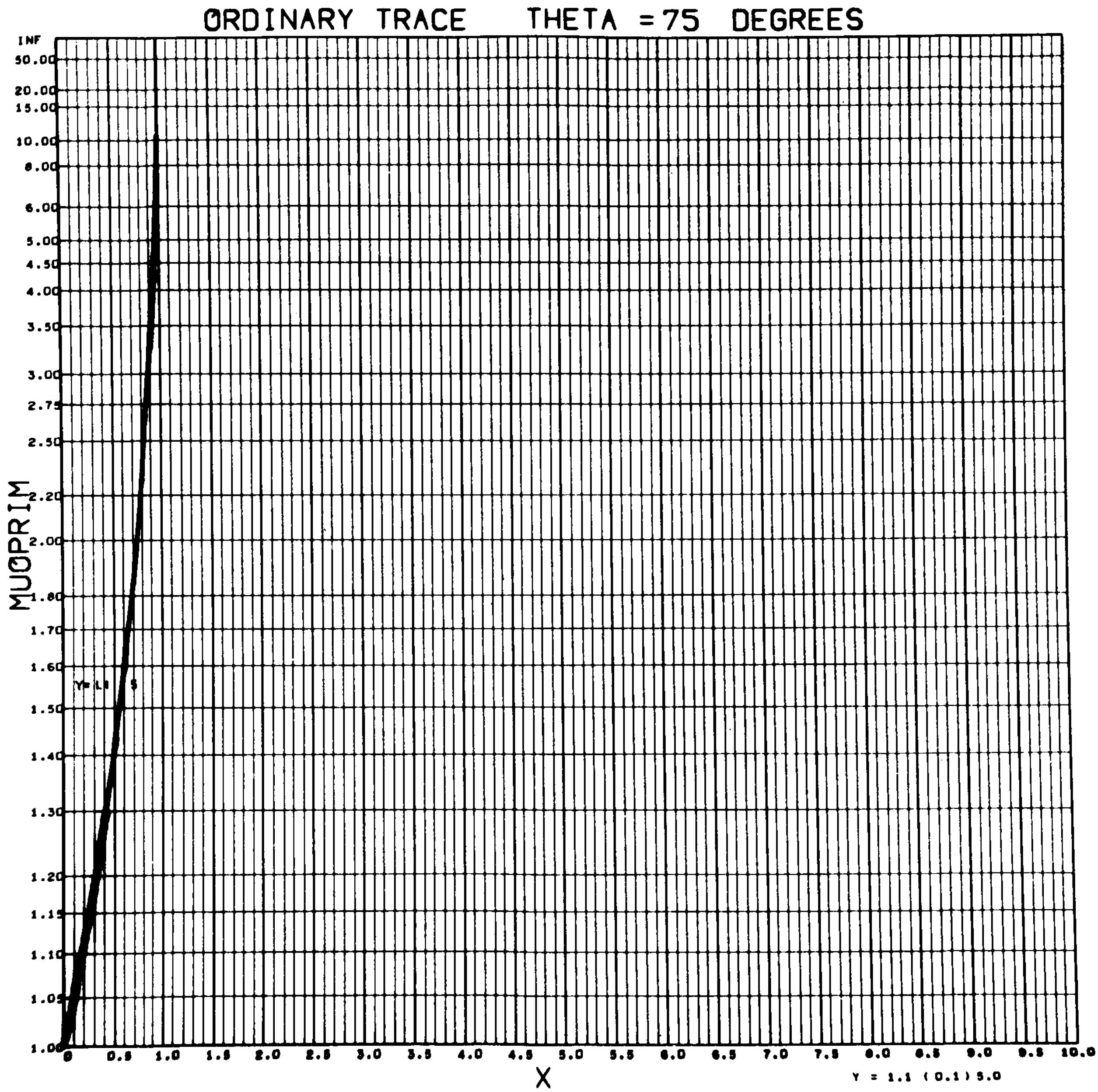

Figure 64.- Variation of μ' vs. X; Y = 1.1 - 5.0; $\theta = 75^{\circ}$.

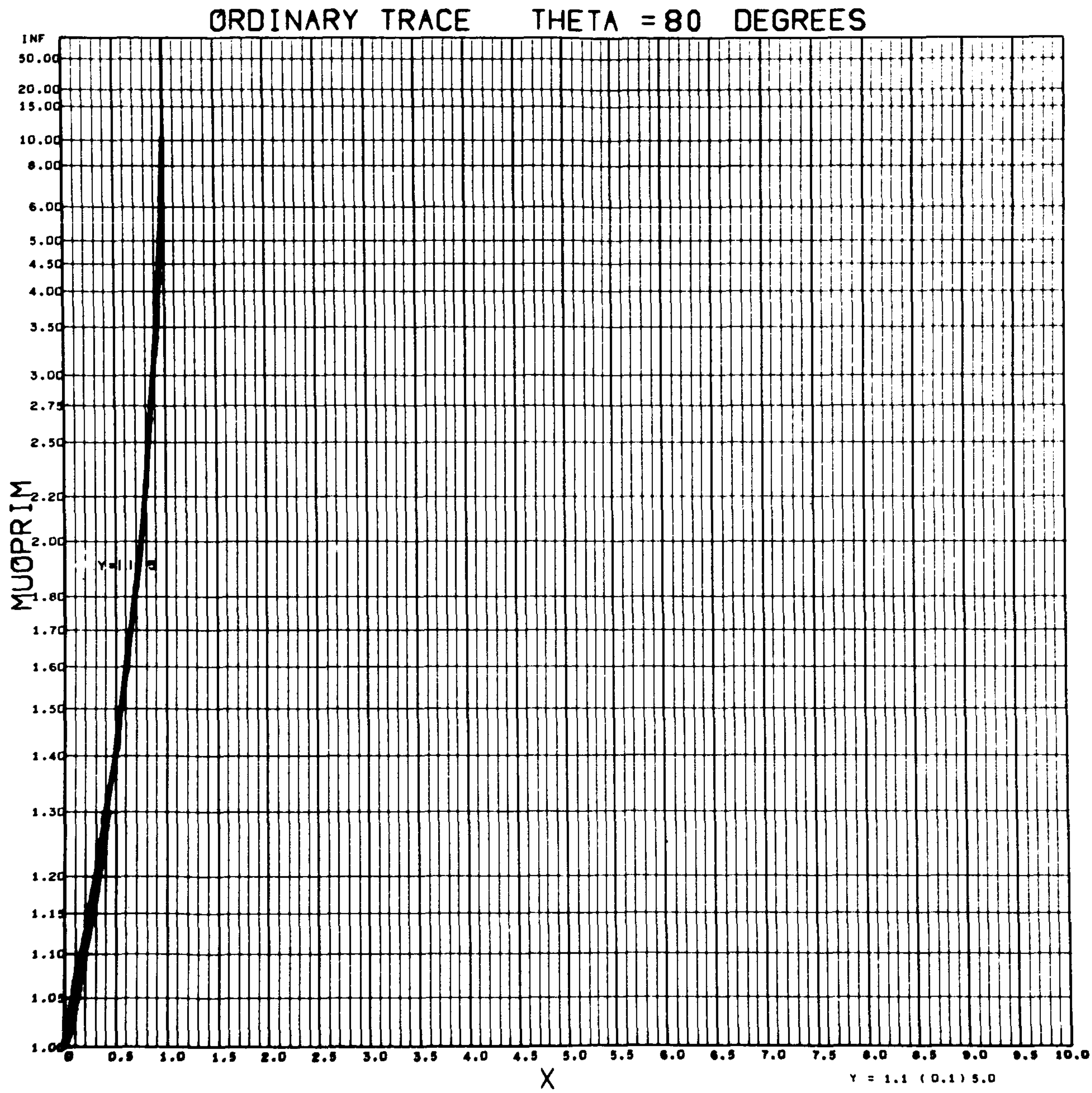

Figure 65.- Variation of μ' vs. X; Y = 1.1 - 5.0; θ = 80°.

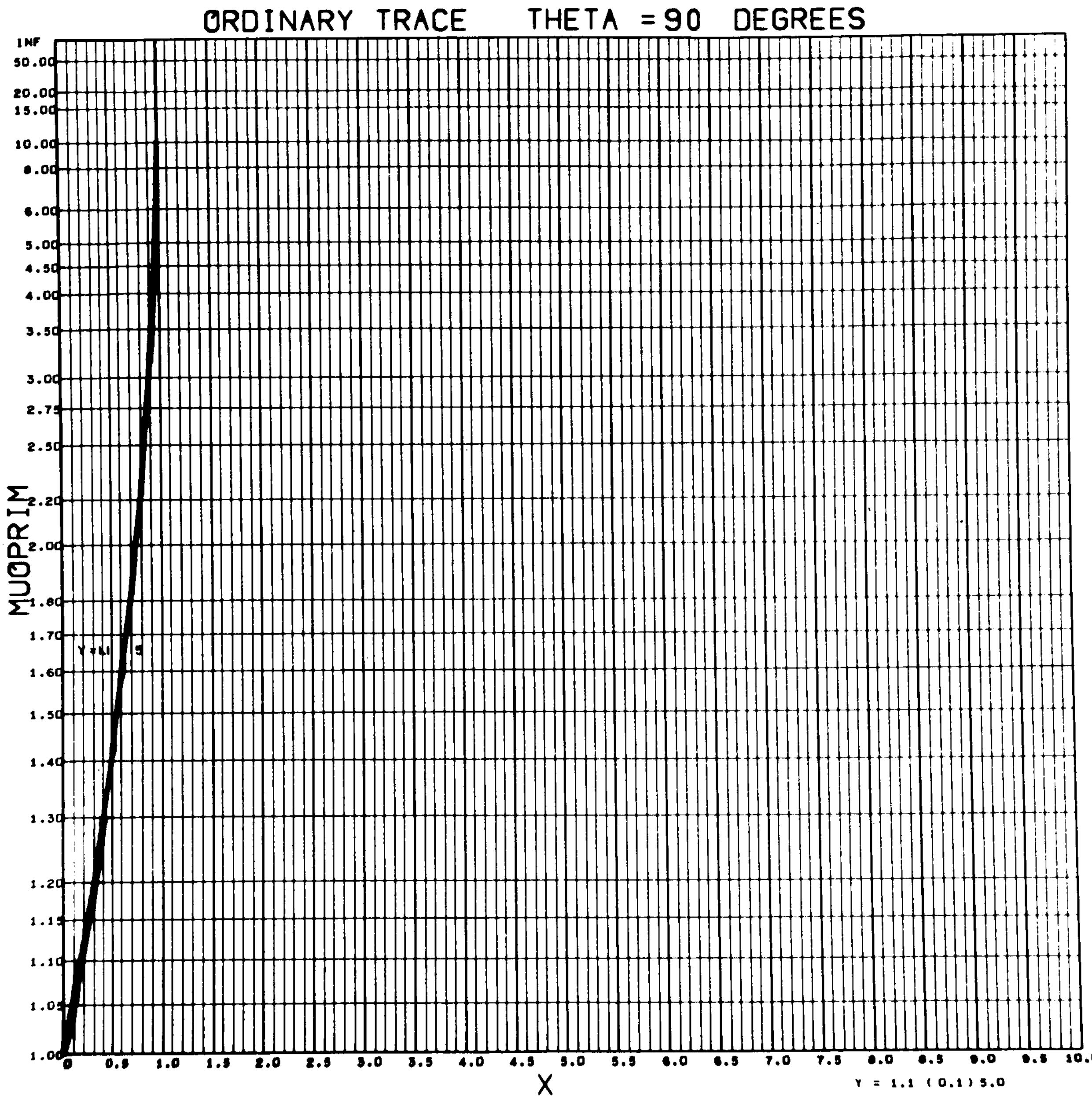

Figure 66.- Variation of μ' vs. X; Y = 1.1 - 5.0; θ = 90°.

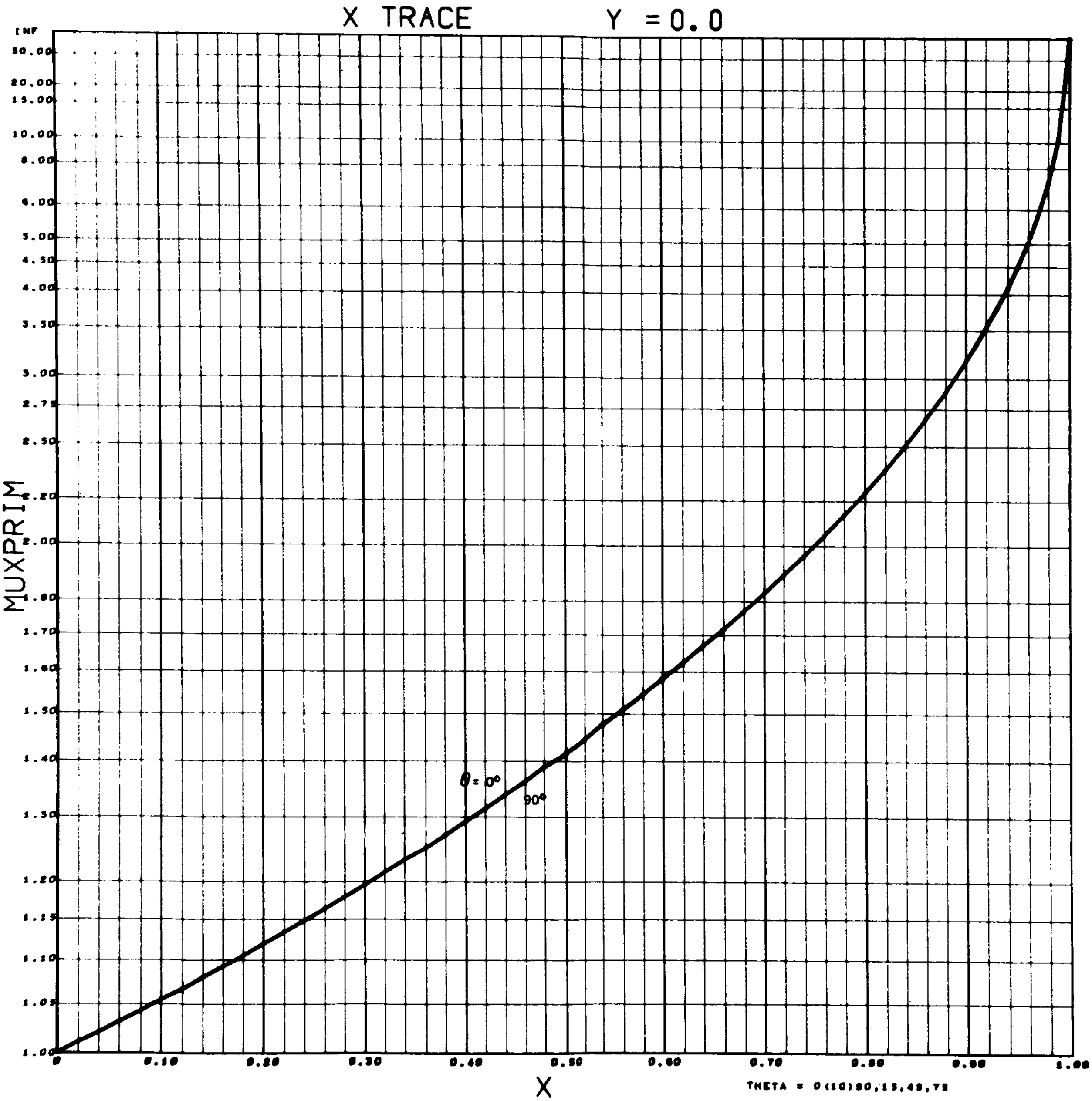

Figure 67.- Variation of μ' vs. X; Y = 0; θ = 0° - 90°.

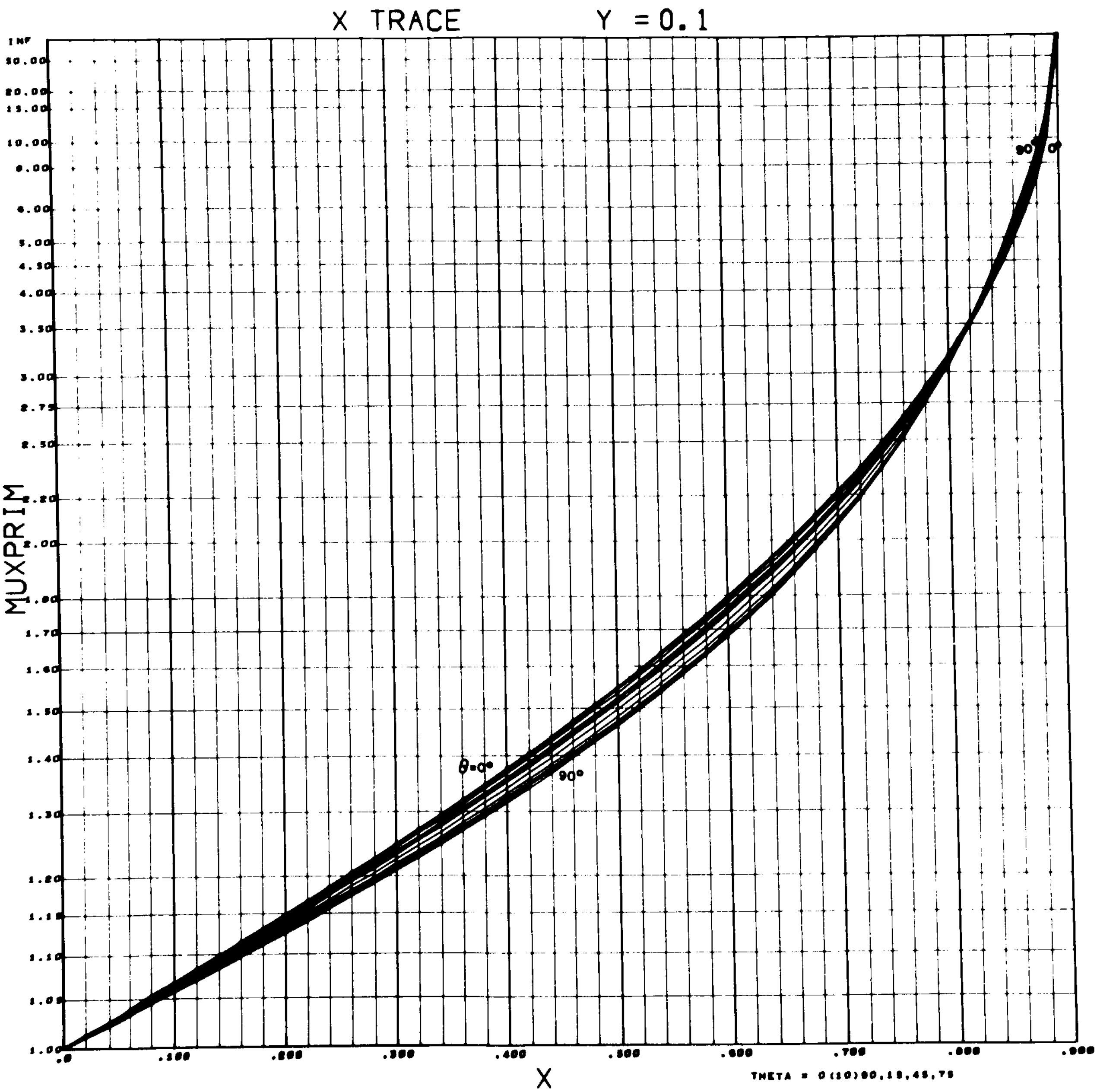

Figure 68.- Variation of μ' vs. X; Y = 0.1; θ = 0° - 90°.

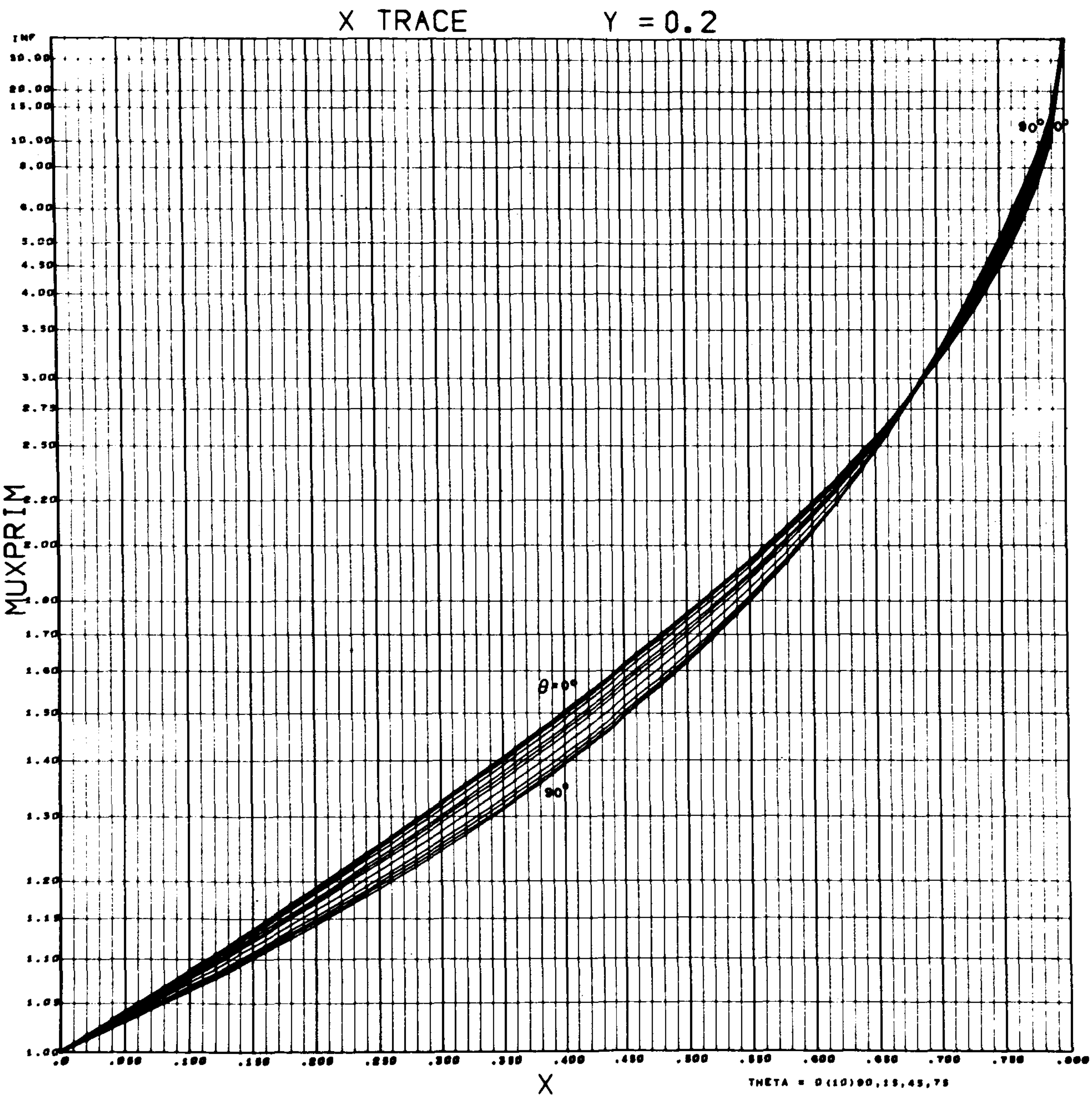

Figure 69.- Variation of μ' vs. X; Y = 0.2; θ = 0° - 90°.

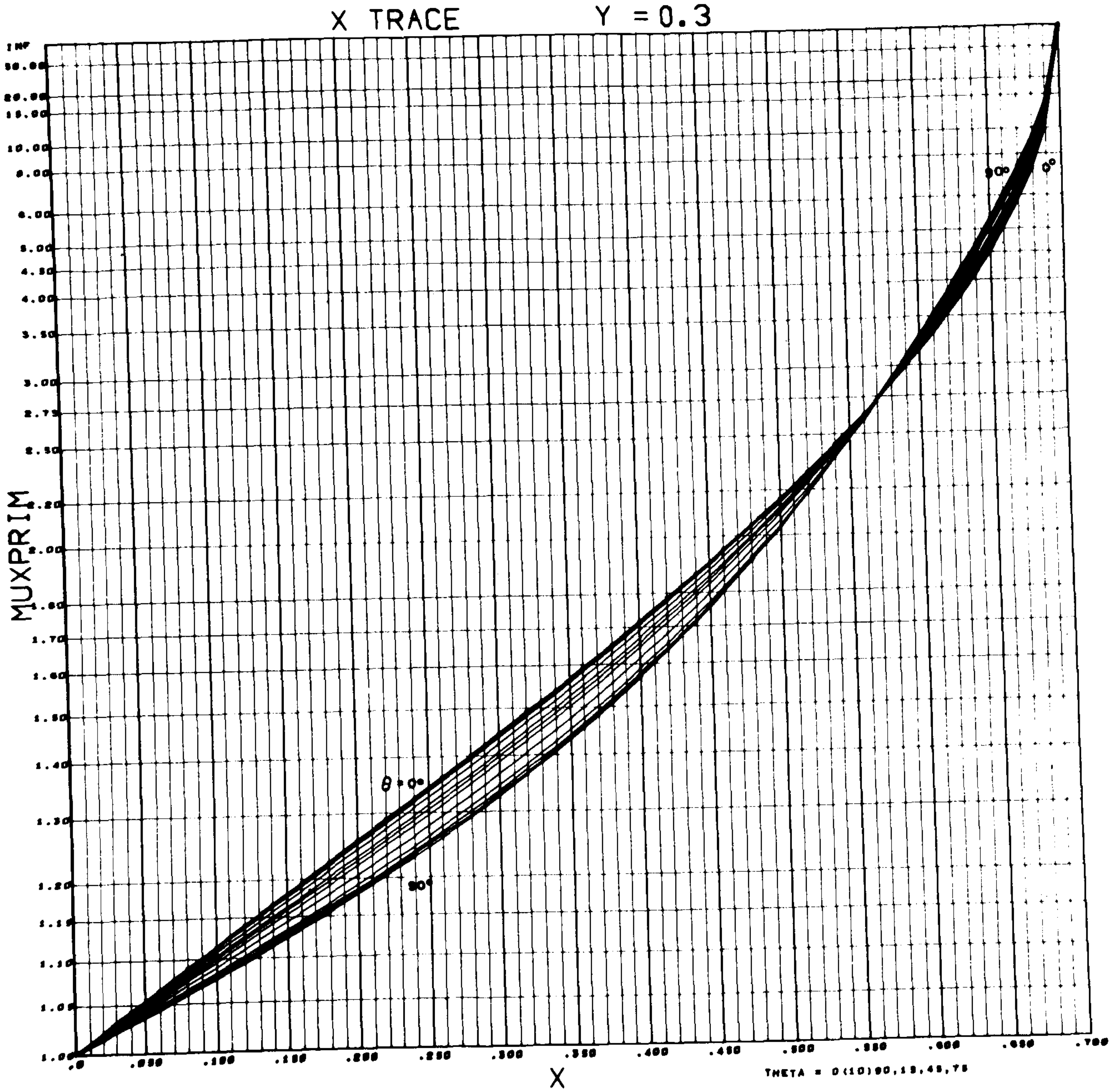

Figure 70.- Variation of μ' vs. X; Y = 0.3; θ = 0° - 90°.

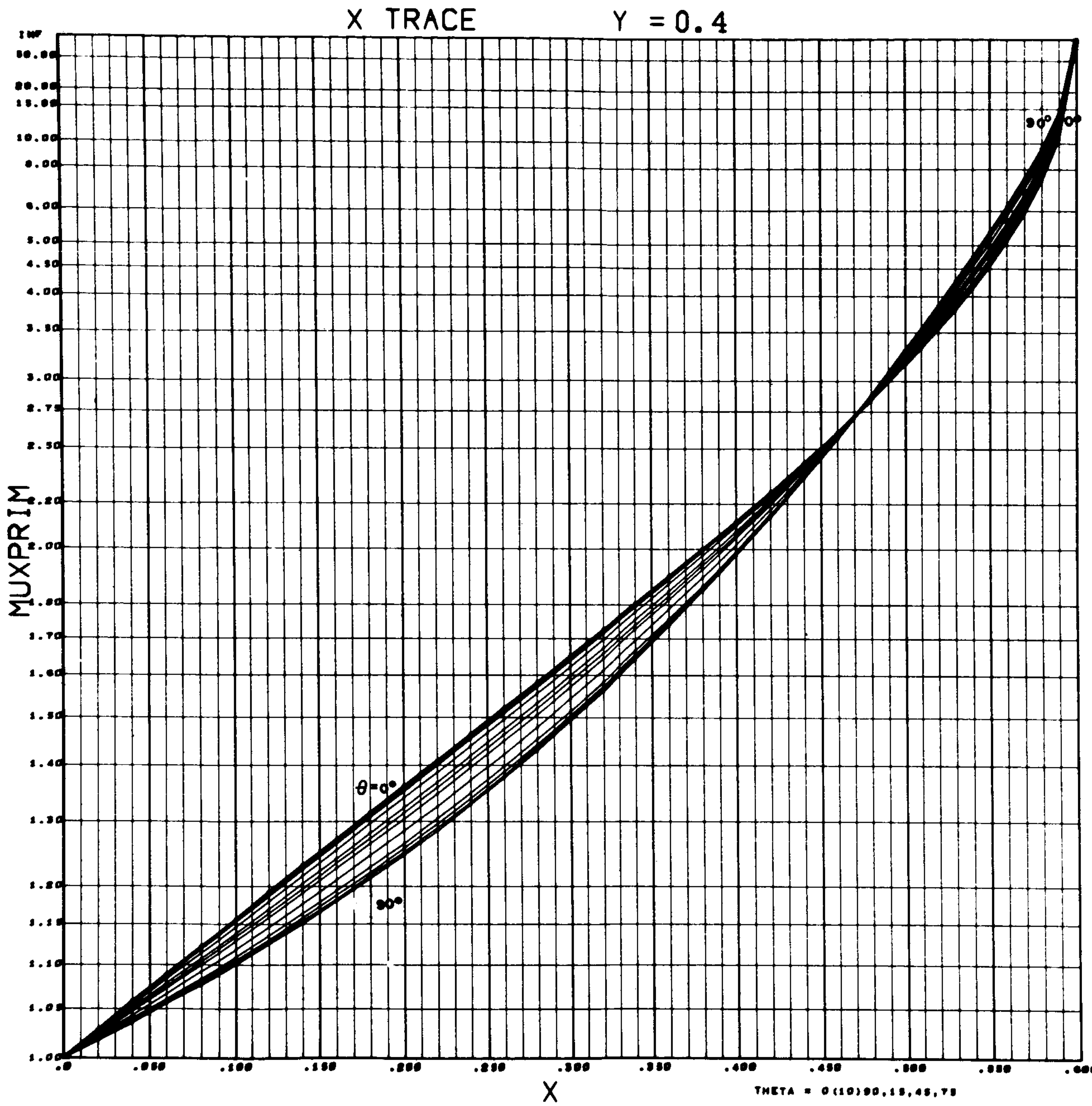

Figure 71.- Variation of μ' vs. X; Y = 0.4; θ = 0° - 90°.

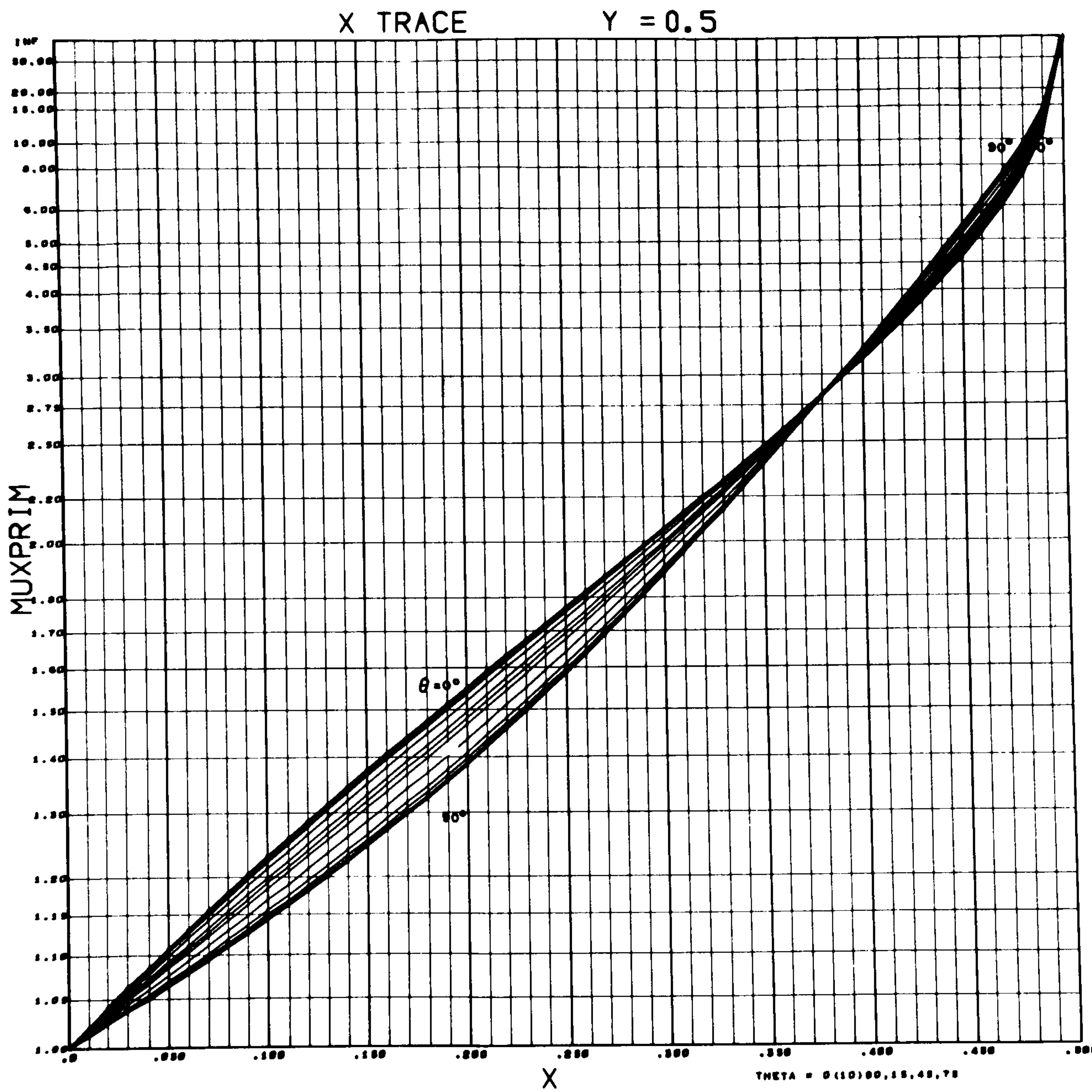

Figure 72.- Variation of μ' vs. X; Y = 0.5; θ = 0° - 90°.

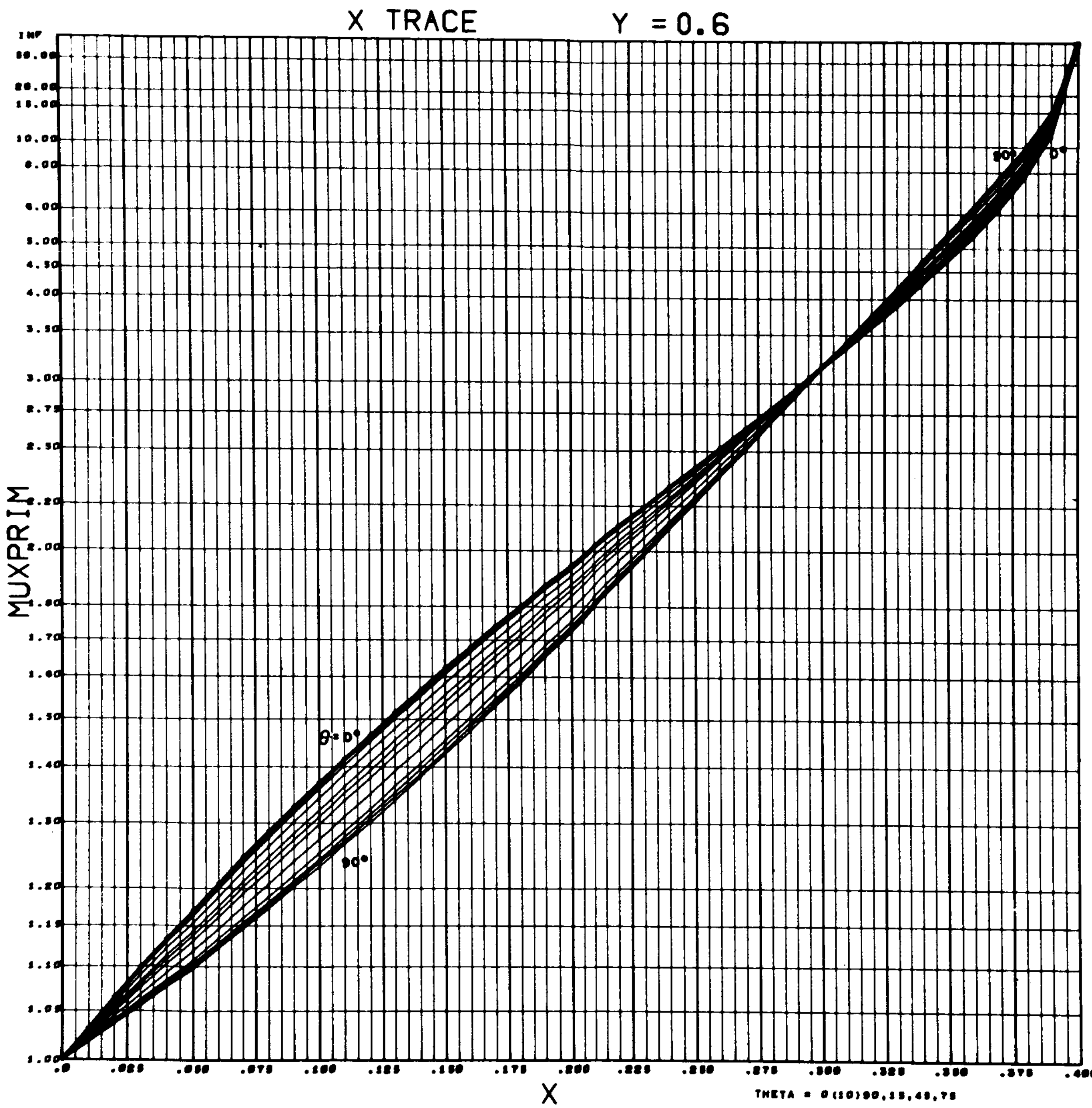

Figure 73.- Variation of μ' vs. X; Y = 0.6; $\theta = 0^{\circ} - 90^{\circ}$.

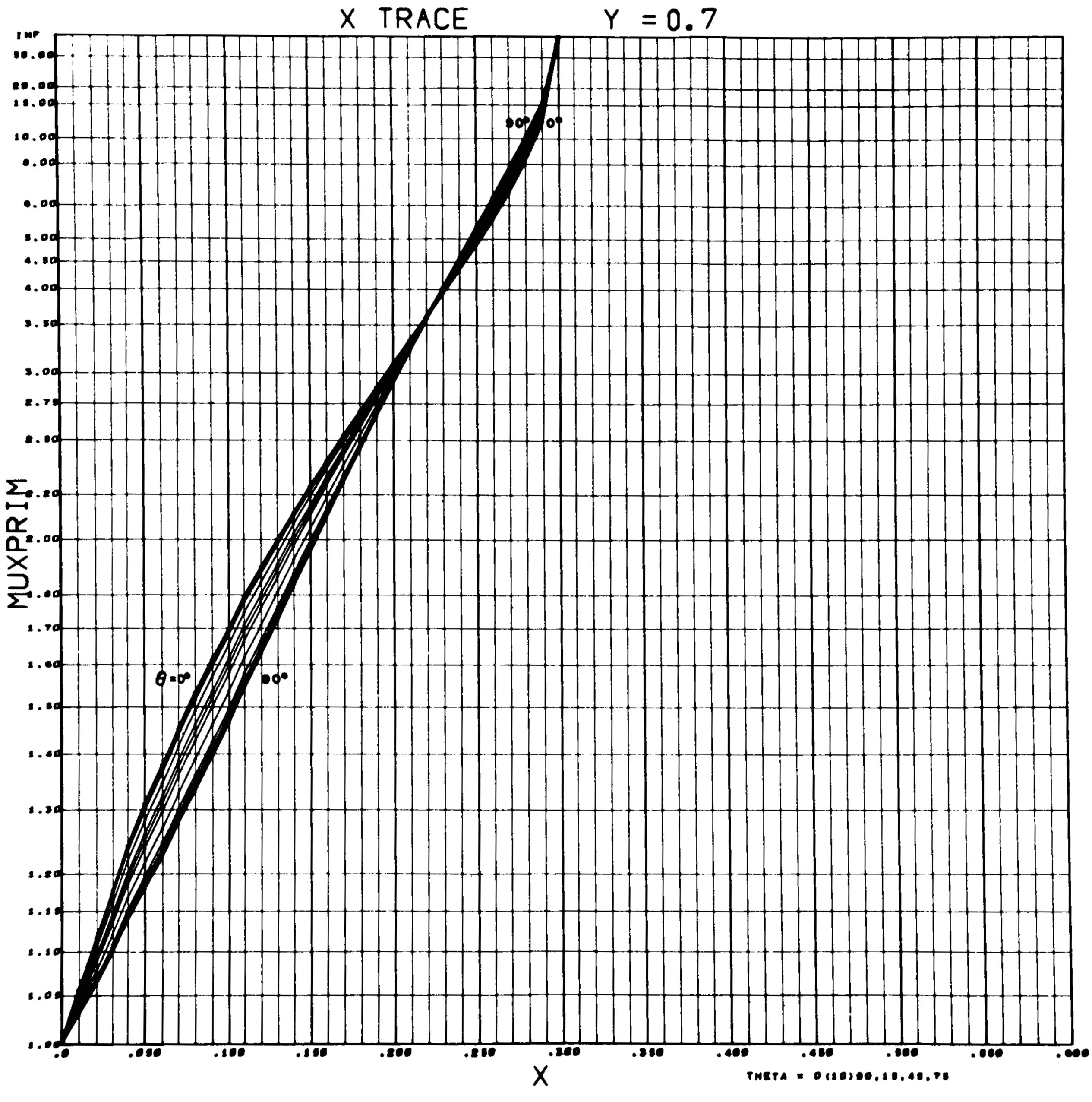

Figure 74.- Variation of μ' vs. X; Y = 0.7; $\theta = 0^{\circ} - 90^{\circ}$.

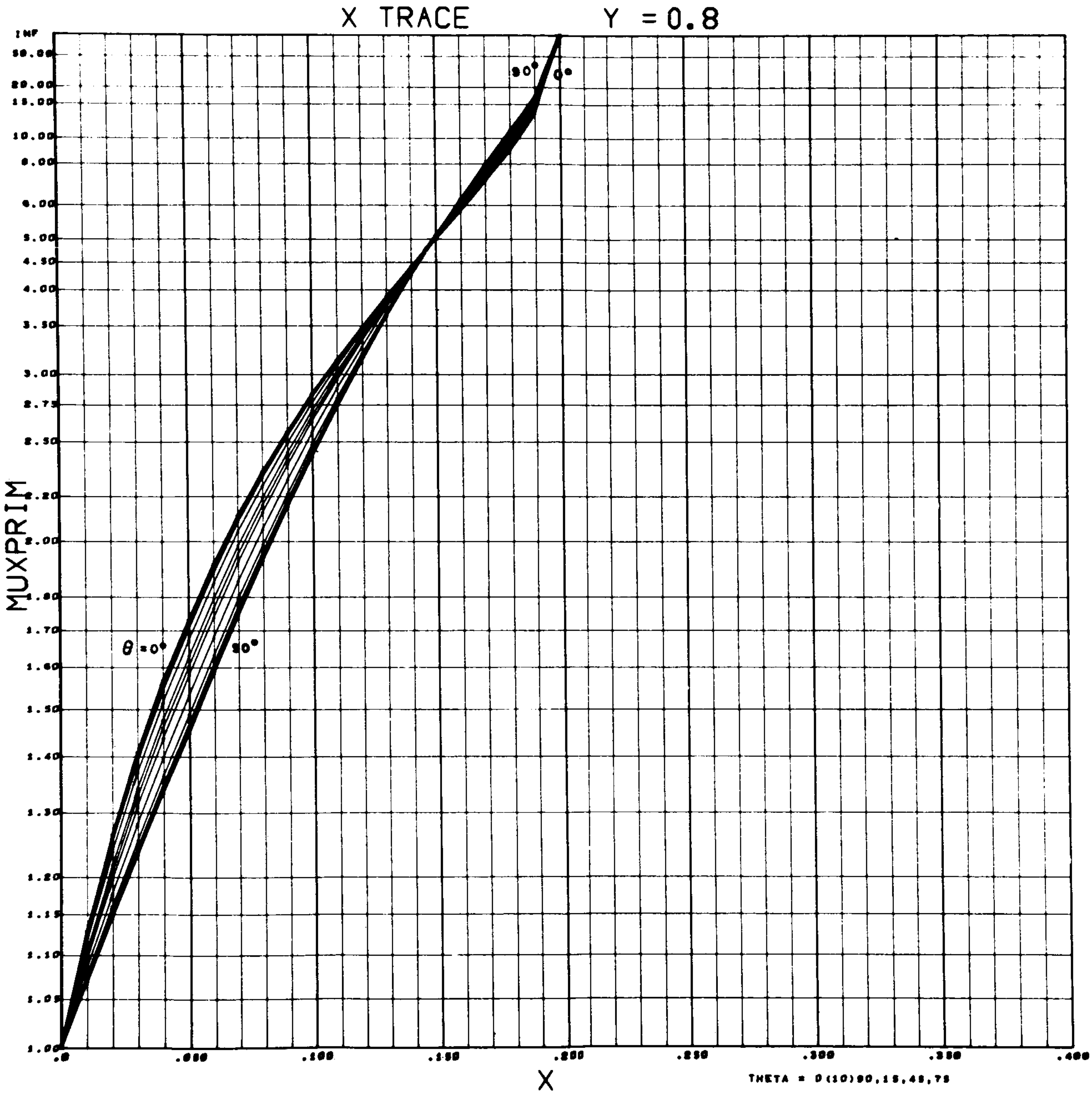

Figure 75.- Variation of μ' vs. X; Y = 0.8; $\theta = 0^{\circ} - 90^{\circ}$.

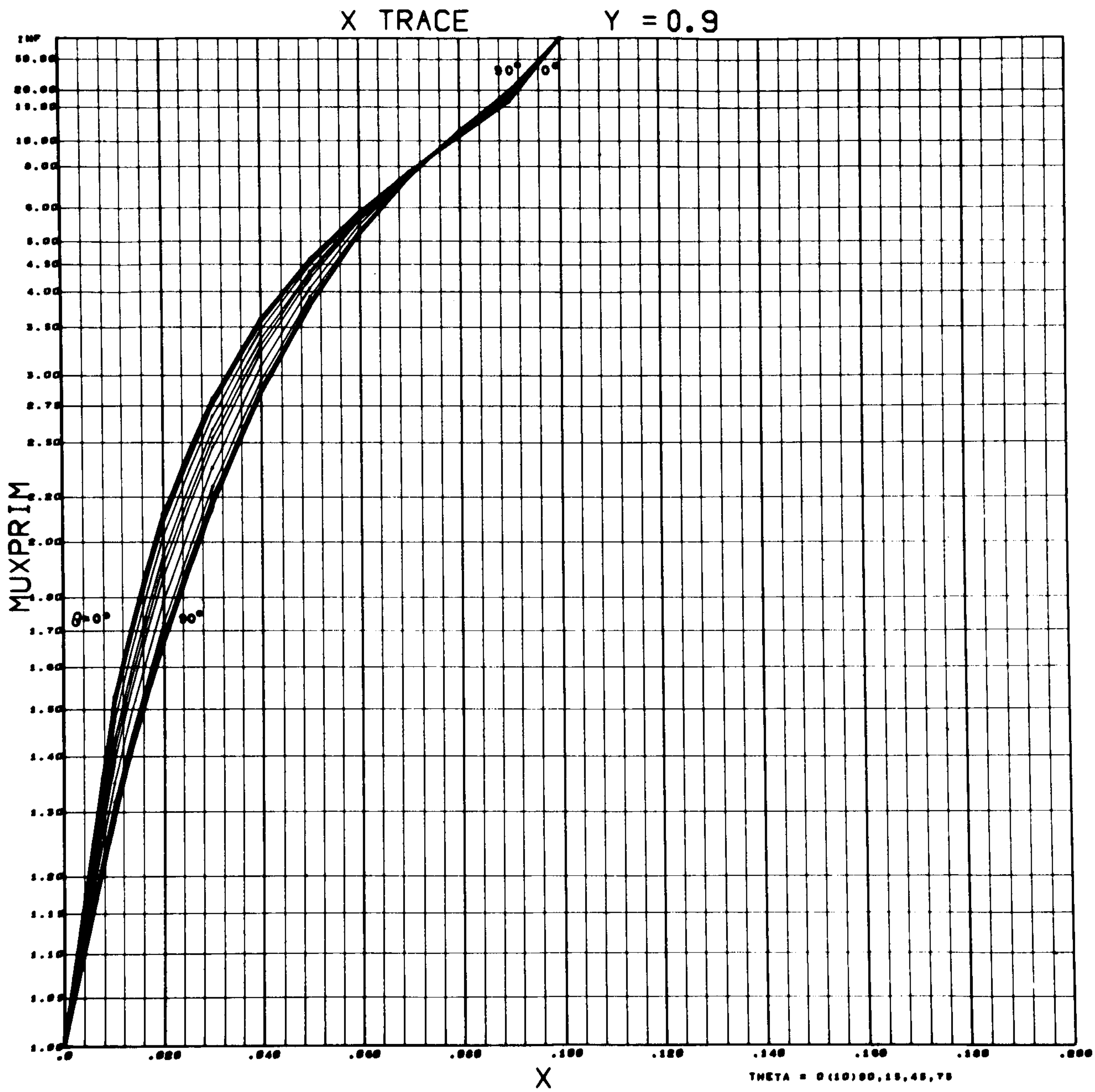

Figure 76.- Variation of μ' vs. X; Y = 0.9; θ = 0° - 90°.

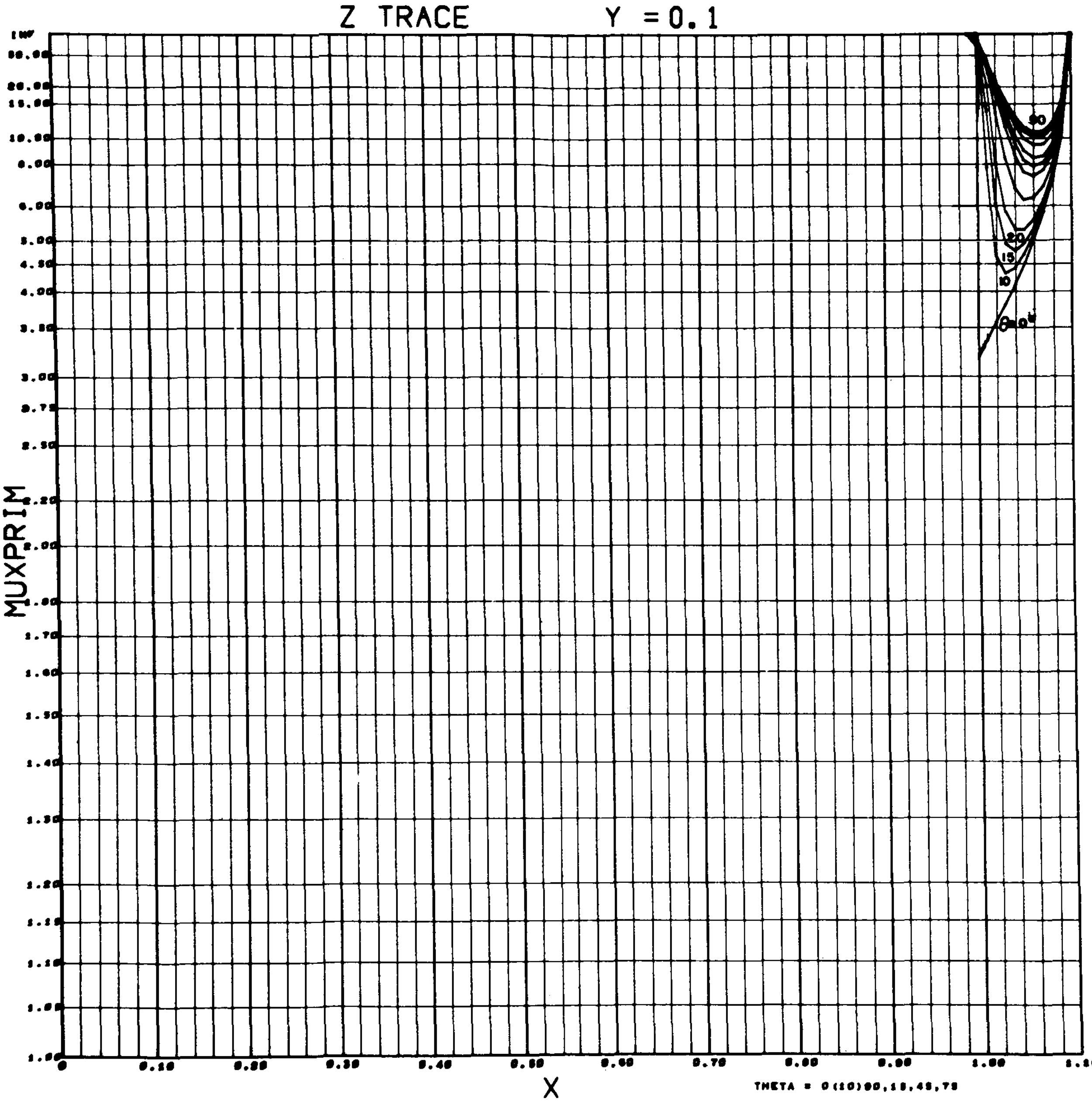

Figure 77.- Variation of μ' vs. X; Y = 0.1; θ = 0° - 90°.

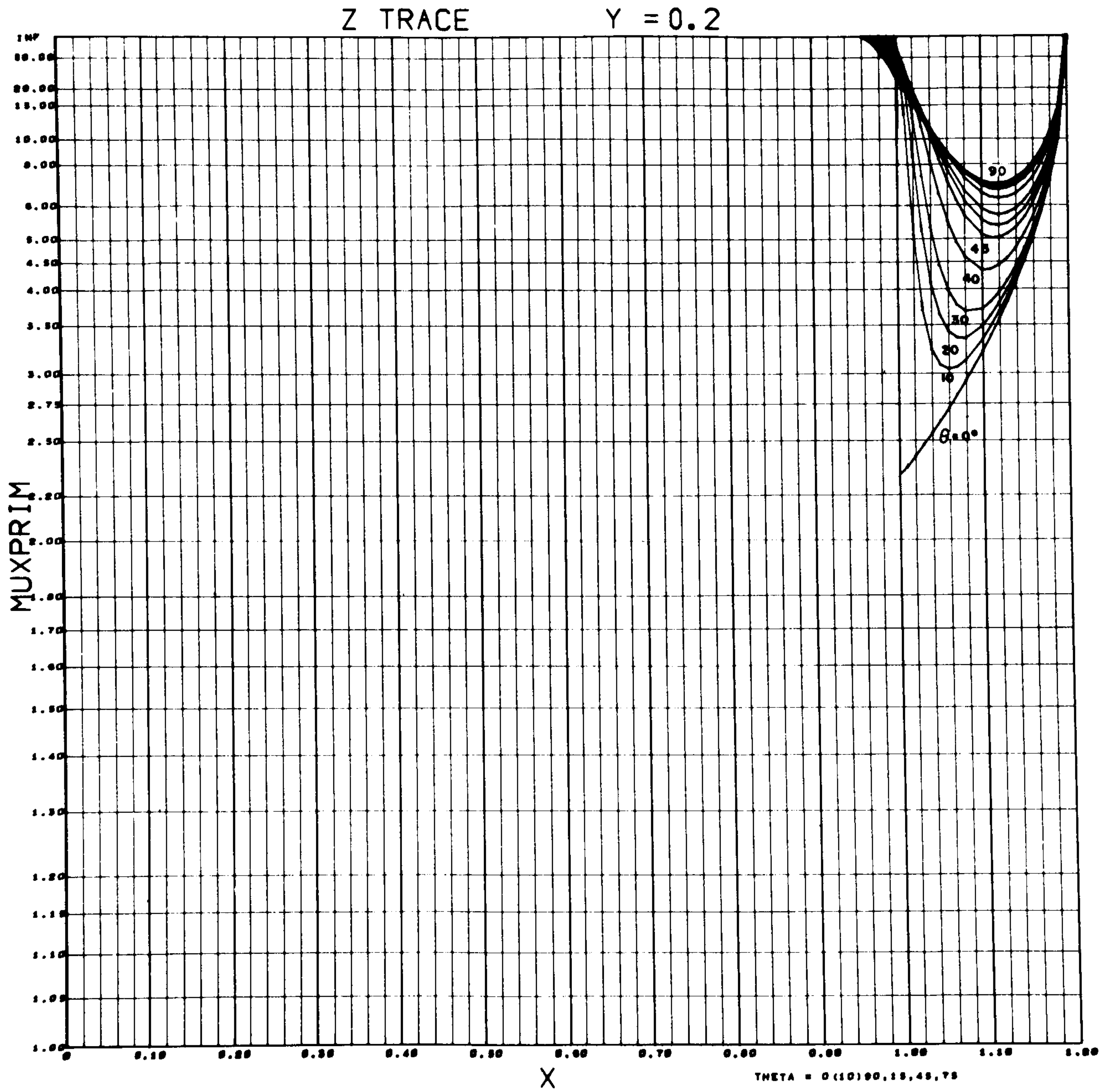

Figure 78.- Variation of μ' vs. X; Y = 0.2; θ = 0° - 90°.

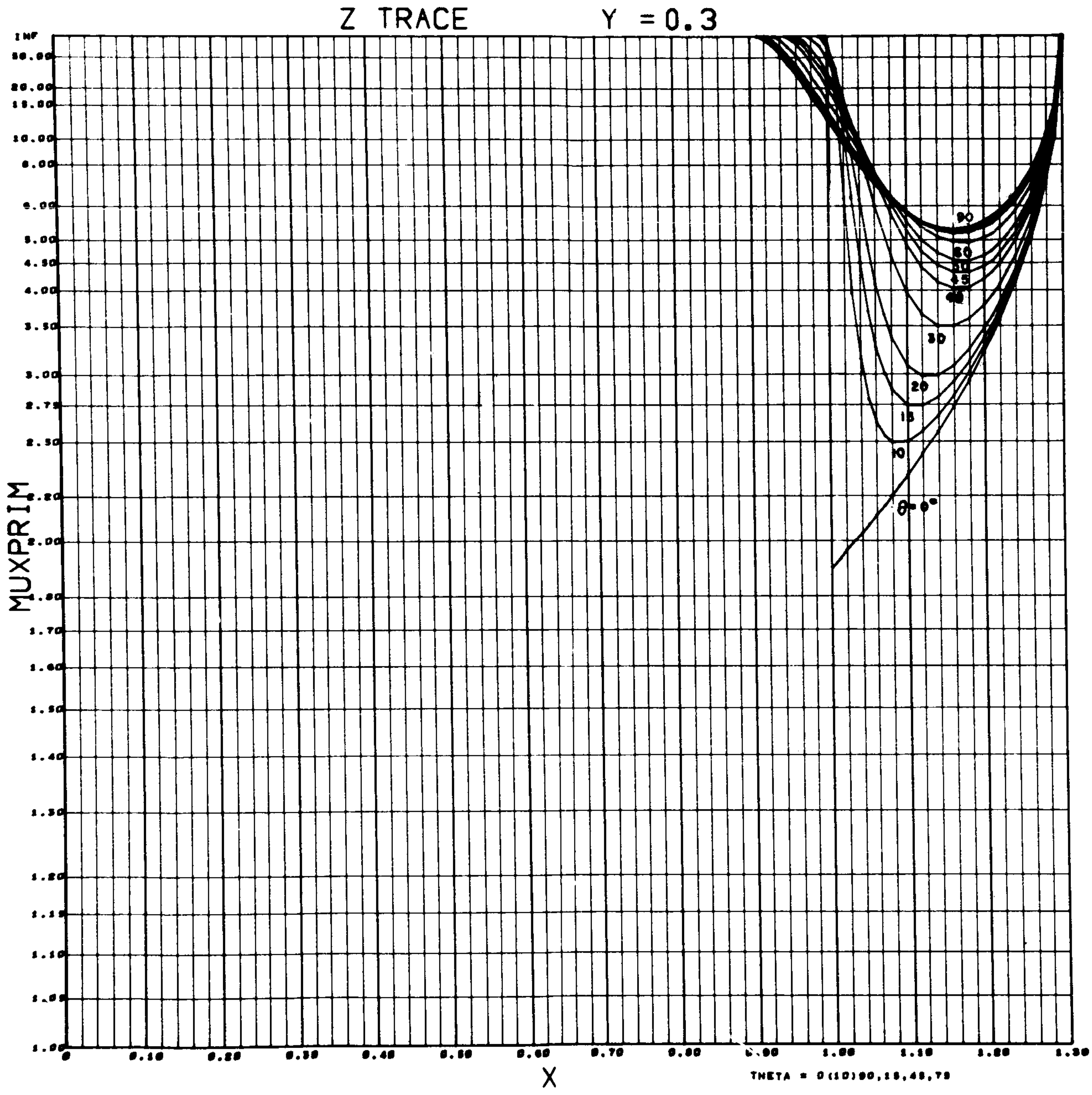

Figure 79.- Variation of μ' vs. X; Y = 0.3; $\theta = 0^{\circ} - 90^{\circ}$.

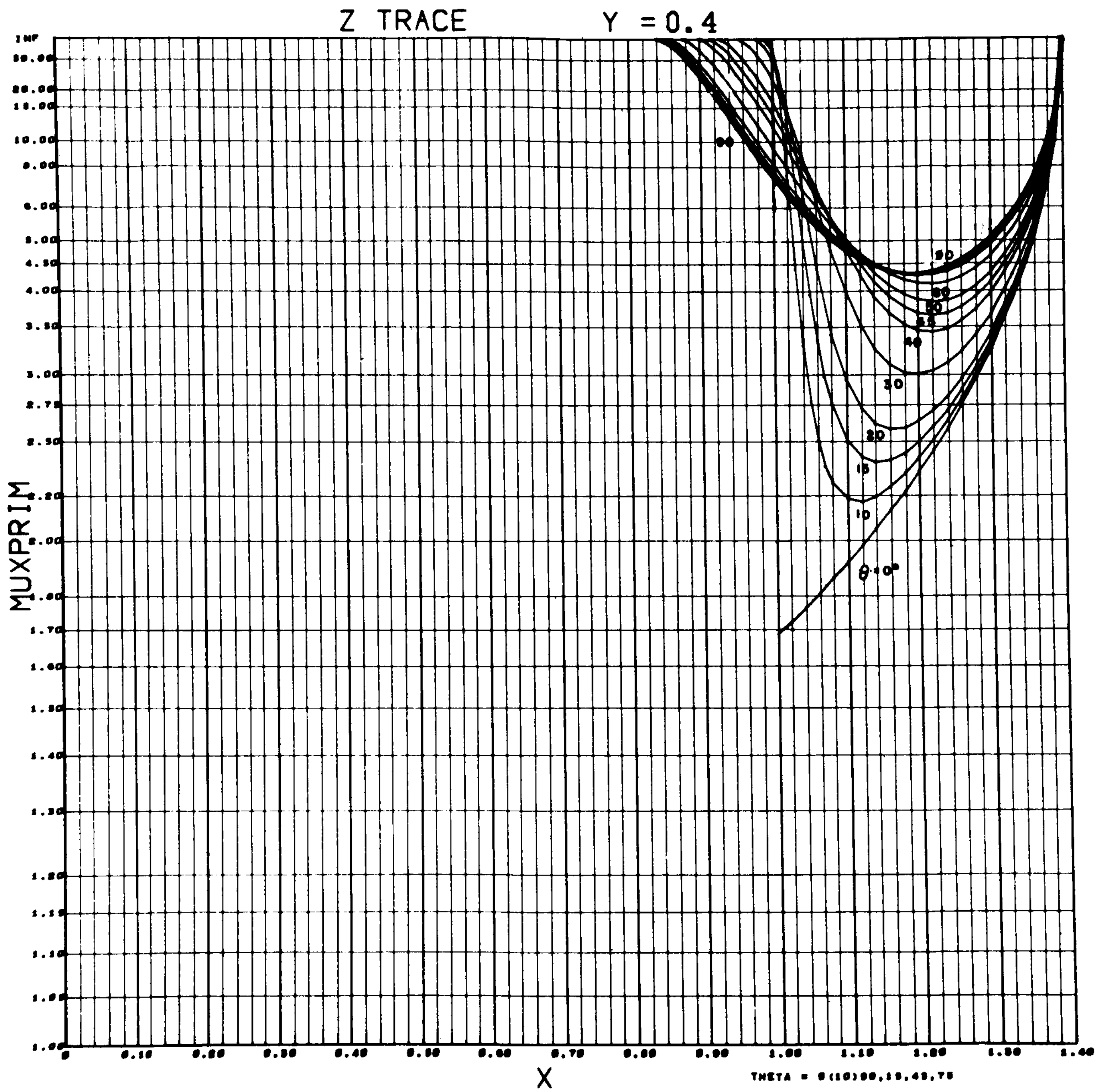

Figure 80.- Variation of μ' vs. X; Y = 0.4; $\theta = 0^\circ - 90^\circ$.

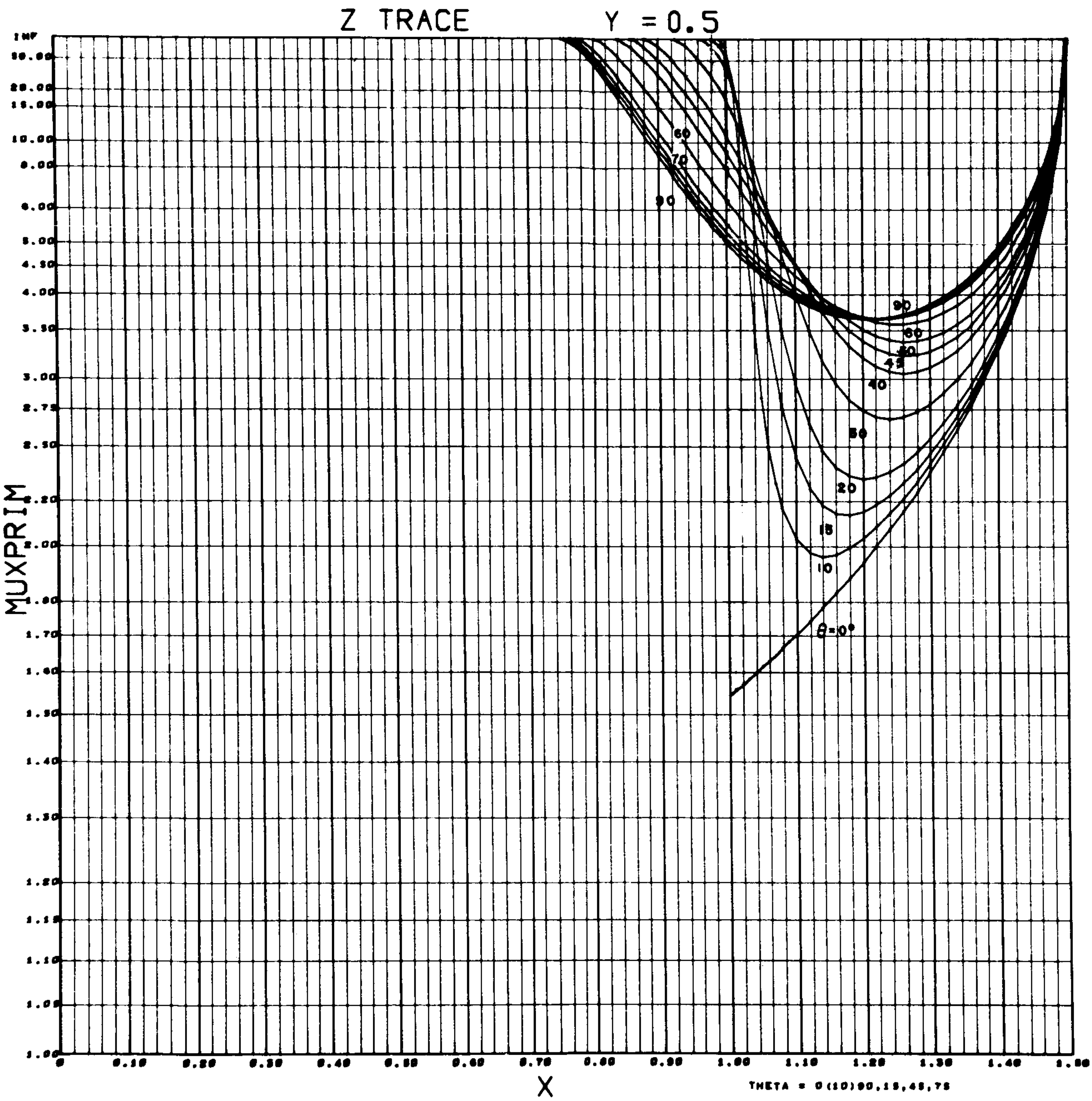

Figure 81.- Variation of μ' vs. X; Y = 0.5; θ = 0° - 90°.

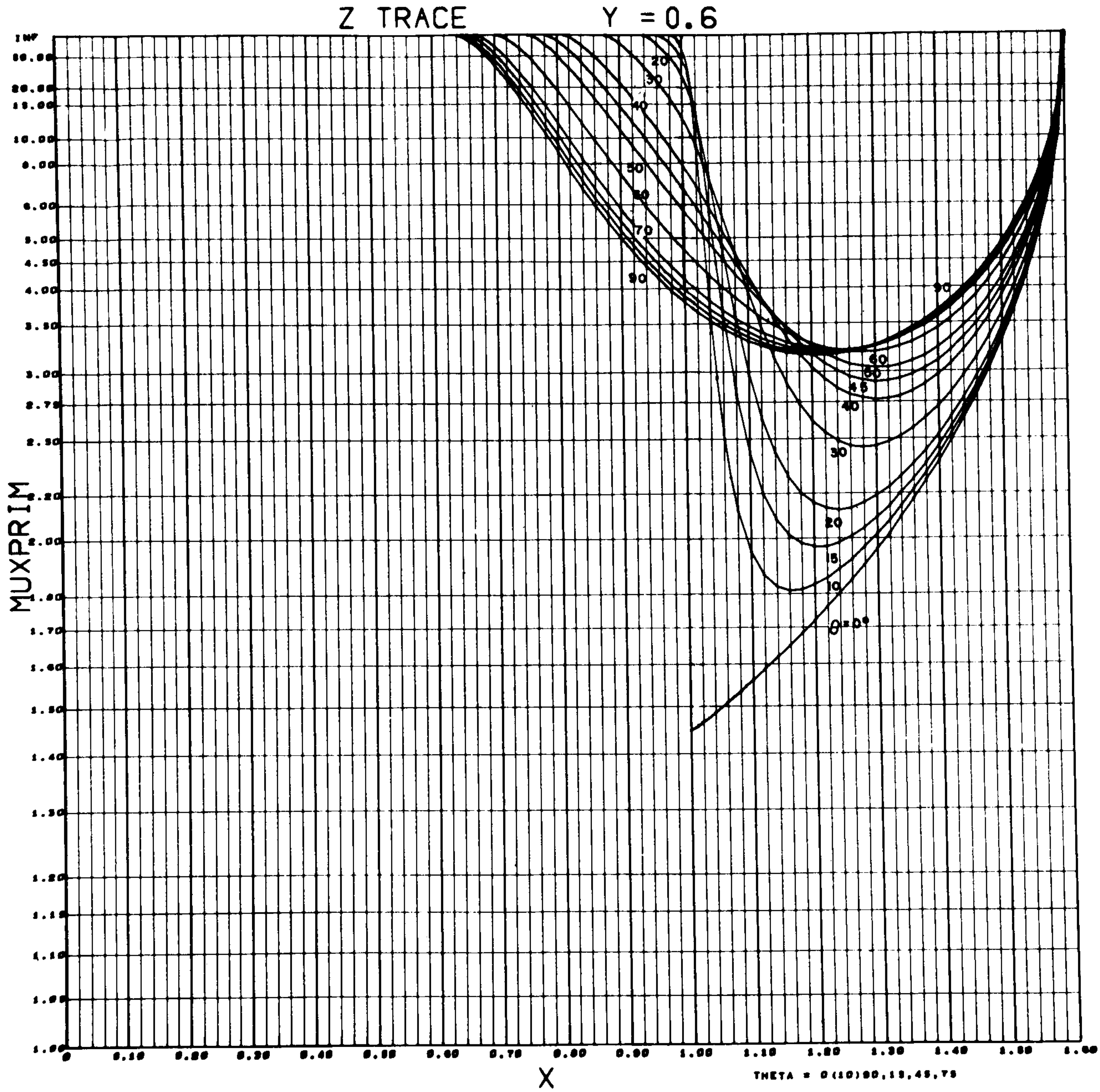

Figure 82.- Variation of μ' vs. X; Y = 0.6; $\theta = 0^{o} - 90^{o}$.

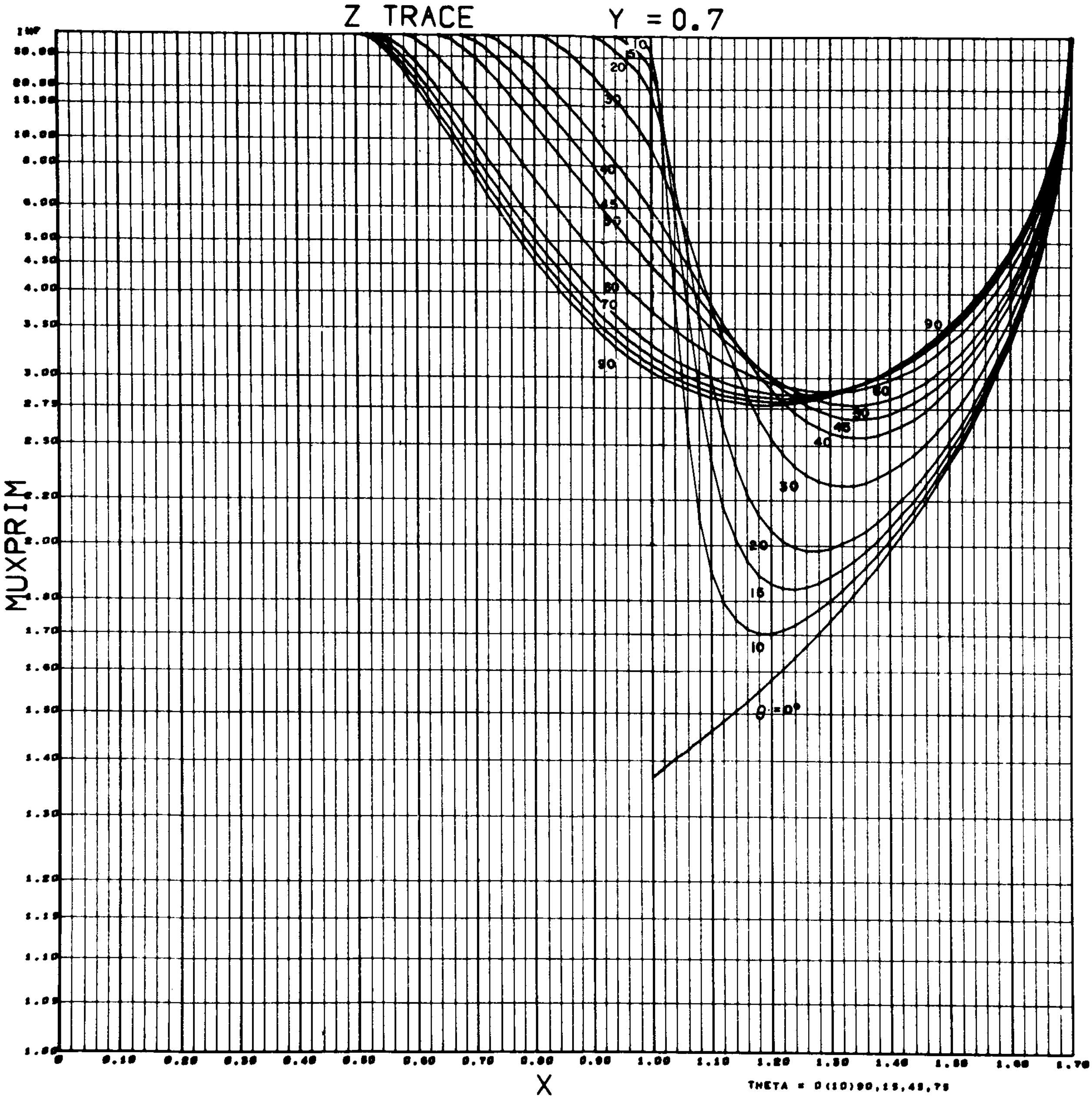

Figure 83.- Variation of μ' vs. X; Y = 0.7; $\theta = 0^\circ - 90^\circ$.

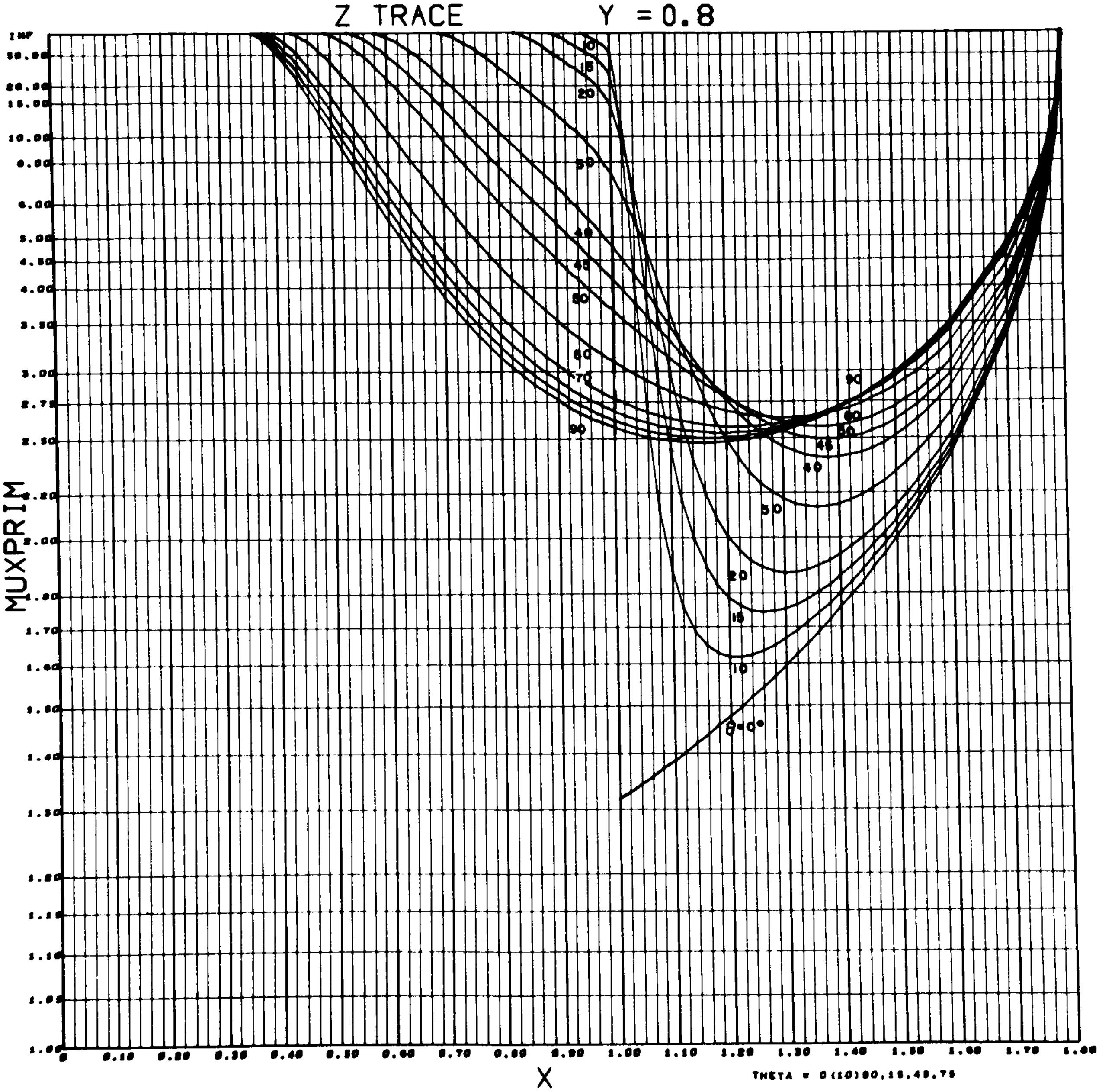

Figure 84.- Variation of μ' vs. X; Y = 0.8; $\theta = 0^{\circ} - 90^{\circ}$.

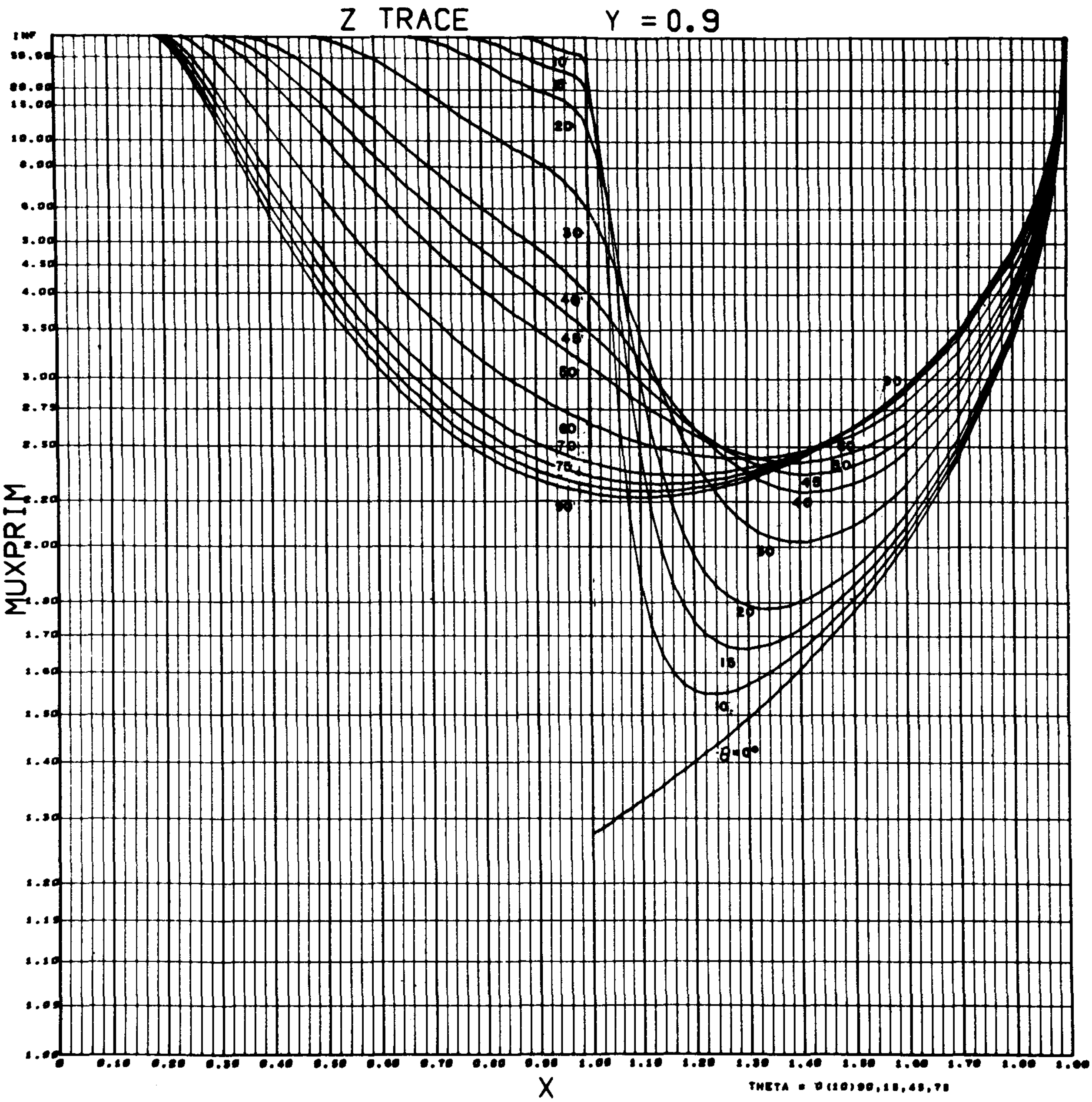

Figure 85.- Variation of μ' vs. X; Y = 0.9; $\theta = 0^{\circ} - 90^{\circ}$.

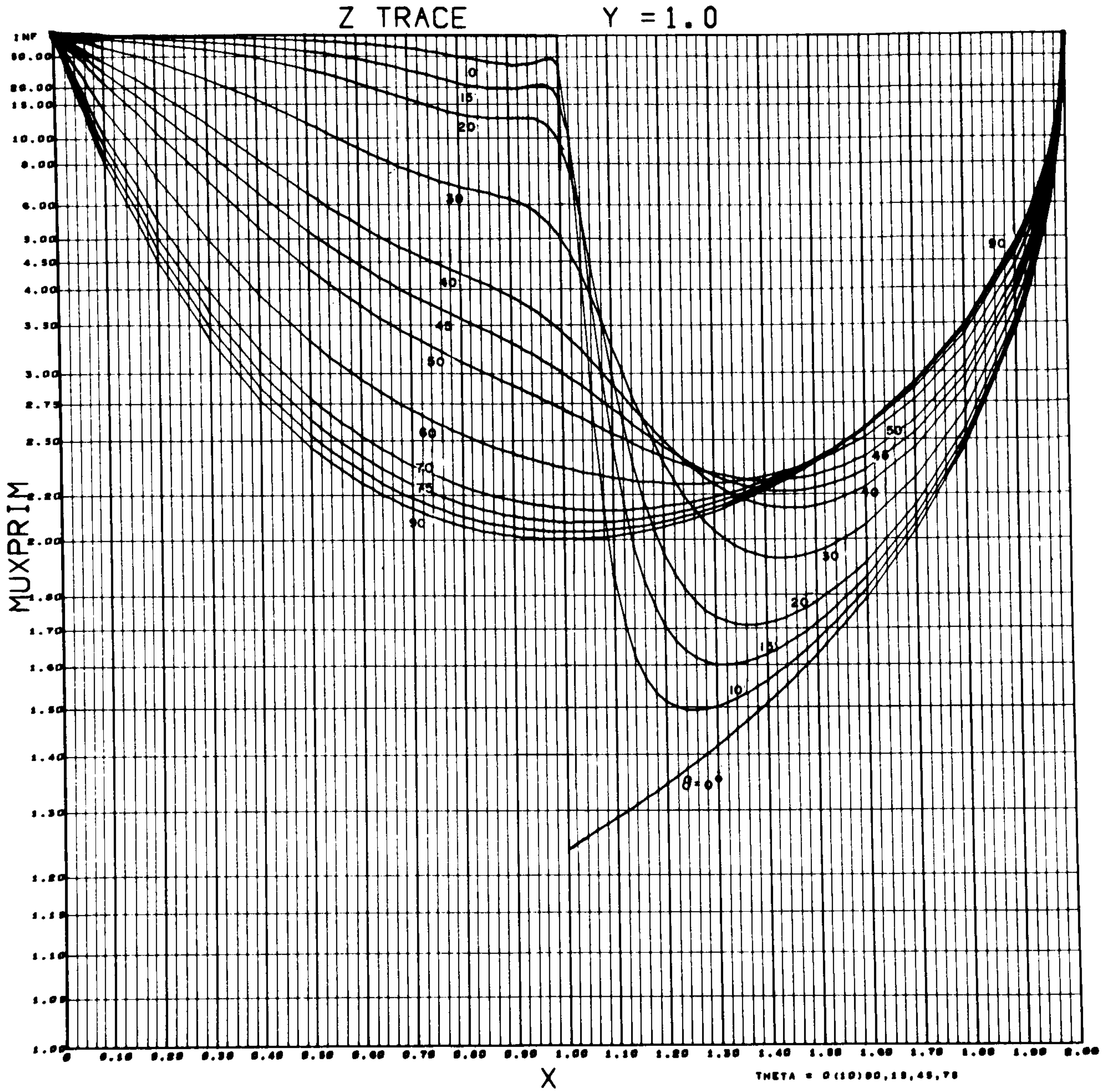

Figure 86.- Variation of μ' vs. X; Y = 1.0; $\theta = 0^\circ - 90^\circ$.

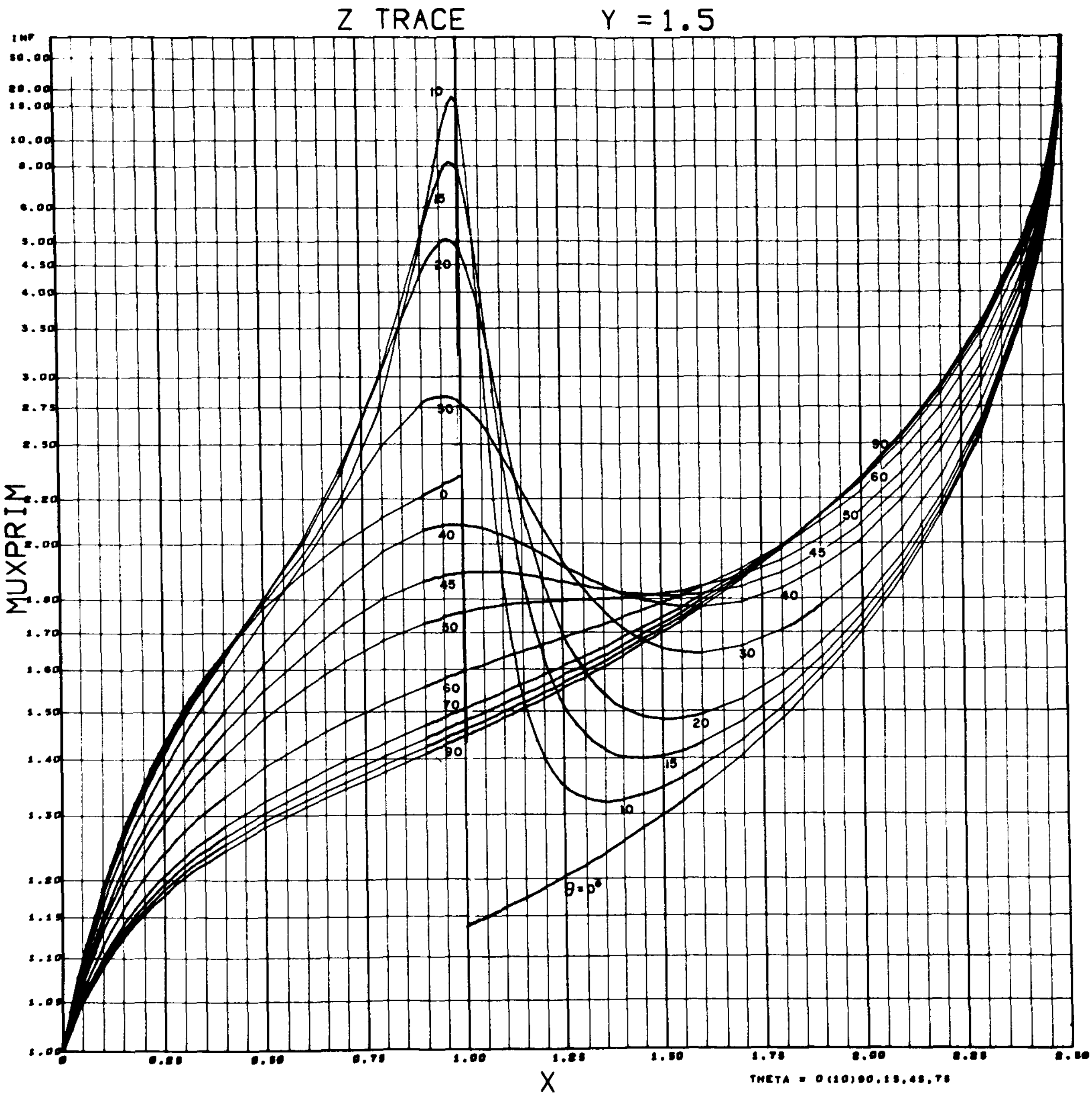

Figure 87.- Variation of μ' vs. X; Y = 1.5; $\theta = 0^{\circ} - 90^{\circ}$.

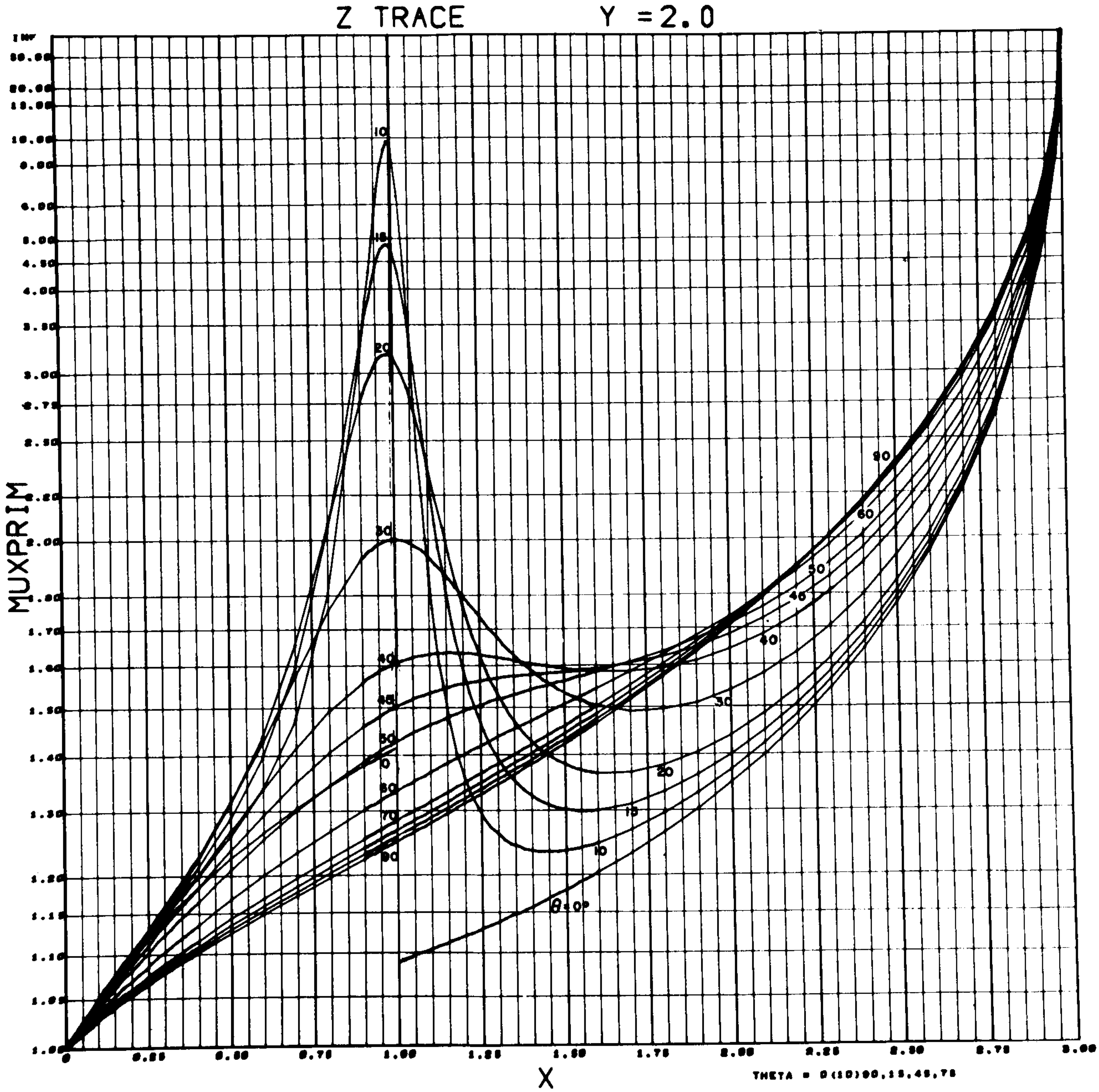

Figure 88.- Variation of μ' vs. X; Y = 2.0; $\theta = 0^\circ - 90^\circ$.

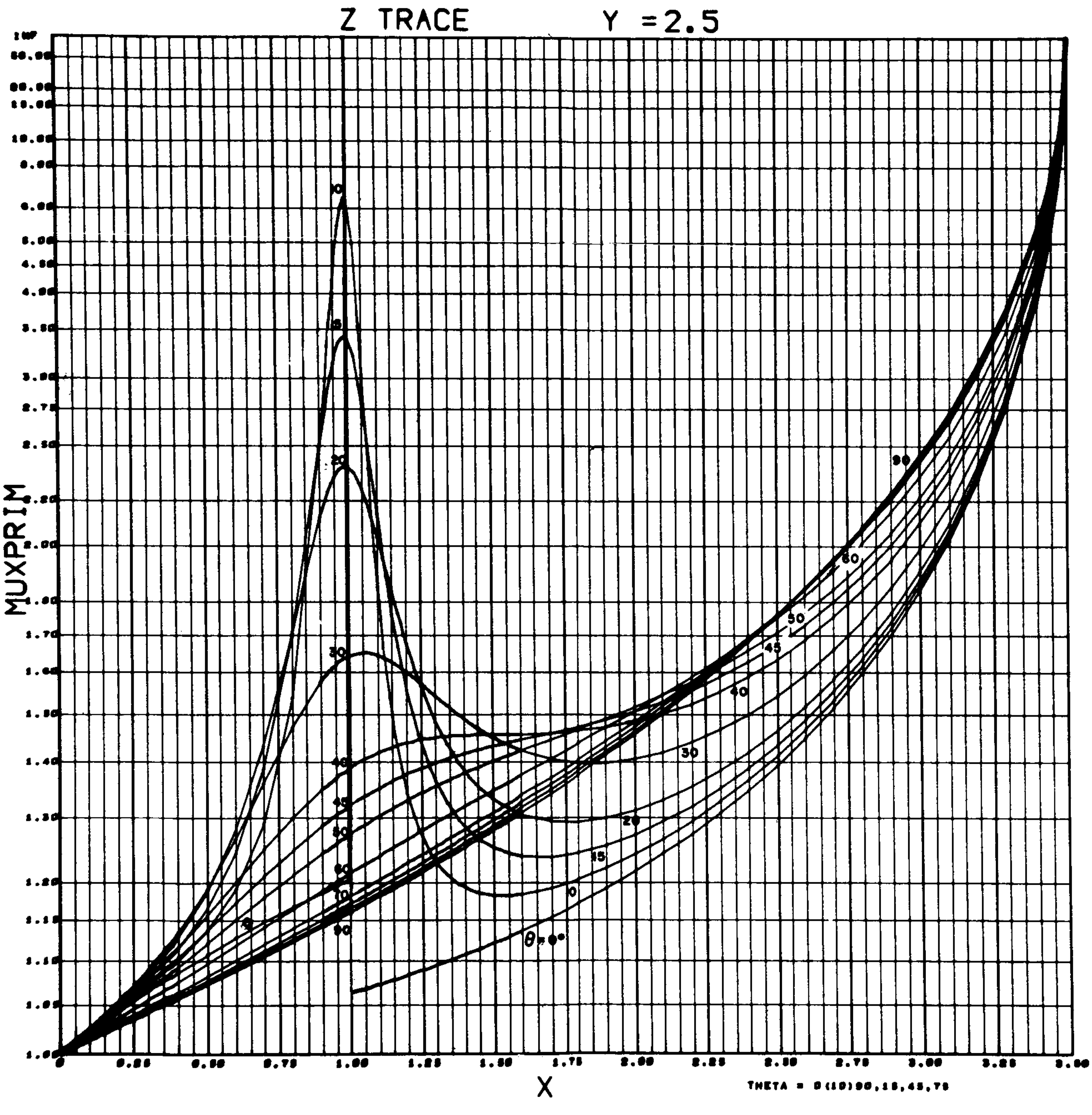

Figure 89.- Variation of μ' vs. X; Y = 2.5; θ = 0° - 90°.

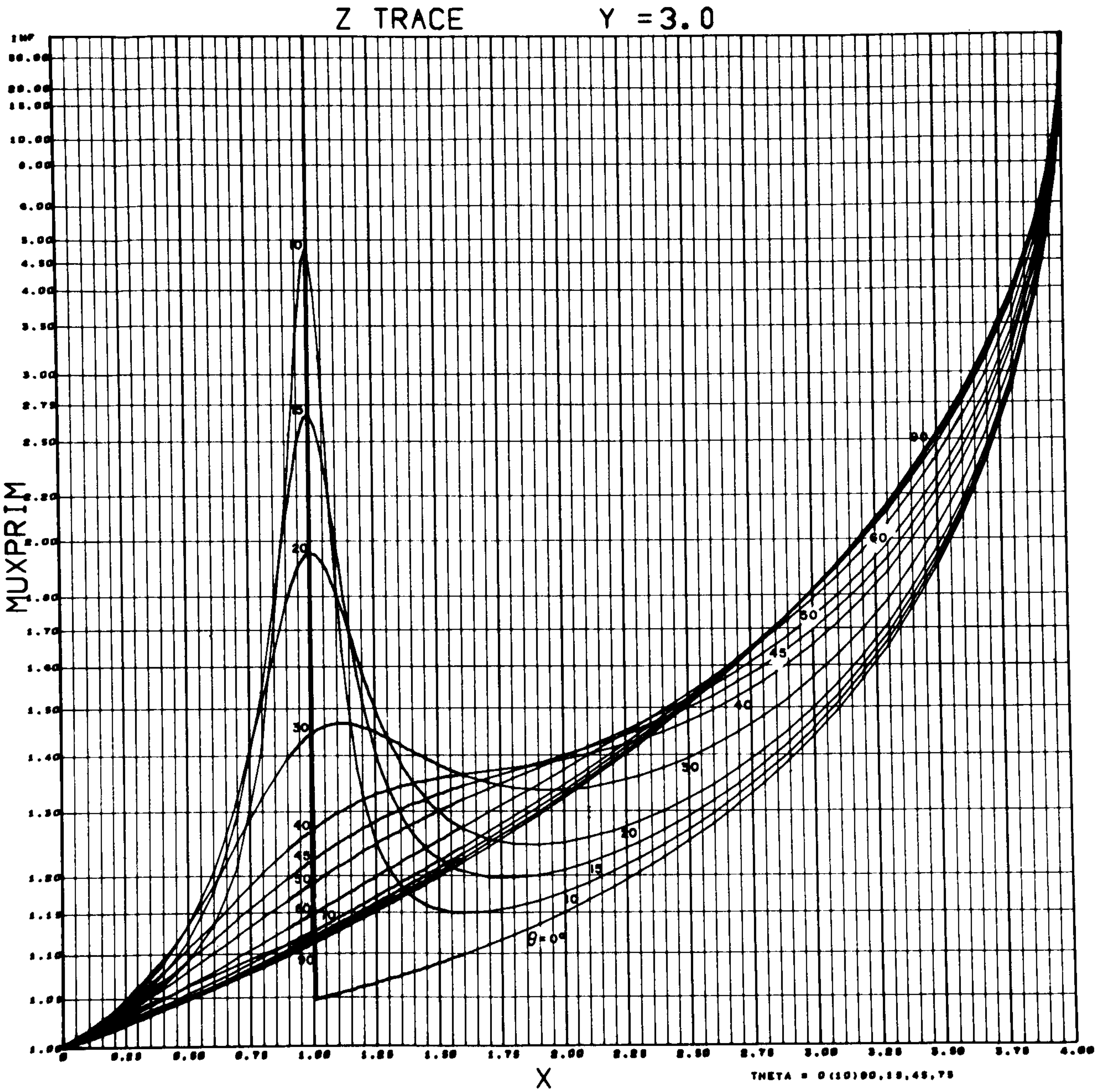

Figure 90.- Variation of μ' vs. X; Y = 3.0; $\theta = 0^{\circ} - 90^{\circ}$.

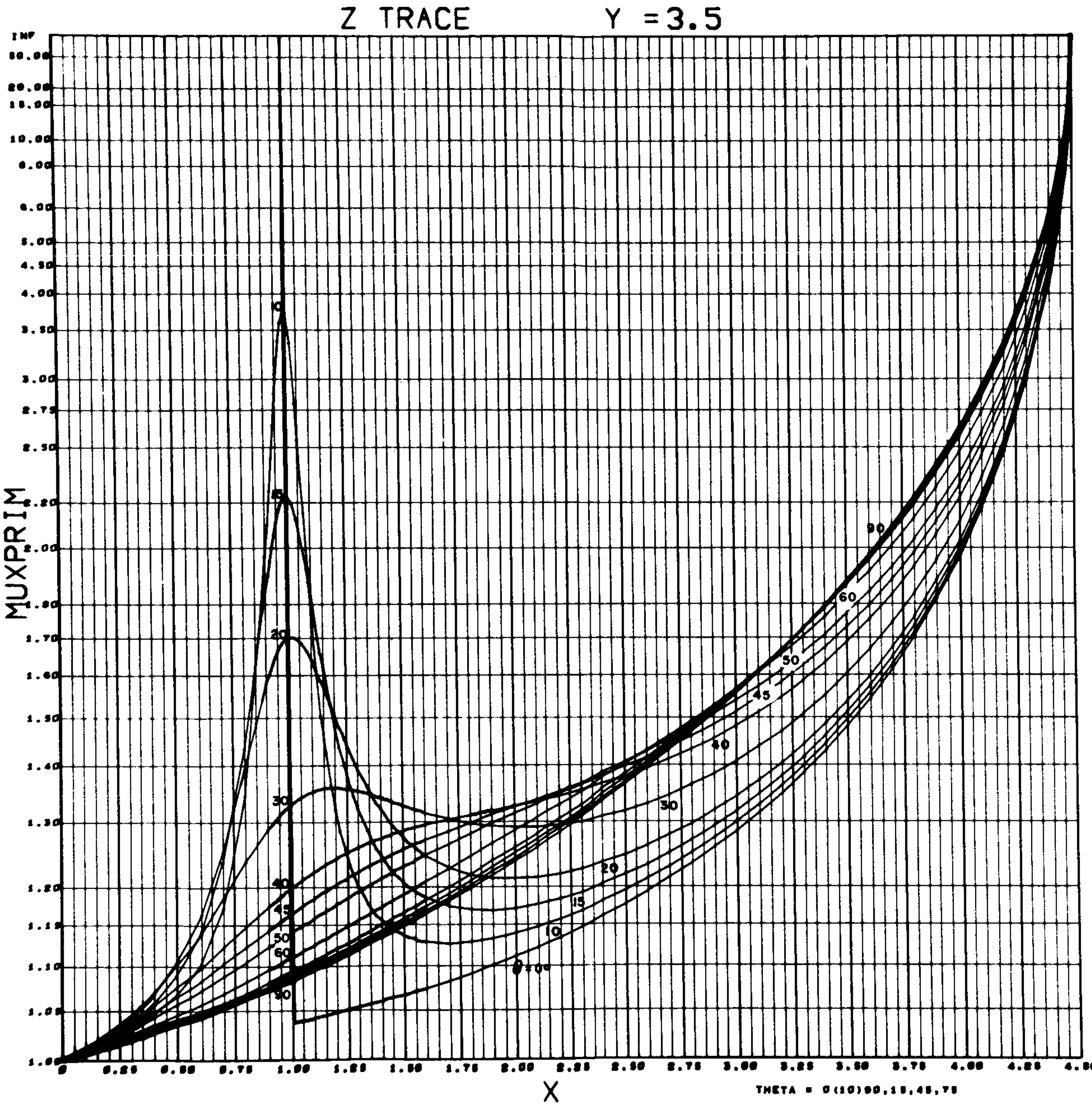

Figure 91.- Variation of μ' vs. X; Y = 3.5; θ = 0° - 90°.

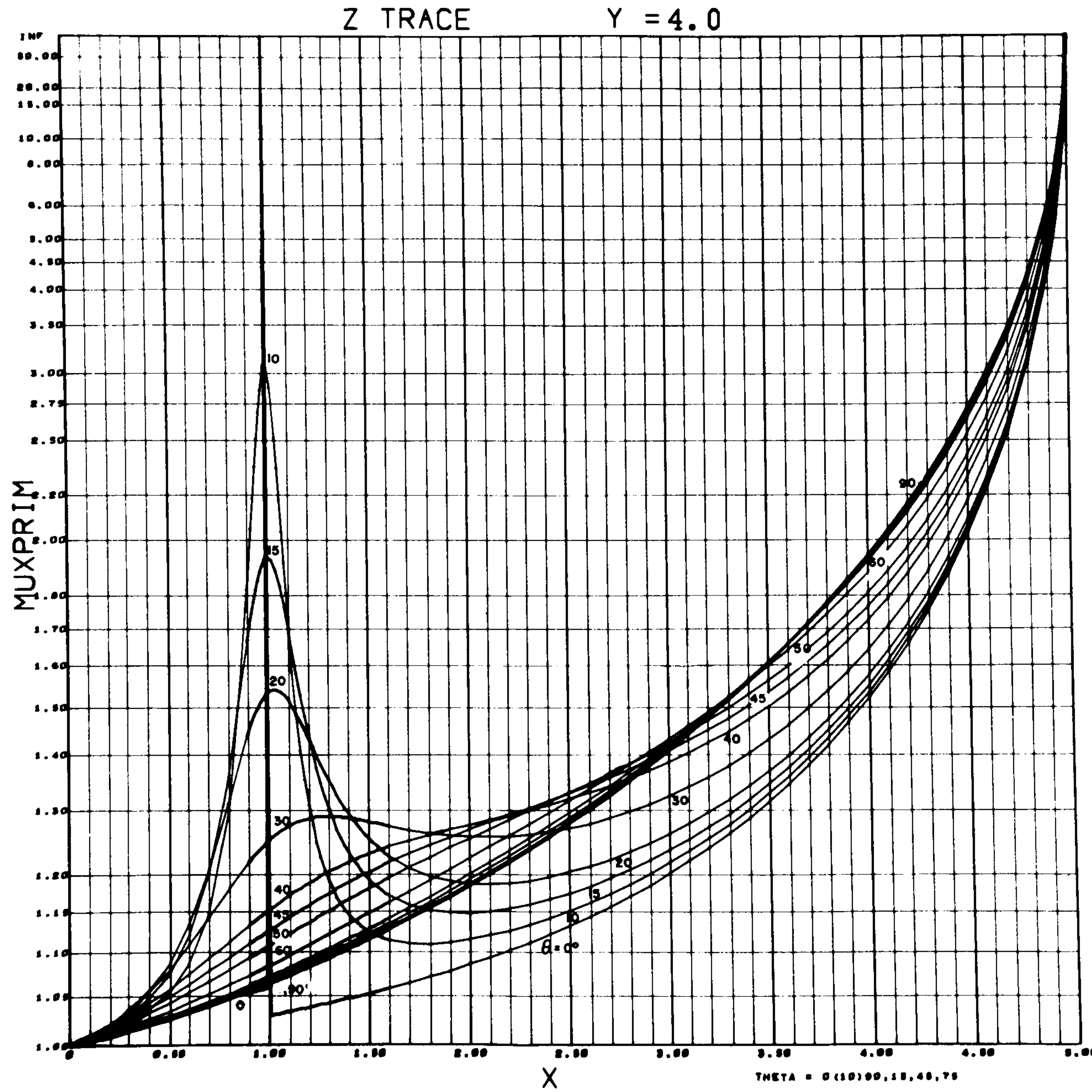

Figure 92.- Variation of μ' vs. X; Y = 4.0; $\theta = 0^\circ - 90^\circ$.

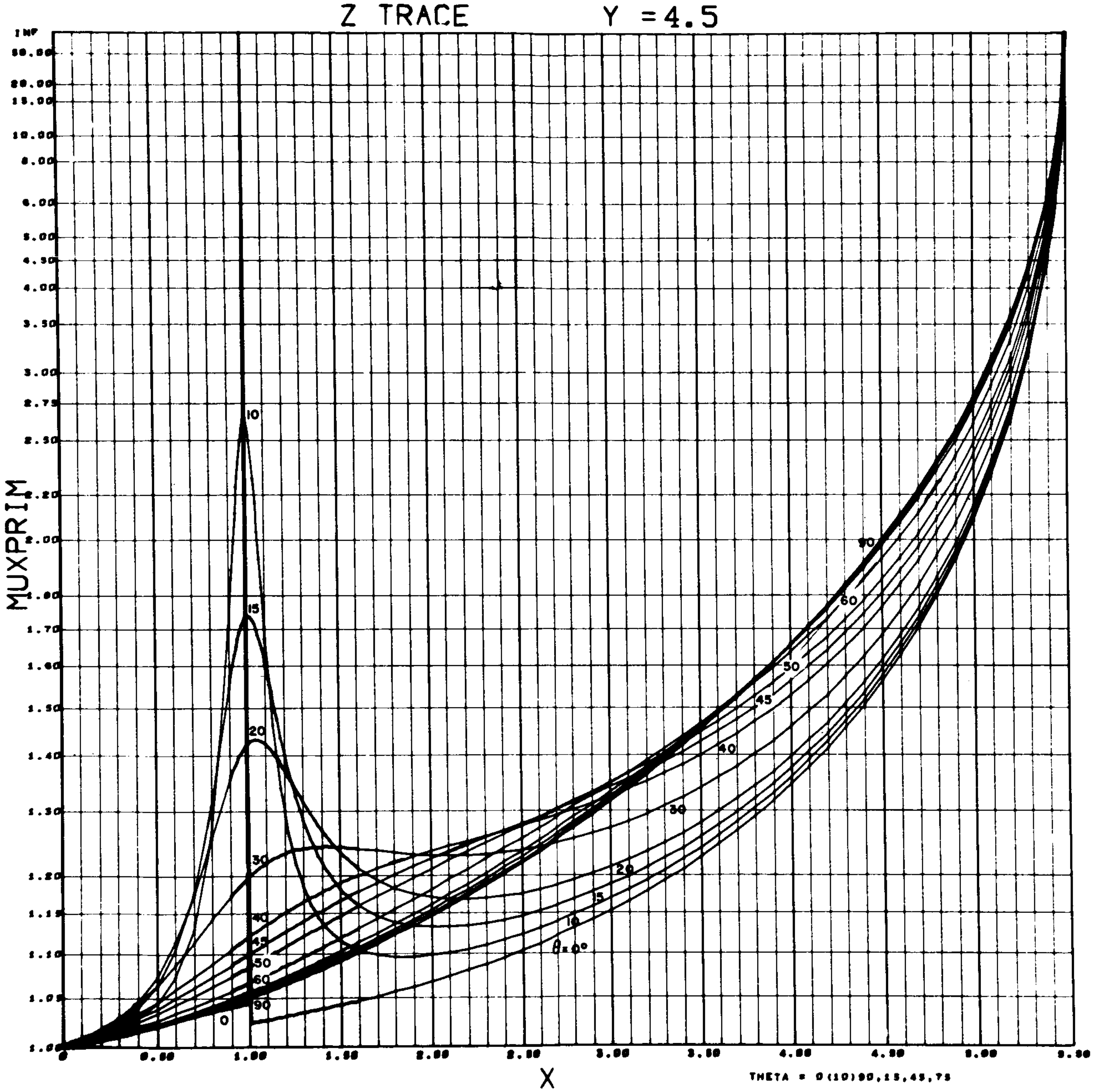

Figure 93.- Variation of μ' vs. X; Y = 4.5; θ = 0° - 90°.

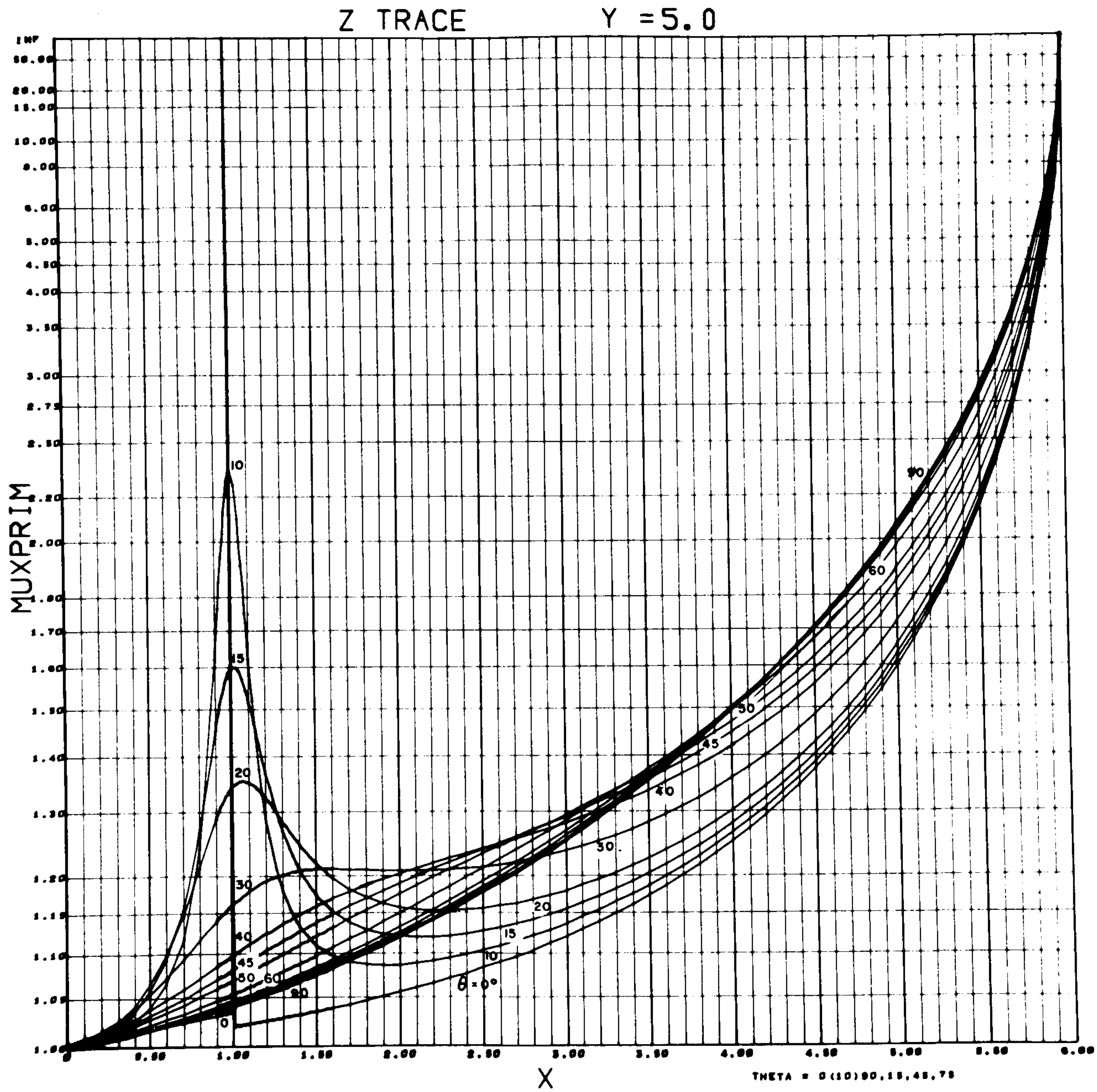

Figure 94.- Variation of μ' vs. X; Y = 5.0; $\theta = 0^{\circ} - 90^{\circ}$.

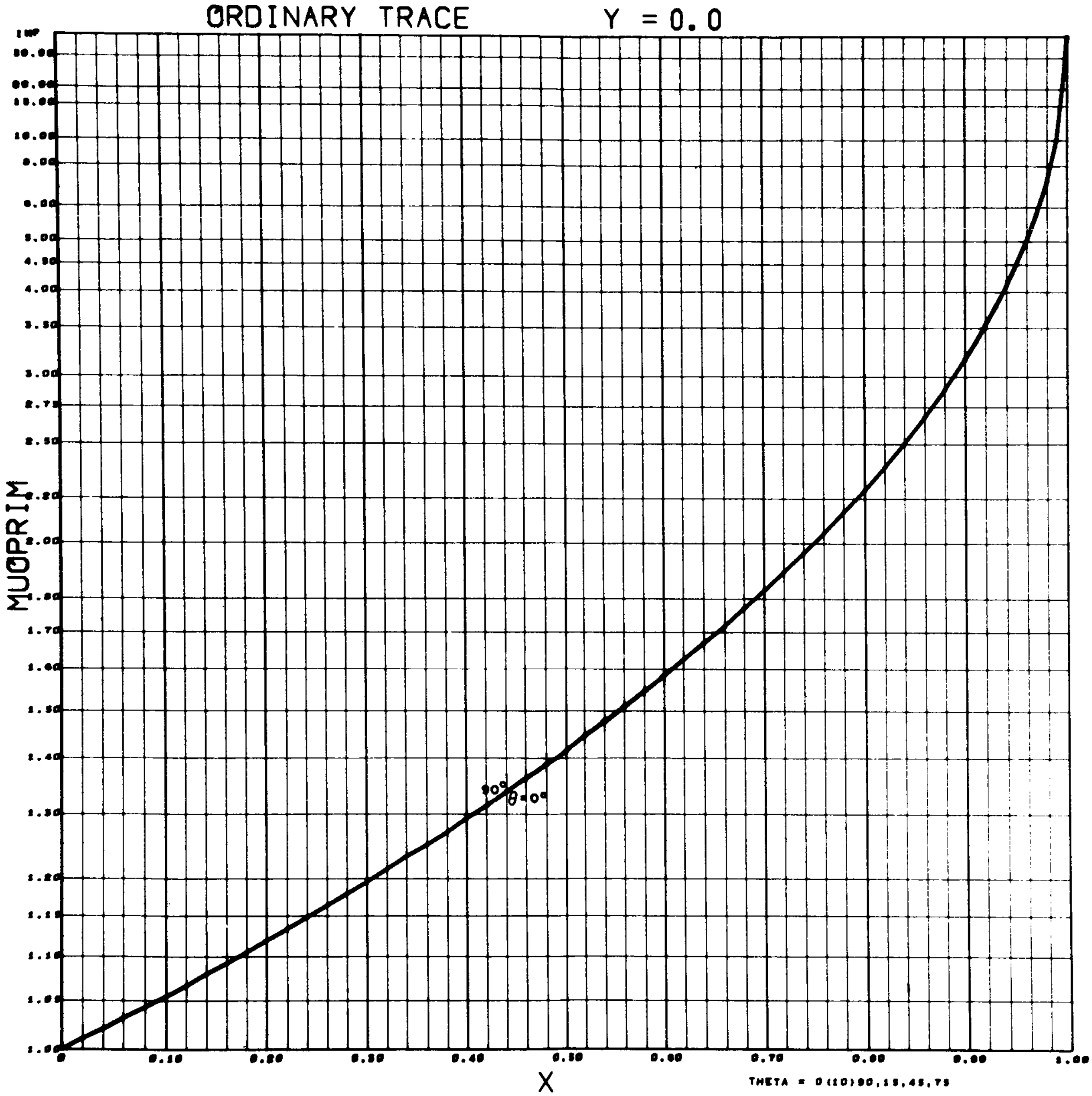

Figure 95.- Variation of μ' vs. X; Y = 0; $\theta = 0^{\circ} - 90^{\circ}$.

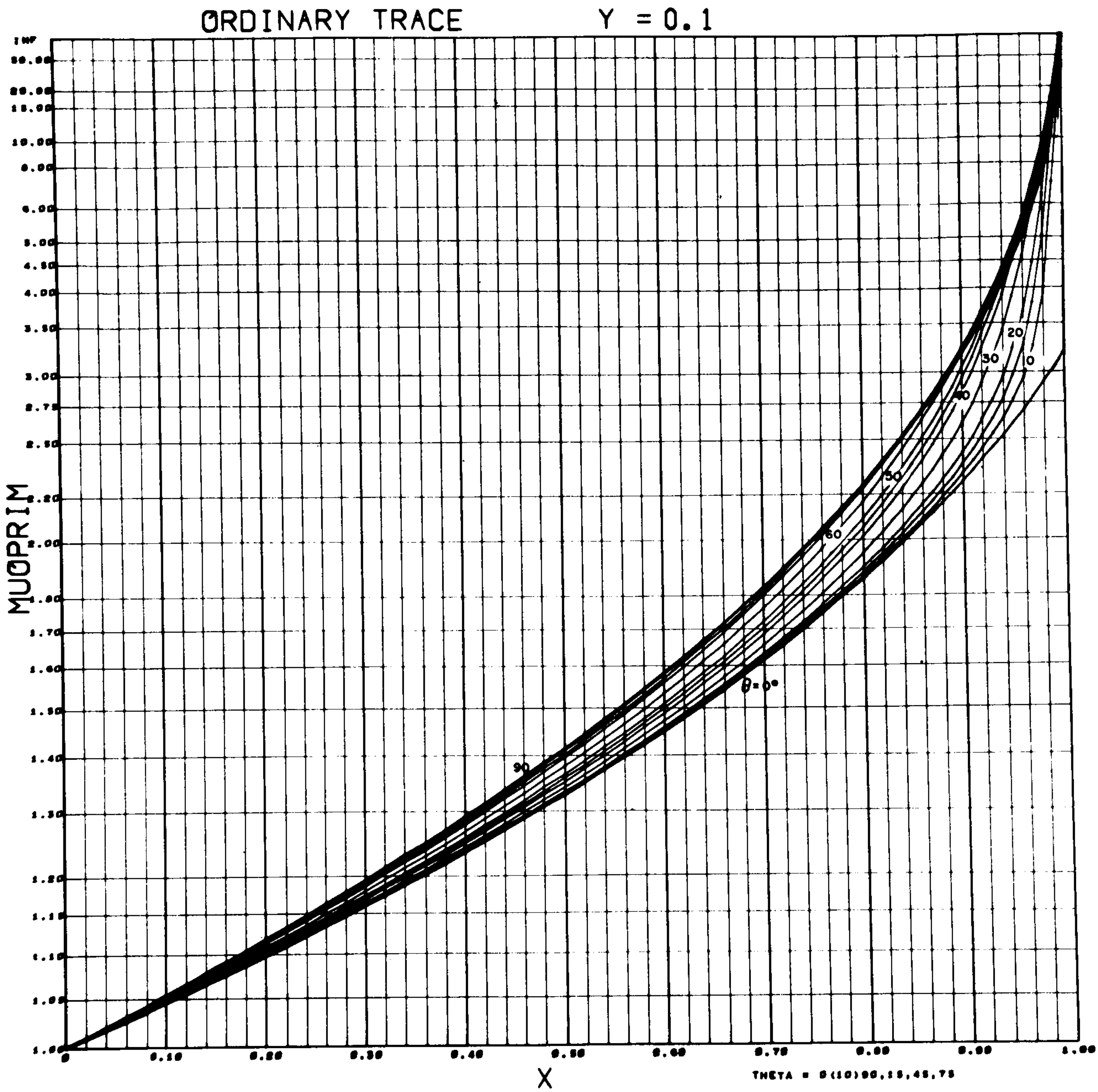

Figure 96.- Variation of μ' vs. X; Y = 0.1; θ = 0° - 90°.

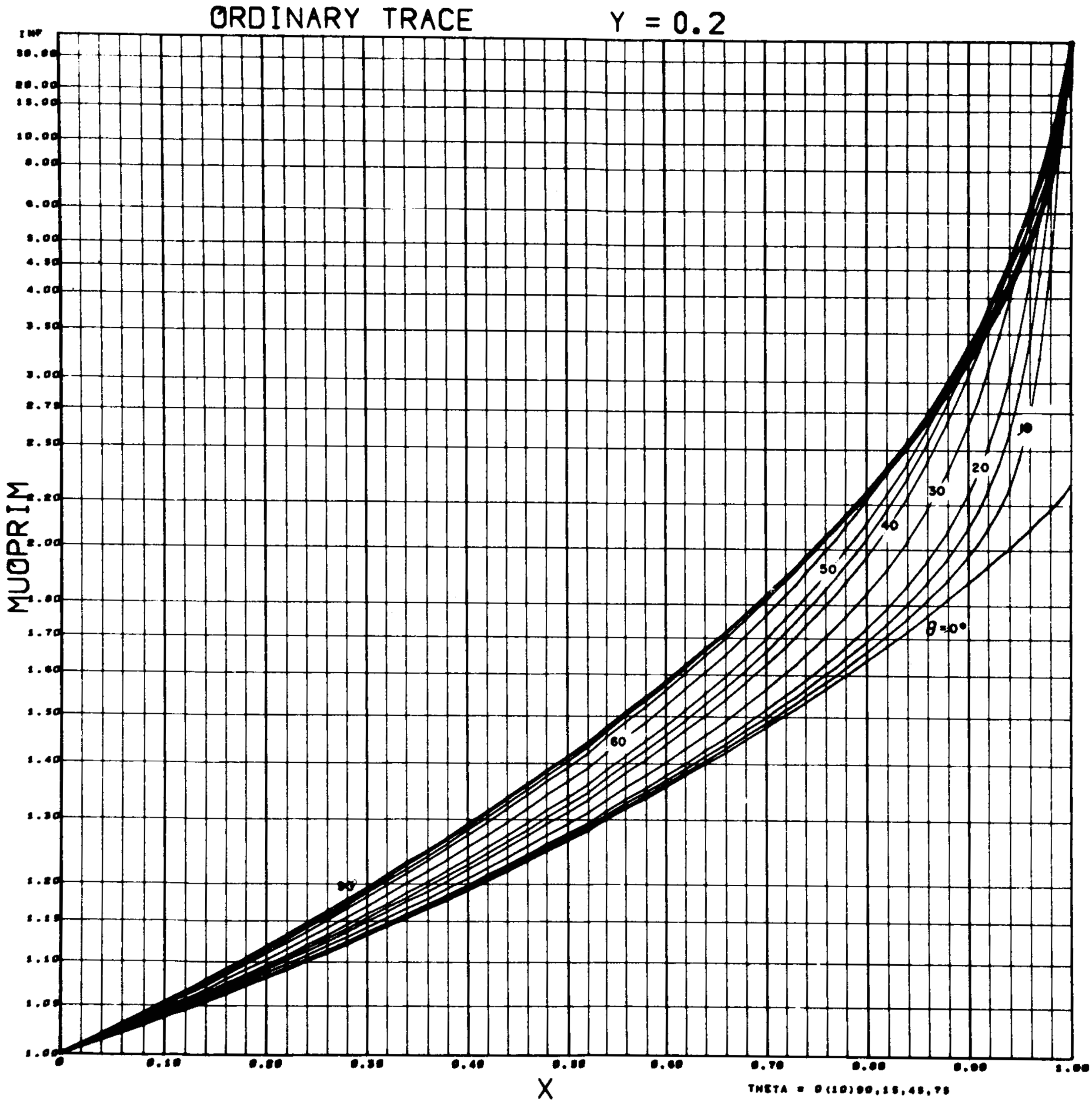

Figure 97.- Variation of μ' vs. X; Y = 0.2; θ = 0° - 90°.

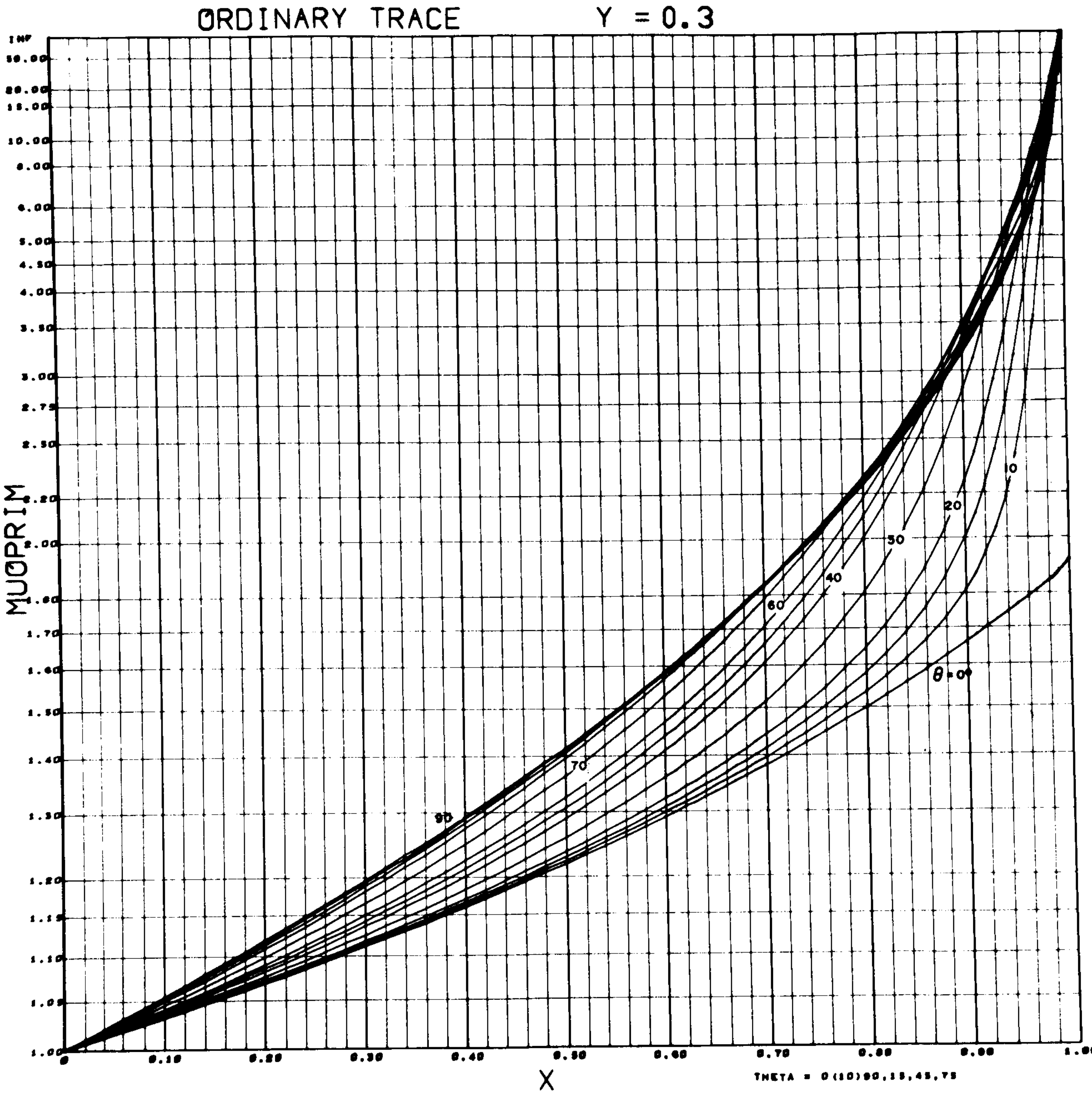

Figure 98.- Variation of μ' vs. X; Y = 0.3; $\theta = 0^{\circ} - 90^{\circ}$.

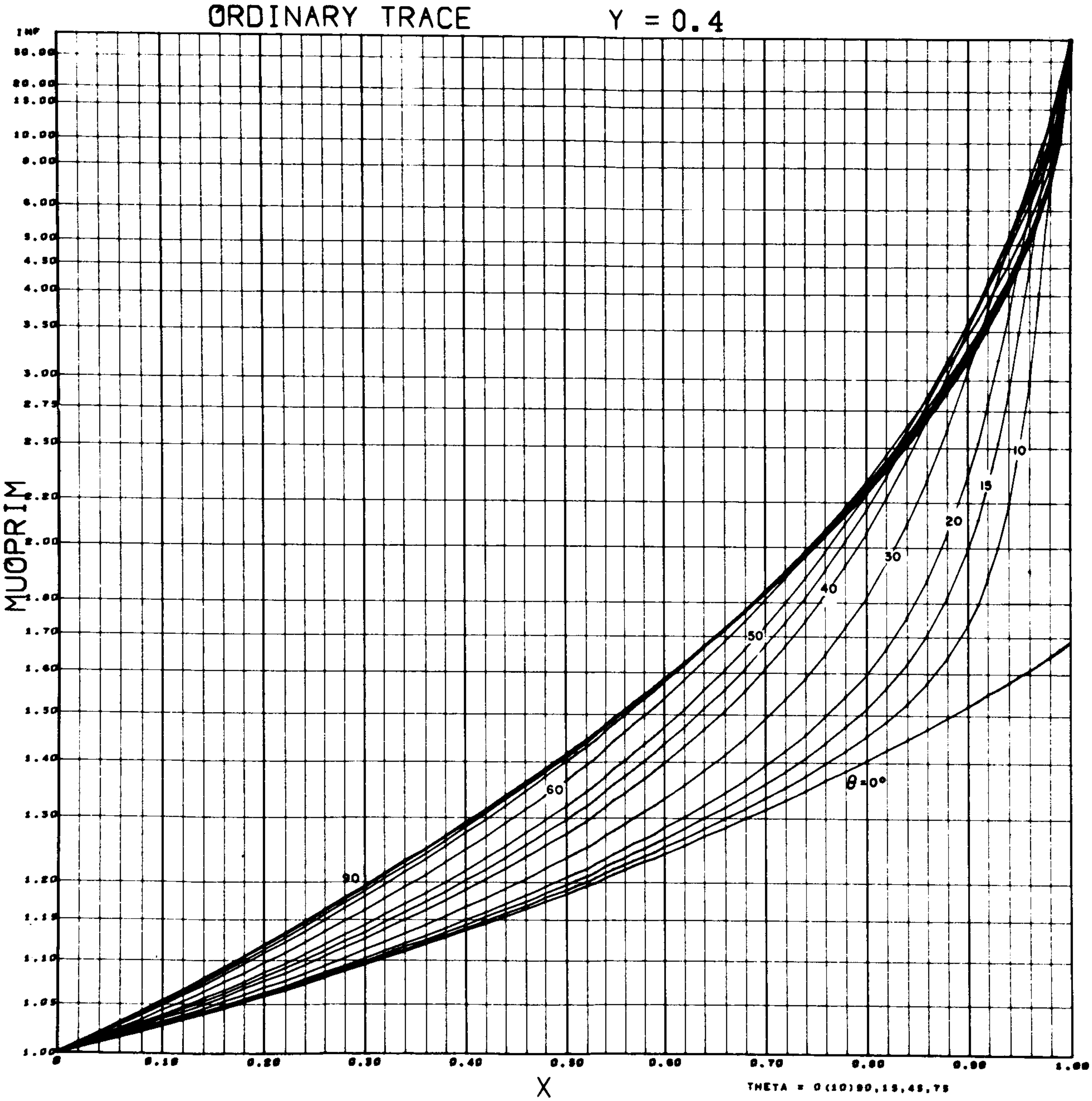

Figure 99.- Variation of μ' vs. X; Y = 0.4; $\theta = 0^{\circ} - 90^{\circ}$.

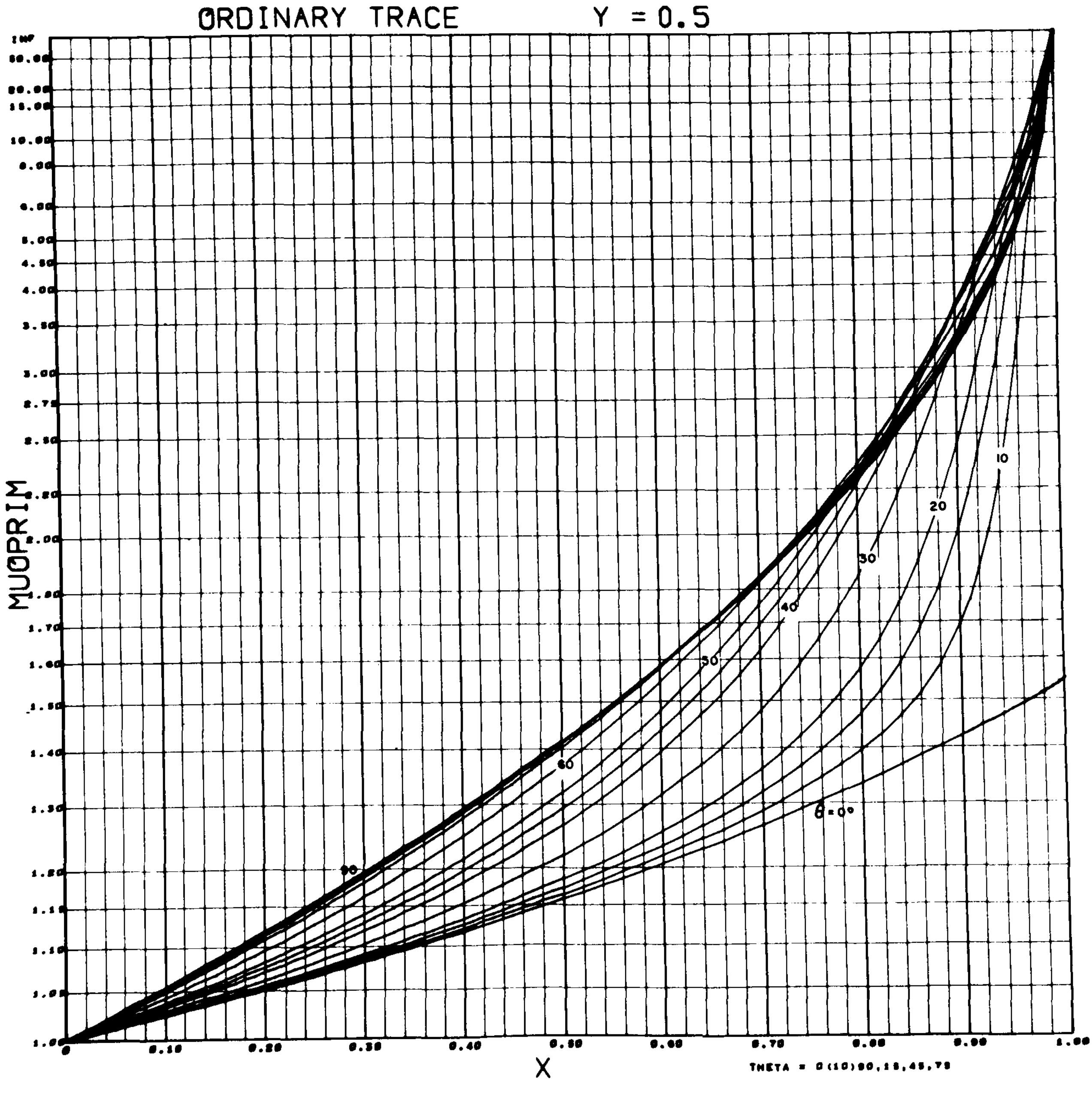

Figure 100.- Variation of μ' vs. X; Y = 0.5; θ = 0° - 90°.

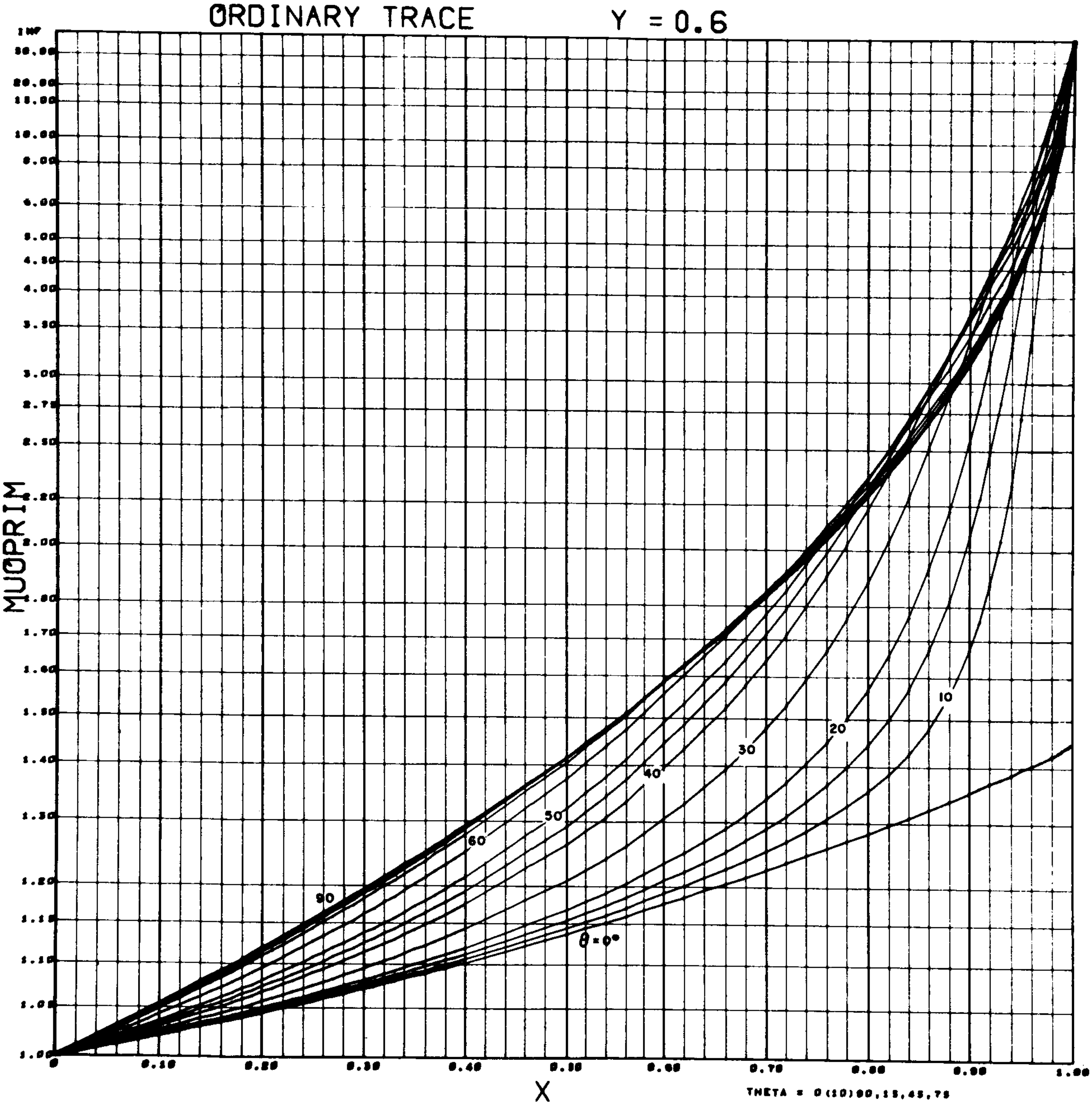

Figure 101.- Variation of μ' vs. X; Y = 0.6; $\theta = 0^{\circ} - 90^{\circ}$.

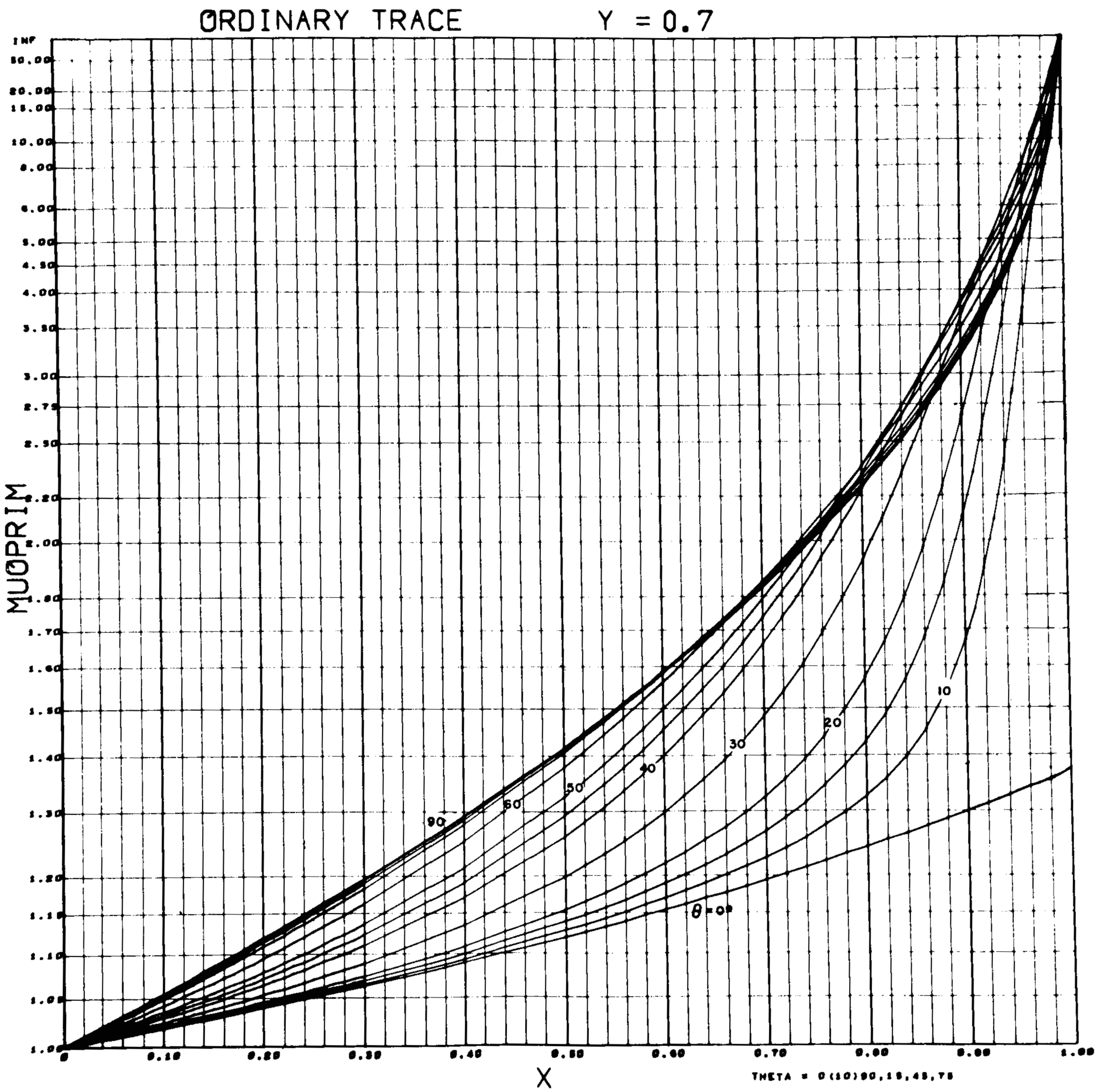

Figure 102.- Variation of μ' vs. X; Y = 0.7; θ = 0° - 90°.

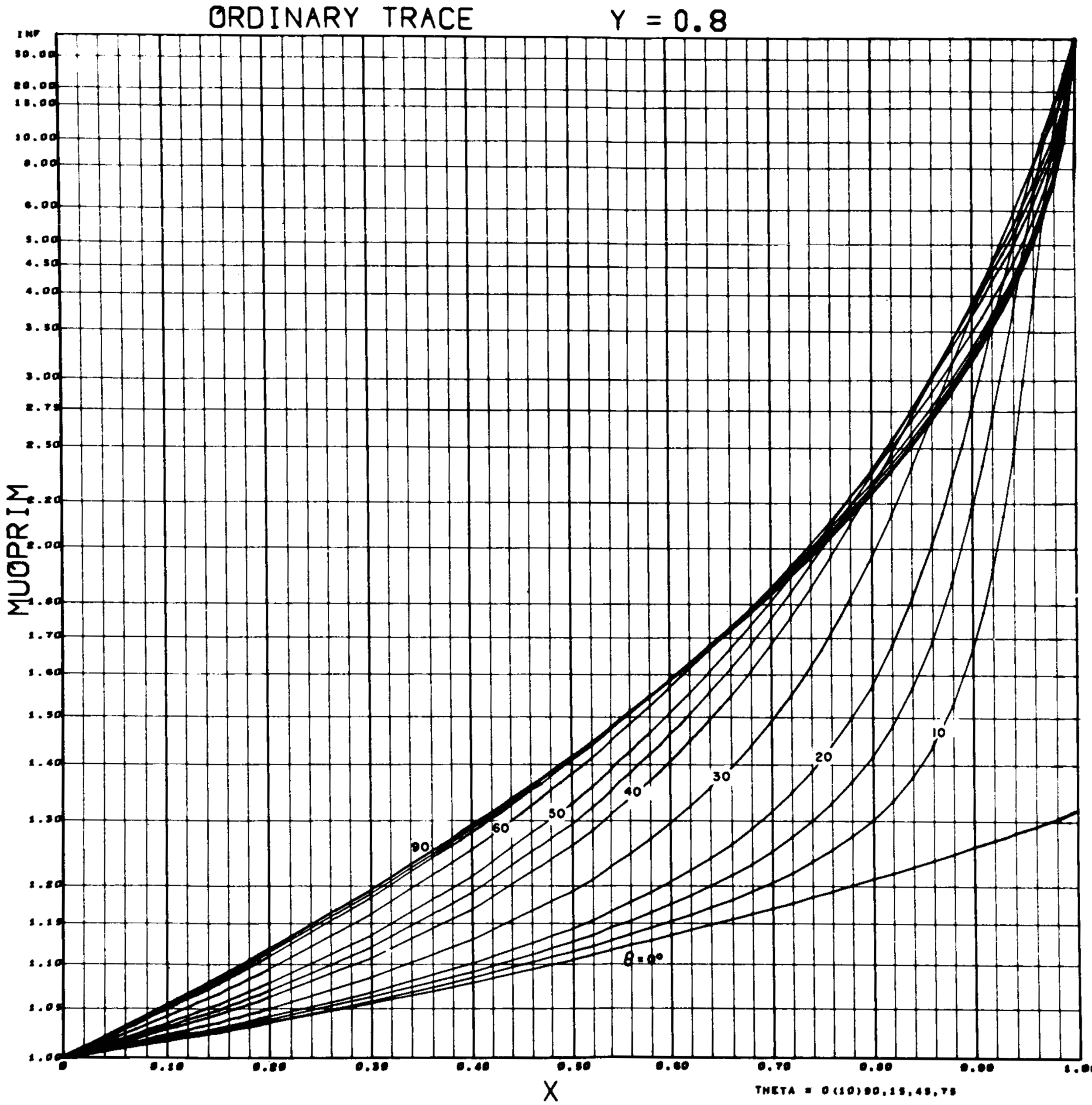

Figure 103.- Variation of μ' vs. X; Y = 0.8; $\theta = 0^{\circ} - 90^{\circ}$.

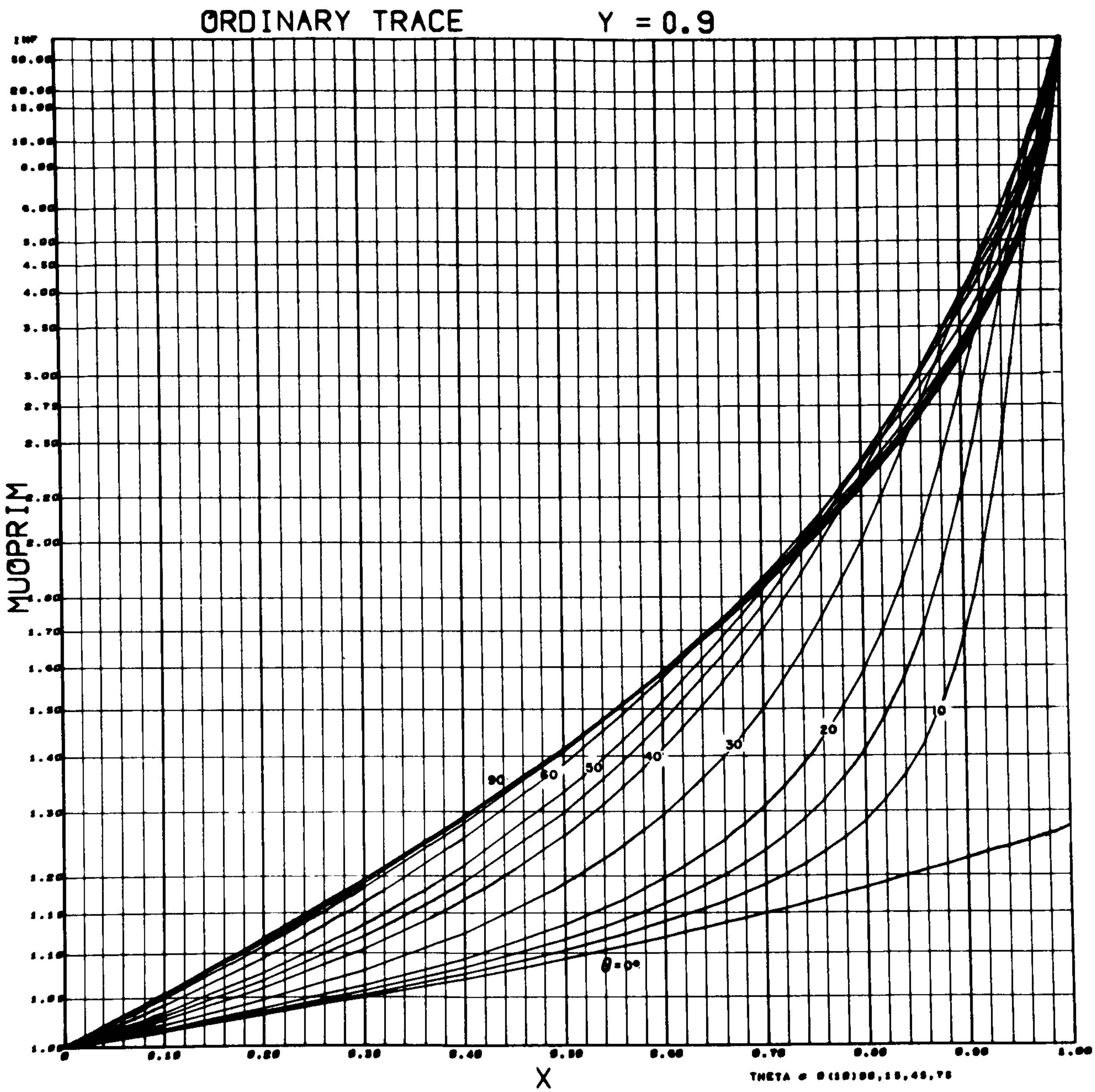

Figure 104.- Variation of μ' vs. X; Y = 0.9; θ = 0° - 90°.

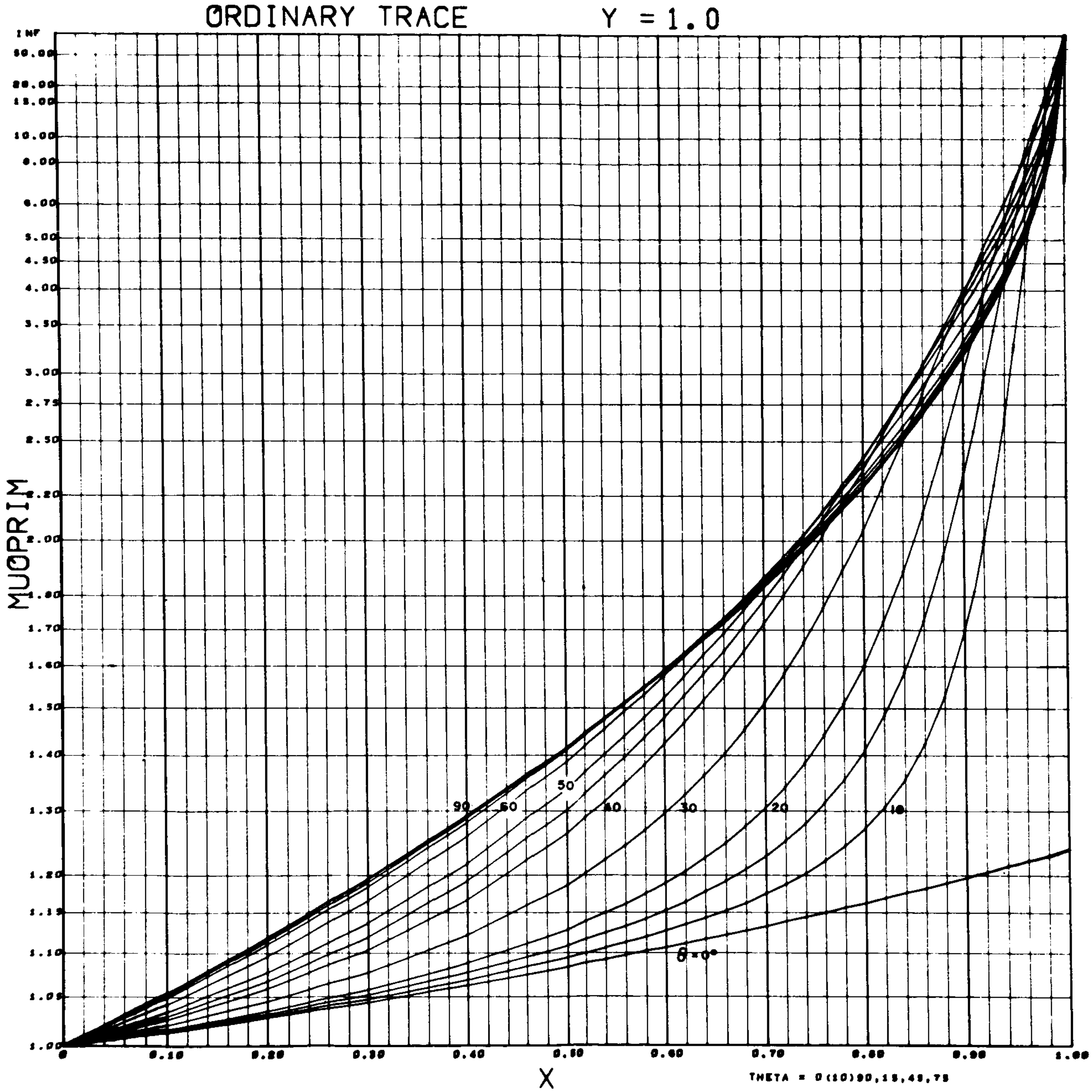

Figure 105.- Variation of μ' vs. X; Y = 1.0; θ = 0° - 90°.

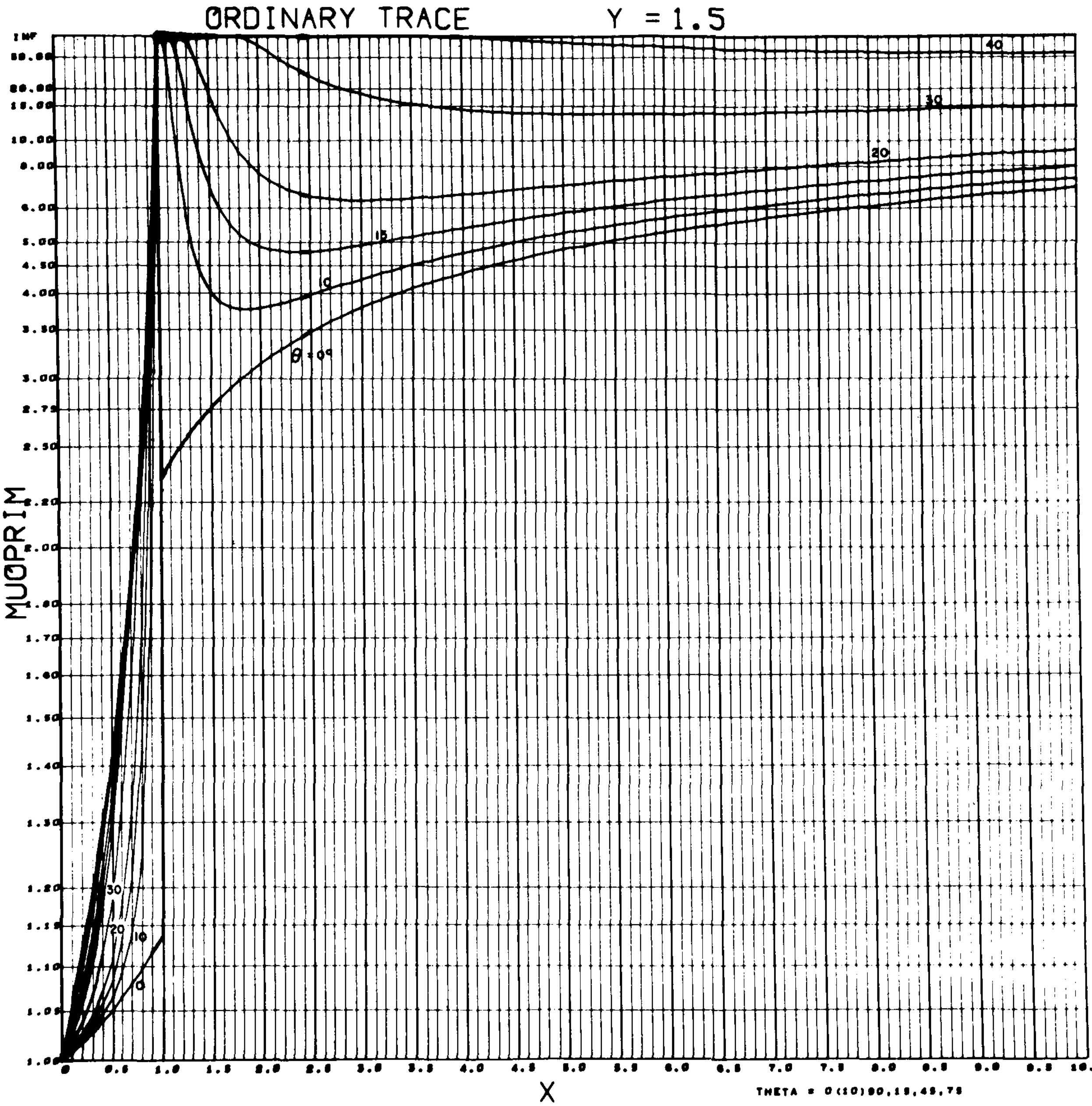

Figure 106.- Variation of μ' vs. X; Y = 1.5; $\theta = 0^{\circ} - 90^{\circ}$.

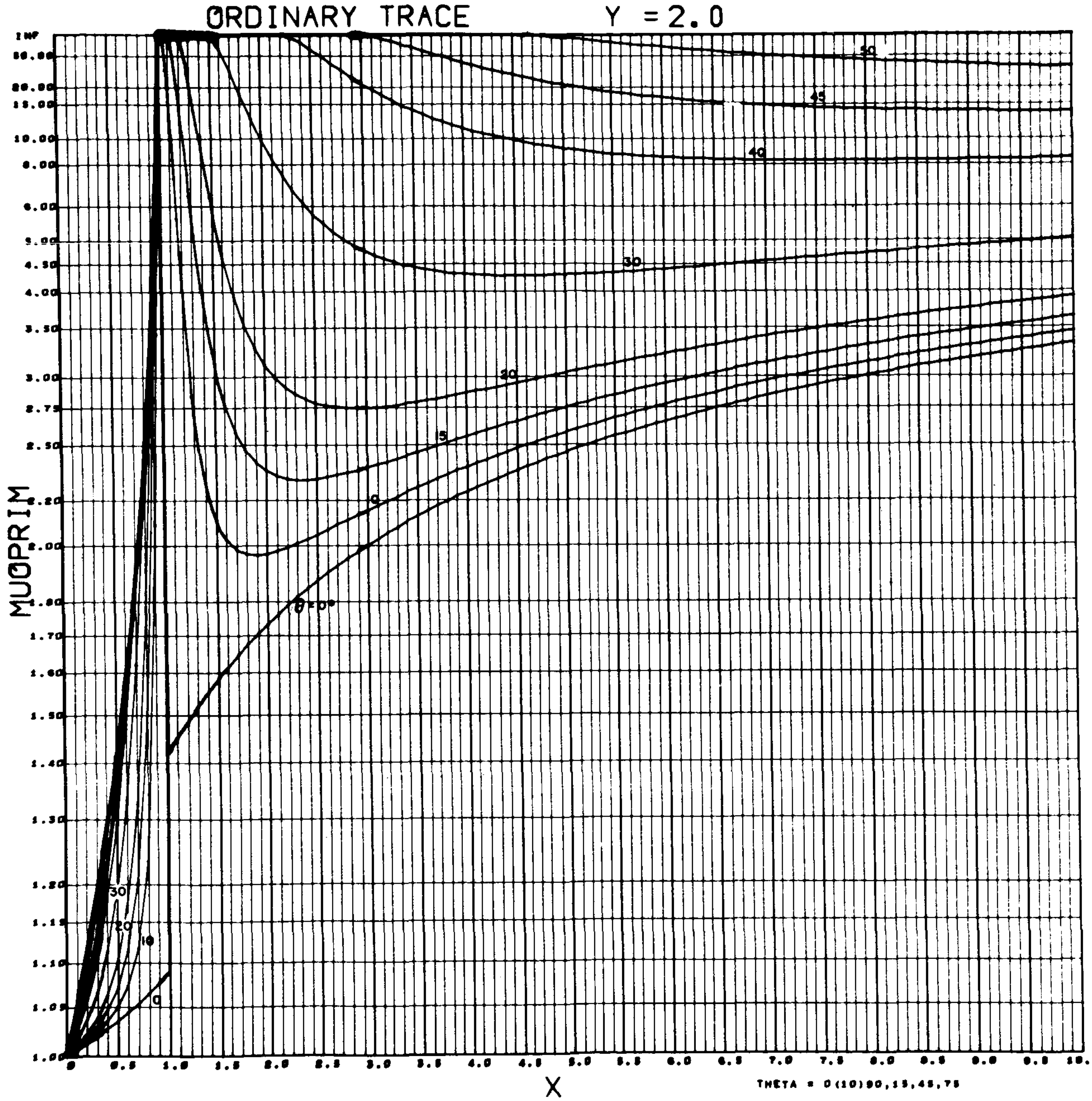

Figure 107.- Variation of μ' vs. X; Y = 2.0; θ = 0° - 90°.

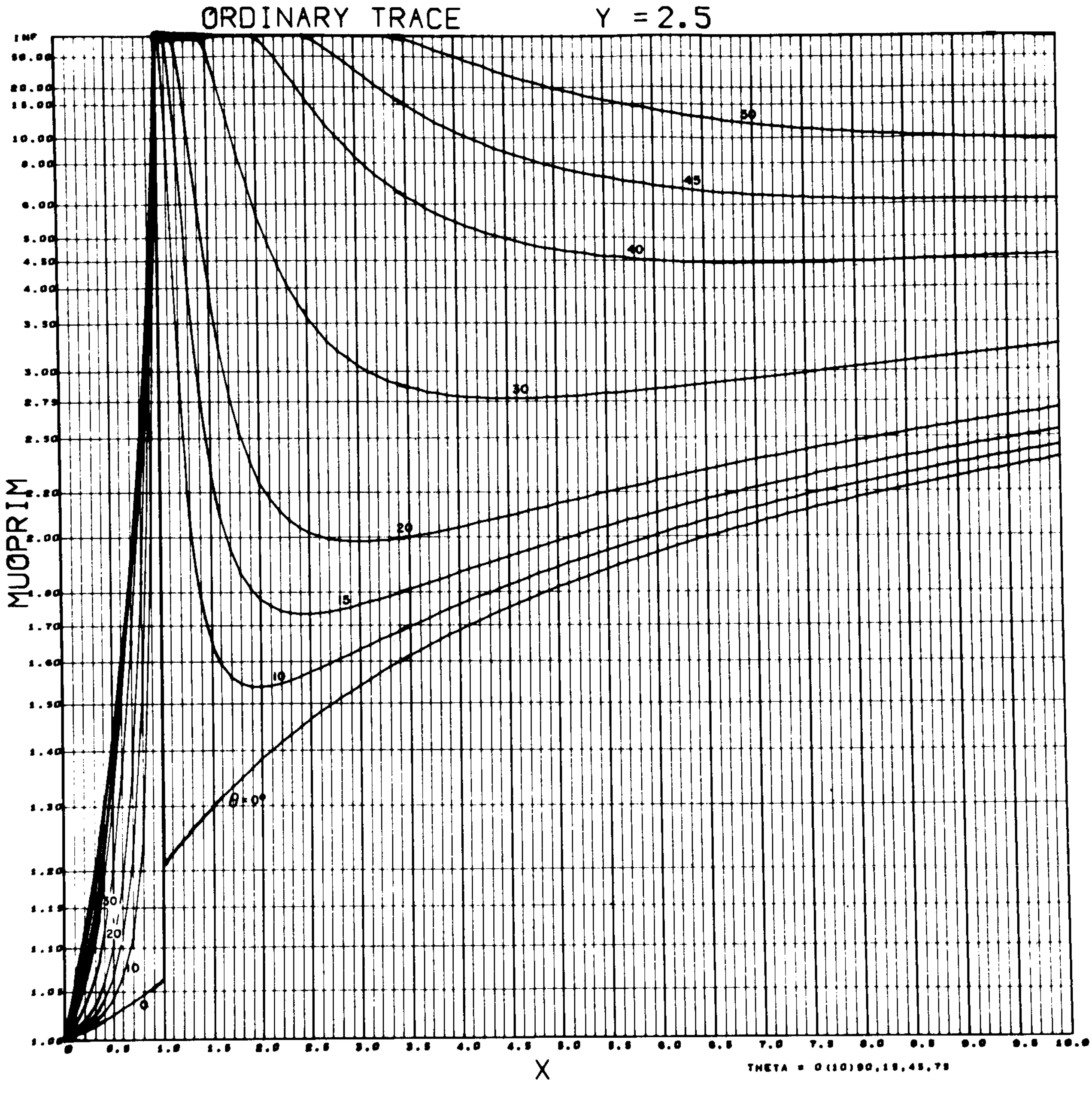

Figure 108.- Variation of μ' vs. X; Y = 2.5; $\theta = 0^{\circ} - 90^{\circ}$.

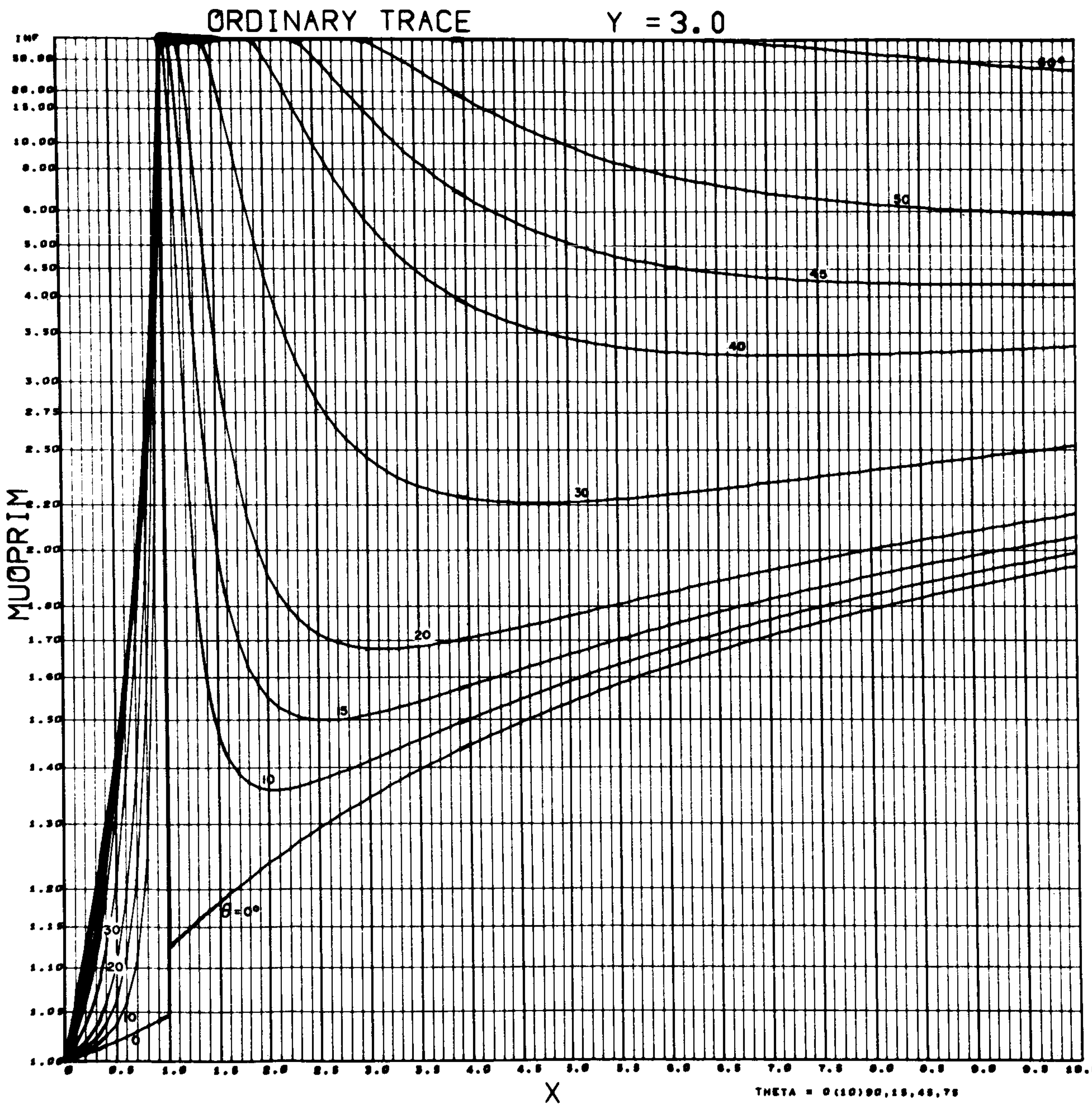

Figure 109.- Variation of μ' vs. X; Y = 3.0; θ = 0° - 90°.

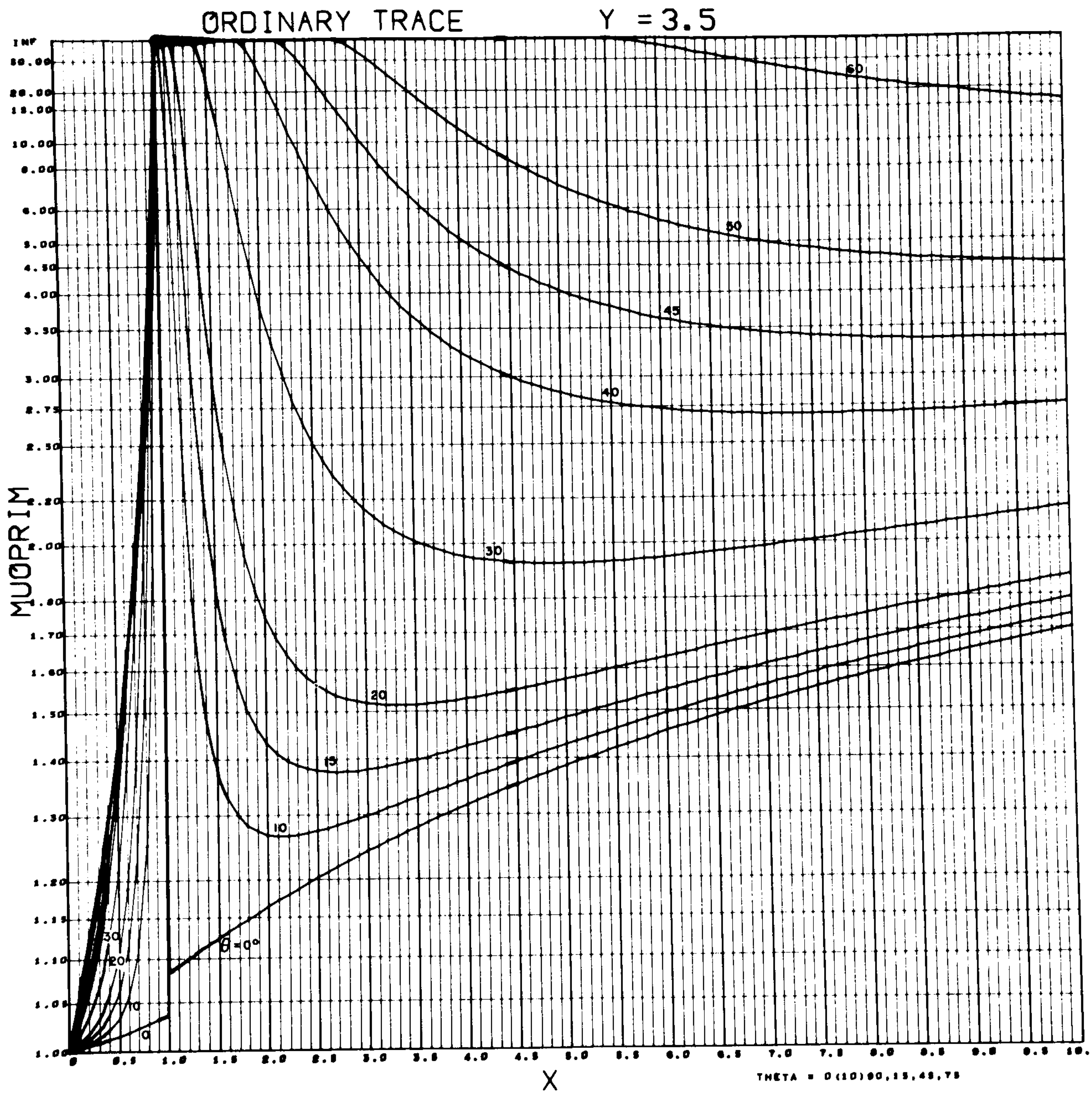

Figure 110.- Variation of μ' vs. X; Y = 3.5; θ = 0° - 90°.

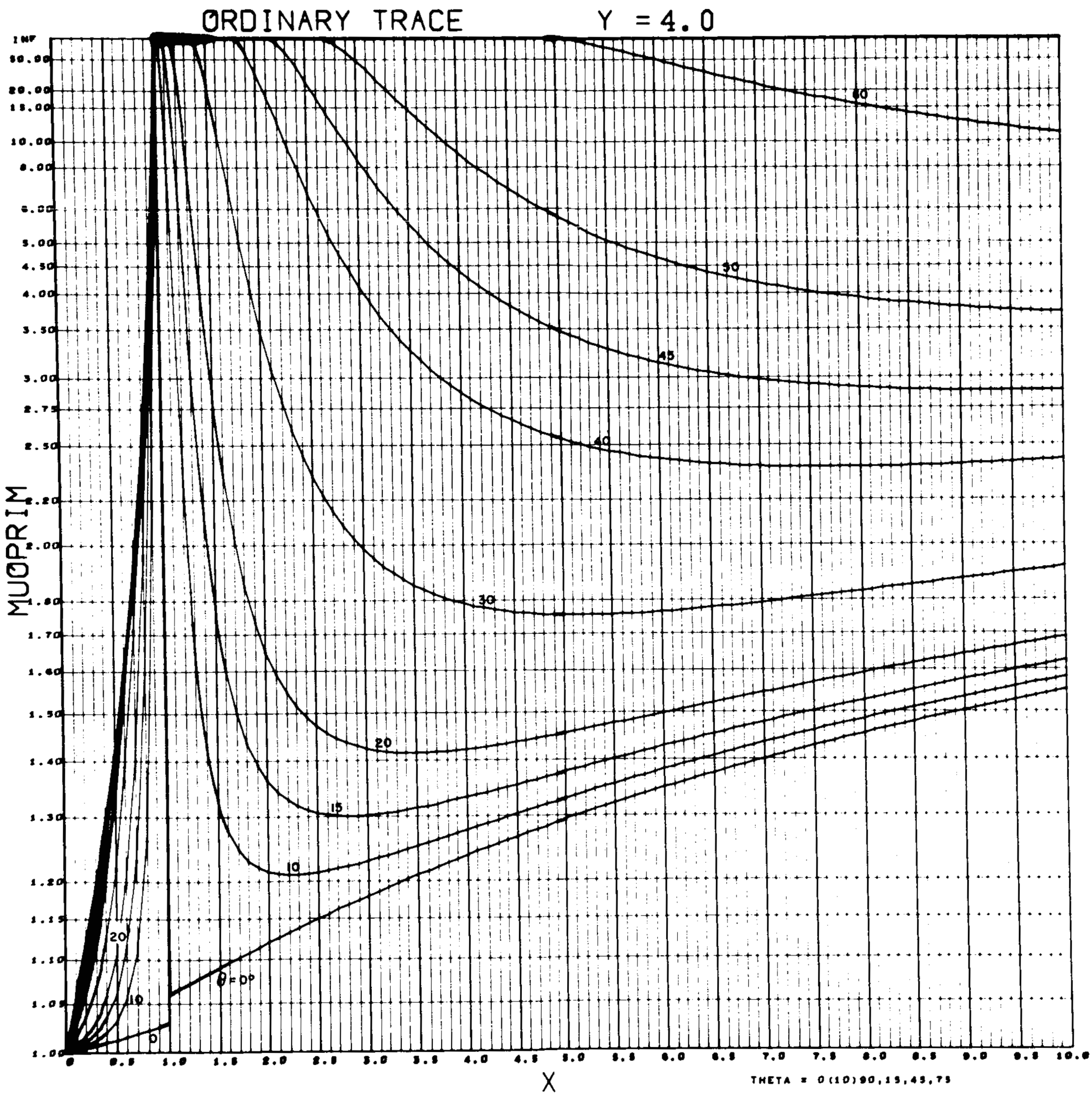

Figure 111.- Variation of μ' vs. X; Y = 4.0; $\theta = 0^{\circ} - 90^{\circ}$.

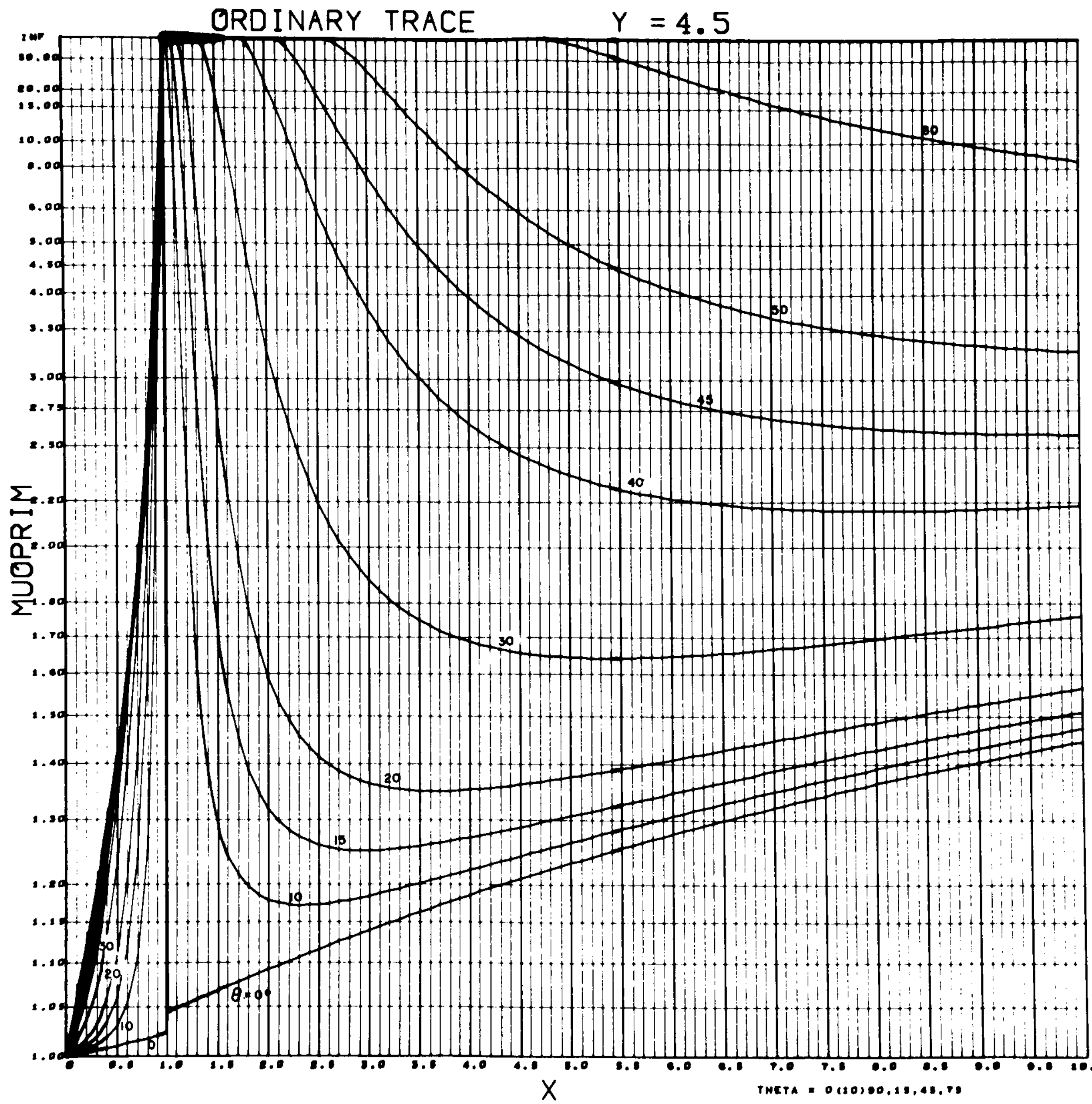

Figure 112.- Variation of μ' vs. X; Y = 4.5; $\theta = 0^{\circ} - 90^{\circ}$.

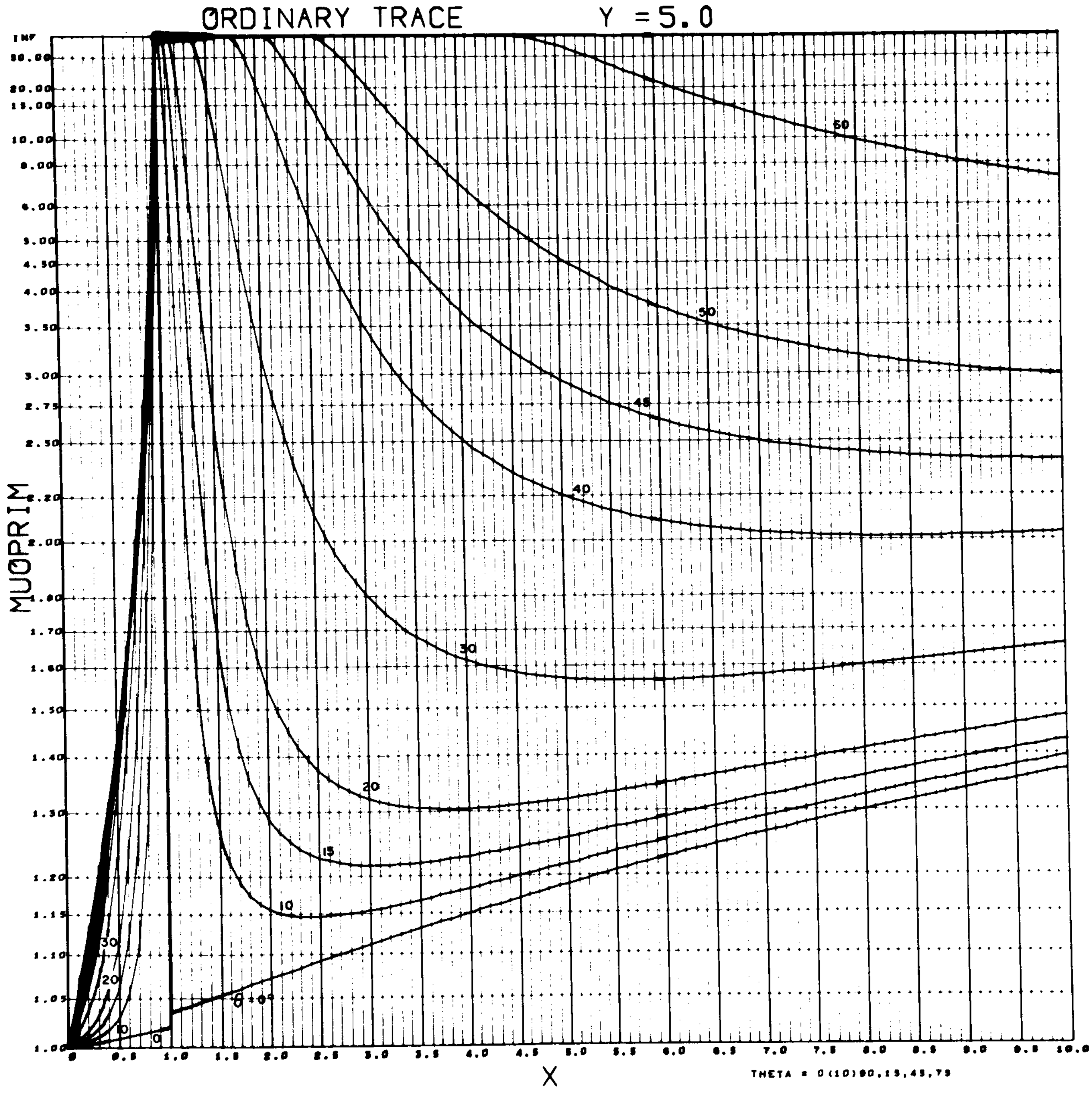

Figure 113.- Variation of μ' vs. X; Y = 5.0; θ = 0° - 90°.

National Aeronautics and Space Administration
WASHINGTON, D. C.

OFFICIAL BUSINESS

FIRST CLASS MAIL

POSTAGE AND FEES PAID
NATIONAL AERONAUTICS AND
SPACE ADMINISTRATION

POSTMASTER: If Undeliverable (Section 158 Postal Manual) Do Not Return

"The aeronautical and space activities of the United States shall be conducted so as to contribute . . . to the expansion of human knowledge of phenomena in the atmosphere and space. The Administration shall provide for the widest practicable and appropriate dissemination of information concerning its activities and the results thereof."

—NATIONAL AERONAUTICS AND SPACE ACT OF 1958

NASA SCIENTIFIC AND TECHNICAL PUBLICATIONS

TECHNICAL REPORTS: Scientific and technical information considered important, complete, and a lasting contribution to existing knowledge.

TECHNICAL NOTES: Information less broad in scope but nevertheless of importance as a contribution to existing knowledge.

TECHNICAL MEMORANDUMS: Information receiving limited distribution because of preliminary data, security classification, or other reasons.

CONTRACTOR REPORTS: Scientific and technical information generated under a NASA contract or grant and considered an important contribution to existing knowledge.

TECHNICAL TRANSLATIONS: Information published in a foreign language considered to merit NASA distribution in English.

SPECIAL PUBLICATIONS: Information derived from or of value to NASA activities. Publications include conference proceedings, monographs, data compilations, handbooks, sourcebooks, and special bibliographies.

TECHNOLOGY UTILIZATION PUBLICATIONS: Information on technology used by NASA that may be of particular interest in commercial and other non-aerospace applications. Publications include Tech Briefs, Technology Utilization Reports and Notes, and Technology Surveys.

Details on the availability of these publications may be obtained from:

SCIENTIFIC AND TECHNICAL INFORMATION DIVISION

NATIONAL AERONAUTICS AND SPACE ADMINISTRATION

Washington, D.C. 20546